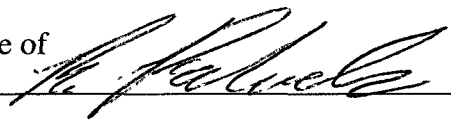


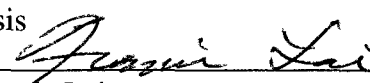
Validation of Moldflow™ Simulation with Experimental Data from Mold with
Viewing Window

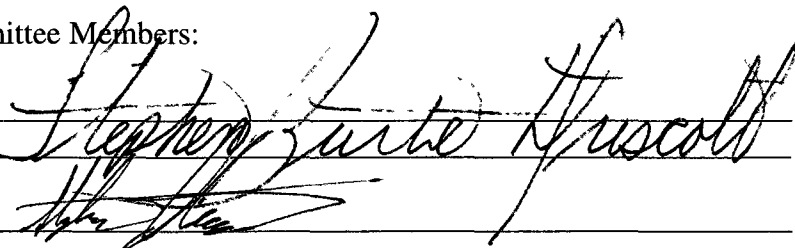

BY

BRIAN PALIWODA
B.S. University of Massachusetts Lowell (2008)

SUBMITTED IN PARTIAL FULFILLMENT OF THE REQUIREMENTS
FOR THE DEGREE OF MASTER OF SCIENCE
DEPARTMENT OF PLASTICS ENGINEERING
UNIVERSITY OF MASSACHUSETTS LOWELL

Signature of Author:  Date: 7/15/11

Signature of Thesis Supervisor:  Date: July 15, 2011
Name Typed: Francis Lai

Signature of other Thesis Committee Members:
Committee Member Signature: 
Name Typed: Stephen Driscoll
Committee Member Signature: 
Name Typed: Stephen Johnston

UMI Number: 1504016

All rights reserved

INFORMATION TO ALL USERS

The quality of this reproduction is dependent upon the quality of the copy submitted.

In the unlikely event that the author did not send a complete manuscript and there are missing pages, these will be noted. Also, if material had to be removed, a note will indicate the deletion.



UMI 1504016

Copyright 2011 by ProQuest LLC.

All rights reserved. This edition of the work is protected against unauthorized copying under Title 17, United States Code.



ProQuest LLC
789 East Eisenhower Parkway
P.O. Box 1346
Ann Arbor, MI 48106-1346

Validation of Moldflow™ Simulation with Experimental Data

BY

BRIAN PALIWODA

ABSTRACT OF A THESIS SUBMITTED TO THE FACULTY OF THE
DEPARTMENT OF PLASTICS ENGINEERING
IN PARTIAL FULFILLMENT OF THE REQUIREMENTS
FOR THE DEGREE OF
MASTER OF SCIENCE
UNIVERSITY OF MASSACHUSETTS LOWELL
2011

Thesis Supervisor: Francis Lai
Professor, Plastics Engineering Department

ABSTRACT

In this thesis benchmarking was used to determine the accuracy of the injection molding CAE software Moldflow™. The benchmarking data were obtained by experiments; the visualized melt filling behaviors inside rib shape cavities, step-change cavities, and obstacle-pin cavities with tapered thickness using a three-dimensional (3-D) glass-inserted mold. The measured melt temperature distributions along the thickness direction using an integrated thermocouple sensor was developed based on many different molding conditions. The database includes all these important data in addition to material data generally required for numerical simulation.

To determine the accuracy of the simulation software the following three characteristics were compared: fill pattern, injection pressure at three locations, and temperature profile in the runner just before the gate.

The results indicate that the Moldflow™ software makes some assumptions that cause the simulation to be not entirely accurate; however the simulation does give a very good understanding of how the mold cavity will fill.

ACKNOWLEDGEMENTS

I would like to thank Autodesk for allowing me use the Moldflow™ software. I would also like to thank Professor Francis Lai for providing support, his time, and academic guidance during the long process of researching, writing, and editing this thesis.

I would also like to thank my family and girlfriend Aly for their support and understanding during the researching, writing, and editing this thesis.

Table of Contents

I. Introduction	1
II. Literature review	13
III. Methodology	15
IV. RESULTS and DISCUSSION.....	17
Analysis of Flow path and Fill time.....	17
Comparison 1 – Obstacle Pin Cavity, J-2000GP at 37.7 cc/s.....	18
Comparison 2 – Obstacle Pin Cavity, J-2000GP at 6.3 cc/s.....	19
Comparison 3 – Obstacle Pin Cavity, CR-3500 at 37.7 cc/s.....	20
Comparison 4 – Obstacle Pin Cavity, CR-3500 at 6.3 cc/s.....	20
Comparison 5 – 2 mm Parallel Rib Cavity, J-2000GP at 37.7 cc/s.....	21
Comparison 6 – 2 mm Parallel Rib Cavity, J-2000GP at 6.3 cc/s.....	22
Comparison 7 – 2 mm Parallel Rib Cavity, CR-3500 at 37.7 cc/s.....	22
Comparison 8 – 2 mm Parallel Rib Cavity, CR-3500 at 6.3 cc/s.....	23
Comparison 9 – 4 mm Parallel Rib Cavity, J-2000GP at 37.7 cc/s.....	24
Comparison 10 – 4 mm Parallel Rib Cavity, J-2000GP at 6.3 cc/s.....	25
Comparison 11 – 4 mm Parallel Rib Cavity, CR-3500 at 37.7 cc/s.....	25
Comparison 12 – 4 mm Parallel Rib Cavity, CR-3500 at 6.3 cc/s.....	26
Comparison 13 – 2 mm Perpendicular Rib Cavity, J-2000GP at 18.8 cc/s.....	27
Comparison 14 – 2 mm Perpendicular Rib Cavity, J-2000GP at 6.3 cc/s.....	28
Comparison 15 – 2 mm Perpendicular Rib Cavity, CR-2500 at 18.8 cc/s.....	28
Comparison 16 – 2 mm Perpendicular Rib Cavity, CR-2500 at 6.3 cc/s.....	29
Comparison 17 – 4 mm Perpendicular Rib Cavity, J-2000GP at 18.8 cc/s.....	30
Comparison 18 – 4 mm Perpendicular Rib Cavity, J-2000GP at 6.3 cc/s.....	31
Comparison 19 – 4 mm Perpendicular Rib Cavity, CR-2500 at 18.8 cc/s.....	31
Comparison 20 – 4 mm Perpendicular Rib Cavity, CR-2500 at 6.3 cc/s.....	32
Comparison 21 – 3D meshed Obstacle Pin Cavity, J-2000GP at 37.7 cc/s.....	33
Analysis of Peak Injection Pressure.....	33
Comparison 22 – Obstacle Pin cavity, mtl: J-2000GP.....	34
Comparison 23 – Obstacle Pin cavity, mtl: J-2000GP.....	35
Comparison 24 – 4 mm perpendicular rib cavity, mtl: CR-3500.....	36
Comparison 25 – 4 mm parallel rib cavity, mtl: CR-3500.....	37

V. CONCLUSIONS.....	38
VI. RECOMMENDATIONS.....	39
VII. LITERATURE CITED.....	40
Appendix A – Flow Patterns.....	41
Figure 1a – Flow Front Profile in Obstacle Pin cavity, mtl: 700GP @ 37.7 cc/s injection rate	41
Figure 2a - Flow Front Profile in Obstacle Pin cavity, mtl: 700GP @ 6.3 cc/s injection rate..	42
Figure 3a - Flow Front Profile in Obstacle Pin cavity, mtl: 2000GP @ 37.7 cc/s injection rate	43
Figure 4a - Flow Front Profile in Obstacle Pin cavity, mtl: 2000GP @ 6.3 cc/s injection rate	44
Figure 5a - Flow Front Profile in Obstacle Pin cavity, mtl: CR3500 @ 37.7 cc/s injection rate	45
Figure 6a - Flow Front Profile in Obstacle Pin cavity, mtl: CR3500 @ 6.3 cc/s injection rate	46
Figure 7a - Flow Front Profile in Obstacle Pin cavity, mtl: CR4500 @ 37.7 cc/s injection rate	47
Figure 8a - Flow Front Profile in Obstacle Pin cavity, mtl: CR4500 @ 6.3 cc/s injection rate	48
Figure 9-1a - Flow Front Profile (side) in 2 mm parallel rib cavity, mtl: CR3500 @ 37.7 cc/s injection rate.....	49
Figure 9-2a - Flow Front Profile in 2 mm parallel rib cavity, mtl: CR3500 @ 37.7 cc/s injection rate.....	50
Figure 10-1a - Flow Front Profile (side) in 2 mm parallel rib cavity, mtl: CR3500 @ 6.3 cc/s injection rate.....	51
Figure 10-2a - Flow Front Profile in 2 mm parallel rib cavity, mtl: CR3500 @ 6.3 cc/s injection rate.....	52
Figure 11-1a - Flow Front Profile (side) in 2 mm parallel rib cavity, mtl: CR4500 @ 37.7 cc/s injection rate.....	53
Figure 11-2a - Flow Front Profile in 2 mm parallel rib cavity, mtl: CR4500 @ 37.7 cc/s injection rate.....	54
Figure 12-1a - Flow Front Profile (side) in 2 mm parallel rib cavity, mtl: CR4500 @ 6.3 cc/s injection rate.....	55
Figure 12-2a - Flow Front Profile in 2 mm parallel rib, mtl: CR4500 @ 6.3 cc/s injection rate	56
Figure 13-1a - Flow Front Profile (side) in 2 mm parallel rib cavity, mtl: 700GP @ 37.7 cc/s injection rate.....	57
Figure 13-2a - Flow Front Profile in 2 mm parallel rib cavity, mtl: 700GP @ 37.7 cc/s injection rate.....	58
Figure 14-1a - Flow Front Profile (side) in 2 mm parallel rib cavity, mtl: 700GP @ 6.3 cc/s injection rate.....	59

Figure 14-2a - Flow Front Profile in 2 mm parallel rib cavity, mtl: 700GP @ 6.3 cc/s injection rate.....	60
Figure 15-1a - Flow Front Profile (side) in 2 mm parallel rib cavity, mtl: 2000GP @ 37.7 cc/s injection rate.....	61
Figure 15-2a - Flow Front Profile in 2 mm parallel rib cavity, mtl: 2000GP @ 37.7 cc/s injection rate.....	62
Figure 16-1a - Flow Front Profile (side) in 2 mm parallel rib cavity, mtl: 2000GP @ 6.3 cc/s injection rate.....	63
Figure 16-2a - Flow Front Profile in 2 mm parallel rib cavity, mtl: 2000GP @ 6.3 cc/s injection rate.....	64
Figure 17-1a - Flow Front Profile (last rib) in 2 mm perpendicular rib cavity, mtl: CR3500 @ 18.8 cc/s injection rate	65
Figure 17-2a - Flow Front Profile (top) in 2 mm perpendicular rib cavity, mtl: CR3500 @ 18.8cc/s injection rate	66
Figure 18-1a - Flow Front Profile (last rib) in 2 mm perpendicular rib cavity, mtl: CR3500 @ 6.3 cc/s injection rate	67
Figure 18-2a - Flow Front Profile (top) in 2 mm perpendicular rib cavity, mtl: CR3500 @ 6.3 cc/s injection rate	68
Figure 19-1a - Flow Front Profile (last rib) in 2 mm perpendicular rib cavity, mtl: CR4500 @ 18.8cc/s injection rate	69
Figure 19-2a - Flow Front Profile (top) in 2 mm perpendicular rib cavity, mtl: CR4500 @ 18.8 cc/s injection rate	70
Figure 20-1a - Flow Front Profile (last rib) in 2 mm perpendicular rib cavity, mtl: CR4500 @ 6.3 cc/s injection rate	71
Figure 20-2a - Flow Front Profile (top) in 2 mm perpendicular rib cavity, mtl: CR4500 @ 6.3 cc/s injection rate	72
Figure 21-1a - Flow Front Profile (last rib) in 2 mm perpendicular rib cavity, mtl: 700GP @ 18.8cc/s injection rate	73
Figure 21-2a - Flow Front Profile (top) in 2 mm perpendicular rib cavity, mtl: 700GP @ 18.8cc/s injection rate	74
Figure 22-1a - Flow Front Profile (last rib) in 2 mm perpendicular rib cavity, mtl: 700GP @ 6.3 cc/s injection rate	75
Figure 22-2a - Flow Front Profile (top) in 2 mm perpendicular rib cavity, mtl: 700GP @ 6.3 cc/s injection rate	76
Figure 23-1a - Flow Front Profile (last rib) in 2 mm perpendicular rib cavity, mtl: 2000GP @ 18.8 cc/s injection rate	77
Figure 23-2a - Flow Front Profile (top) in 2 mm perpendicular rib cavity, mtl: 2000GP @ 18.8 cc/s injection rate	78
Figure 24-1a - Flow Front Profile (last rib) in 2 mm perpendicular rib cavity, mtl: 2000GP @ 6.3 cc/s injection rate	79

Figure 24-2a - Flow Front Profile (top) in 2 mm perpendicular rib cavity, mtl: 2000GP @ 6.3 cc/s injection rate 80

Figure 25-1a - Flow Front Profile (side) in 4 mm parallel rib cavity, mtl: CR3500 @ 18.8 cc/s injection rate..... 81

Figure 25-2a - Flow Front Profile (top) in 4 mm parallel rib cavity, mtl: CR3500 @ 37.7 cc/s injection rate..... 82

Figure 26-1a - Flow Front Profile (side) in 4 mm parallel rib cavity, mtl: CR3500 @ 6.3 cc/s injection rate..... 83

Figure 26-2a - Flow Front Profile (top) in 4 mm parallel rib cavity, mtl: CR3500 @ 6.3 cc/s injection rate..... 84

Figure 27-1a - Flow Front Profile (side) in 4 mm parallel rib cavity, mtl: CR4500 @ 37.7 cc/s injection rate..... 85

Figure 27-2a - Flow Front Profile (top) in 4 mm parallel rib cavity, mtl: CR4500 @ 37.7 cc/s injection rate..... 86

Figure 28-1a - Flow Front Profile (side) in 4 mm parallel rib cavity, mtl: CR4500 @ 6.3 cc/s injection rate..... 87

Figure 28-2a - Flow Front Profile (top) in 4 mm parallel rib cavity, mtl: CR4500 @ 6.3 cc/s injection rate..... 88

Figure 29-1a - Flow Front Profile (side) in 4 mm parallel rib cavity, mtl: 700GP @ 37.7 cc/s injection rate..... 89

Figure 29-2a - Flow Front Profile (top) in 4 mm parallel rib cavity, mtl: 700GP @ 37.7 cc/s injection rate..... 90

Figure 30-1a - Flow Front Profile (side) in 4 mm parallel rib cavity, mtl: 700GP @ 6.3 cc/s injection rate..... 91

Figure 30-2a - Flow Front Profile (top) in 4 mm parallel rib cavity, mtl: 700GP @ 6.3 cc/s injection rate..... 92

Figure 31-1a - Flow Front Profile (side) in 4 mm parallel rib cavity, mtl: 2000GP @ 37.7cc/s injection rate..... 93

Figure 31-2a - Flow Front Profile (top) in 4 mm parallel rib cavity, mtl: 2000GP @ 37.7cc/s injection rate..... 94

Figure 32-1a - Flow Front Profile (side) in 4 mm parallel rib cavity, mtl: 2000GP @ 6.3 cc/s injection rate..... 95

Figure 32-2a - Flow Front Profile (top) in 4 mm parallel rib cavity, mtl: 2000GP @ 6.3 cc/s injection rate..... 96

Figure 33-1a - Flow Front Profile (last rib) in 4 mm perpendicular rib cavity, mtl: CR3500 @ 18.8 cc/s injection rate 97

Figure 33-2a - Flow Front Profile (top) in 4 mm perpendicular rib cavity, mtl: CR3500 @ 18.8 cc/s injection rate 98

Figure 34-1a - Flow Front Profile (last rib) in 4 mm perpendicular rib cavity, mtl: CR3500 @ 6.3 cc/s injection rate 99

Figure 34-2a - Flow Front Profile (top) in 4 mm perpendicular rib cavity, mtl: CR3500 @ 6.3 cc/s injection rate	100
Figure 35-1a - Flow Front Profile (last rib) in 4 mm perpendicular rib cavity, mtl: CR4500 @ 18.8 cc/s injection rate	101
Figure 35-2a - Flow Front Profile (top) in 4 mm perpendicular rib cavity, mtl: CR4500 @ 18.8 cc/s injection rate	102
Figure 36-1a - Flow Front Profile (last rib) in 4 mm perpendicular rib cavity, mtl: CR4500 @ 6.3 cc/s injection rate	103
Figure 36-2a - Flow Front Profile (top) in 4 mm perpendicular rib cavity, mtl: CR4500 @ 6.3 cc/s injection rate	104
Figure 37-1a - Flow Front Profile (last rib) in 4 mm perpendicular rib cavity, mtl: 700GP @ 18.8 cc/s injection rate	105
Figure 37-2a - Flow Front Profile (top) in 4 mm perpendicular rib cavity, mtl: 700GP @ 18.8 cc/s injection rate	106
Figure 38-1a - Flow Front Profile (last rib) in 4 mm perpendicular rib cavity, mtl: 700GP @ 6.3 cc/s injection rate	107
Figure 38-2a - Flow Front Profile (top) in 4 mm perpendicular rib cavity, mtl: 700GP @ 6.3 cc/s injection rate	108
Figure 39-1a - Flow Front Profile (last rib) in 4 mm perpendicular rib cavity, mtl: 2000GP @ 18.8 cc/s injection rate	109
Figure 39-2a - Flow Front Profile (top) in 4 mm perpendicular rib cavity, mtl: 2000GP @ 18.8 cc/s injection rate	110
Figure 40-1a - Flow Front Profile (last rib) in 4 mm perpendicular rib cavity, mtl: 2000GP @ 6.3 cc/s injection rate	111
Figure 40-2a - Flow Front Profile (top) in 4 mm perpendicular rib cavity, mtl: 2000GP @ 6.3 cc/s injection rate	112
Figure 41a – Experimental Flow Pattern – 4 mm parallel rib cavity.....	113
Figure 42a – Experimental Flow Pattern – 2 mm parallel rib cavity.....	114
Figure 43a – Experimental Flow Pattern – 2 mm parallel rib cavity.....	115
Figure 44a – Experimental Flow Pattern – 4 mm parallel rib cavity.....	116
Figure 45a – Experimental Flow Pattern – 2 mm perpendicular rib cavity.....	117
Figure 46a – Experimental Flow Pattern – 4 mm perpendicular rib cavity.....	118
Figure 47a – Experimental Flow Pattern – 2 mm perpendicular rib cavity.....	119
Figure 48a – Experimental Flow Pattern – 4 mm perpendicular rib cavity.....	120
Figure 49a – Experimental Flow Pattern – Obstacle pin cavity J-2000GP	121
Figure 50a – Experimental Flow Pattern – Obstacle pin cavity CR-3500.....	122
Appendix B – Pressure Profile at Three Locations.....	123

Figure 1b - Pressure profile at three locations in Obstacle Pin cavity, mtl: 700GP @ 37.7 cc/s injection rate.....	123
Figure 2b - Pressure profile at three locations in Obstacle Pin cavity, mtl: 700GP @ 6.3 cc/s injection rate.....	123
Figure 3b - Pressure profile at three locations in Obstacle Pin cavity, mtl: 2000GP @ 37.7 cc/s injection rate.....	124
Figure 4b - Pressure profile at three locations in Obstacle Pin cavity, mtl: 2000GP @ 6.3 cc/s injection rate.....	124
Figure 5b - Pressure profile at three locations in Obstacle Pin cavity, mtl: CR3500 @ 37.7 cc/s injection rate.....	125
Figure 6b - Pressure profile at three locations in Obstacle Pin cavity, mtl: CR3500 @ 6.3 cc/s injection rate.....	125
Figure 7b- Pressure profile at three locations in Obstacle Pin cavity, mtl: CR4500 @ 37.7 cc/s injection rate.....	126
Figure 8b - Pressure profile at three locations in Obstacle Pin cavity, mtl: CR4500 @ 6.3 cc/s injection rate.....	126
Figure 9b - Pressure profile at three locations in 2 mm parallel rib cavity, mtl: CR3500 @ 37.7 cc/s injection rate	127
Figure 10b - Pressure profile at three locations in 2 mm parallel rib cavity, mtl: CR4500 @ 37.7 cc/s injection rate	127
Figure 11b - Pressure profile at three locations in 2 mm parallel rib cavity, mtl: CR4500 @ 6.3 cc/s injection rate	128
Figure 12b - Pressure profile at three locations in 2 mm parallel rib cavity, mtl: 2000GP @ 37.7 cc/s injection rate	128
Figure 13b - Pressure profile at three locations in 2 mm parallel rib cavity, mtl: CR3500 @ 6.3 cc/s injection rate	129
Figure 14b - Pressure profile at three locations in 2 mm parallel rib cavity, mtl: 700GP @ 6.3 cc/s injection rate	129
Figure 15b - Pressure profile at three locations in 2 mm parallel rib cavity, mtl: 700GP @ 37.7 cc/s injection rate	130
Figure 16b - Pressure profile at three locations in 2 mm parallel rib cavity, mtl: 2000GP @ 6.3 cc/s injection rate	130
Figure 17b - Pressure profile at three locations in 2 mm perpendicular rib cavity, mtl: CR3500 @ 18.8 cc/s injection rate.....	131
Figure 18b - Pressure profile at three locations in 2 mm perpendicular rib cavity, mtl: CR3500 @ 6.3 cc/s injection rate.....	131
Figure 19b - Pressure profile at three locations in 2 mm perpendicular rib cavity, mtl: CR4500 @ 18.8 cc/s injection rate.....	132
Figure 20b - Pressure profile at three locations in 2 mm perpendicular rib cavity, mtl: CR4500 @ 6.3 cc/s injection rate.....	132

Figure 21b - Pressure profile at three locations in 2 mm perpendicular rib cavity, mtl: 700GP @ 18.8 cc/s injection rate.....	133
Figure 22b - Pressure profile at three locations in 2 mm perpendicular rib cavity, mtl: 700GP @ 6.3 cc/s injection rate.....	133
Figure 23b - Pressure profile at three locations in 2 mm perpendicular rib cavity, mtl: 2000GP @ 18.8 cc/s injection rate.....	134
Figure 24b - Pressure profile at three locations in 2 mm perpendicular rib cavity, mtl: 2000GP @ 6.3 cc/s injection rate.....	134
Figure 25b - Pressure profile at three locations in 4 mm parallel rib cavity, mtl: CR3500 @ 37.7 cc/s injection rate	135
Figure 26b - Pressure profile at three locations in 4 mm parallel rib cavity, mtl: CR3500 @ 6.3 cc/s injection rate	135
Figure 27b - Pressure profile at three locations in 4 mm parallel rib cavity, mtl: CR4500 @ 37.7 cc/s injection rate	136
Figure 28b - Pressure profile at three locations in 4 mm parallel rib cavity, mtl: CR4500 @ 6.3 cc/s injection rate	136
Figure 29b - Pressure profile at three locations in 4 mm parallel rib cavity, mtl: 700GP @ 37.7 cc/s injection rate	137
Figure 30b - Pressure profile at three locations in 4 mm parallel rib cavity, mtl: 700GP @ 6.3 cc/s injection rate	137
Figure 31b - Pressure profile at three locations in 4 mm parallel rib cavity, mtl: 2000GP @ 37.7 cc/s injection rate	138
Figure 32b - Pressure profile at three locations in 4 mm parallel rib cavity, mtl: 2000GP @ 6.3 cc/s injection rate	138
Figure 33b - Pressure profile at three locations in 4 mm perpendicular rib cavity, mtl: CR3500 @ 18.8 cc/s injection rate.....	139
Figure 34b - Pressure profile at three locations in 4 mm perpendicular rib cavity, mtl: CR3500 @ 6.3 cc/s injection rate.....	139
Figure 35b - Pressure profile at three locations in 4 mm perpendicular rib cavity, mtl: CR4500 @ 18.8 cc/s injection rate.....	140
Figure 36b - Pressure profile at three locations in 4 mm perpendicular rib cavity, mtl: CR4500 @ 6.3 cc/s injection rate.....	140
Figure 37b - Pressure profile at three locations in 4 mm perpendicular rib cavity, mtl: 700GP @ 18.8 cc/s injection rate.....	141
Figure 38b - Pressure profile at three locations in 4 mm perpendicular rib cavity, mtl: 700GP @ 6.3 cc/s injection rate.....	141
Figure 39b - Pressure profile at three locations in 4 mm perpendicular rib cavity, mtl: 2000GP @ 18.8 cc/s injection rate.....	142
Figure 40b - Pressure profile at three locations in 4 mm perpendicular rib cavity, mtl: 2000GP @ 6.3 cc/s injection rate.....	142

Figure 41b – Experimental data of Pressure profile at three locations in obstacle pin cavity, mtl: J-2000GP 143

Figure 42b – Experimental data of Pressure profile at three locations in 4 mm parallel rib cavity, mtl: CR-2500..... 144

Figure 43b – Experimental data of Pressure profile at three locations in 4 mm perpendicular rib cavity, mtl: CR-2500 144

Appendix C -Tables 145

 Table 1 – Pressure at different locations in obstacle pin cavity..... 145

 Table 2 – Peak injection pressure in obstacle pin cavity 146

 Table 3 – Fill time comparison in obstacle pin cavity 146

Appendix D –Temperature at Flow Front..... 147

 Figure 1d - Temperature at flow front in obstacle pin cavity, mtl: J700GP @ 37.7 cc/s 147

 Figure 2d - Temperature at flow front in obstacle pin cavity, mtl: J700GP @ 6.3cc/s 147

 Figure 3d - Temperature at flow front in obstacle pin cavity, mtl: J2000GP @ 37.7 cc/s 148

 Figure 4d - Temperature at flow front in obstacle pin cavity, mtl: J2000GP @ 6.3 cc/s 148

 Figure 5d - Temperature at flow front in obstacle pin cavity, mtl: CR3500 @ 37.7 cc/s..... 149

 Figure 6d - Temperature at flow front in obstacle pin cavity, mtl: CR3500 @ 6.3 cc/s..... 149

 Figure 7d - Temperature at flow front in obstacle pin cavity, mtl: CR4500 @ 37.7 cc/s..... 150

 Figure 8d - Temperature at flow front in obstacle pin cavity, mtl: CR4500 @ 6.3 cc/s..... 150

 Figure 9d - Temperature at flow front in 2 mm parallel rib cavity, mtl: CR3500 @ 37.7 cc/s 151

 Figure 10d - Temperature at flow front in 2 mm parallel rib cavity, mtl: CR4500 @ 37.7 cc/s 151

 Figure 11d - Temperature at flow front in 2 mm parallel rib cavity, mtl: J2000GP @ 37.7 cc/s 152

 Figure 12d - Temperature at flow front in 2 mm parallel rib cavity, mtl: J700GP @ 37.7 cc/s 152

 Figure 13d - Temperature at flow front in 2 mm parallel rib cavity, mtl: CR3500 @ 6.3 cc/s 153

 Figure 14d - Temperature at flow front in 2 mm parallel rib cavity, mtl: CR4500 @ 6.3 cc/s 153

 Figure 15d - Temperature at flow front in 2 mm parallel rib cavity, mtl: J700GP @ 6.3 cc/s..... 154

 Figure 16d - Temperature at flow front in 2 mm parallel rib cavity, mtl: J2000GP @ 6.3 cc/s 154

 Figure 17d - Temperature at flow front in 2 mm perpendicular rib cavity, mtl: CR3500 @ 18.8 cc/s 155

Figure 18d - Temperature at flow front in 2 mm perpendicular rib cavity, mtl: CR3500 @ 6.3 cc/s	155
Figure 19d - Temperature at flow front in 2 mm perpendicular rib cavity, mtl: CR4500 @ 18.8 cc/s	156
Figure 20d - Temperature at flow front in 2 mm perpendicular rib cavity, mtl: CR4500 @ 6.3 cc/s	156
Figure 21d - Temperature at flow front in 2 mm perpendicular rib cavity, mtl: J700GP @ 18.8 cc/s	157
Figure 22d - Temperature at flow front in 2 mm perpendicular rib cavity, mtl: J700GP @ 6.3 cc/s	157
Figure 23d - Temperature at flow front in 2 mm perpendicular rib cavity, mtl: J2000GP @ 18.8 cc/s	158
Figure 24d - Temperature at flow front in 2 mm perpendicular rib cavity, mtl: J2000GP @ 6.3 cc/s	158
Figure 25d - Temperature at flow front in 4 mm parallel rib cavity, mtl: CR3500 @ 37.7 cc/s	159
Figure 26d - Temperature at flow front in 4 mm parallel rib cavity, mtl: CR3500 @ 6.3 cc/s	159
Figure 27d - Temperature at flow front in 4 mm parallel rib cavity, mtl: CR4500 @ 37.7 cc/s	160
Figure 28d - Temperature at flow front in 4 mm parallel rib cavity, mtl: CR4500 @ 6.3 cc/s	160
Figure 29d - Temperature at flow front in 4 mm parallel rib cavity, mtl: J700GP @ 37.7 cc/s	161
Figure 30d - Temperature at flow front in 4 mm parallel rib cavity, mtl: J700GP @ 6.3 cc/s	161
Figure 31d - Temperature at flow front in 4 mm parallel rib cavity, mtl: J2000GP @ 37.7 cc/s	162
Figure 32d - Temperature at flow front in 4 mm parallel rib cavity, mtl: J2000GP @ 6.3 cc/s	162
Figure 33d - Temperature at flow front in 4 mm perpendicular rib cavity, mtl: CR3500 @ 18.8 cc/s	163
Figure 34d - Temperature at flow front in 4 mm perpendicular rib cavity, mtl: CR3500 @ 6.3 cc/s	163
Figure 35d - Temperature at flow front in 4 mm perpendicular rib cavity, mtl: CR4500 @ 18.8 cc/s	164
Figure 36d - Temperature at flow front in 4 mm perpendicular rib cavity, mtl: CR4500 @ 6.3 cc/s	164
Figure 37d - Temperature at flow front in 4 mm perpendicular rib cavity, mtl: J700GP @ 18.8 cc/s	165

Figure 38d - Temperature at flow front in 4 mm perpendicular rib cavity, mtl: J700GP @ 6.3 cc/s	165
Figure 39d - Temperature at flow front in 4 mm perpendicular rib cavity, mtl: J2000GP @ 18.8 cc/s	166
Figure 40d - Temperature at flow front in 4 mm perpendicular rib cavity, mtl: J2000GP @ 6.3 cc/s	166
Appendix E – Engineering Drawings of Cavities.....	167
Figure 1e – Engineering Drawing of Obstacle Pin Cavity	167
Figure 2e – Engineering Drawing of 2 mm Parallel Rib Cavity.....	167
Figure 3e – Engineering Drawing of 4 mm Parallel Rib Cavity.....	168
Figure 4e – Engineering Drawing of 2 mm Perpendicular Rib Cavity.....	168
Figure 5e – Engineering Drawing of 4 mm Perpendicular Rib Cavity.....	169
Biographical Sketch of Author	170

I. Introduction

A remarkable development in the injection molding process is the application of computer simulation to part and mold design, material selection, and process control. Before computer simulation became available, the large number of interactive process variables limited the molding engineer's ability to predict accurately the outcome of a particular set of design parameters, material selections, and processing conditions. Furthermore, many engineers are not aware of the limitations of plastics that are imposed by inappropriate design and processing. The results were often poor performance, over-design, high costs, and missed project milestones. In today's competitive climate, these approaches have become increasingly inadequate and inefficient when applied to the molding of larger, more complex, more precise, and costlier parts, to the processing of new materials, or to emerging processes. It is a misconception to think that OEM designers are performing mold filling simulations all the time. In most instances, the designers focus on components, not on tools. It is most often the toolmaker or molder who puts in runner systems and gates and sizes for shrinkage. If these considerations were part of the initial design, production problems would be greatly reduced.

In these days, more and more commercial products are made of plastics. There are two major reasons. The first reason is the useful inherent property of plastics materials, such as lightness, cheapness, toughness, chemical resistance, etc. The second reason is the simplicity, flexibility, and speed of the shaping operations into useful objects. Injection molding is one of the major processes for plastics forming. Injection molding has good features for mass production of complicated parts, such as automated process, high degree of dimensional accuracy, and good reproducibility of production. Now injection molding has an increasing

global market for industrial parts, such as automobile parts, medical devices, computer data storage compact disk (CD), digital video disk (DVD), optical lenses, and others.

Traditionally, in injection molding, engineers use trial-and-error method to figure out the optimal molding conditions. However, it is very time consuming and costly to perform this trial-and-error method. To make the parts more cost effective, we need to seek a more efficient way to do this work. CAE (Computer Aided Engineering) is a very useful and common tool used in industry to substitute the traditional trial-and-error method.

CAE is a technology using computer software to simulate and analyze the complicated process. Injection Molding CAE can simulate the molding filling/packing/cooling processes without doing any molding trial. The simulation results provide valuable graphical information such as filling pattern, cavity temperature, cavity pressure, shear stress, mold outside temperature distribution, etc. From these results, engineers can predict some possible problems, such as weld line location, flow problem, air trap position, etc. Accordingly, the cost in mold design can be optimized and the time-to-market can be minimized as well. Injection Molding CAE is yet to be perfected. The CAE system is required to be more user friendly, that is simpler and easier to use, shorter simulation time, more seamless integration with CAD software, improved accuracy in simulation results, and enhanced material data/database.

Review of Basic Injection Molding

In this thesis, the fundamental knowledge of injection molding is reviewed below:

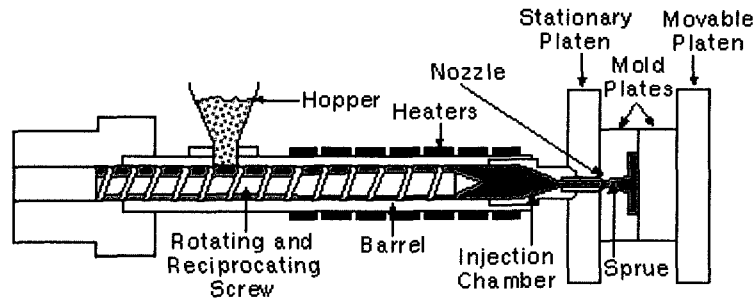


Figure 1. A single screw injection-molding machine

The injection system consists of a hopper, a reciprocating screw and barrel assembly, and an injection nozzle as seen in figure 1 above. This system confines and transports the plastics as it progresses through the feeding, compressing, degassing, melting, injection, and packing/cooling stages.

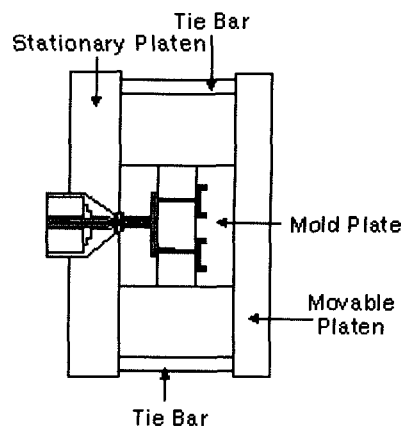


Figure 2. A typical molding system

A mold is a tool used for shaping a plastics product. It is the most important part of a molding machine. The mold is an arrangement, in one assembly, of one/some vacant cavity

spaces built to the shape of the desired product, with the purpose of producing large numbers of plastics parts. Thus the primary purpose of the injection mold is to determine the final shape of the molded part. The mold design, construction, and cooling channel arrangement largely determine the quality of the parts and its manufacturing cost. Figure 2, above, is an example of a typical mold. Figure 3, below, shows the molded parts with the runner system still attached.

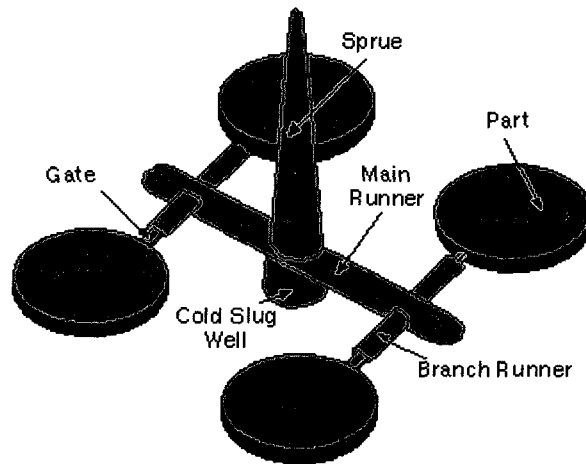
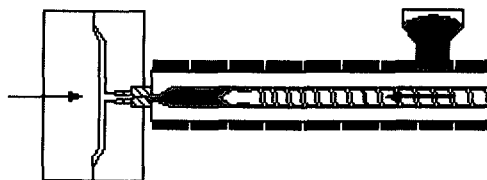


Figure 3. The molded system includes a delivery system and molded parts



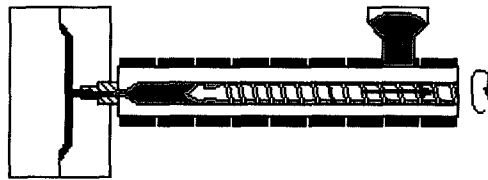
(1) Filling/Injection Phase

The plastics material is heated to a hot molten state in the injection-molding machine. The screw moves toward the runner in the mold. The nozzle is opened, and the material is injected into the cavity of the mold by the forward motion of the screw.



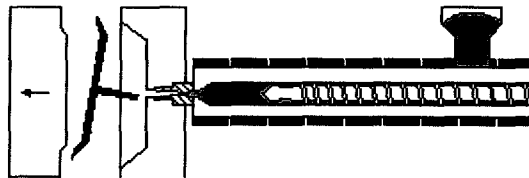
(2) Packing Phase

As soon as the material is injected in the mold, it begins to cool and solidify, because it contacts the cold mold surface. Additional material is fed into the mold by packing pressure in order to compensate for part shrinkage until the sprue has frozen.



(3) Cooling Phase

The part is then cooled in the mold. During a cooling phase, most of a dissipated thermal energy is removed by coolant in the cooling lines via a heat convection mechanism.



(4) Mold opening/Part ejection Phase

When the molded part is cool and solid enough, the mold opens and the molding is ejected from the cavity with assistance from an ejector system inside the mold. This completes a cycle and the next production cycle can begin.

Figure 4. Injection Molding Process

Injection molding is a cyclic process, consisting of the filling, packing, cooling phases. During the injection molding process, the machine undertakes a sequence of operations in a cyclic fashion. A process cycle is one complete operation of an injection-molding machine.

Basic Principles of Injection Molding CAE Simulation

1. Geometric Modeling

In traditional 2.5D CAE, the injection-molded solid object is represented by a 2.5D surface model, called mid-plan model, to perform simulation. Surface modeling or solid modeling could create this mid-plane model. The former can be performed in one of the CAE module called pre-processor, whereas using 3D CAD can do the latter. The former requires a great amount of time and effort investments in surface modeling, and the latter requires extra effort to correct the geometric error due to file transformation from solid model to surface model. On the contrary, in 3D CAE, solid element will be used in simulation. The geometric modeling can be performed in 3D CAD and then imported into 3D CAE pre-processor. Since 3D CAE is based on the true geometric shape of the injection-molded part, no geometry simplification is needed as in 2D CAE. In addition, no extra effort is required to correct the error due to file transformation as in 2D CAE.

2. Meshing

After the geometric modeling is done, the geometry model will be meshed into many partitions, called elements, in order to perform flow calculations. The meshed geometry model is called analysis model. For 2.5D CAE, a two-dimensional shell-type element is utilized, whereas 3-dimensional solid elements will be used in 3D CAE. It is noted that in 2D CAE the thickness has to be assigned in element properties, by the user.

3. Mechanical Modeling

The simulation of mold filling process for molten polymer within the mold cavity is very complex and challenging in computer modeling. The inherent difficulties include:

1. The associated non-isothermal
2. Non-Newtonian and transient fluid flow
3. Moving boundary
4. Temperature-dependent viscosity of the polymer melt
5. The irregular shape of the mold cavity.

2.5D Mathematical Formulation

During the injection filling stage, the following assumptions are adopted:

1. Molten plastics flow is incompressible ($\nabla \cdot \mathbf{v} = 0$)

2. Pseudo-steady state flow

3. Viscous flow behavior

4. Fully developed flow

5. Part is thin. No flow component in gap-wise direction and velocity gradient is only considered in gap-wise direction (z-direction)

6. Molten plastics flow behaves as generalized Newtonian flow

7. Neglect of conventional heat transfer

8. 1-dimensional heat conduction

Based on these assumptions, the governing equations of the filling process are governed by:

Continuity Equation

$$\frac{\partial v_x}{\partial x} + \frac{\partial v_y}{\partial y} = 0 \quad (1)$$

Momentum Equation

x-component

$$\frac{\partial P}{\partial x} = \frac{\partial^2 v_x}{\partial z^2} \quad (2)$$

y-component

$$\frac{\partial P}{\partial y} = \frac{\partial^2 v_y}{\partial z^2} \quad (3)$$

Energy Equation

$$\rho C_p \frac{\partial T}{\partial t} = \kappa \left(\frac{\partial^2 T}{\partial k^2} \right) + \mu \dot{\gamma}^2 \quad (4)$$

3D Mathematical Formulation

During the injection filling stage, the following assumptions are adopted:

1. Molten plastics flow is incompressible
2. Pseudo-steady state
3. Viscous flow behavior
4. Fully developed flow
5. Molten plastics flow behaves as generalized Newtonian flow
6. Neglect of conventional heat transfer
7. 3-dimensional heat conduction

Based on these assumptions, the governing equations of the filling process are by

Continuity Equation

$$\frac{\partial v_x}{\partial x} + \frac{\partial v_y}{\partial y} + \frac{\partial v_z}{\partial z} = 0 \quad (5)$$

Momentum Equation

x-component

$$\frac{\partial P}{\partial x} = \frac{\partial^2 v_x}{\partial x^2} + \frac{\partial^2 v_x}{\partial y^2} + \frac{\partial^2 v_x}{\partial z^2} \quad (6)$$

y-component

$$\frac{\partial P}{\partial y} = \frac{\partial^2 v_y}{\partial x^2} + \frac{\partial^2 v_y}{\partial y^2} + \frac{\partial^2 v_y}{\partial z^2} \quad (7)$$

z-component

$$\frac{\partial P}{\partial z} = \frac{\partial^2 v_z}{\partial x^2} + \frac{\partial^2 v_z}{\partial y^2} + \frac{\partial^2 v_z}{\partial z^2} \quad (8)$$

Energy Equation

$$\rho C_p \frac{\partial T}{\partial t} = \kappa \left(\frac{\partial^2 T}{\partial x^2} + \frac{\partial^2 T}{\partial y^2} + \frac{\partial^2 T}{\partial z^2} \right) + \mu \dot{\gamma}^2 \quad (9)$$

Where properties ρ , μ , C_p and κ are density, viscosity, specific heat and thermal conductivity, respectively. Vector V_i denotes velocity. Scalar P and T stand for pressure and temperature, respectively. Note that shear rate $\dot{\gamma}$ is defined as

$$\dot{\gamma} = \sqrt{\left(\frac{\partial U}{\partial x} \right)^2 + \left(\frac{\partial U}{\partial y} \right)^2} \quad (10)$$

During the post-filling, the governing equation and the associated assumptions still hold, except the assumption of incompressible flow in filling phase is no longer valid in post-filling stage. We must include the compressibility into the governing equations. That is,

$\nabla \cdot \mathbf{v} = 0$ is not valid.

$$\frac{\partial \rho}{\partial t} + \left(\nabla \cdot \rho \vec{v} \right) = 0 \tag{11}$$

Precise experimental data such as cavity filling patterns, temperature, pressure profiles, etc. are important for the verification of numerical simulation results. Murataa & Yokoi[1] have been conducting a research project on CAE benchmarking, aiming to construct a database on melt filling patterns, melt temperatures, and pressure distributions for CAE verification benchmark tests on injection molding. In their experiments, they visualized melt filling behaviors inside rib shape cavities, step-change cavities, and obstacle-pin cavities with tapered thickness using a three-dimensional (3-D) glass-inserted mold. They also measured melt temperature distributions along the thickness direction using an integrated thermocouple sensor they developed under many different molding conditions. The database includes all of these important data in addition to material data generally required for numerical simulation.

In this thesis, Moldflow™ CAE software will be validated using:

1. The melt filling patterns

2. Melt pressure distribution

3. Melt temperature distribution along the cavity thickness

Inside an obstacle-pin cavity with tapered thickness and cavities with various rib patterns from the database constructed.

II. Literature review

The continued improvement of the Injection molding process drives injection molding CAE software manufacturers to continually improve their softwares as well. This drives research which both promotes improvement and provides data to validate the assessments. In this Literature review a research papers will be reviewed for the research that has been done which is relevant to this thesis. The paper will be used to support and show contrast to the conclusions of this thesis.

In a research paper by Gelotte and Broadbent [2007] two parameters guided their study: flow patterns and injection pressures of actual molded parts and molding simulation software predictions. In this study the short shot method was used for the “actual” flow pattern and machine readout was used for the actual injection pressure. The short shot method is when a percentage of the amount of material necessary to fill the mold is injected and cooled to show how the mold will fill at 10%, 20%, 50%, etc. This method is widely used because of how easy it is to perform, however it does not simulate a true molding environment and therefore is not entirely accurate. However this study did find a way to increase the accuracy of the injection pressure prediction of the software by manipulating the Heat Transfer Coefficient (HTC). By adjusting the HTC value in the software Gelotte et al. were able to increase the accuracy of the injection pressure predictor to within 29.5% of the actual molding pressure. This is an improvement over the 40% difference seen in this thesis without adjusting the HTC. As for the results of the short shot method vs. Moldflow™ the same differences that have been observed in this thesis are seen here. The Moldflow™ “simplifies” the shape of the flow front, when in reality the flow reacts very sensitively to the differences in the cavity geometry. For example in figure 2 of the research paper at 24.98% filled the short shot shows that when the melt front

reached the top edge of the part it “race tracked” for approximately half the length of the part leaving the rest of the part barely filled. In contrast the Moldflow™ simulated fill at 24.98% shows that the flow front splits flow fronts which are moving through the part at an even pace. At 50% these observations are still valid: the short shot now has two “race tracks” top and bottom, and the Moldflow™ simulation is practically flat across with only a slight “race track” near the top edge.

The research done by Gellote et al. [2007] shows how CAE injection molding softwares can improve with just a little research in the right areas.

III. Methodology

Since this thesis was only looking at the accuracy of the CAE software Moldflow™ MPI the procedure that was followed, in molding the parts and record the data that was used in this thesis will not be included. The procedure used to gather the data that is used in this study is cited in either *Database for Validation of Numerical Simulation Results in Melt Filling Process* by Murata and Yokoi, or *Visualization Analysis of Flow Front Behavior During Filling Process of Injection Mold Cavity by Two Axis Tracking System* by Yokoi, Masuda and Mitsuhashi.

To run the simulations:

1. The five parts being examined were first modeled in SolidWorks™ without the runner system
2. The models were then saved as .stl files, and then imported into MPI.
3. The models were meshed using a mid plane mesh because the parts are very simple geometries that can be simulated well with this type of mesh. A global edge length of 1mm was used to get a mesh that was fine enough to show a smooth flow front, but not so fine that it took too long to run.
4. The runner system was created using beams, the runner was given one element per mm length.
5. The next step was to set the material and process settings.
6. For the process settings, the injection rate controlled was used and set to 6.3 cm³/s, 18.8 cm³/s, or 37.7 cm³/s depending upon which study was being evaluated.
7. The four materials that were used for this experiment are two PPs by Idemitsu Petrochemical Co., Ltd - grades J-2000GP (low viscosity) and J-700GP (high viscosity)

and two GPPSs by Dainippon Ink and Chemical, Inc. grades - CR-3500 (low viscosity) and CR-4500 (high viscosity).

8. The rest of the settings, such as melt temperature etc., were left at the MPI default setting.

9. Then the simulations were run.

The simulations took between two and 15 minutes, depending upon the study and if multiple simulations were running at the same time.

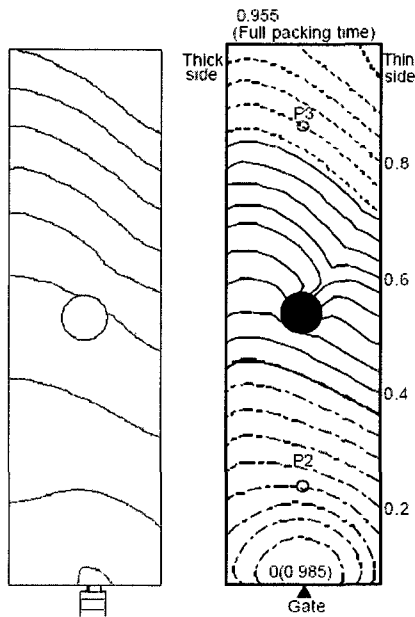
IV. RESULTS and DISCUSSION

The data from the Moldflow™ simulations appear in the Appendices.

Analysis of Flow path and Fill time

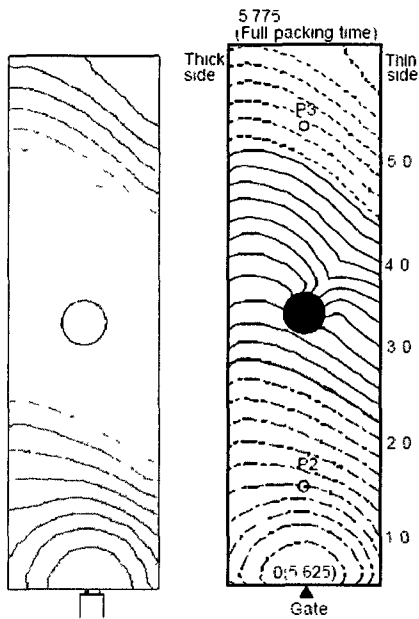
When comparing the pictures of the fill pattern generated by the Moldflow™ simulation to the sketches generated with the experimental data it was clear that the simulation became more accurate the further it was away from the gate. The only area in all of the forty comparisons that was significantly different was the fill pattern just past the gate, (Figures 4a and 49a). The experimental sketch was more arced than in the simulation. That is, the simulation represented the forward and transverse flow close in velocity, and the experiment showed the forward velocity was higher than the transverse velocity. Also the fill time comparison was very accurate; the Moldflow™ simulations averaged 7.59% lower than the experimental data with a 1.38% standard deviation.

Comparison 1 is a side by side contrasting of all of the available flow pattern figures from the research done by Yokoi, Masuda and Mitsuata and the Moldflow™ simulations. In all of these comparisons the image(s) on the left are from Moldflow™ simulations and the experimental data is on the right. In the Moldflow™ images the contours were all set to the maximum of 100.



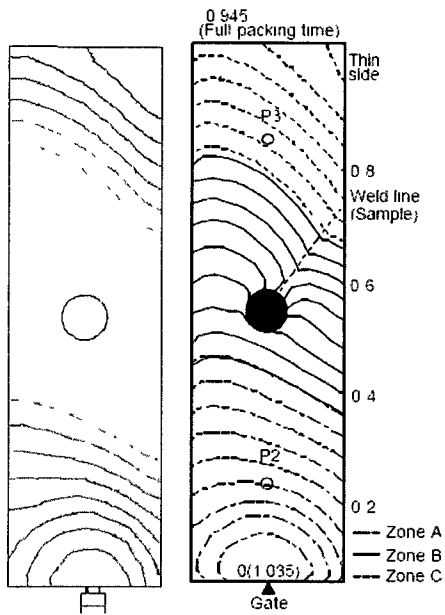
Comparison 1 – Obstacle Pin Cavity, J-2000GP at 37.7 cc/s

In this comparison it is clear that in the Moldflow™ simulation (left) that the speed of the flow front was moving faster in the longitudinal direction and slightly more slowly in the transverse direction, but in the experimental data (right) the flow was slightly faster in the longitudinal direction. This could be due to momentum exhibited by the actual flow front not accounted for by the assumptions, in the Moldflow™ software, that the polymer exhibited a perfect fountain flow. Also in this comparison it becomes clear that for future analysis it would be more accurate to have the contour setting in Moldflow™ be adjustable by time increments.

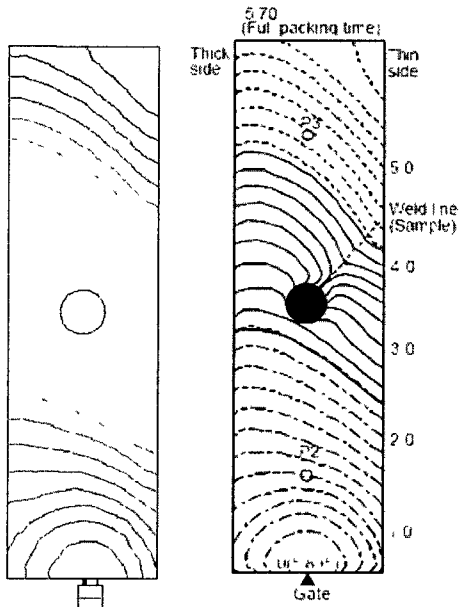


Comparison 2 – Obstacle Pin Cavity, J-2000GP at 6.3 cc/s

Now it is clear that the assumption of fountain flow was not perfect; the flow front moves longitudinally slightly faster than transverse. Also on the left side of the cavity, in the experimental image, the flow was slowed by the wall and created an arc. That happens to a much lesser extent in the Moldflow™ image and in some contours did not occur at all. Lastly, in the experimental image, the area just to the right and past the obstacle pin showed two distinct flow fronts that eventually merged to form one flow front, that is not the case in the Moldflow™ simulation, the flow fronts merge almost immediately after the obstacle pin indicating a much smaller weld line which could influence a designer to disregard a possible weak point. In reality the weld line will be larger and weaker and might cause a failure.



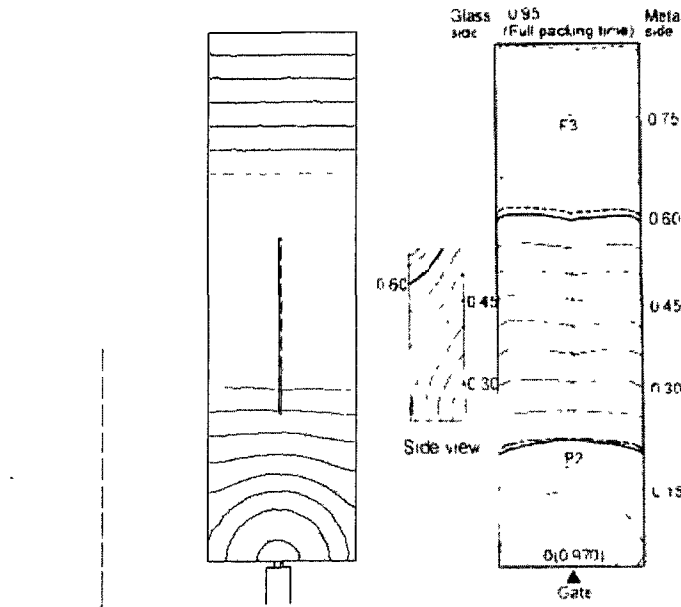
Comparison 3 – Obstacle Pin Cavity, CR-3500 at 37.7 cc/s



Comparison 4 – Obstacle Pin Cavity, CR-3500 at 6.3 cc/s

In Comparisons 3 and 4 there are further examples of what was explained in comparisons 1 and 2. In short, at the gate the flow was not a perfect fountain the longitudinal speed was faster than the transverse speed, two flow front existed after the obstacle pin for a longer period of time

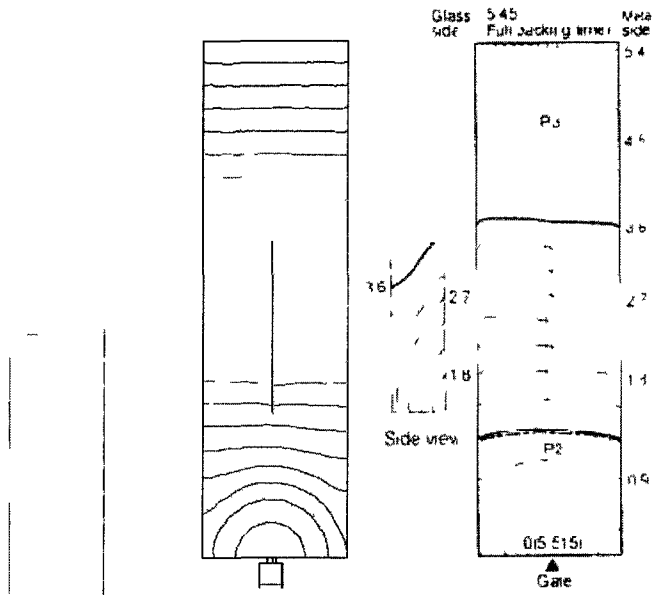
than Moldflow™ showed, and the resistance by the left wall of the cavity created another small flow front on the left side of the part.



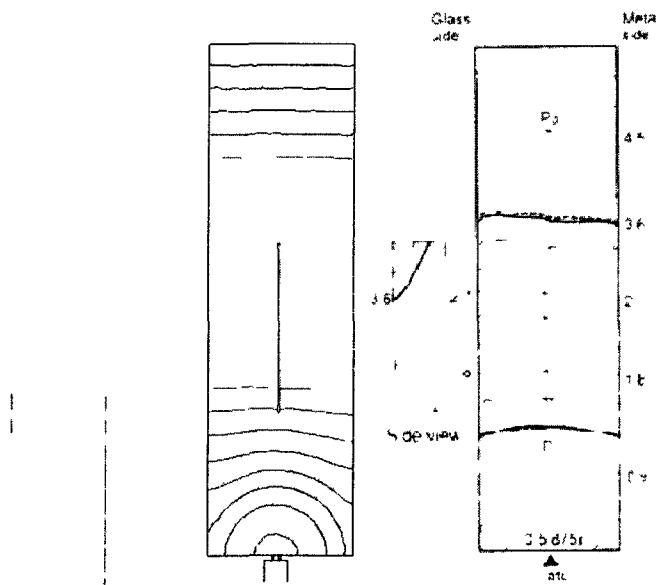
Comparison 5 – 2 mm Parallel Rib Cavity, J-2000GP at 37.7 cc/s

The cavities with 2 mm ribs running parallel to the flow showed some of the same differences as the obstacle pin cavity. First, the resistance from both the left and right walls created small arcs in the flow front, in the experimental image, which did not appear in the Moldflow™ image. Also, the effect of the rib on the flow front after the rib was not seen in the Moldflow™ image like it was in the experimental image. In the experimental image the flow front, from mid-way through the rib to the end of the cavity, looked like an “m” with two distinct flow fronts. In the Moldflow™ image the flow front at the rib looks like a “v”, and was completely flat across after the rib. Also, the observation about the longitudinal speed being higher than the transverse speed from the obstacle pin cavity seemed to be holding true to all the simulations in all cavity types. This observation was further confirmed in the side view, in the experimental image the flow front arched so the flow front hit the top of the rib before filling the

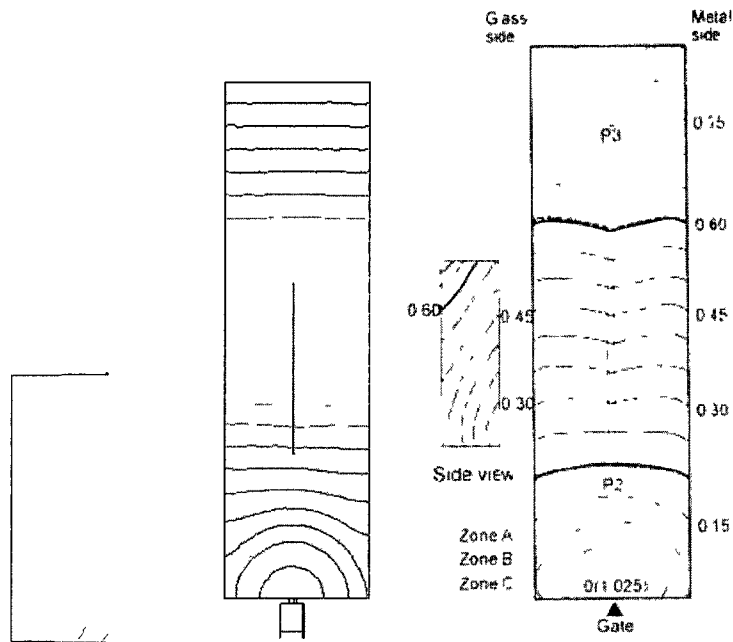
near corner. In the Moldflow™ image the contours showed that the polymer flowed up the near wall of the rib filling the corner first.



Comparison 6 – 2 mm Parallel Rib Cavity, J-2000GP at 6.3 cc/s



Comparison 7 – 2 mm Parallel Rib Cavity, CR-3500 at 37.7 cc/s

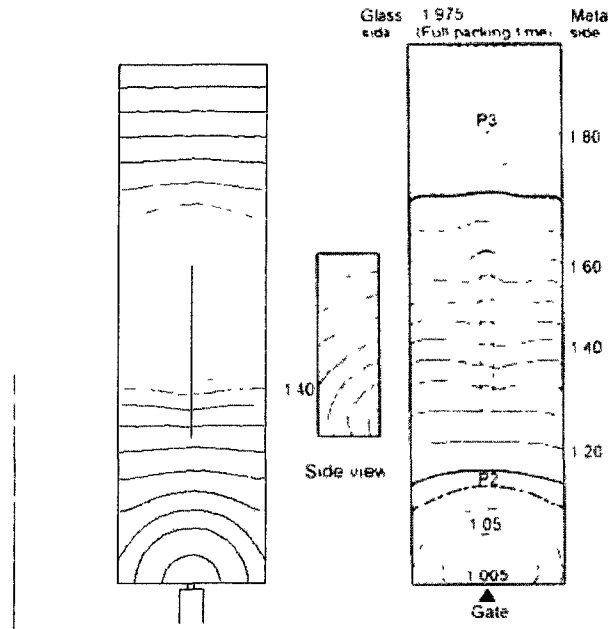


Comparison 8 – 2 mm Parallel Rib Cavity, CR-3500 at 6.3 cc/s

Comparisons 6, 7, and 8 all showed the same differences that were seen in comparison 5.

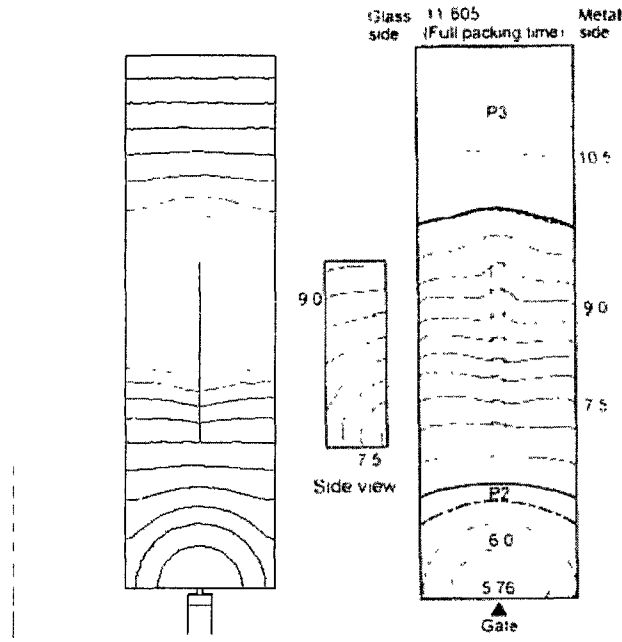
Those differences were;

1. Faster longitudinal flow than transverse flow
2. “M” shape flow from the rib to the end of fill in the experimental image
3. “V” shape flow in the rib section of the Moldflow™ image
4. A flat flow front at the end of fill in the Moldflow™ image.

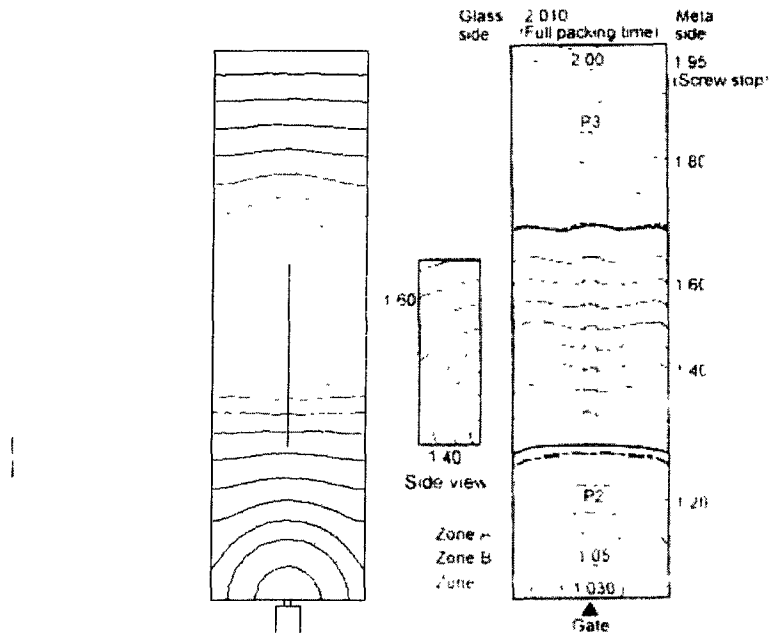


Comparison 9 – 4 mm Parallel Rib Cavity, J-2000GP at 37.7 cc/s

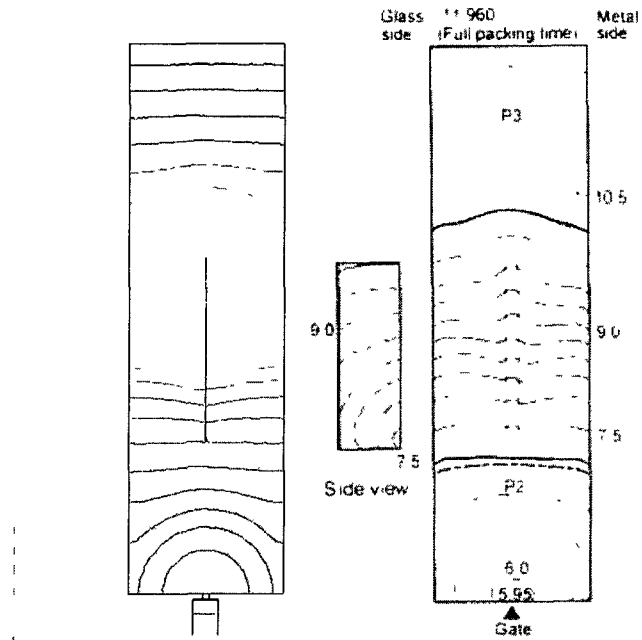
In the comparisons of cavities with a 4 mm thick rib parallel to flow a much different flow pattern than in the cavities with a 2 mm thick rib parallel to flow was observed. First, in the experimental image, the flow from the start of the rib to the end of fill had three fronts, with the middle front being the fastest, after the rib the middle front became wider and by the end of fill only the two side fronts existed. In the Moldflow™ image the flow had the shape of an arrow, with only one front which, after the rib ends, quickly faded to a flat flow front. As in the other cavities longitudinal speed of the flow front was faster than the transverse speed. One possible explanation why there was only the one flow front in the Moldflow™ image was because the simulation was only affected by the rib and not the resistance of the cavity wall that created fronts on either side of the rib.



Comparison 10 – 4 mm Parallel Rib Cavity, J-2000GP at 6.3 cc/s

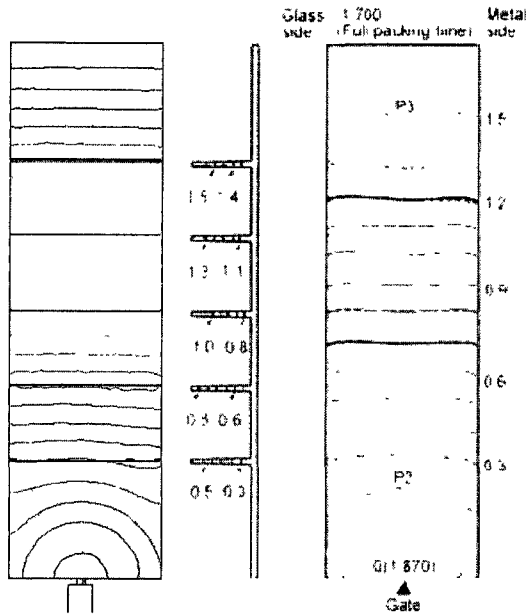


Comparison 11 – 4 mm Parallel Rib Cavity, CR-3500 at 37.7 cc/s



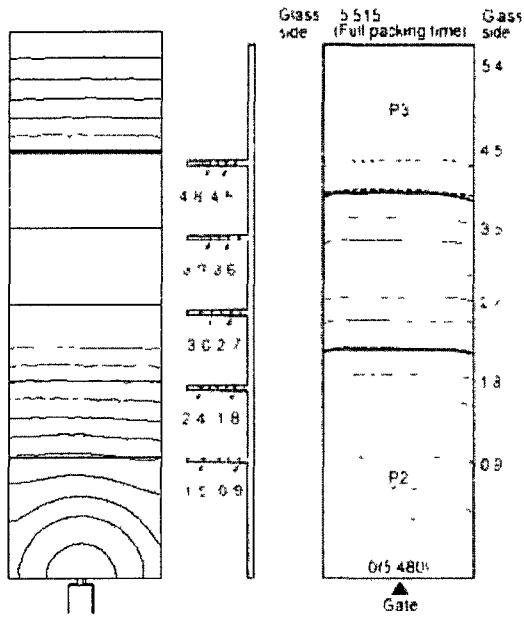
Comparison 12 – 4 mm Parallel Rib Cavity, CR-3500 at 6.3 cc/s

In comparisons 10, 11, and 12 the same differences were observed in comparison 9. In short, Moldflow™ showed one flow front in the rib area becoming one after the rib ended while the experimental image showed three fronts in the rib becoming two after the end of the rib at the high injection rate and one at the low injection rate, and the longitudinal flow speed was slightly higher than the transverse which was not shown by Moldflow™. An additional observation was that Moldflow™ showed, like in the experimental image, that the flow front slowed down significantly in the area with the rib. Also the flow front at the end of fill was more accurate in the Moldflow™ image when the injection rate was slow.

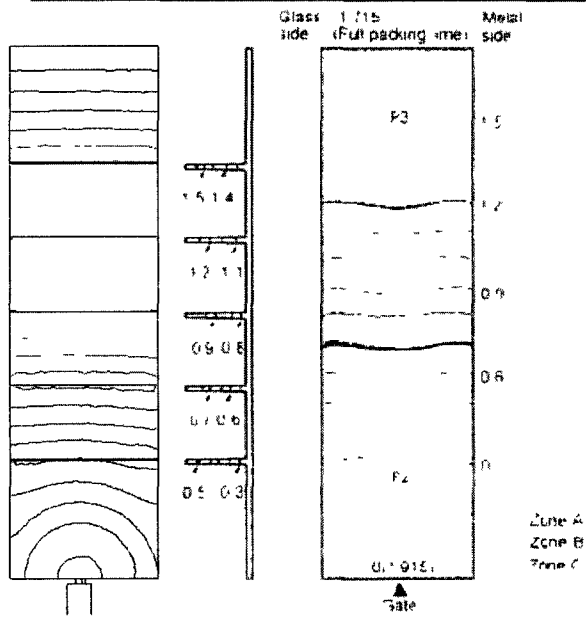


Comparison 13 – 2 mm Perpendicular Rib Cavity, J-2000GP at 18.8 cc/s

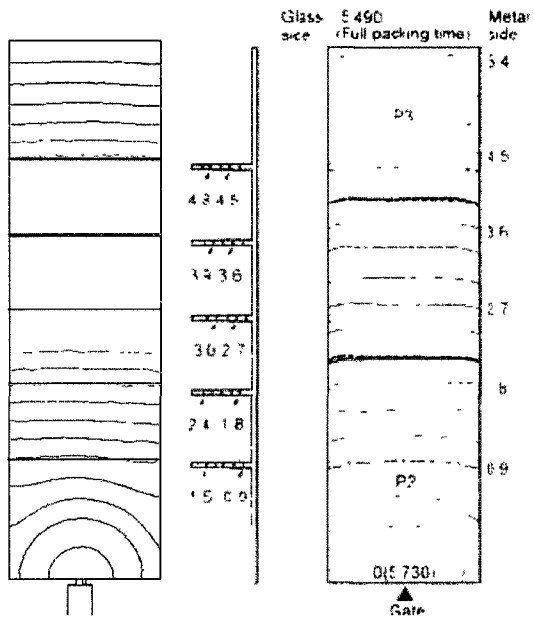
In the cavities with 2 mm ribs perpendicular to flow the Moldflow™ simulation was very close to the experimental image. The only differences were that, as in all of the cavities thus far, the longitudinal flow speed was faster than the transverse speed and the flow front in the experimental image had a slight “m” shape while the Moldflow™ image showed a flat flow front.



Comparison 14 – 2 mm Perpendicular Rib Cavity, J-2000GP at 6.3 cc/s

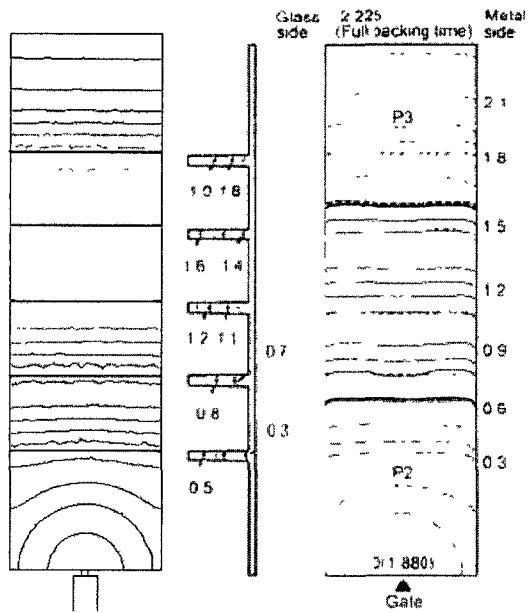


Comparison 15 – 2 mm Perpendicular Rib Cavity, CR-2500 at 18.8 cc/s



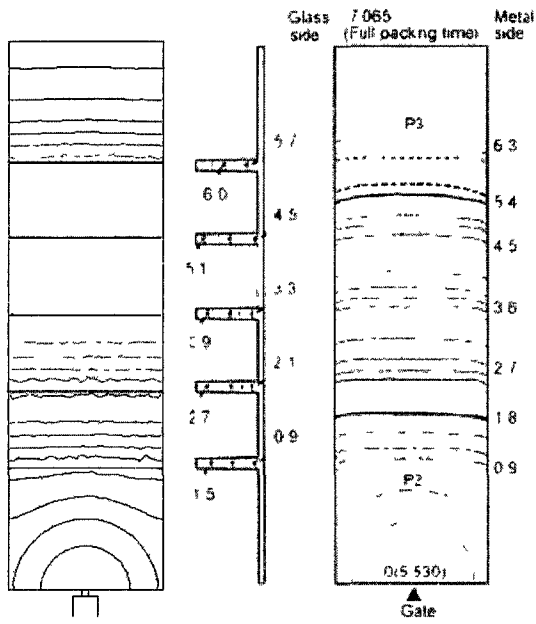
Comparison 16 – 2 mm Perpendicular Rib Cavity, CR-2500 at 6.3 cc/s

In comparisons 14, 15, and 16 the differences are the same as in comparison 13. One additional observation is that Moldflow™ showed a good representation of the flow front slowing down and speeding up as it passed and filled the ribs.

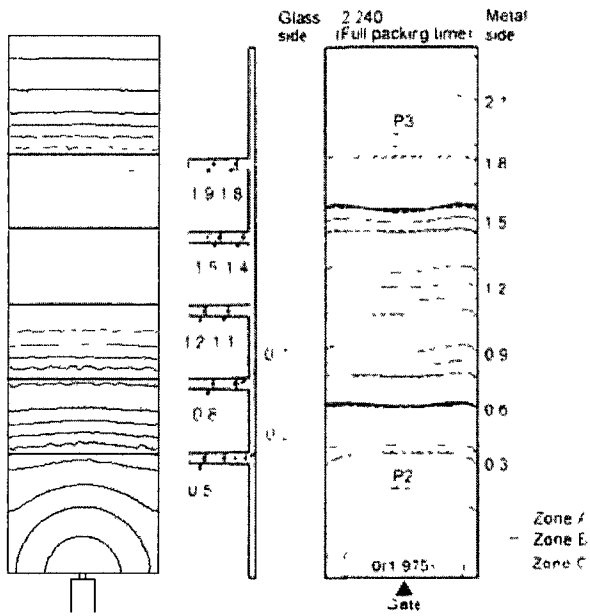


Comparison 17 – 4 mm Perpendicular Rib Cavity, J-2000GP at 18.8 cc/s

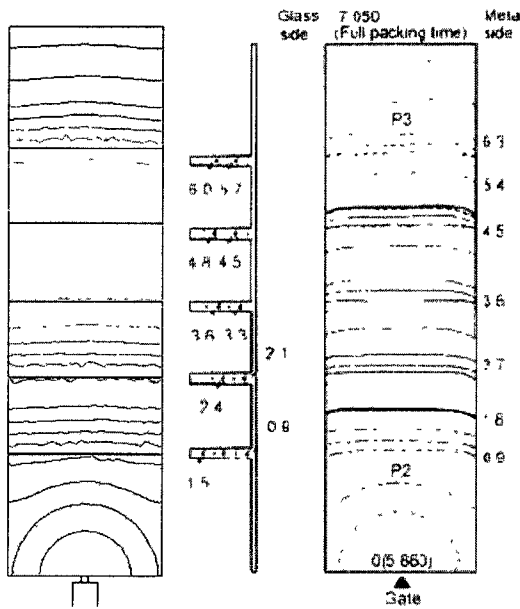
The differences between Moldflow™ and experimental images in the cavities with 4 mm ribs perpendicular to flow are the same as in the cavities with 2 mm ribs perpendicular to flow except the slowing and surging of the flow front due to the ribs was much more significant than in the cavities with 2 mm ribs perpendicular to flow. The thickness of the base was only 2 mm; so when the front reached a rib there was three times the area to fill as before the rib, causing the significant fluctuations in flow front speed.



Comparison 18 – 4 mm Perpendicular Rib Cavity, J-2000GP at 6.3 cc/s



Comparison 19 – 4 mm Perpendicular Rib Cavity, CR-2500 at 18.8 cc/s

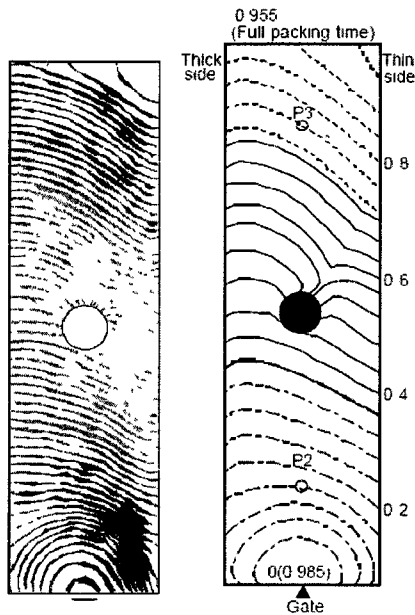


Comparison 20 – 4 mm Perpendicular Rib Cavity, CR-2500 at 6.3 cc/s

The differences among comparisons 18, 19 and 20 were the same as comparison 17.

Also, as in all of the other comparisons, Moldflow™ did not show that the longitudinal speed of the flow front was slightly faster than the transverse speed as in the experimental images.

It became a concern that these evaluations were not accurate because of the assumptions made by the software while using a mid-plane mesh type. It is generally assumed that when using a mid-plane mesh that the friction due to the side walls is negligible due to the small surface area in comparison to the top and bottom surfaces. Therefore the friction on the walls is considered to be zero. In order to disprove that this assumption was the cause of the results that have been seen throughout these past twenty comparisons one 3D mesh was made to verify the flow patterns in the mid-plane meshed analyses. Below is a side by side comparison of the 3D meshed Moldflow™ analysis and the experimental data.



Comparison 21 – 3D meshed Obstacle Pin Cavity, J-2000GP at 37.7 cc/s

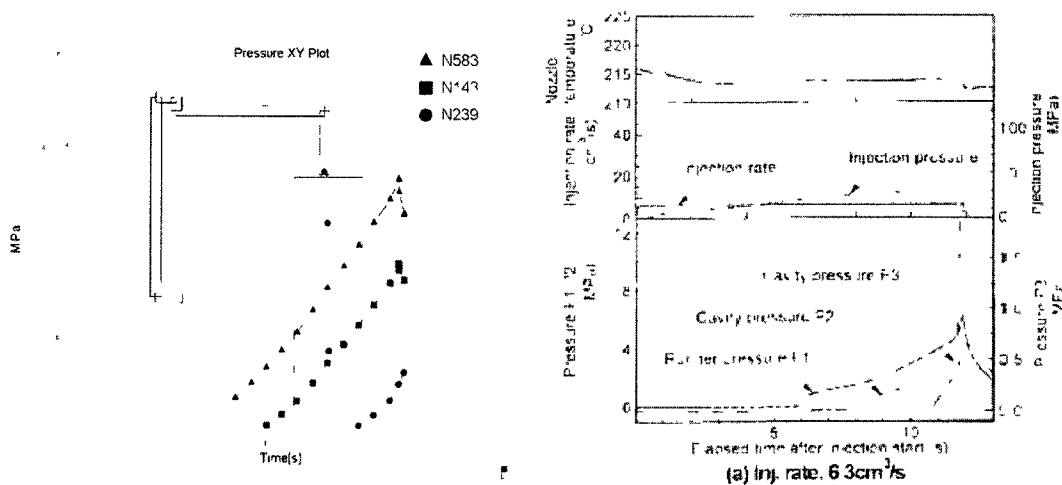
The 3D meshed analysis eliminates any concerns that the mesh type is affecting the results of the rest of the study. It is clear in this comparison that the 3D mesh type shows that the plastic flow will be equal in the transverse and longitudinal directions, which is disproven by the experimental data.

Analysis of Peak Injection Pressure

After conducting a comparison of the data generated by the Moldflow™ simulation to the experimental data it was clear that the simulated data was just that, simulated. The simulated peak injection pressure, on average, was almost 40% lower than the experimental data with approximately a 9% standard deviation. This could be because of a countless number of variances that could have been occurring during the experiment that the simulation does not account for. However, even though the simulation could be looked at by a person untrained in injection molding as inaccurate, the simulation gave an engineer considerable information about how a part will be molded before the mold is ever built.

Furthermore, the simulated injection profile at the three given locations in the experiment was difficult to compare to the Moldflow™ simulation. In Appendix C there is a chart of the injection pressures at only locations P1 and P2 in the obstacle pin cavity. P1 was the runner pressure and P2 was the pressure 30mm from the edge of the part. The data showed that the simulated pressures at the given locations, on average, were only approximately 4% varied from the experimental data. However, the standard deviation of the percent difference was over 14%, indicating that the simulation was not extremely accurate and once again can only be used to get an idea of what will occur while molding. The simulation could not to be taken as an exact representation of what will occur. Also, the data used to calculate these differences were extrapolated from the graphs, which added a degree of error.

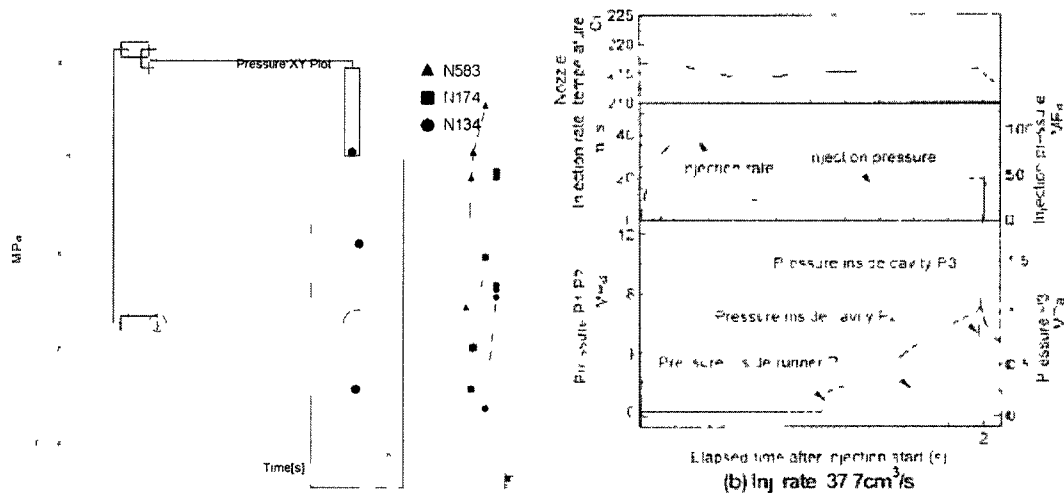
Below is a side-by-side comparison of four pressure profiles from the experimental data in three different cavities, with two materials, and three injection rates.



Comparison 22 – Obstacle Pin cavity, mtl: J-2000GP

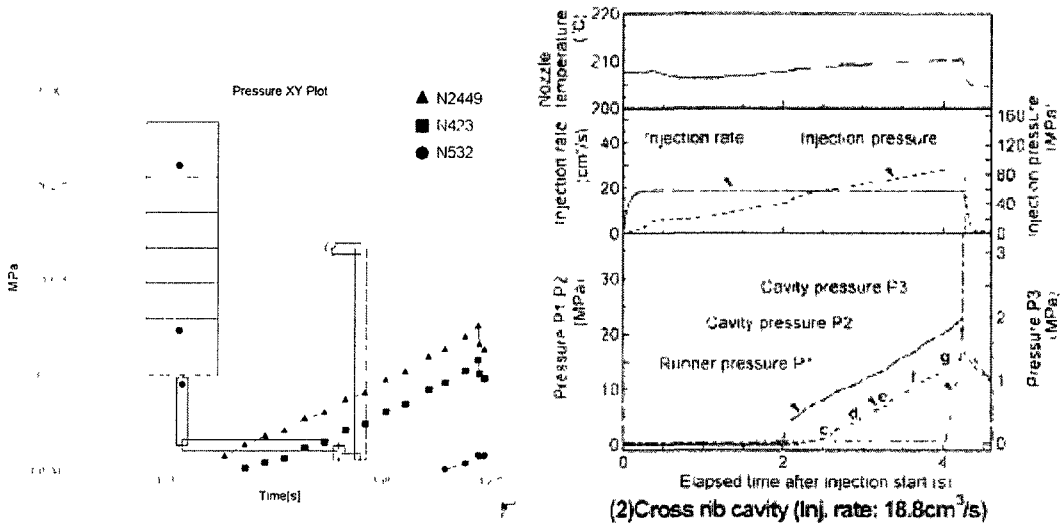
In this side-by-side comparison it is clear that the Moldflow™ simulation was similar, however not very accurate. The peak of P1 was approximately 8.9 MPa in the Moldflow™ simulation and only 7.25 MPa in the experimental data. The peak of P2 in the simulation is

approximately 5.8 MPa and only 4.5 MPa in the experimental data. One reason for the major difference in the appearance of P3 is due to the different scale that P3 followed on the graph of the experimental data. In the graph generated by Moldflow™ the P3 was at the same scale as P1 and P2 therefore it appears to be much different than in the Moldflow™ simulation. However the picture was much clearer when looking at Figure 2b, which is the Moldflow™ generated graph at a larger scale. In Figure 2b it became clear just how inaccurate the simulation was, P1, P2, and P3 all peak around 12 MPa. All followed a nearly vertical rise around the 10th second of injection.



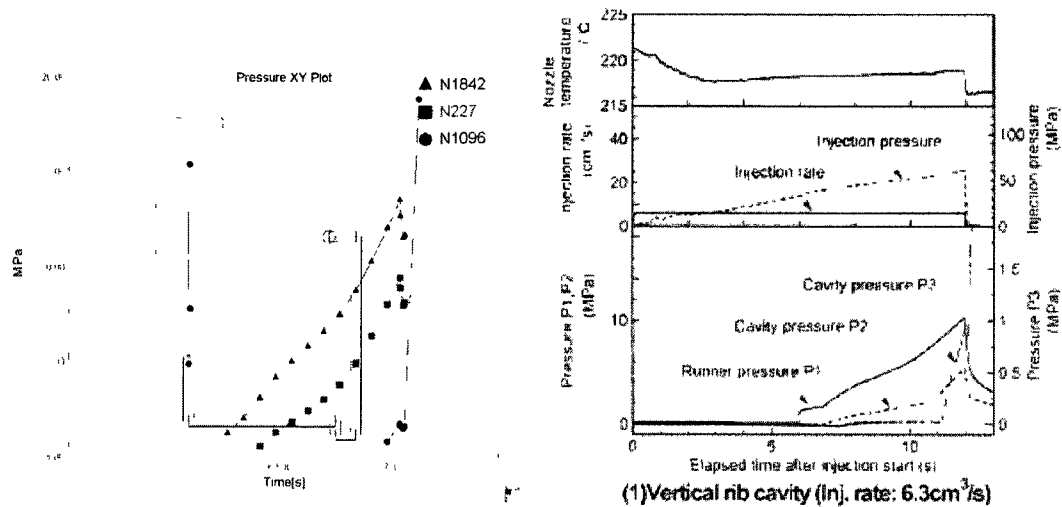
Comparison 23 – Obstacle Pin cavity, mtl: J-2000GP

Unlike the previous comparison it was immediately obvious how inaccurate this simulation was. The only, somewhat, redeeming factor to this simulation was that it agreed with the experimental data that around the 2nd second of injection the pressure at P3 would increase very rapidly. All other aspects of this simulation were inaccurate. Figure 1b showed this same simulation data at a larger scale. This figure shows that the pressure at P1, P2, and P3 all increased at roughly the same time and rate and all plateau and peak at roughly the same time and pressure. This did not agree at all with the experimental data.



Comparison 24 – 4 mm perpendicular rib cavity, mtl: CR-3500

In this comparison the simulation had a similar shape as the experiment but upon a closer look it was clear that the simulation was very inaccurate. Figure 33b showed the same simulation data at a larger scale, in the simulation we see that P1, and P2 both have only dropped momentarily and will peak much higher. Also, their initial peaks at 14MPa and 9.5 MPa, respectively, were significantly lower than the experimental data of 23 MPa and 16 MPa, respectively.



Comparison 25 – 4 mm parallel rib cavity, mtl: CR-3500

This side-by-side comparison appeared to be the closest to the experimental data, but only before taking a deeper look at the simulation. Figure 26b shows that, as in all the other comparisons, the pressure at P1, and P2 dipped and then peaks much higher than in the experimental data. Also the initial peaks of P1, and P2 in the Moldflow™ simulation were 13 MPa and 10 MPa, respectively, compared to 11 MPa and 5 MPa in the experimental data.

Another occurrence in these comparisons was that at the slow injection rates the simulation predicted a higher peak pressure than in the experiment. The higher injection rates predicted a lower peak pressure than in the experiment. Also, the time at which the pressure peaked was predicted accurately by Moldflow™ in the majority of cases. The side-by-side comparisons show the simulated data is not identical to the experimental data, but offers some insight into what will happen before the mold was ever built. This can be an enormous cost saving tool that will also help ensure high quality products every time.

V. CONCLUSIONS

In conclusion, this comparison of a Moldflow™ simulation to experimental data was a good indicator that CAE software was used by Engineers to gain knowledge about how a plastics part would mold before the mold was ever built. The results should not be taken as an exact representation of the quality of the actual molded parts. CAE software, in general, cannot include inputs for every imaginable variable that can change how the simulated action will occur. The conditions during the experiment could have been varying slightly, this could cause the high percenta difference that was seen in the peak injection pressure. The fill time, fill pattern, and pressure at given locations simulations were fairly accurate and would be very useful to a product design engineer trying to bring a part to market.

For further improvement of the mold filling simulation Moldflow™ should make it possible to create contours by time interval to make more easily comparisons with further experimental. Also, the assumption of perfect fountain flow has been disproven by the experimental data used here; this should also be taken into account in future software improvement to predict better the end of fill and possible air traps and weld lines.

CAE software is used by engineers who have been trained to know how the process being simulated is supposed to occur and who are able to decipher good simulated data from bad. CAE software is constantly improving and without a doubt future injection molding CAE software will be so able to predict accurately final products that it will become the standard to use the software before ever building a mold.

VI. RECOMMENDATIONS

Flow line comparison is very difficult because Moldflow™ uses a number of contours and the study puts a line every (x) seconds. This makes the observations only approximate and not exact. If Moldflow™ were to make it possible to create flow front lines spaced by time increments future analysis of the software accuracy would be greatly improved and help Moldflow™ to make its software as accurate as possible.

The assumption of fountain flow is not perfect; it appears that longitudinal flow is slightly faster than transverse flow due to possibly momentum or another force. This should be accounted for to ensure accurate air trap, end of fill, and weld line predictions.

VII. LITERATURE CITED

1. Y. Maekawa, M. Onishi, A. Ando, S. Matsushima and F.S. Lai, "Prediction of Birefringence in Plastics Optical Elements Using 3D CAE for Injection Molding", *Proceedings of SPIE*, Jan 24-Jan 28 2000 p 935-943 0277-786X.
2. C. -H. Chien, Y. Maekawa, H. Kishikawa, M. Onishi, and F. S. Lai, "Influence of processing condition on the formation of birefringence of optical plastics lens using 3D CAE", *ANTEC 2001*, paper number 668.
3. R. Gelotte, M. Broadbent, "Validation of Injection Molding Simulation Results to Actual Molded Product", *ANTEC 2007*, p 2470-2474
4. Y. Murata, H Yokoi, "Database for Validation of Numerical Simulation Results in Melt Filling Process"

Appendix A – Flow Patterns

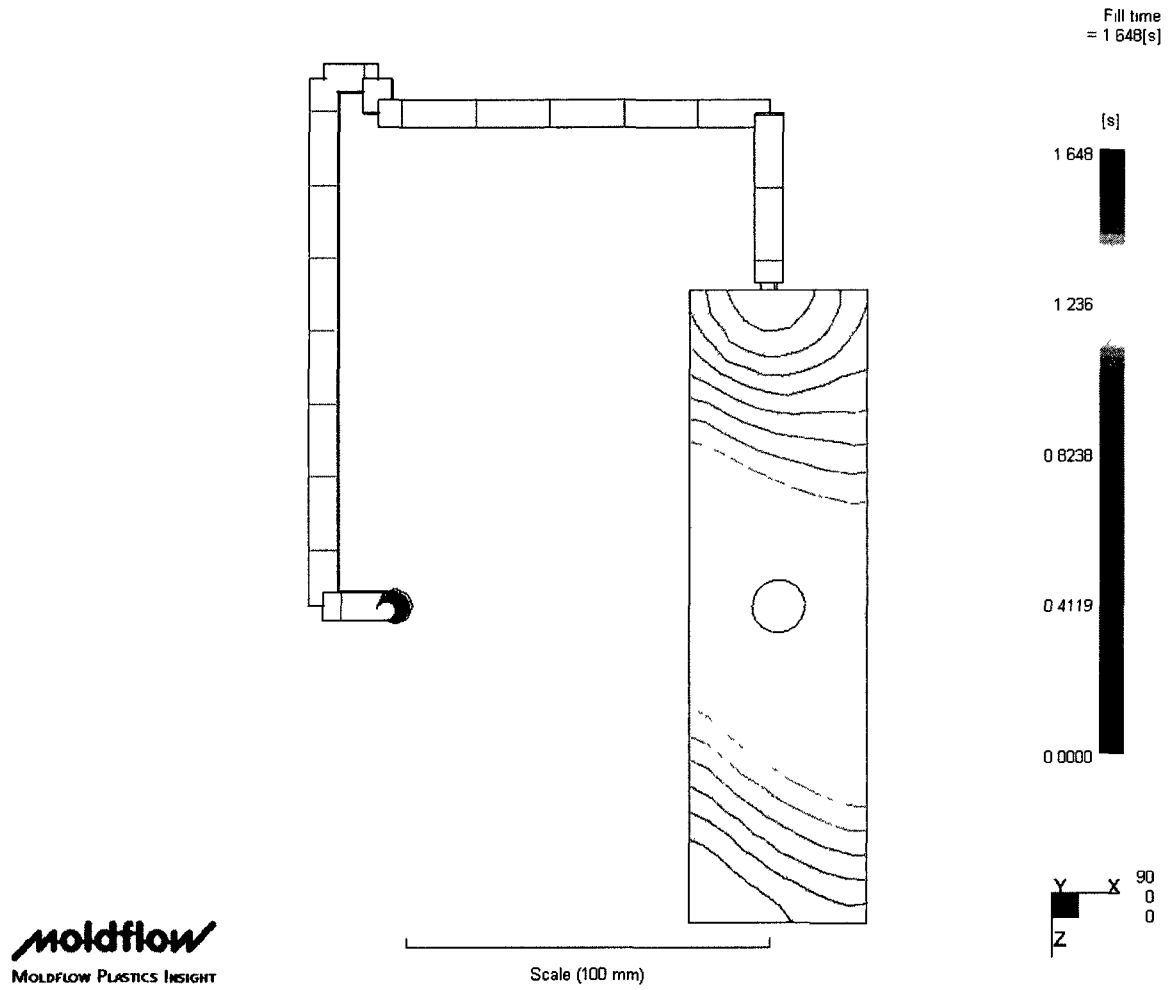


Figure 1a – Flow Front Profile in Obstacle Pin cavity, mtl: 700GP @ 37.7 cc/s injection rate

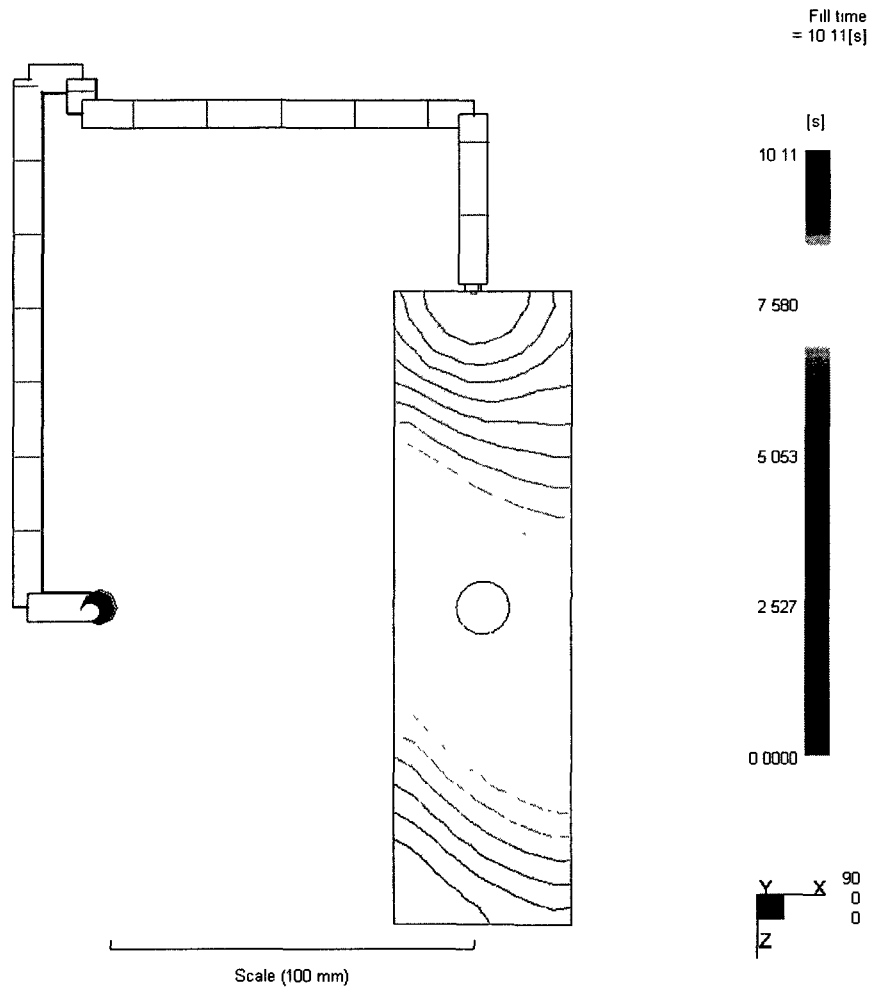
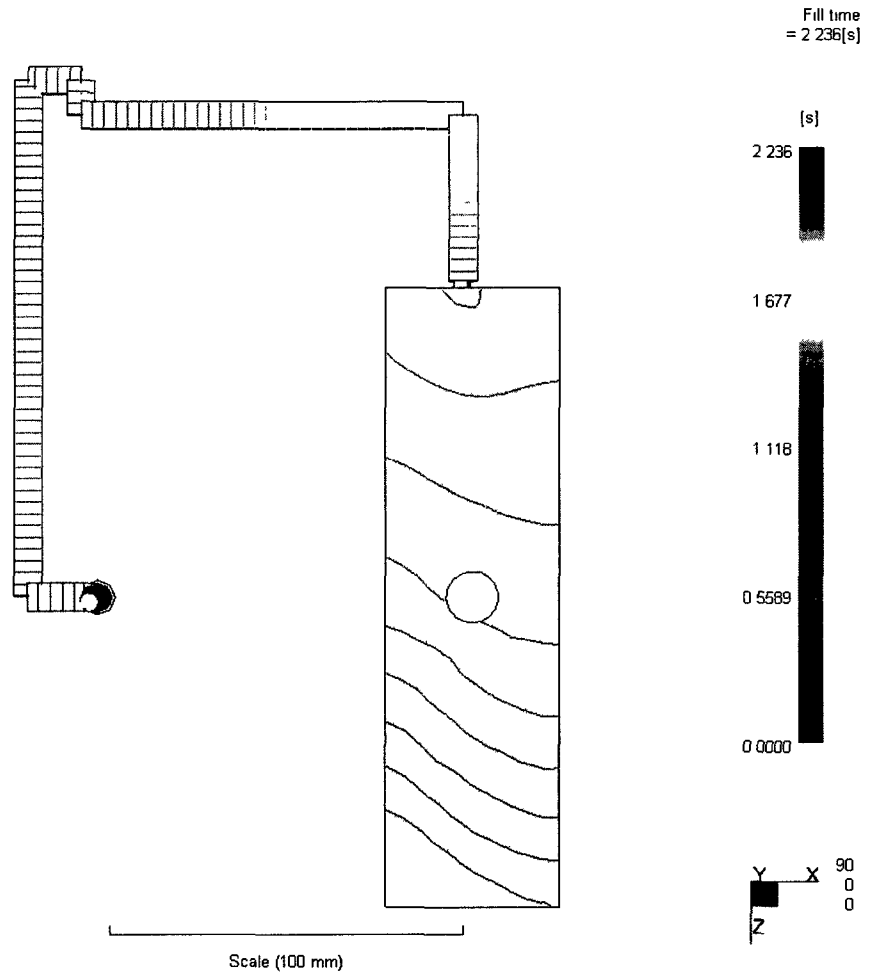
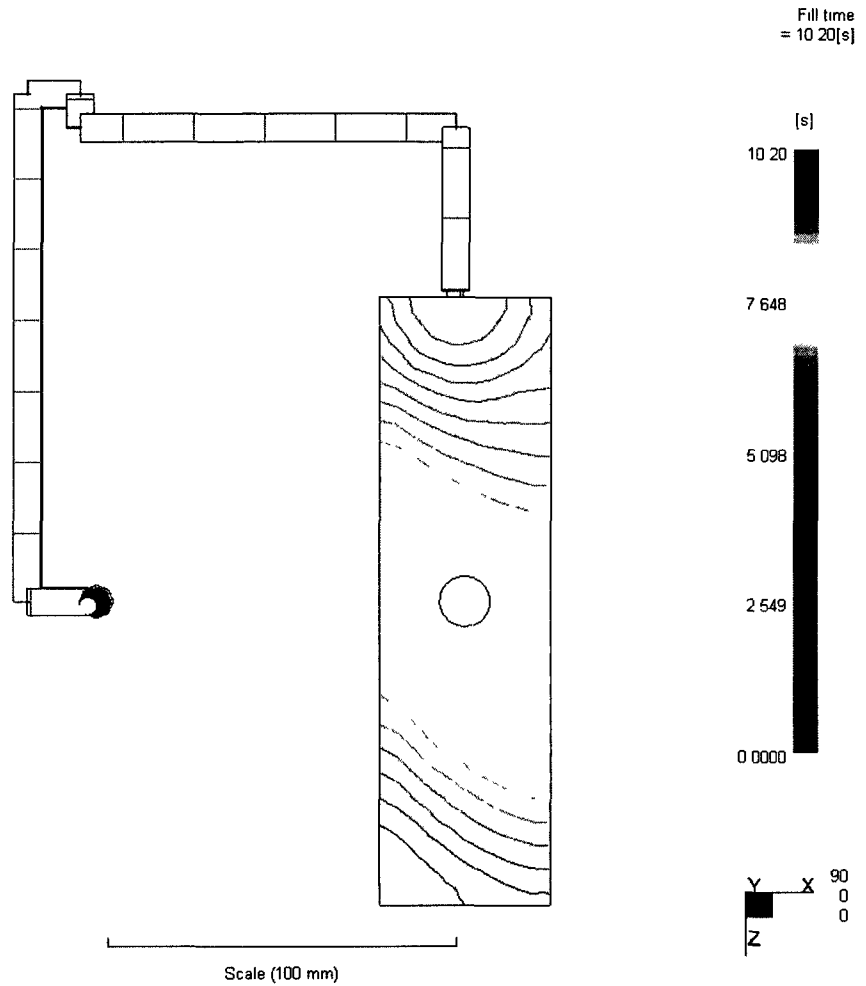


Figure 2a - Flow Front Profile in Obstacle Pin cavity, mtl: 700GP @ 6.3 cc/s injection rate



**Figure 3a - Flow Front Profile in Obstacle Pin cavity, mtl: 2000GP @ 37.7 cc/s
injection rate**



**Figure 4a - Flow Front Profile in Obstacle Pin cavity, mtl: 2000GP @ 6.3 cc/s
injection rate**

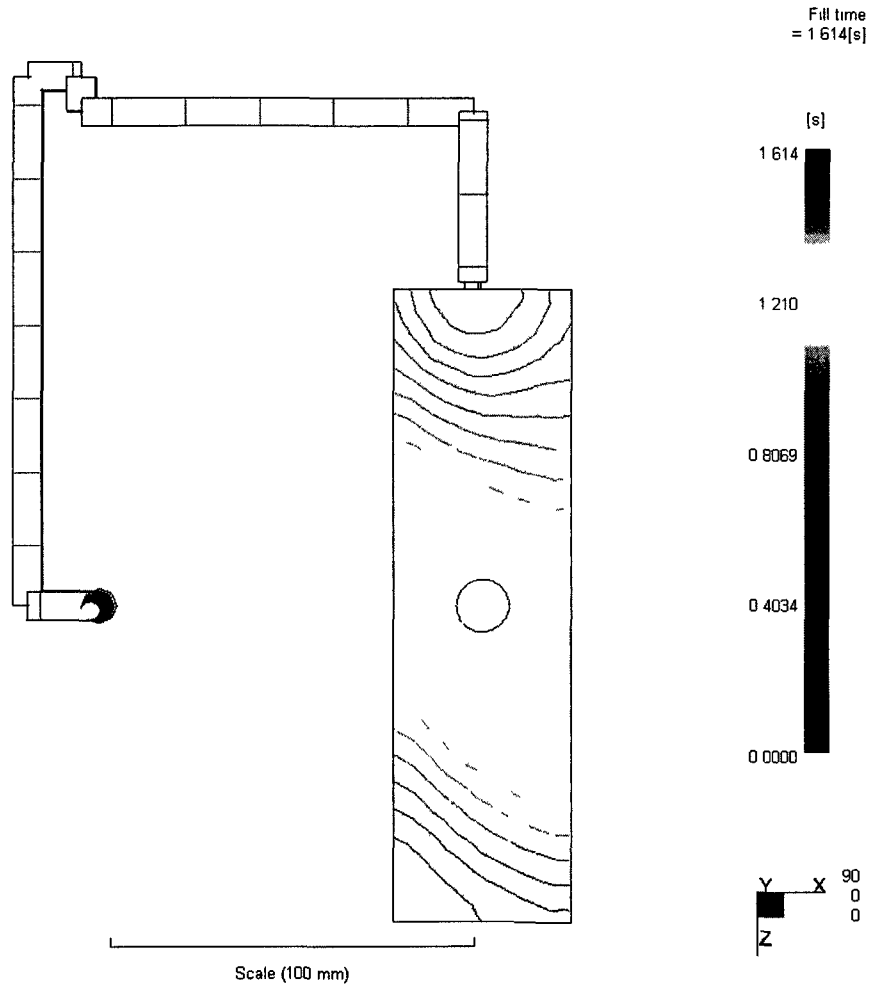


Figure 5a - Flow Front Profile in Obstacle Pin cavity, mtl: CR3500 @ 37.7 cc/s injection rate

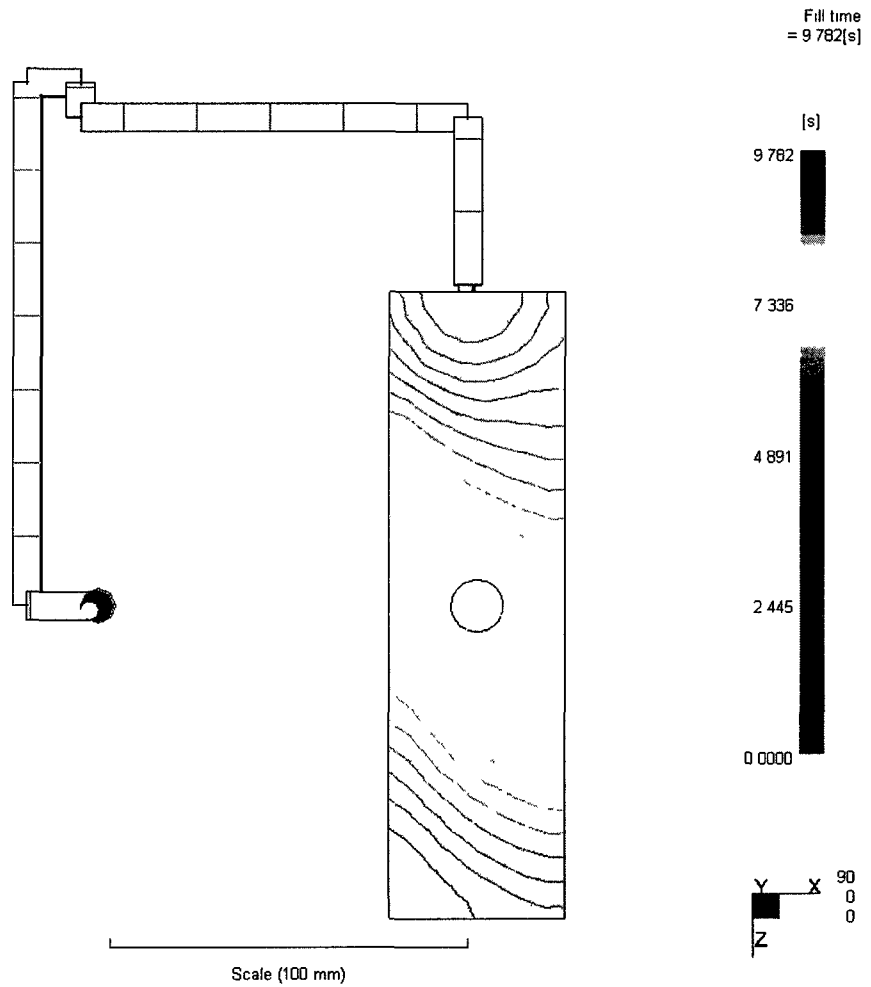


Figure 6a - Flow Front Profile in Obstacle Pin cavity, mtl: CR3500 @ 6.3 cc/s injection rate

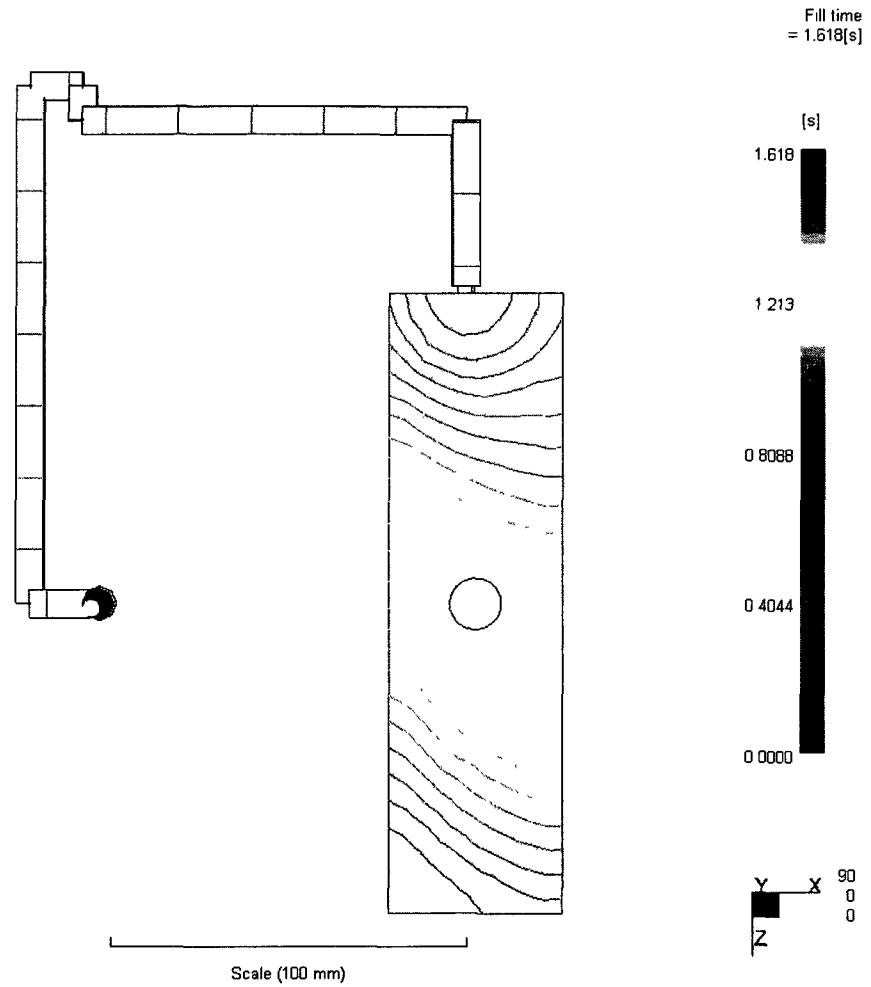
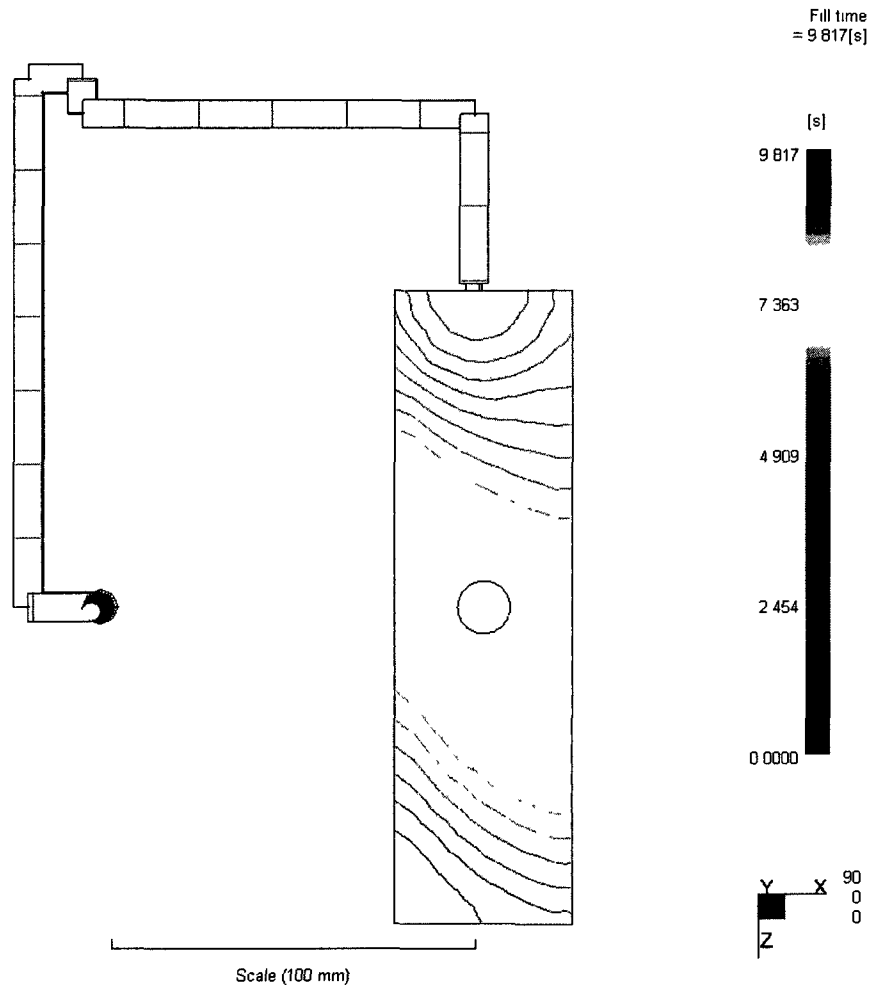


Figure 7a - Flow Front Profile in Obstacle Pin cavity, mtl: CR4500 @ 37.7 cc/s injection rate



**Figure 8a - Flow Front Profile in Obstacle Pin cavity, mtl: CR4500 @ 6.3 cc/s
injection rate**

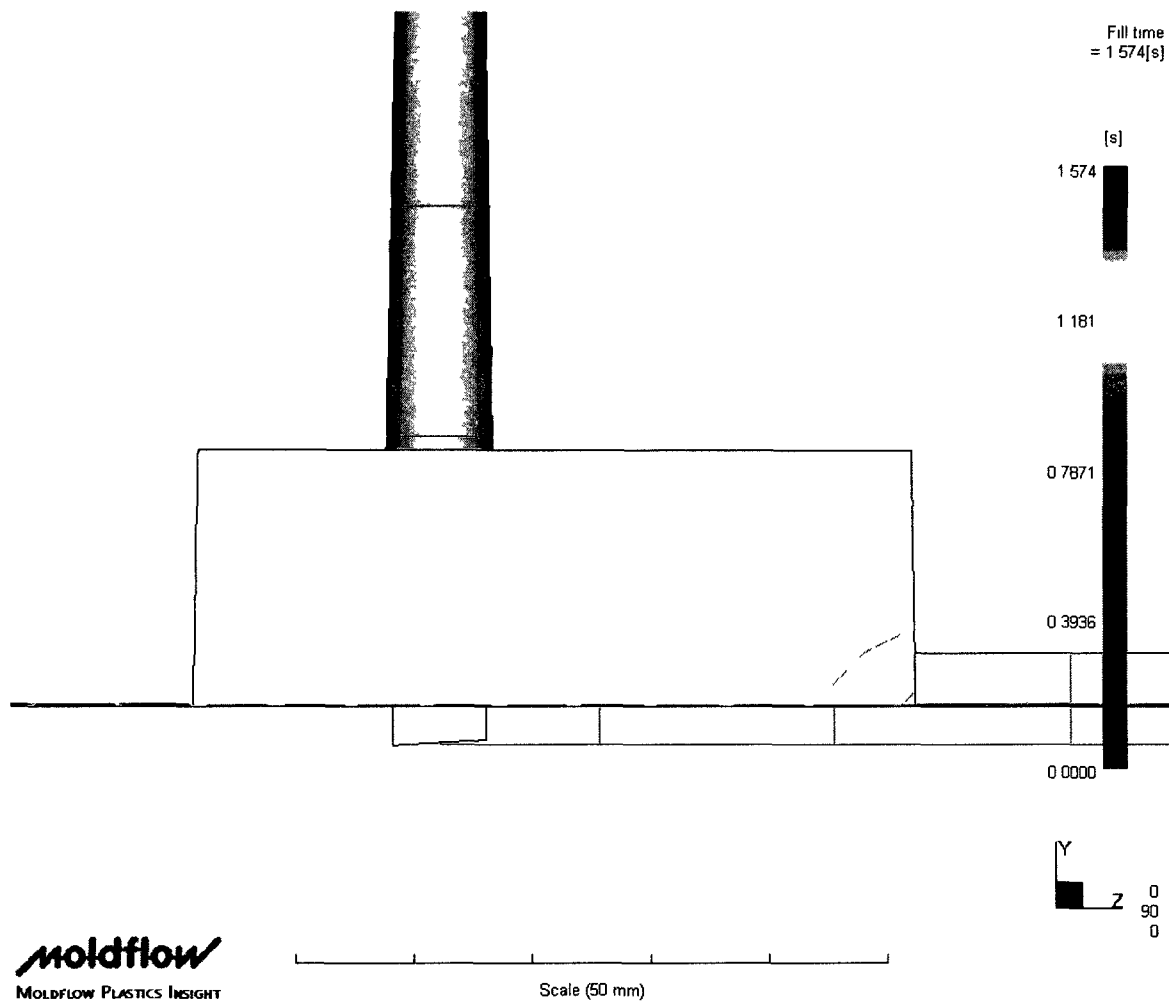


Figure 9-1a - Flow Front Profile (side) in 2 mm parallel rib cavity, mtl: CR3500 @ 37.7 cc/s injection rate

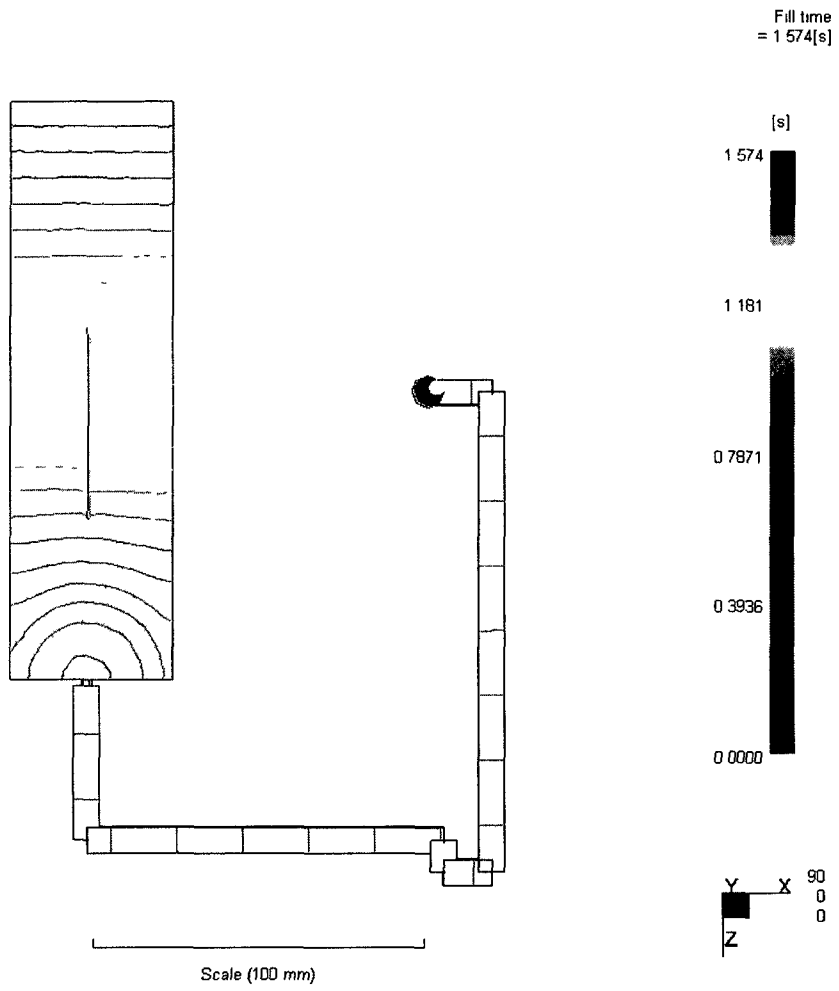


Figure 9-2a - Flow Front Profile in 2 mm parallel rib cavity, mtl: CR3500 @ 37.7 cc/s injection rate

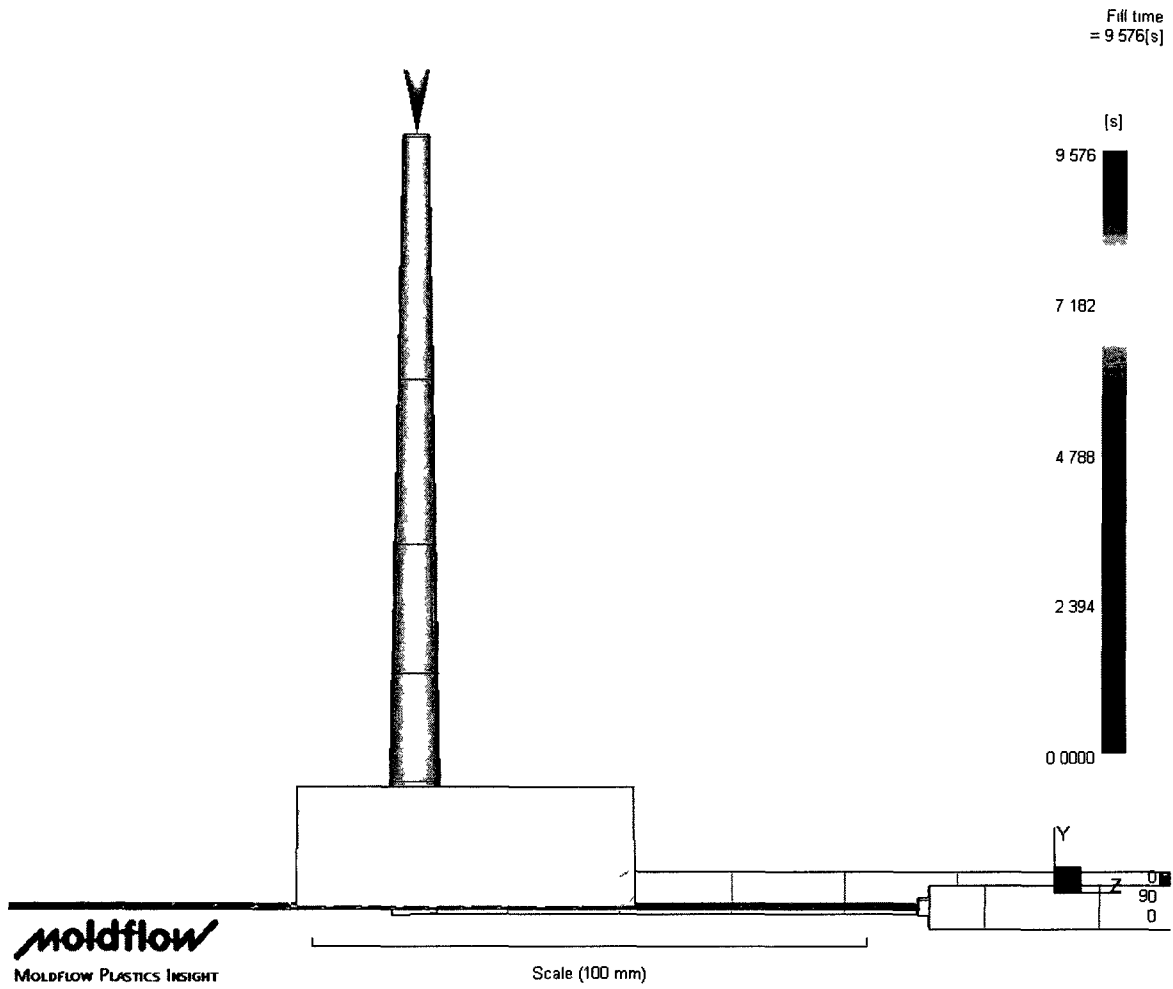
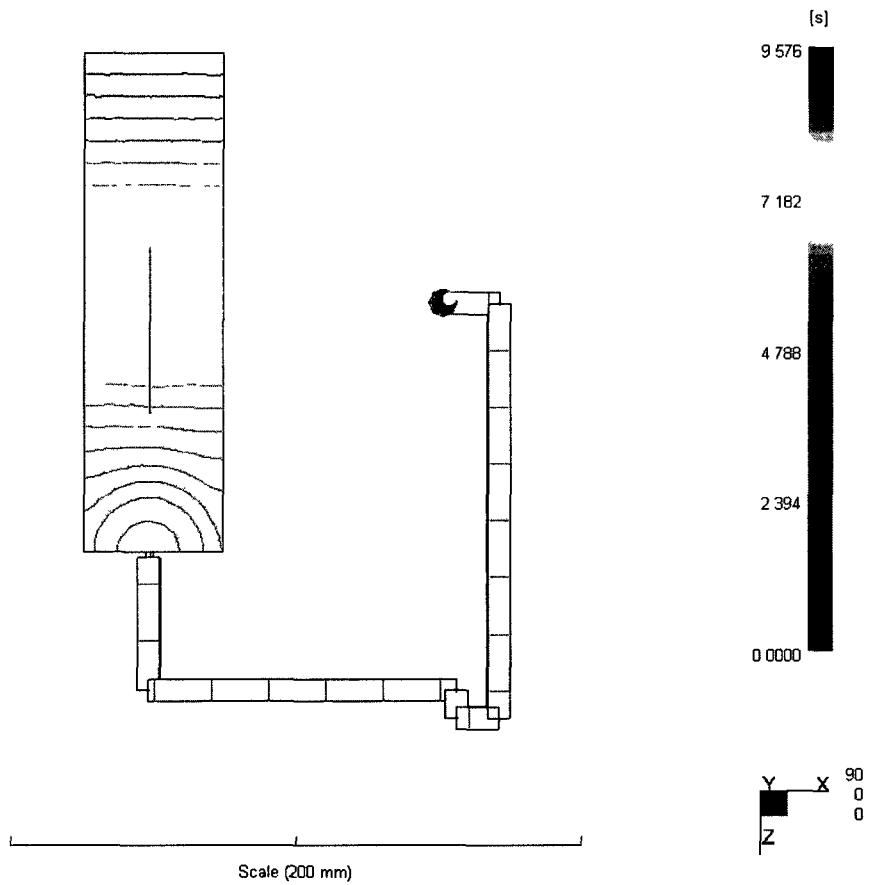


Figure 10-1a - Flow Front Profile (side) in 2 mm parallel rib cavity, mtl: CR3500 @ 6.3 cc/s injection rate

Fill time
= 9.576[s]



moldflow
MOLDFLOW PLASTICS INSIGHT

Figure 10-2a - Flow Front Profile in 2 mm parallel rib cavity, mtl: CR3500 @ 6.3 cc/s injection rate

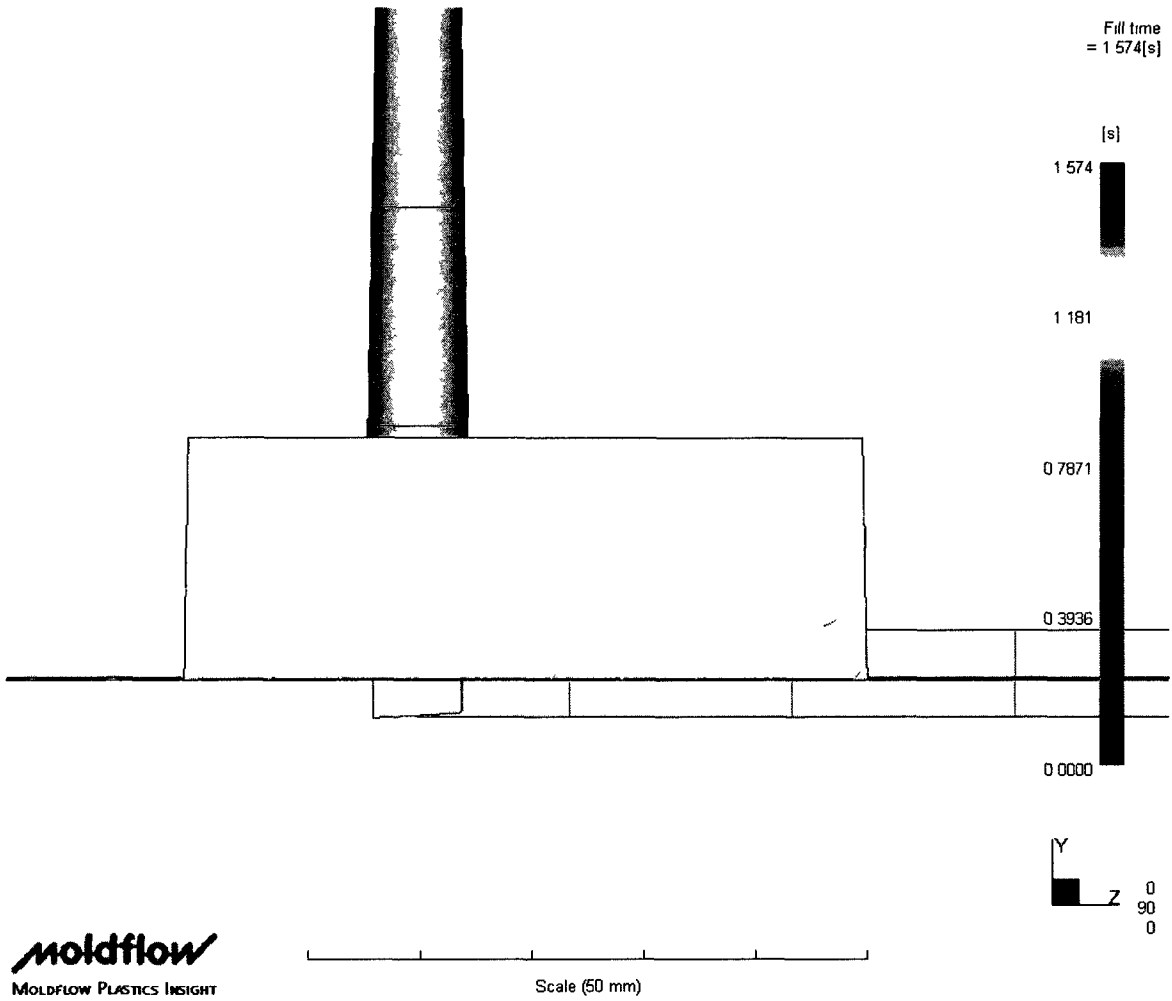


**Figure 11-1a - Flow Front Profile (side) in 2 mm parallel rib cavity, mtl: CR4500 @
37.7 cc/s injection rate**

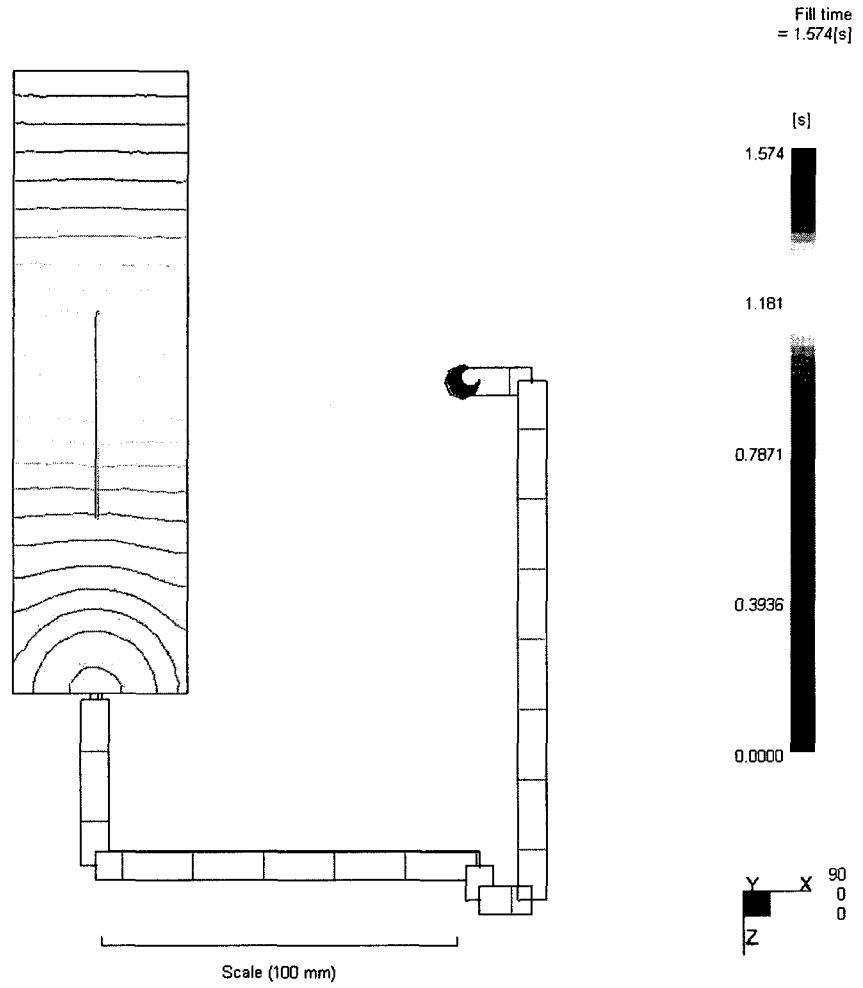
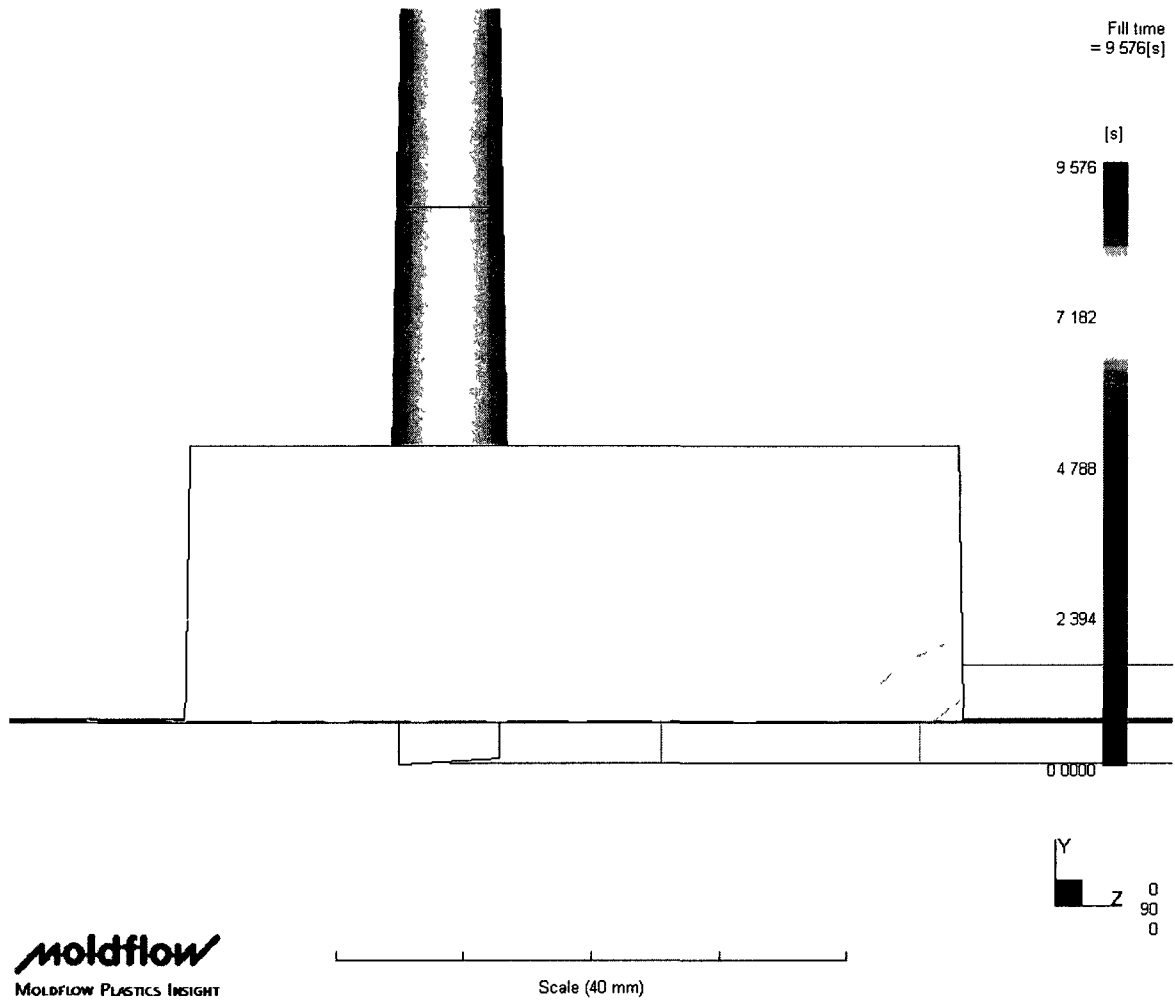


Figure 11-2a - Flow Front Profile in 2 mm parallel rib cavity, mtl: CR4500 @ 37.7 cc/s injection rate



**Figure 12-1a - Flow Front Profile (side) in 2 mm parallel rib cavity, mtl: CR4500 @
6.3 cc/s injection rate**



Scale (200 mm)

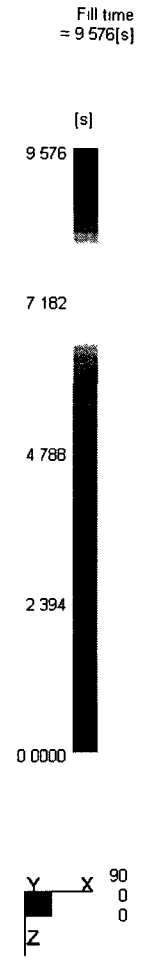


Figure 12-2a - Flow Front Profile in 2 mm parallel rib, mtl: CR4500 @ 6.3 cc/s injection rate

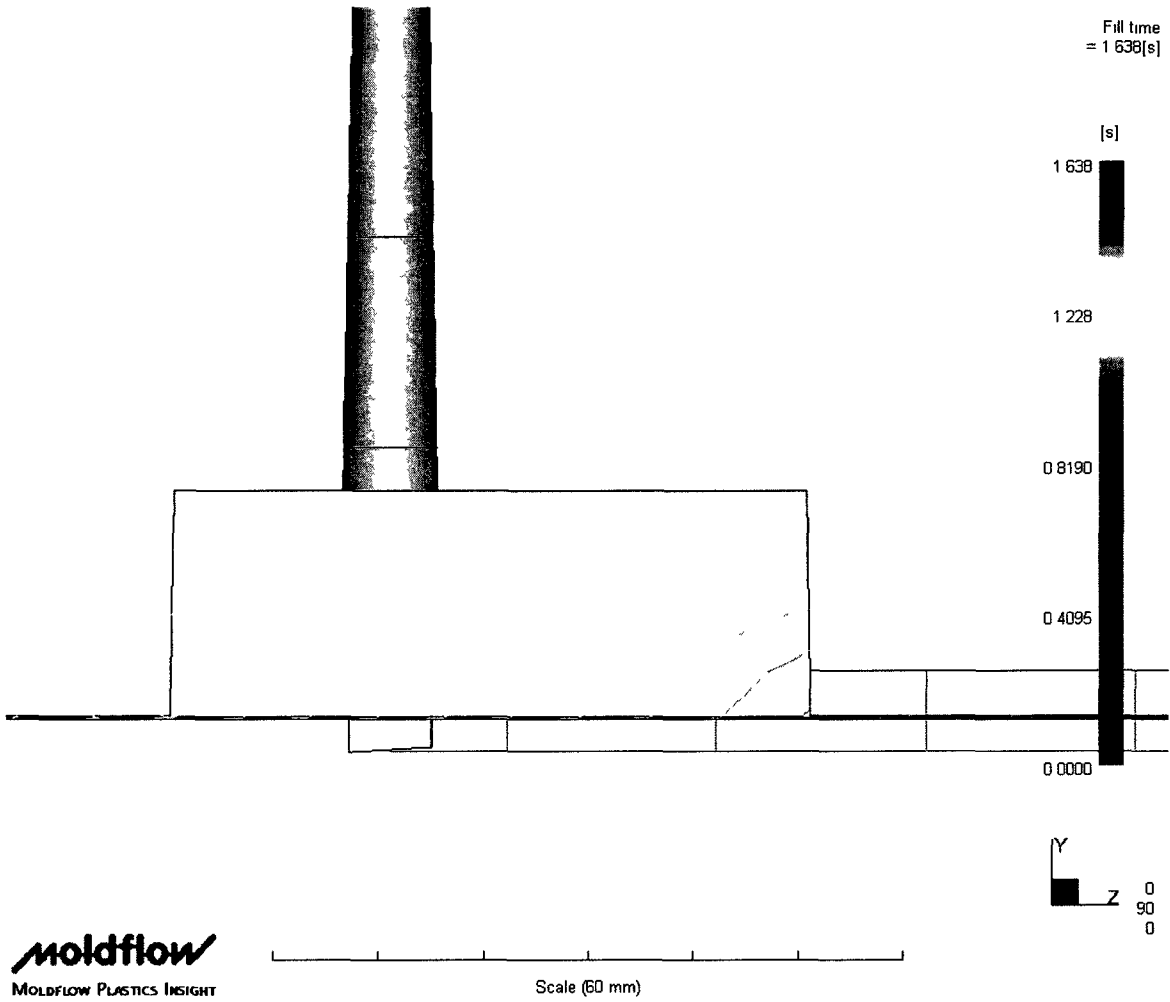


Figure 13-1a - Flow Front Profile (side) in 2 mm parallel rib cavity, mtl: 700GP @ 37.7 cc/s injection rate

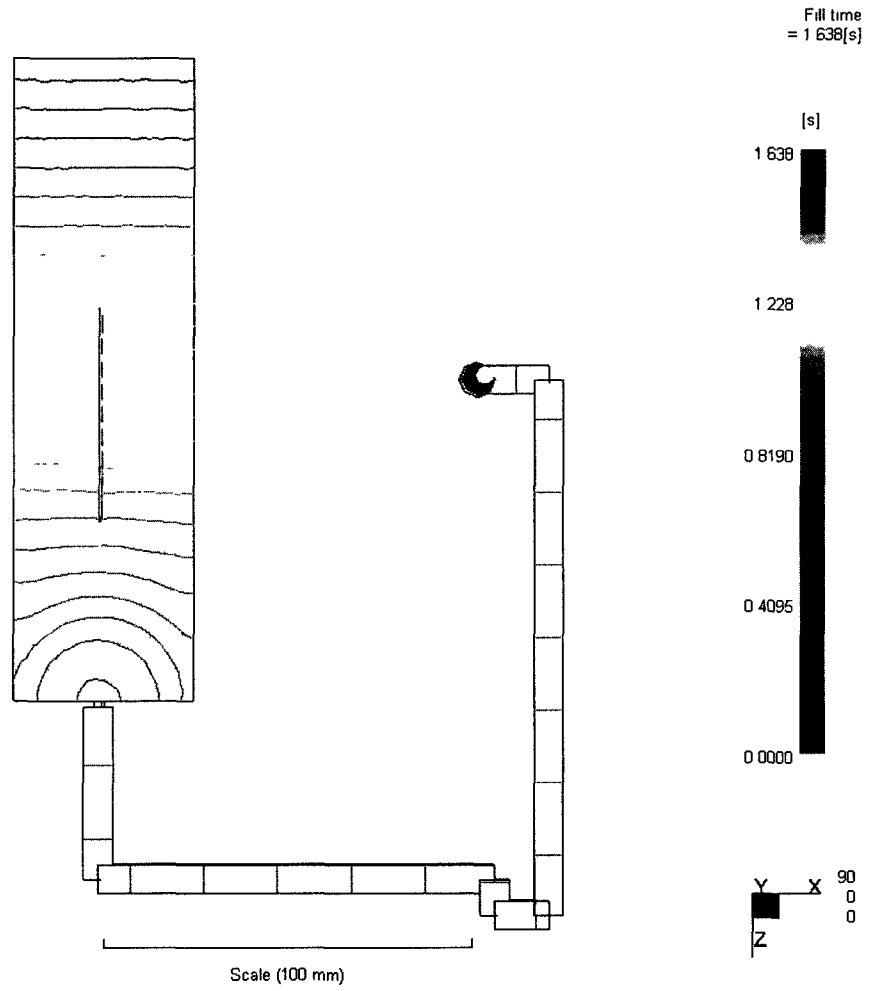


Figure 13-2a - Flow Front Profile in 2 mm parallel rib cavity, mtl: 700GP @ 37.7 cc/s injection rate

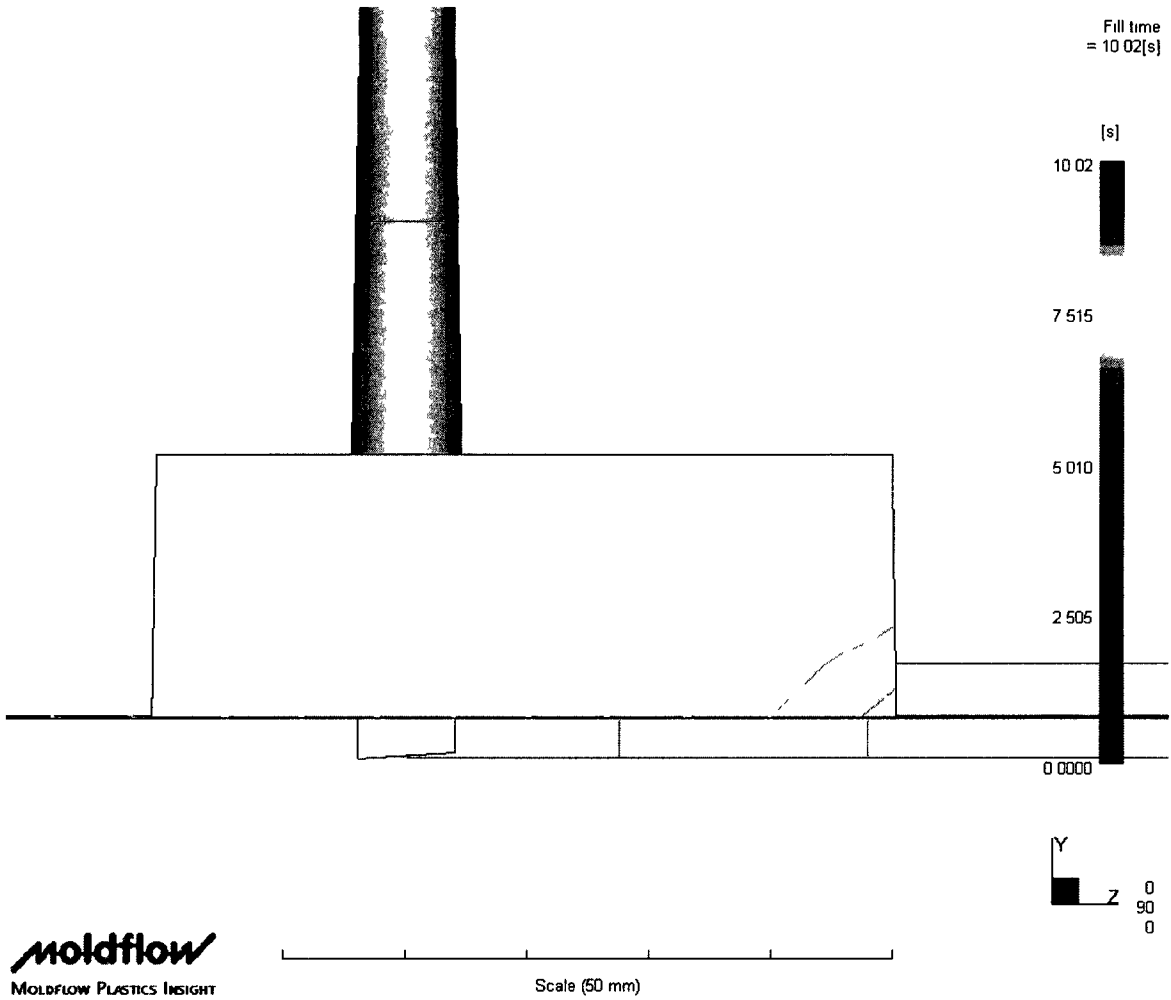


Figure 14-1a - Flow Front Profile (side) in 2 mm parallel rib cavity, mtl: 700GP @ 6.3 cc/s injection rate

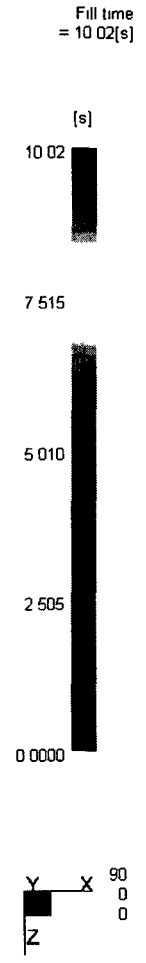
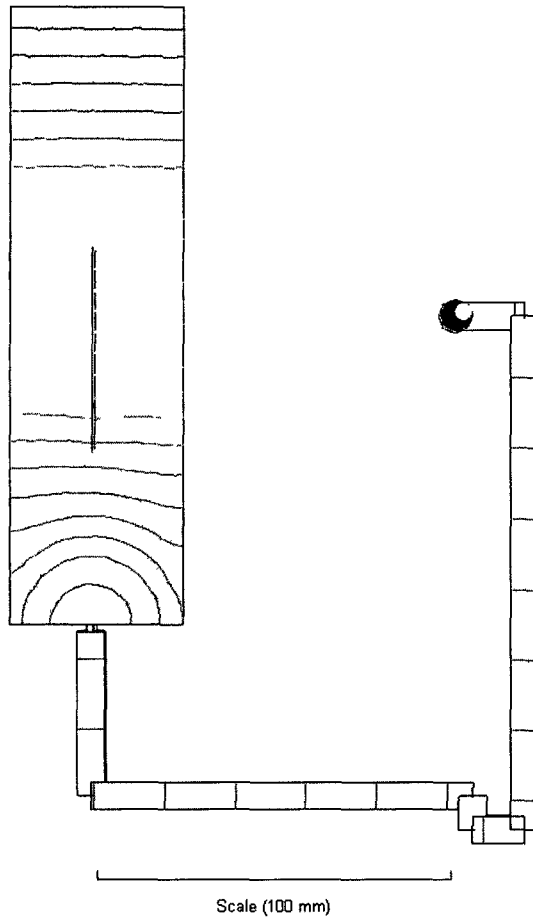


Figure 14-2a - Flow Front Profile in 2 mm parallel rib cavity, mtl: 700GP @ 6.3 cc/s injection rate

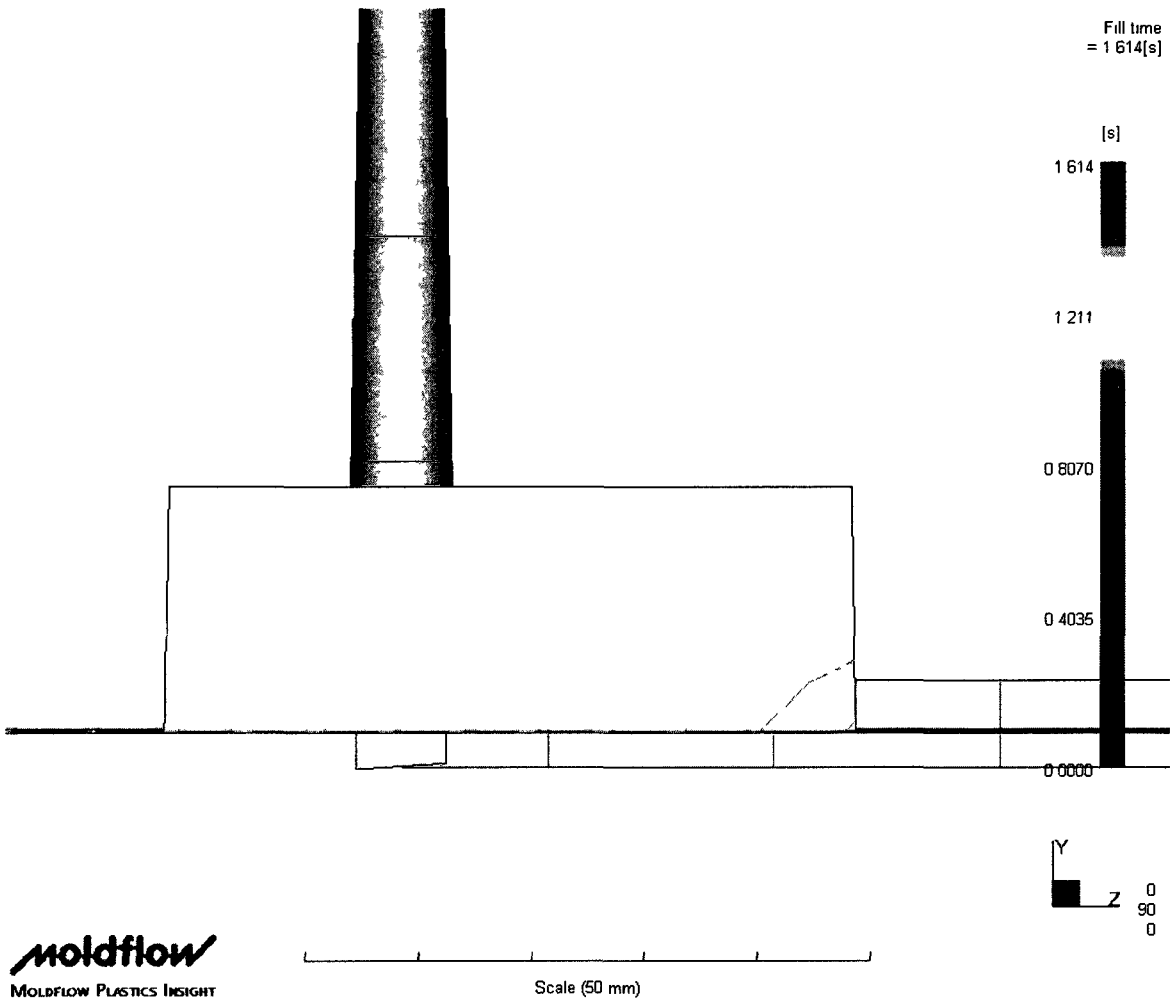


Figure 15-1a - Flow Front Profile (side) in 2 mm parallel rib cavity, mtl: 2000GP @ 37.7 cc/s injection rate

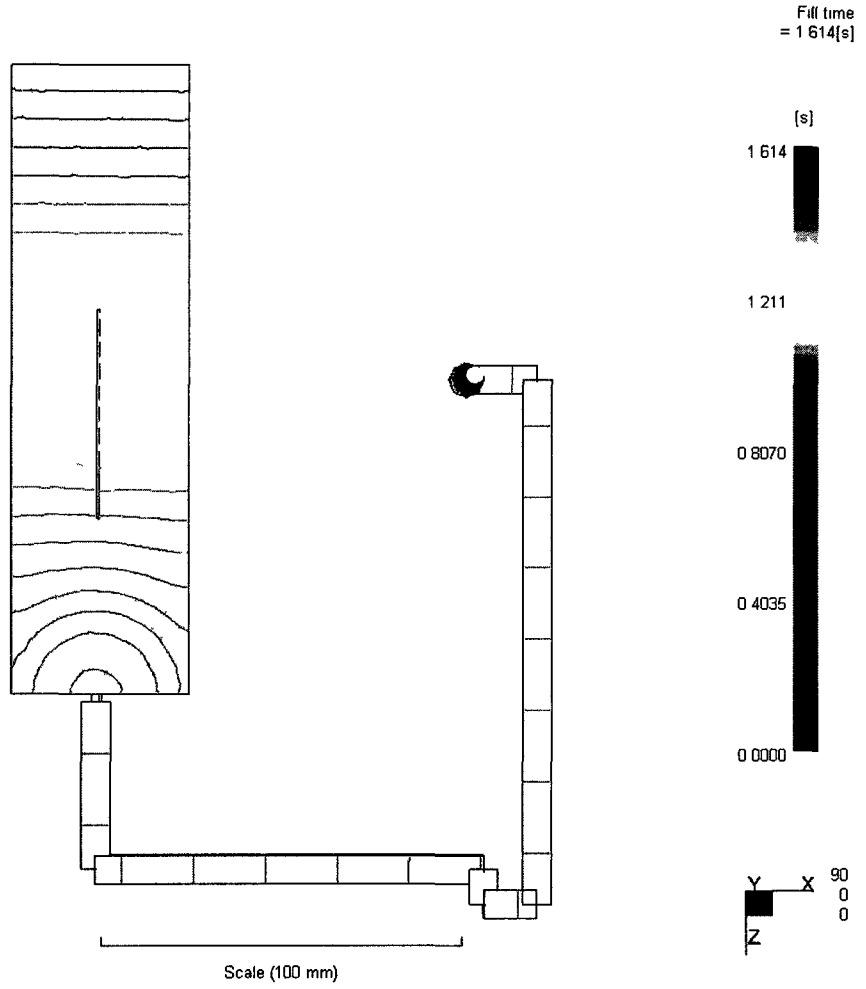


Figure 15-2a - Flow Front Profile in 2 mm parallel rib cavity, mtl: 2000GP @ 37.7 cc/s injection rate

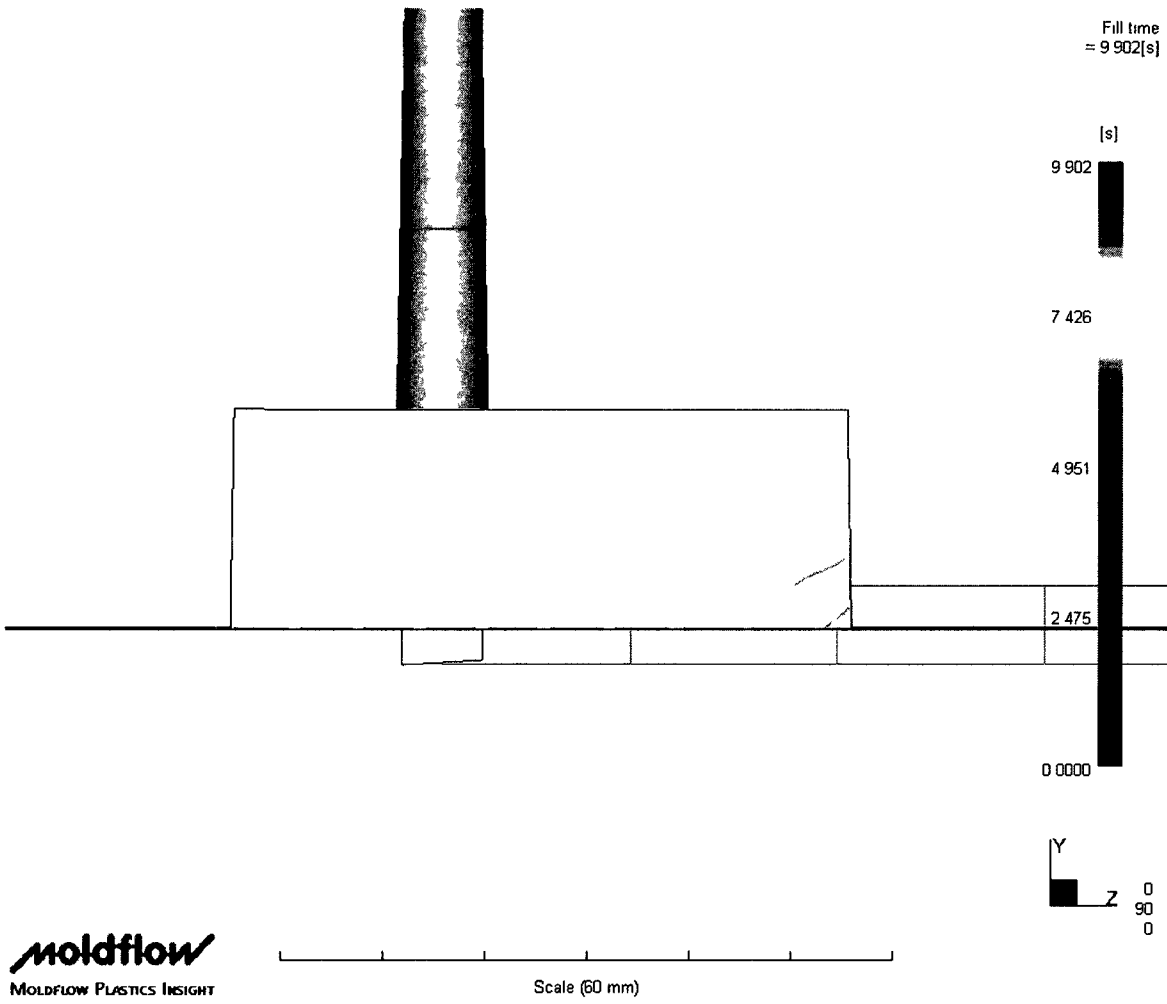


Figure 16-1a - Flow Front Profile (side) in 2 mm parallel rib cavity, mtl: 2000GP @ 6.3 cc/s injection rate

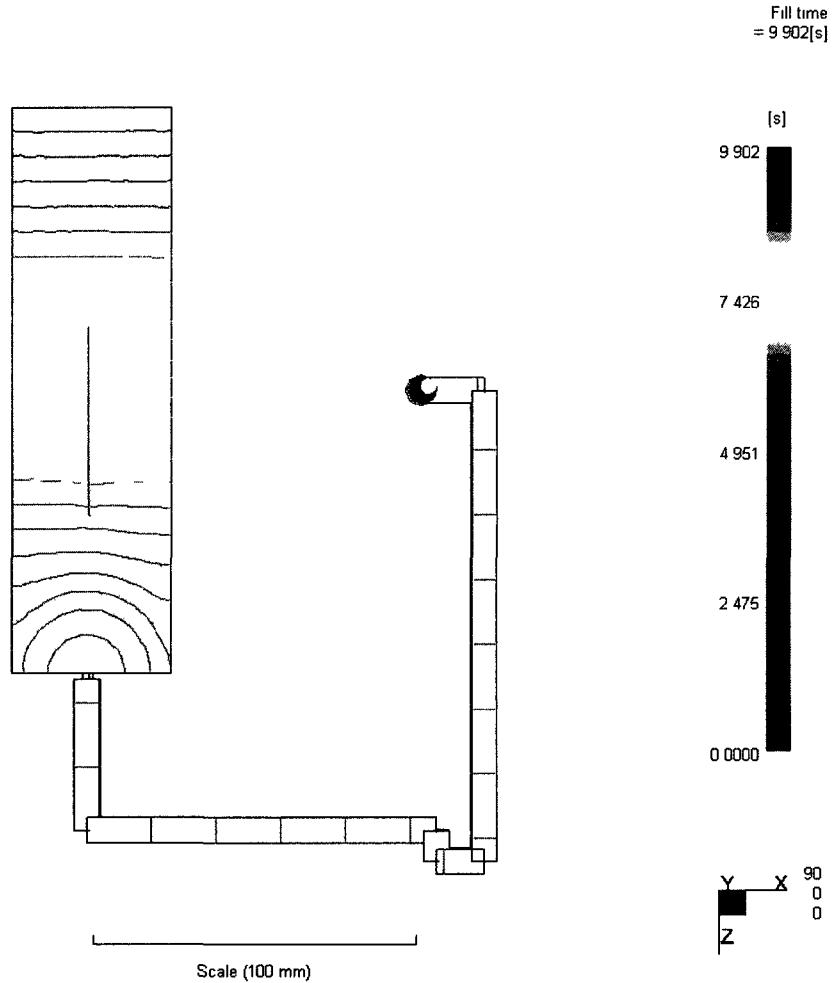
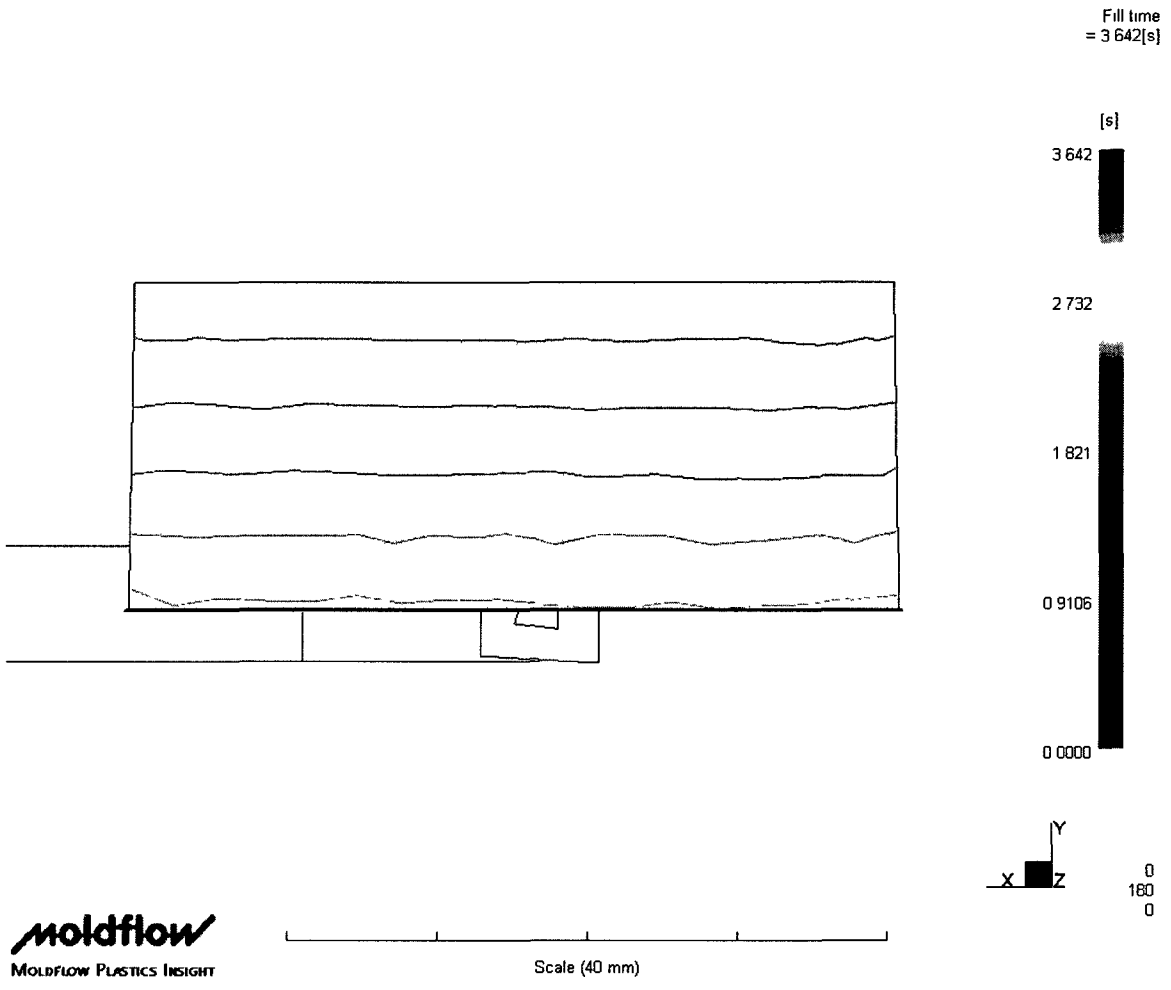
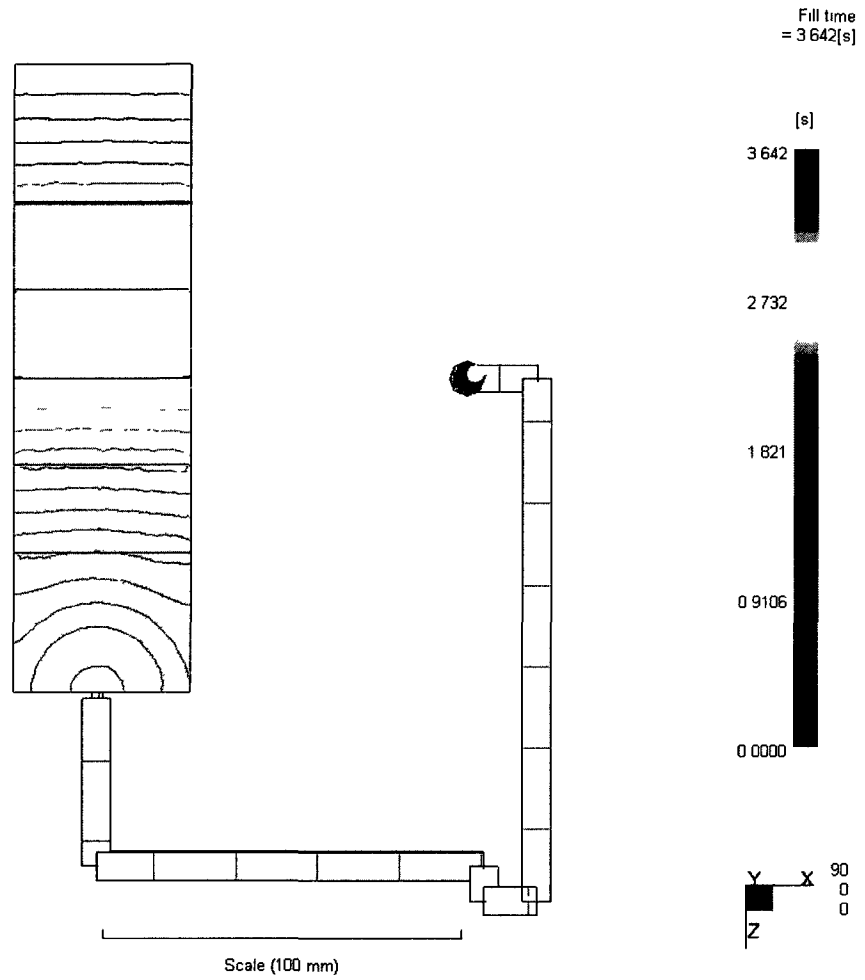


Figure 16-2a - Flow Front Profile in 2 mm parallel rib cavity, mtl: 2000GP @ 6.3 cc/s injection rate



**Figure 17-1a - Flow Front Profile (last rib) in 2 mm perpendicular rib cavity, mtl:
CR3500 @ 18.8 cc/s injection rate**



**Figure 17-2a - Flow Front Profile (top) in 2 mm perpendicular rib cavity, mtl:
CR3500 @ 18.8cc/s injection rate**

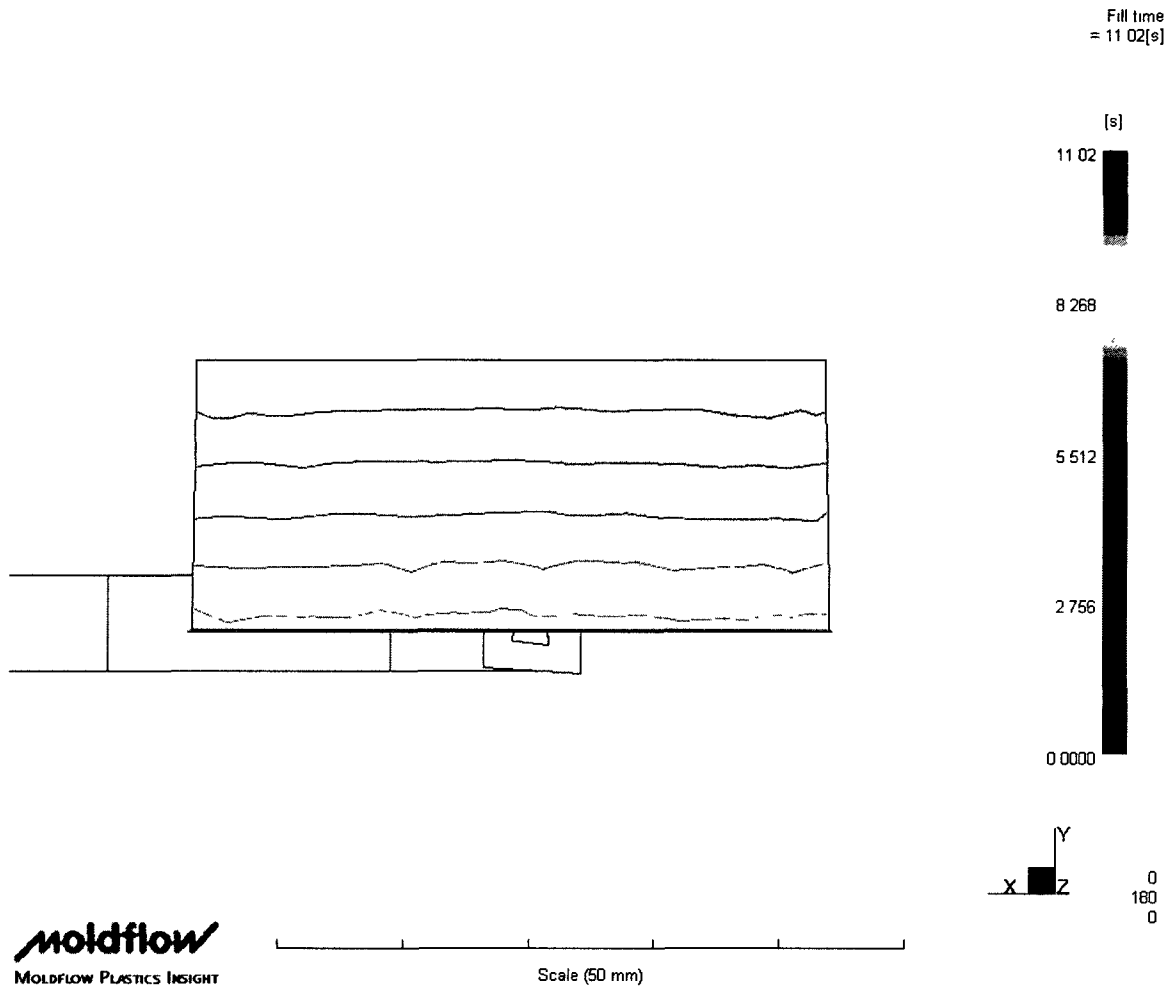


**Figure 18-1a - Flow Front Profile (last rib) in 2 mm perpendicular rib cavity, mtl:
CR3500 @ 6.3 cc/s injection rate**

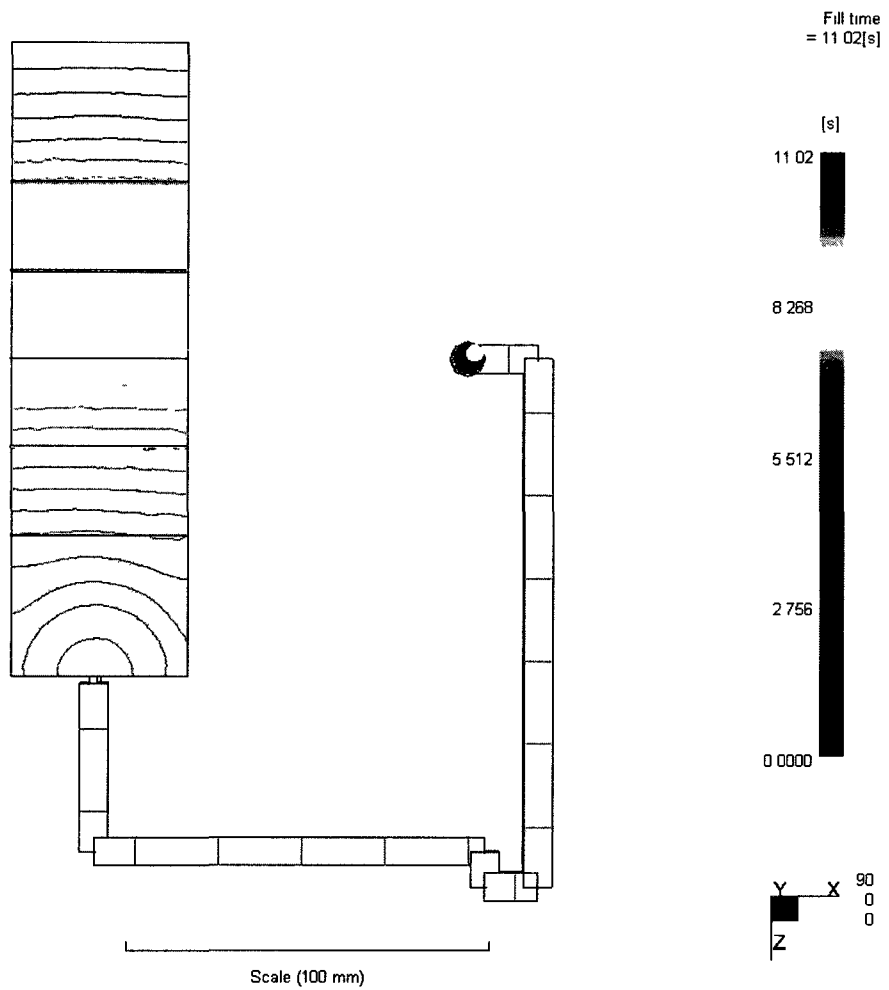


**Figure 18-2a - Flow Front Profile (top) in 2 mm perpendicular rib cavity, mtl:
CR3500 @ 6.3 cc/s injection rate**

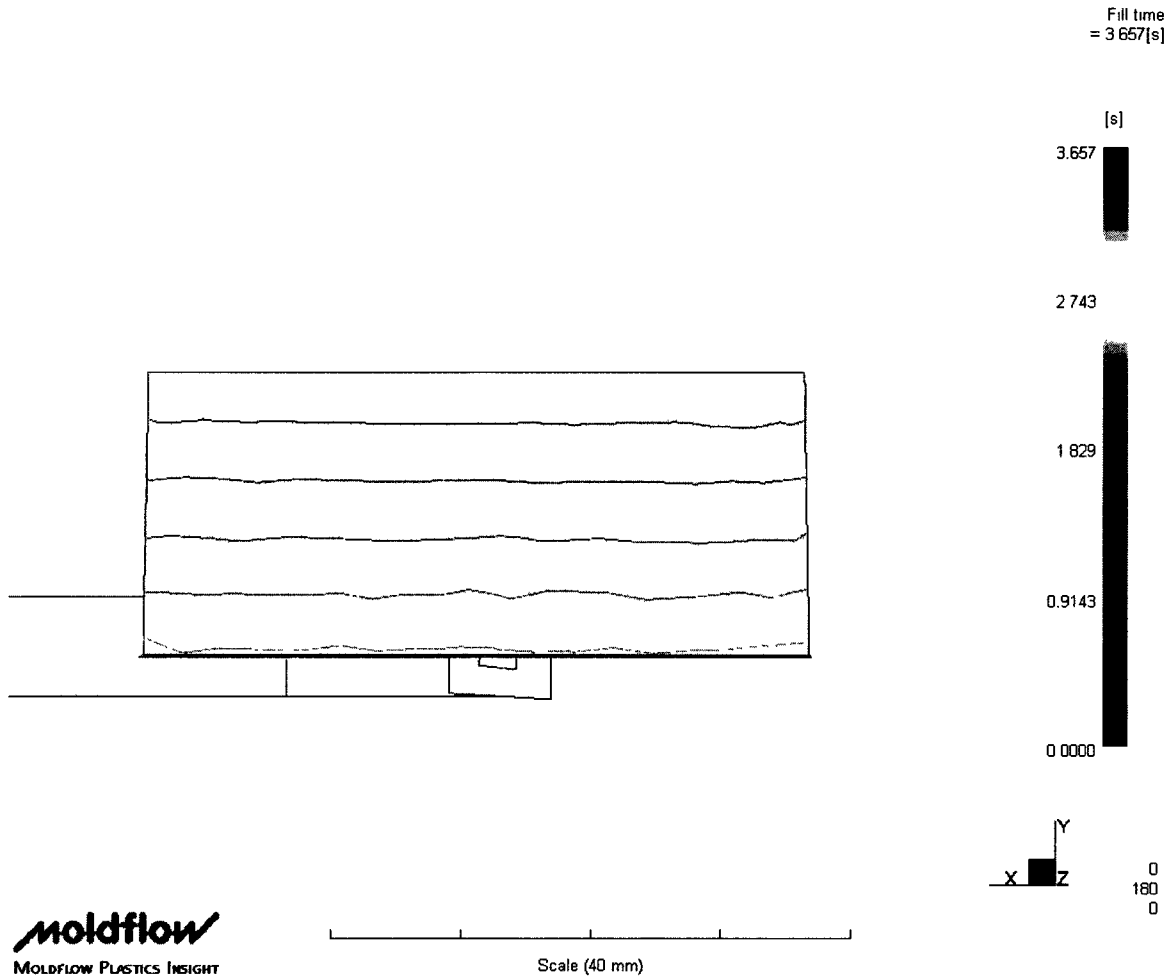


**Figure 19-1a - Flow Front Profile (last rib) in 2 mm perpendicular rib cavity, mtl:
CR4500 @ 18.8cc/s injection rate**

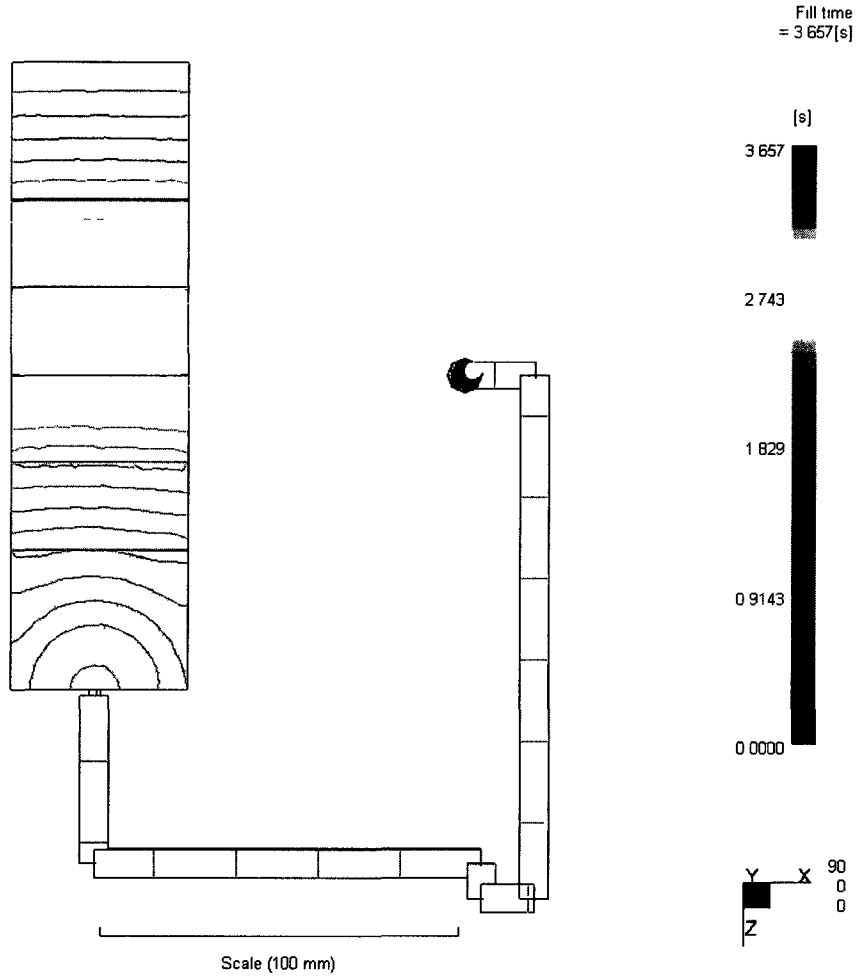


**Figure 19-2a - Flow Front Profile (top) in 2 mm perpendicular rib cavity, mtl:
CR4500 @ 18.8 cc/s injection rate**

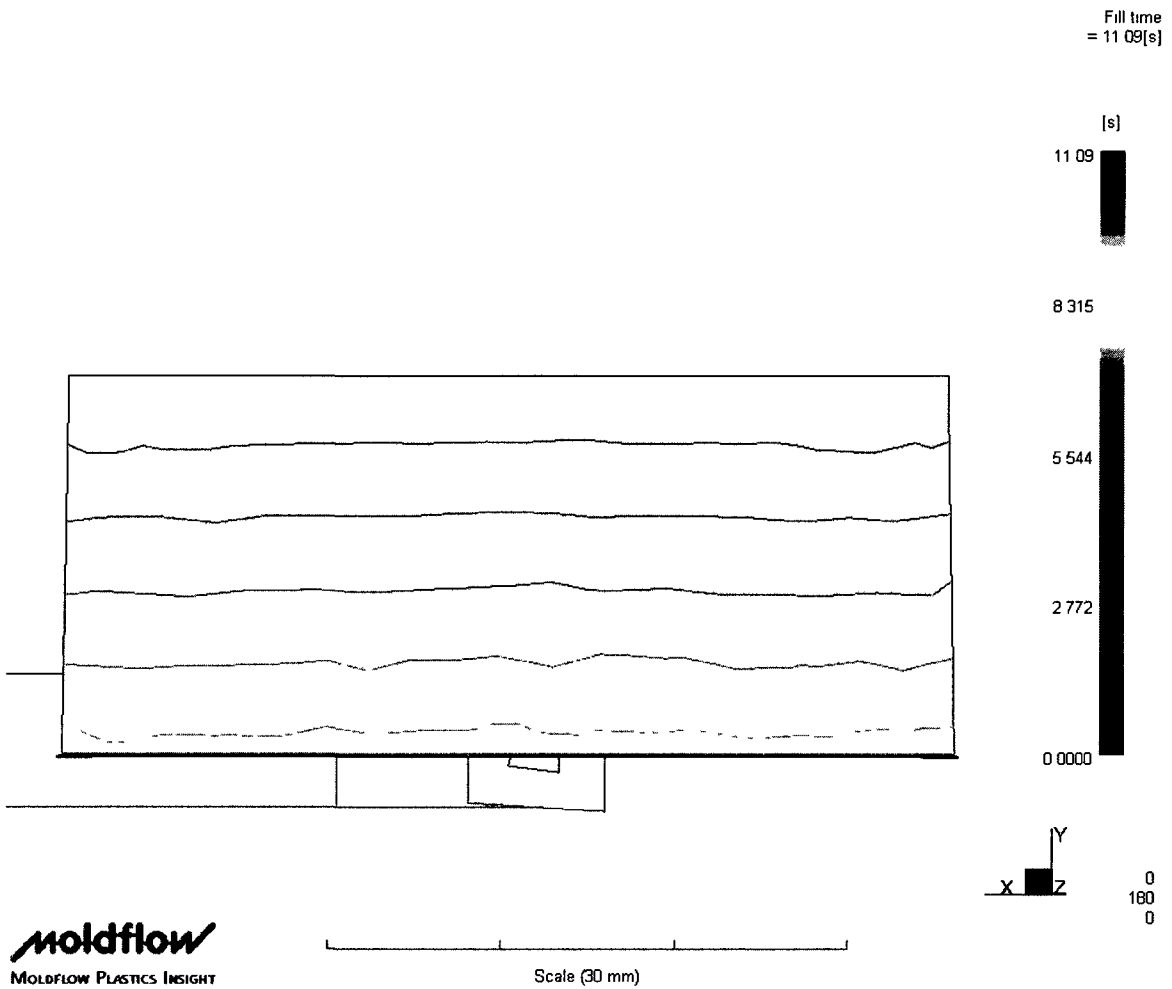


**Figure 20-1a - Flow Front Profile (last rib) in 2 mm perpendicular rib cavity, mtl:
CR4500 @ 6.3 cc/s injection rate**

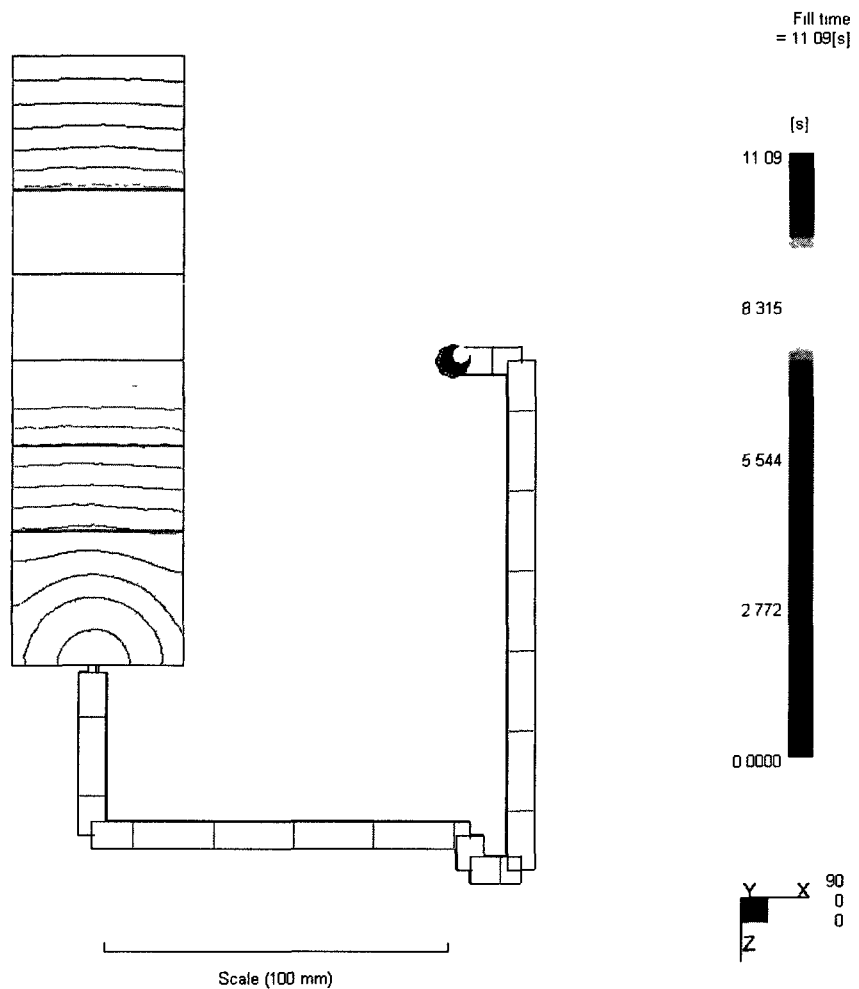


**Figure 20-2a - Flow Front Profile (top) in 2 mm perpendicular rib cavity, mtl:
CR4500 @ 6.3 cc/s injection rate**

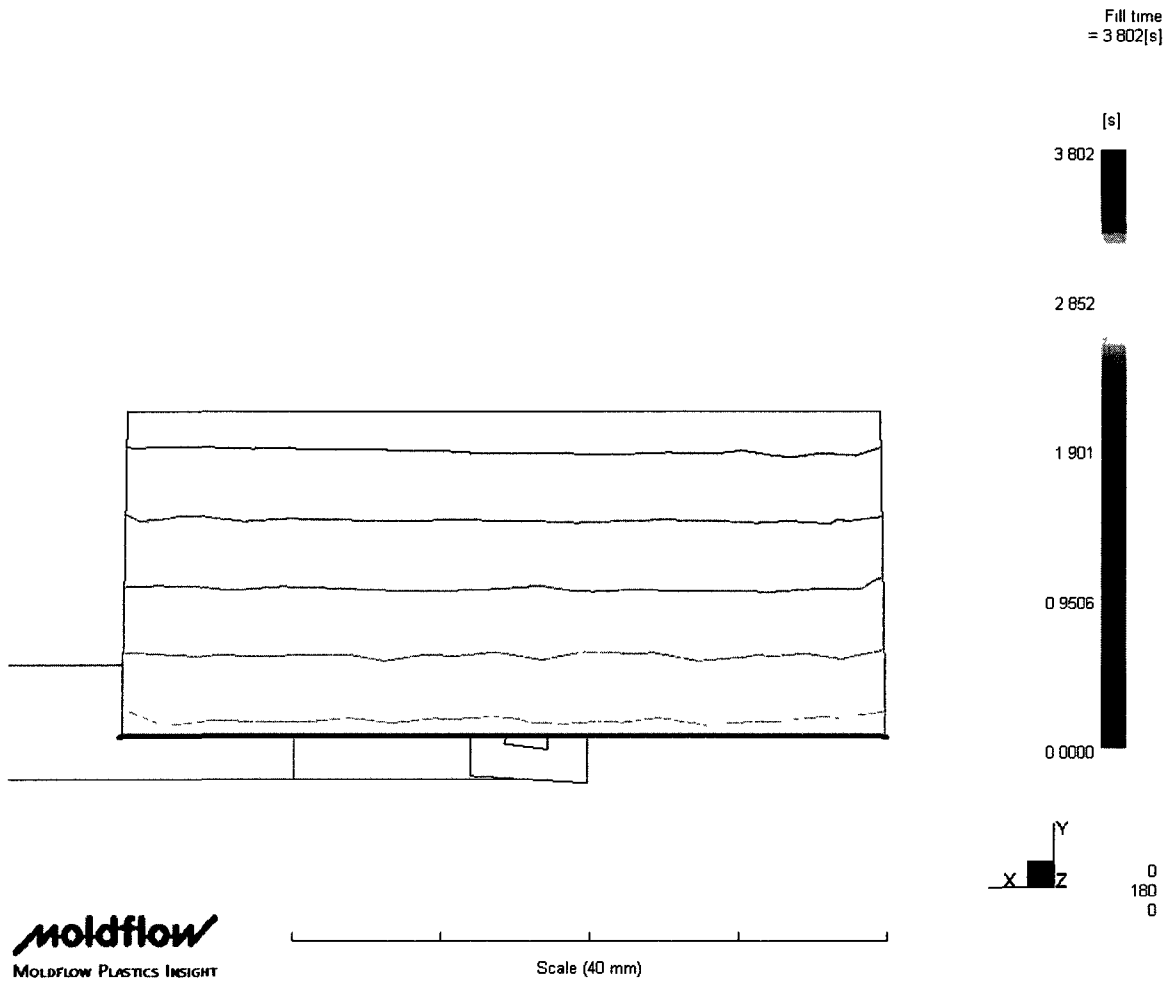


**Figure 21-1a - Flow Front Profile (last rib) in 2 mm perpendicular rib cavity, mtl:
700GP @ 18.8cc/s injection rate**

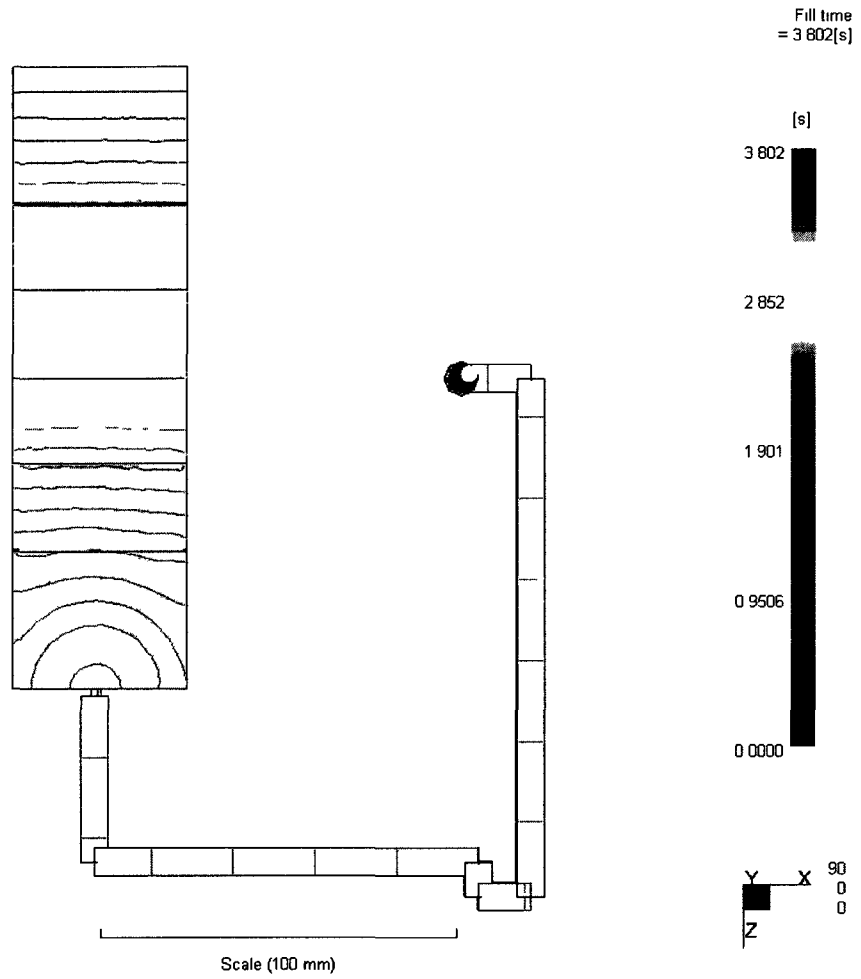


**Figure 21-2a - Flow Front Profile (top) in 2 mm perpendicular rib cavity, mtl:
700GP @ 18.8cc/s injection rate**

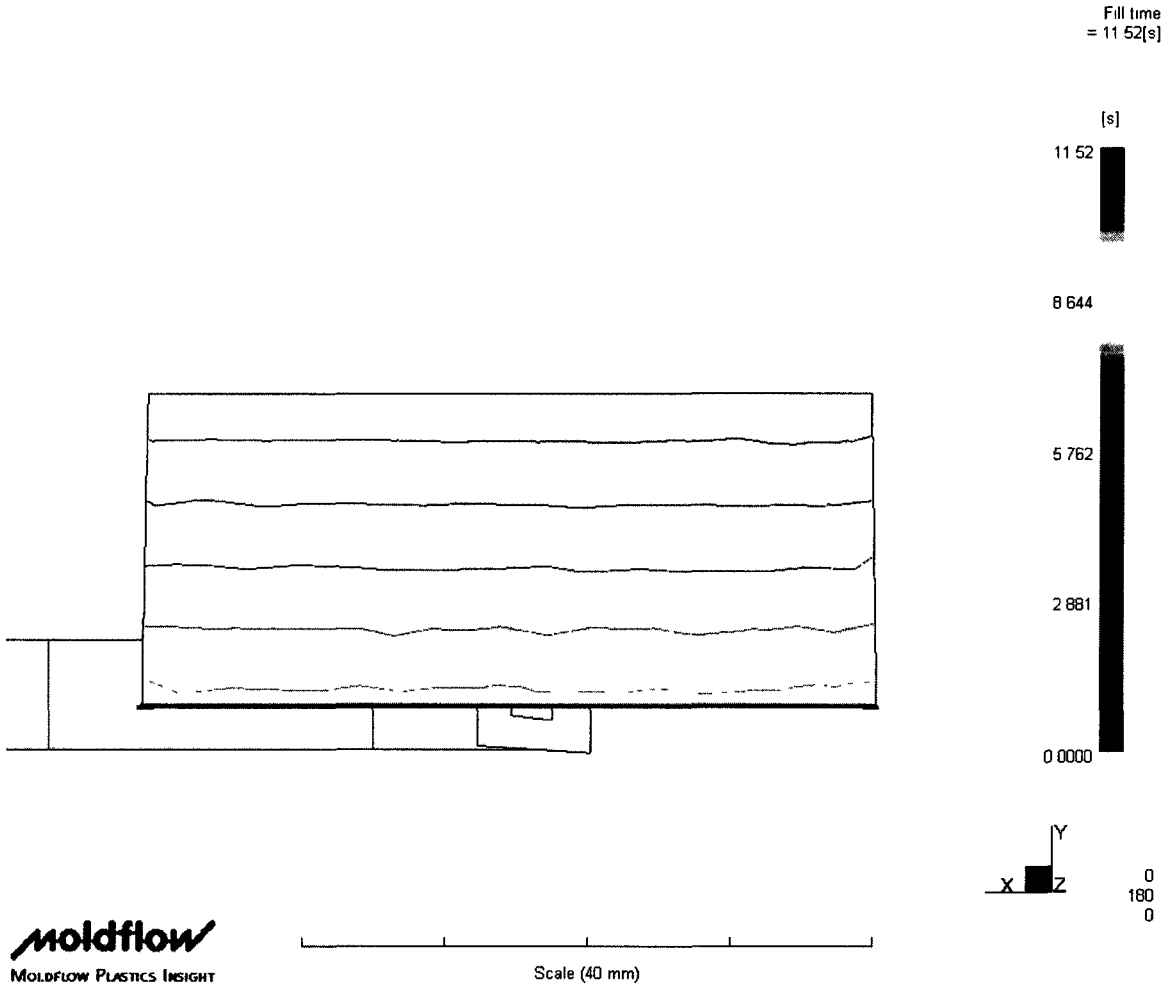


**Figure 22-1a - Flow Front Profile (last rib) in 2 mm perpendicular rib cavity, mtl:
700GP @ 6.3 cc/s injection rate**

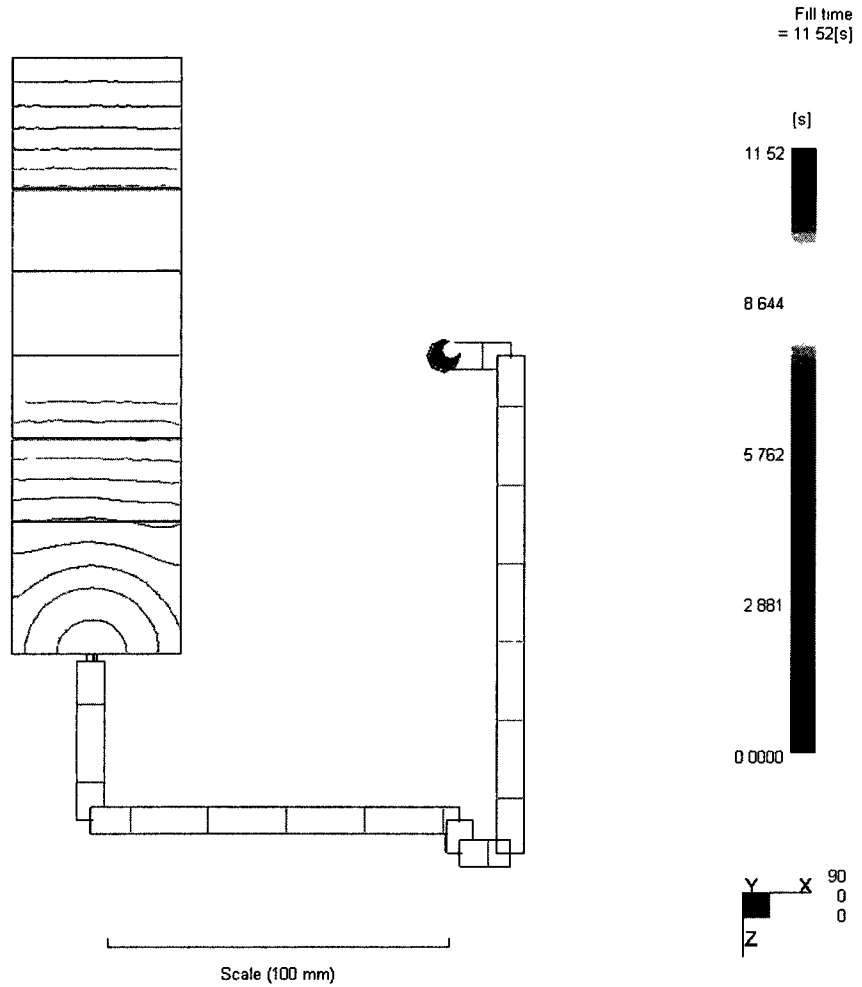


**Figure 22-2a - Flow Front Profile (top) in 2 mm perpendicular rib cavity, mtl:
700GP @ 6.3 cc/s injection rate**

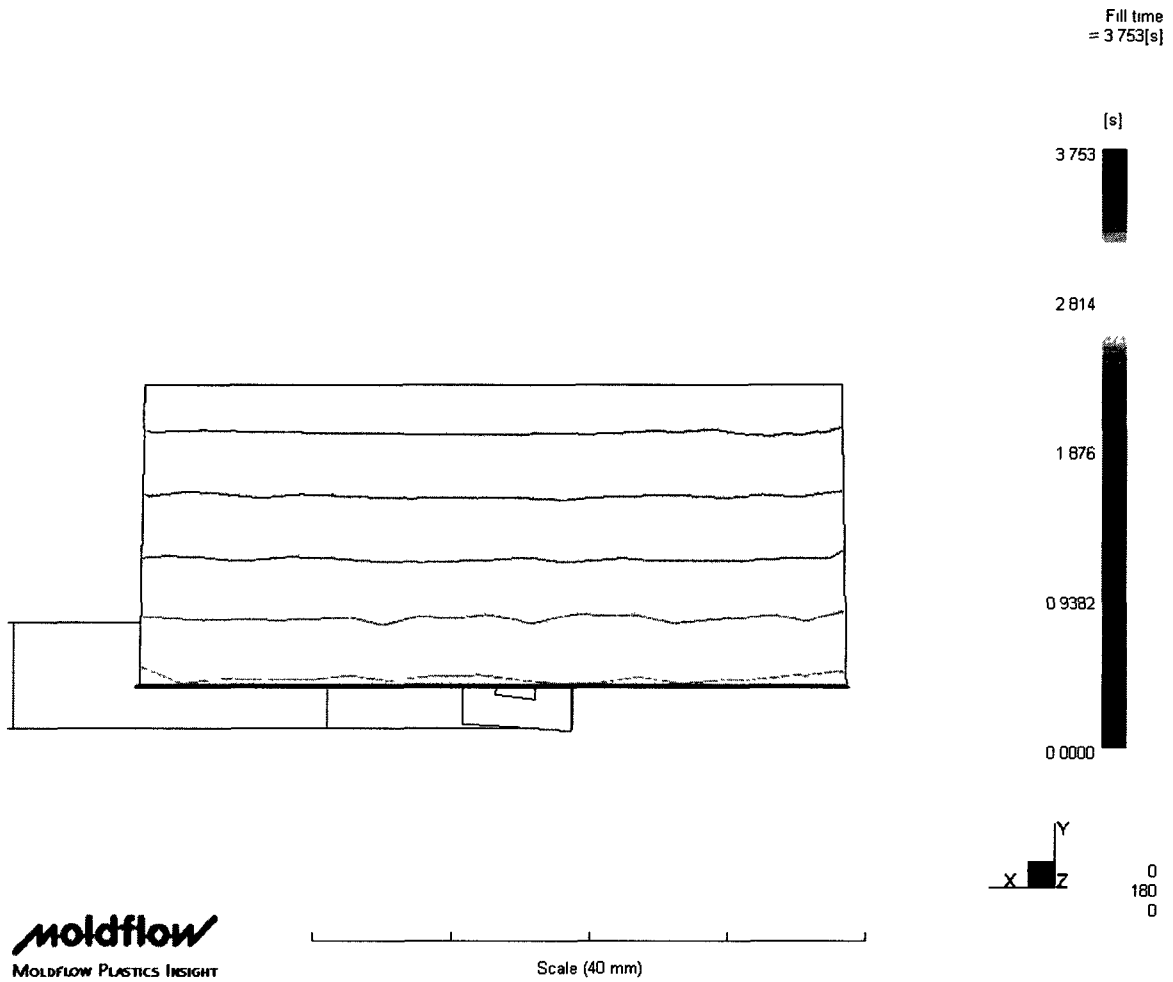


**Figure 23-1a - Flow Front Profile (last rib) in 2 mm perpendicular rib cavity, mtl:
2000GP @ 18.8 cc/s injection rate**

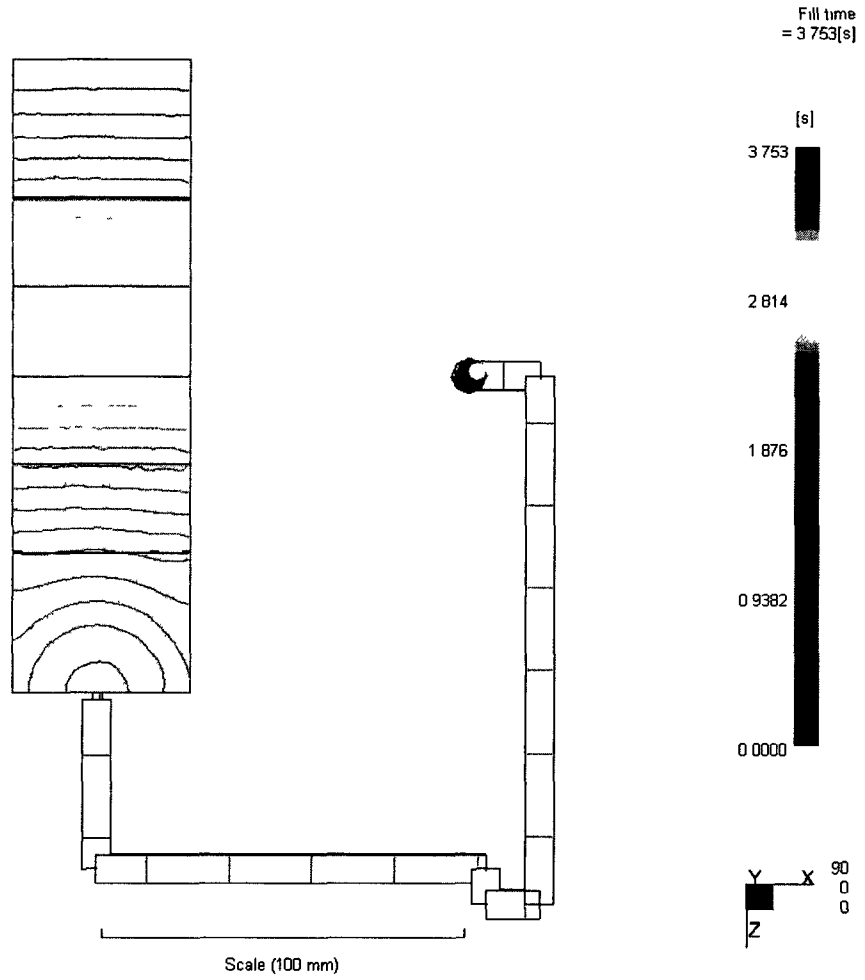


**Figure 23-2a - Flow Front Profile (top) in 2 mm perpendicular rib cavity, mtl:
2000GP @ 18.8 cc/s injection rate**

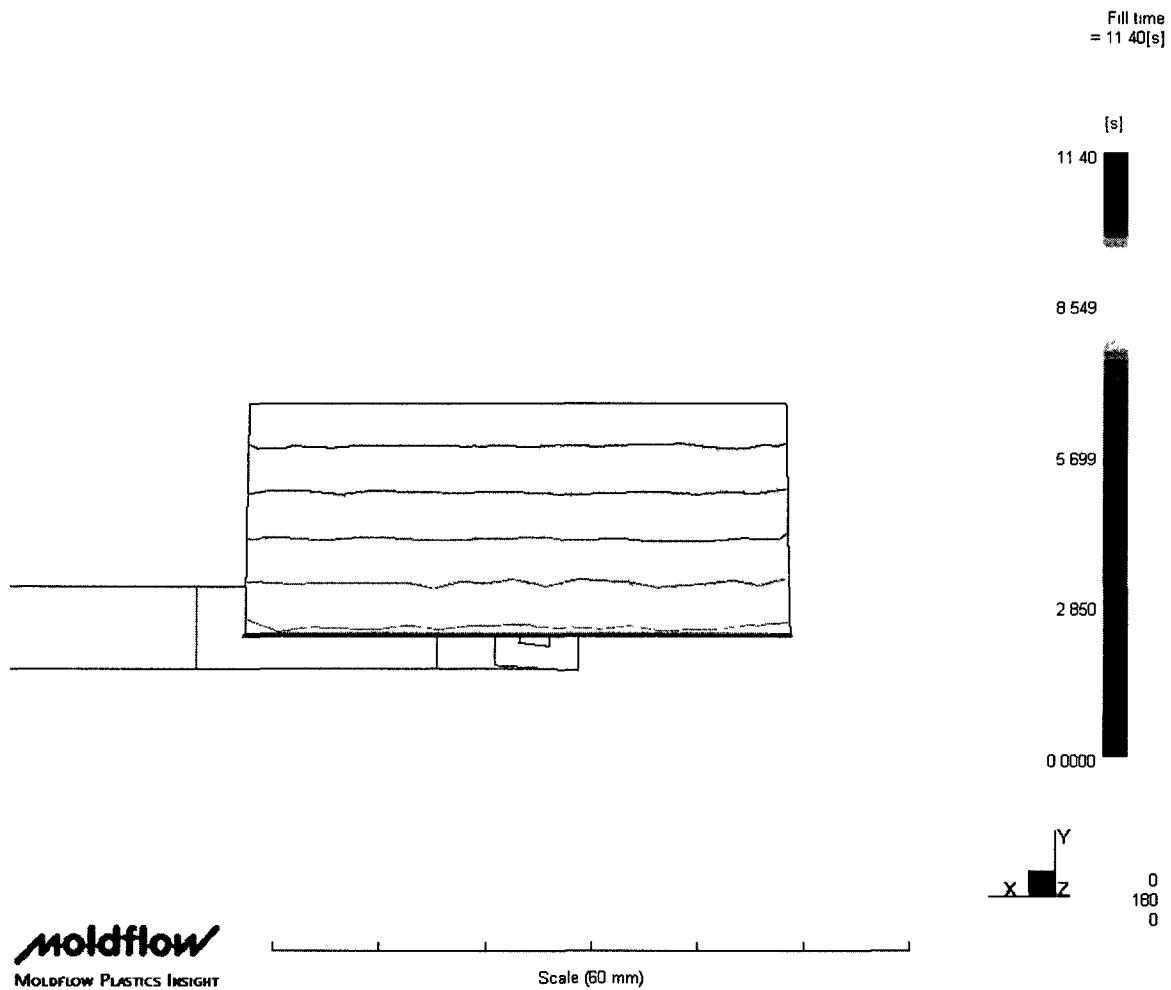


**Figure 24-1a - Flow Front Profile (last rib) in 2 mm perpendicular rib cavity, mtl:
2000GP @ 6.3 cc/s injection rate**

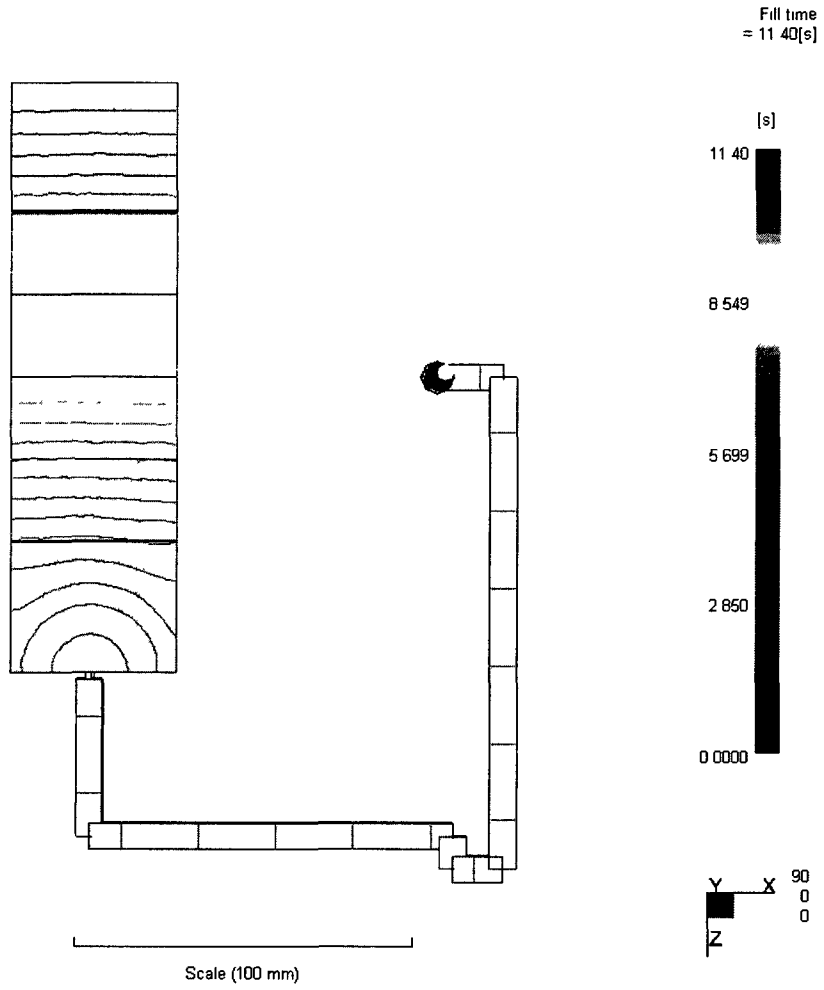


**Figure 24-2a - Flow Front Profile (top) in 2 mm perpendicular rib cavity, mtl:
2000GP @ 6.3 cc/s injection rate**

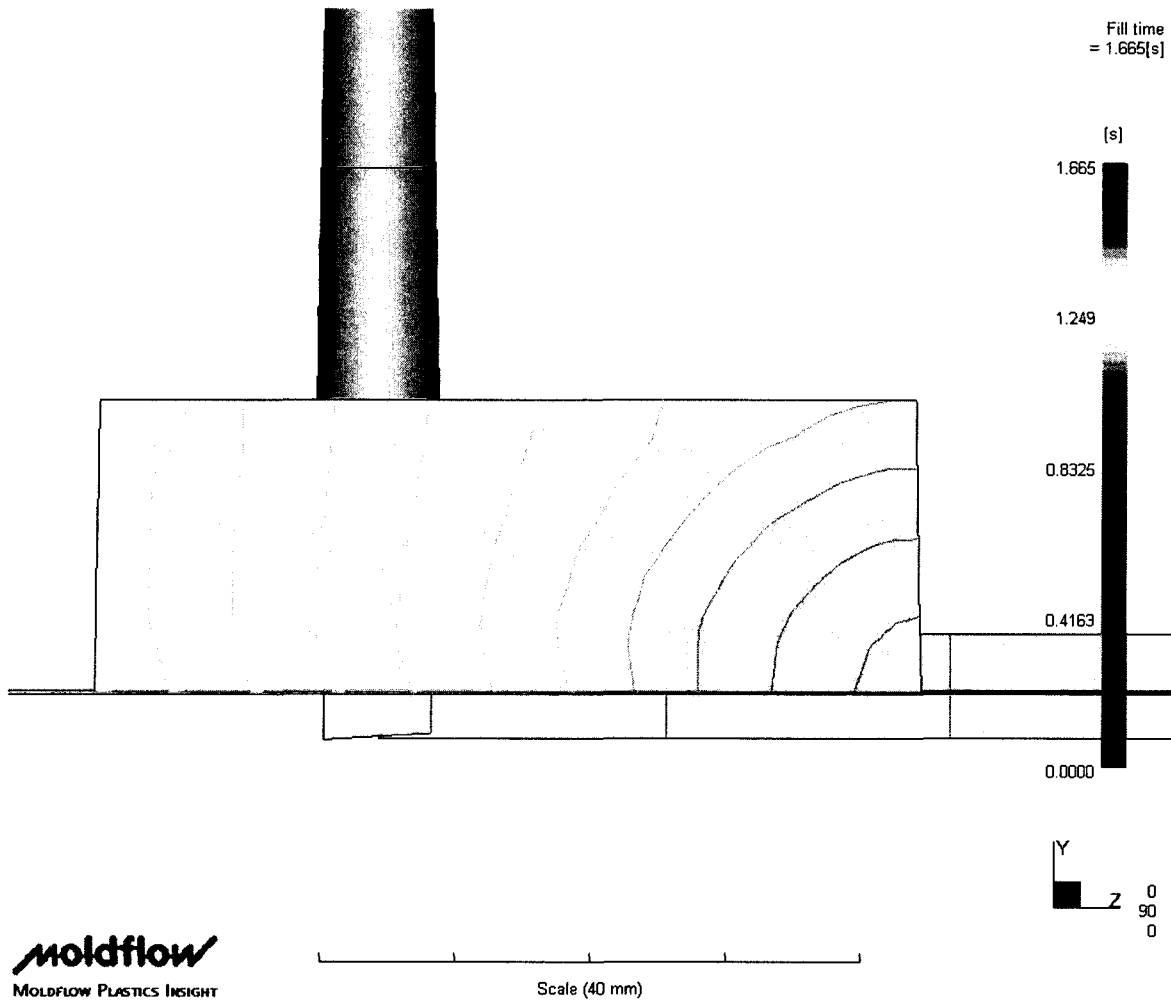


Figure 25-1a - Flow Front Profile (side) in 4 mm parallel rib cavity, mtl: CR3500 @ 18.8 cc/s injection rate

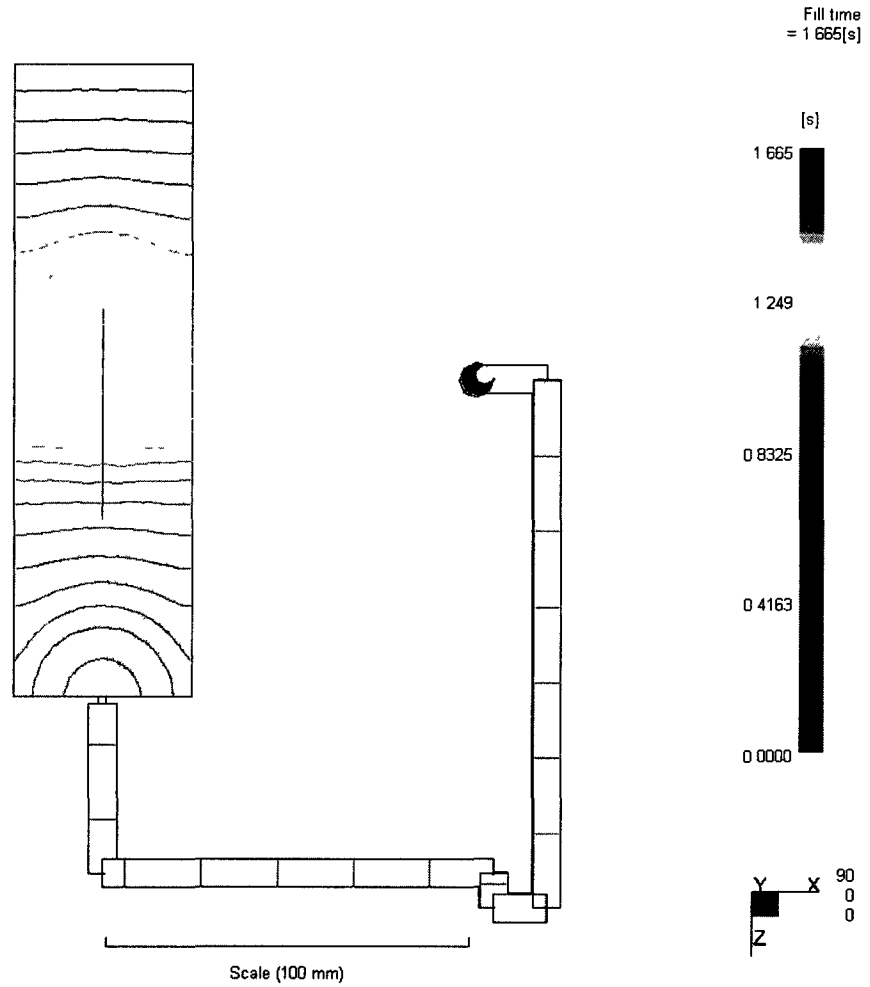


Figure 25-2a - Flow Front Profile (top) in 4 mm parallel rib cavity, mtl: CR3500 @ 37.7 cc/s injection rate

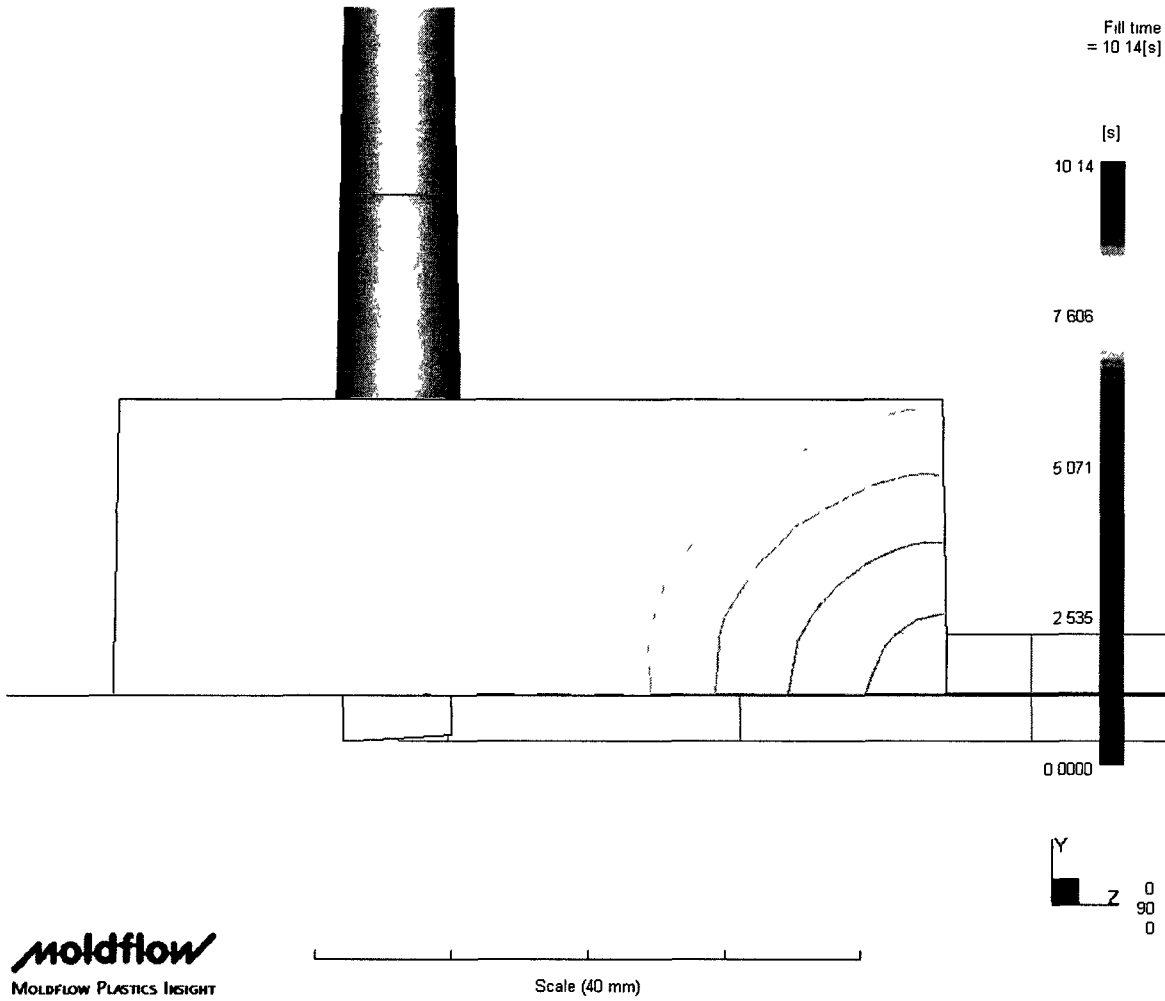


Figure 26-1a - Flow Front Profile (side) in 4 mm parallel rib cavity, mtl: CR3500 @ 6.3 cc/s injection rate

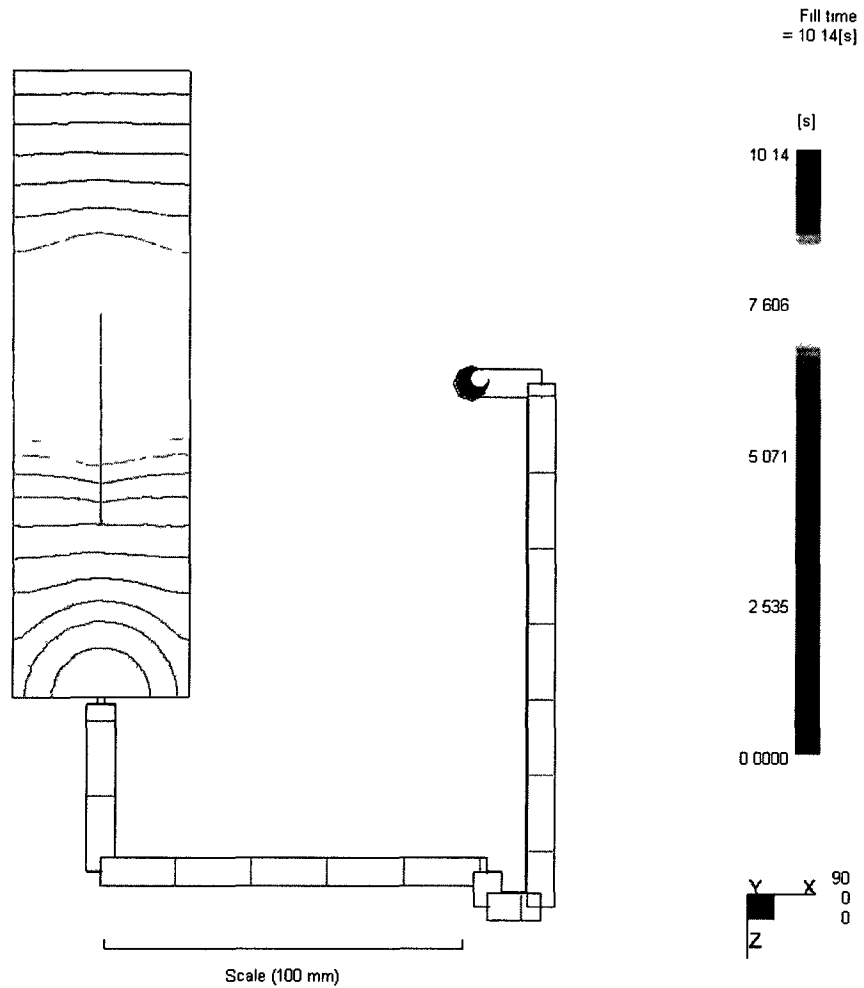


Figure 26-2a - Flow Front Profile (top) in 4 mm parallel rib cavity, mtl: CR3500 @ 6.3 cc/s injection rate

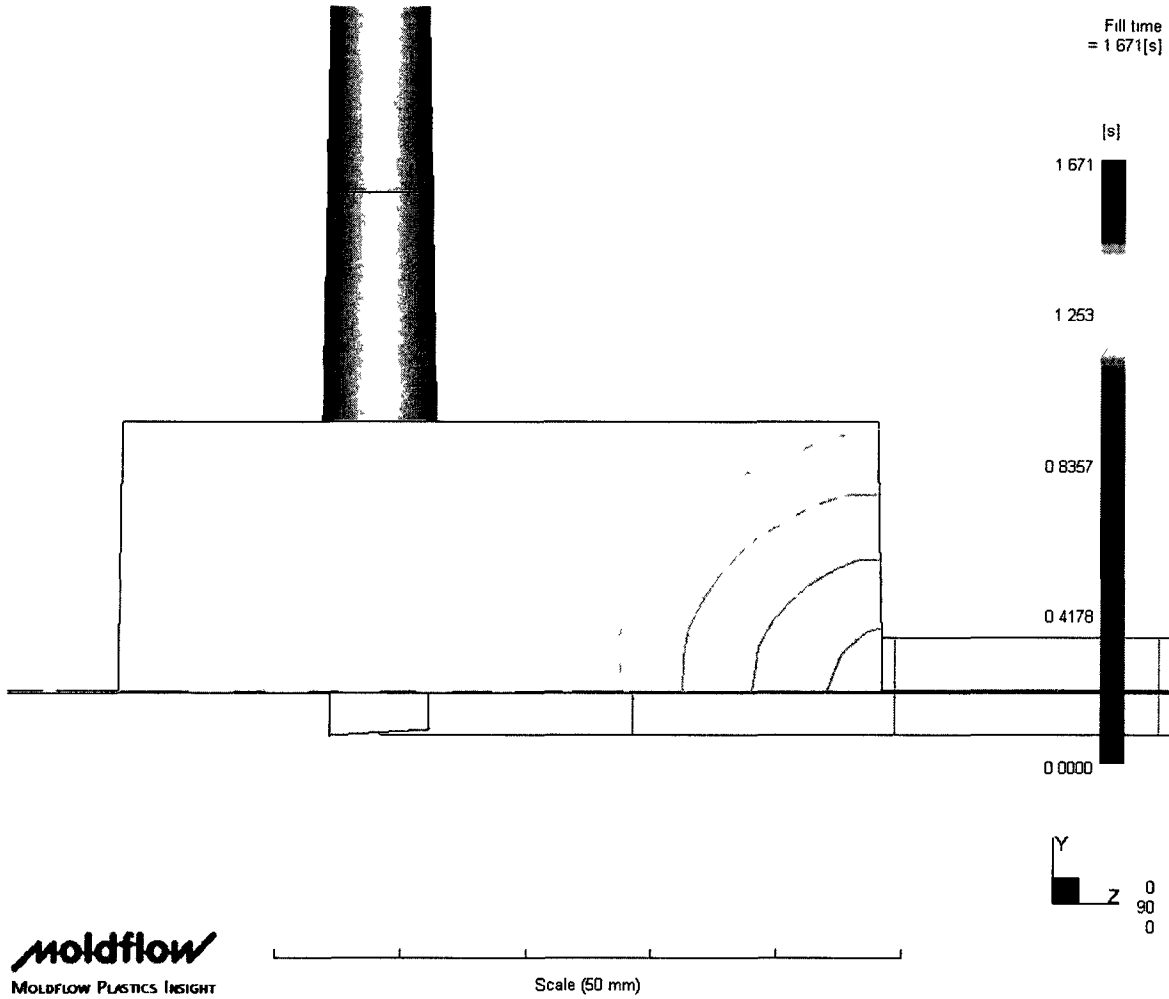


Figure 27-1a - Flow Front Profile (side) in 4 mm parallel rib cavity, mtl: CR4500 @ 37.7 cc/s injection rate

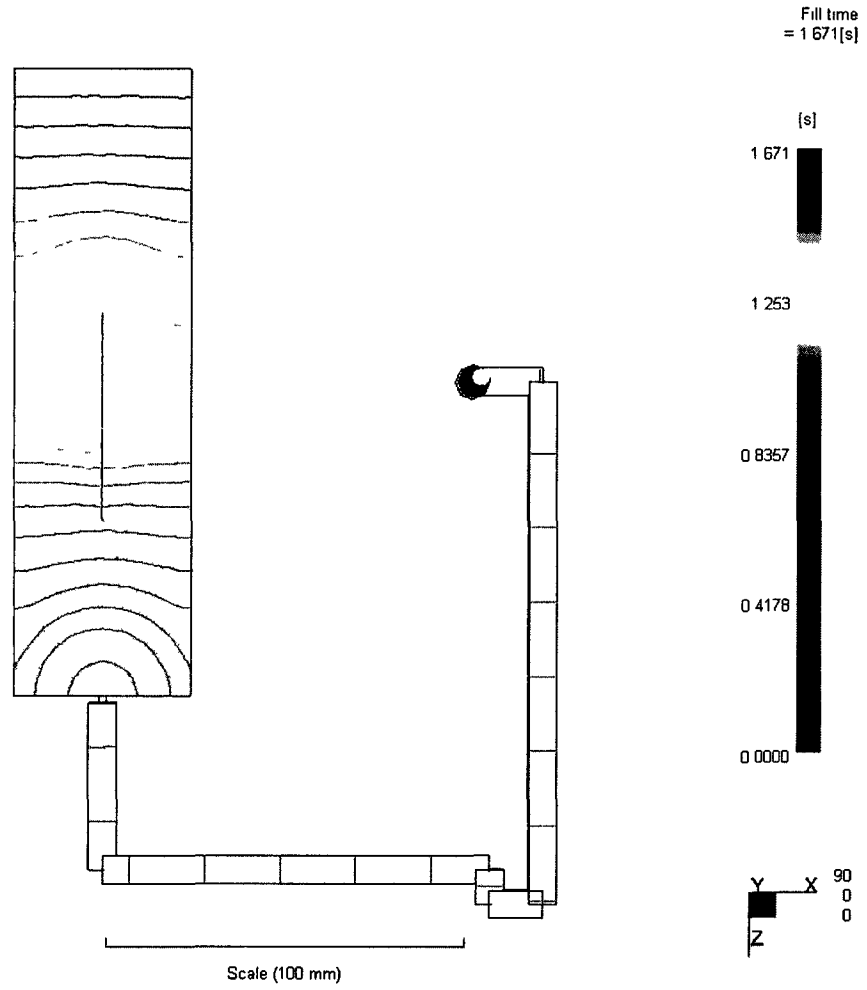


Figure 27-2a - Flow Front Profile (top) in 4 mm parallel rib cavity, mtl: CR4500 @ 37.7 cc/s injection rate

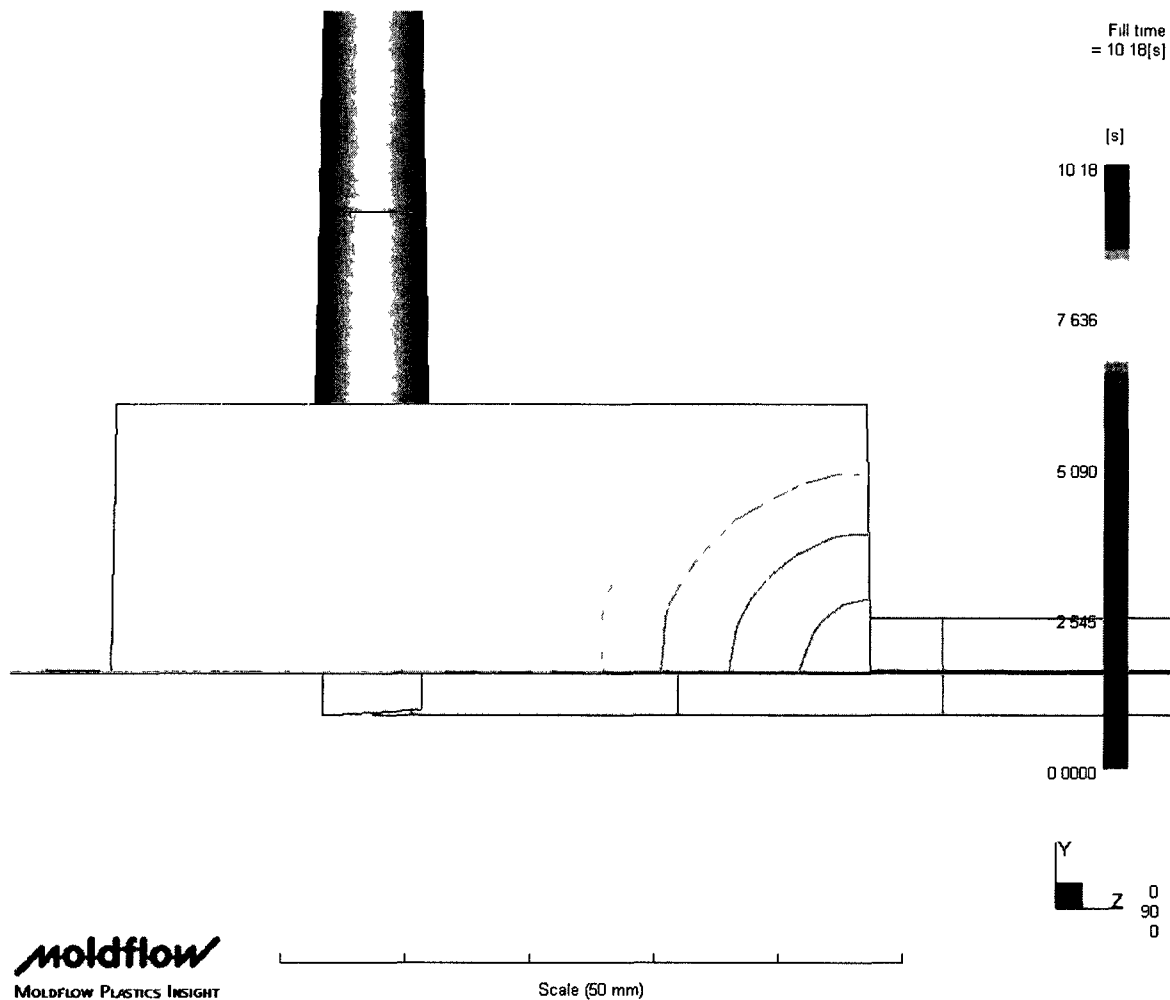


Figure 28-1a - Flow Front Profile (side) in 4 mm parallel rib cavity, mtl: CR4500 @ 6.3 cc/s injection rate

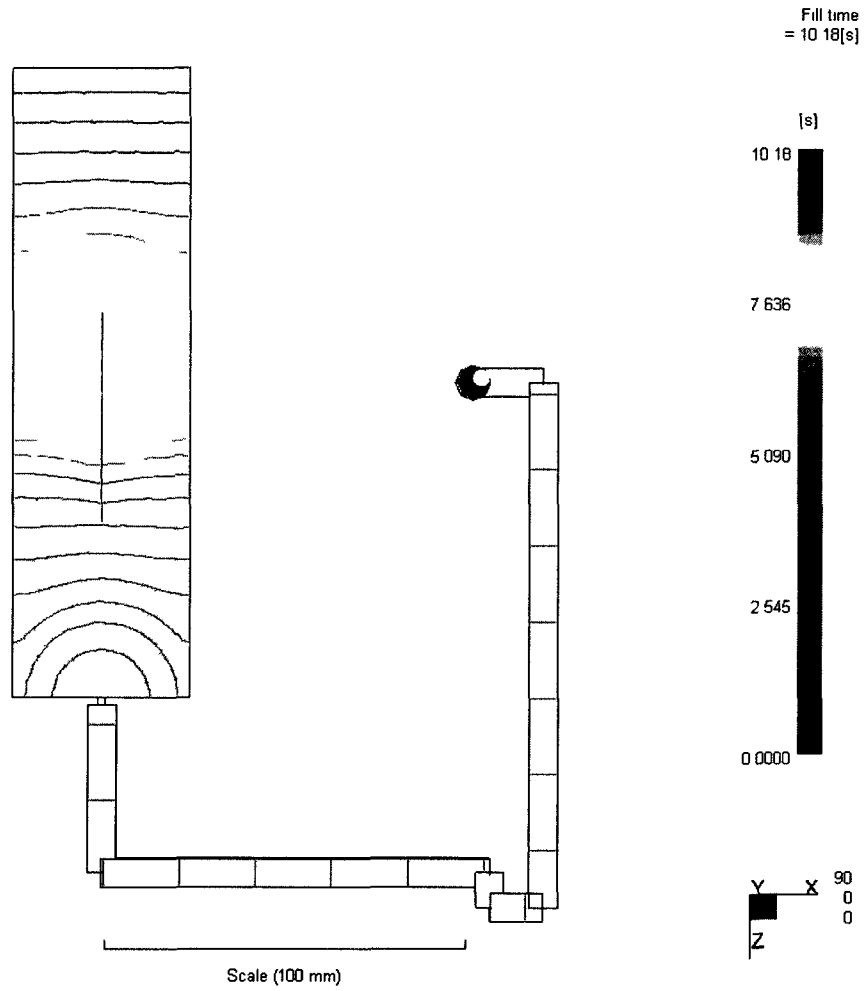


Figure 28-2a - Flow Front Profile (top) in 4 mm parallel rib cavity, mtl: CR4500 @ 6.3 cc/s injection rate

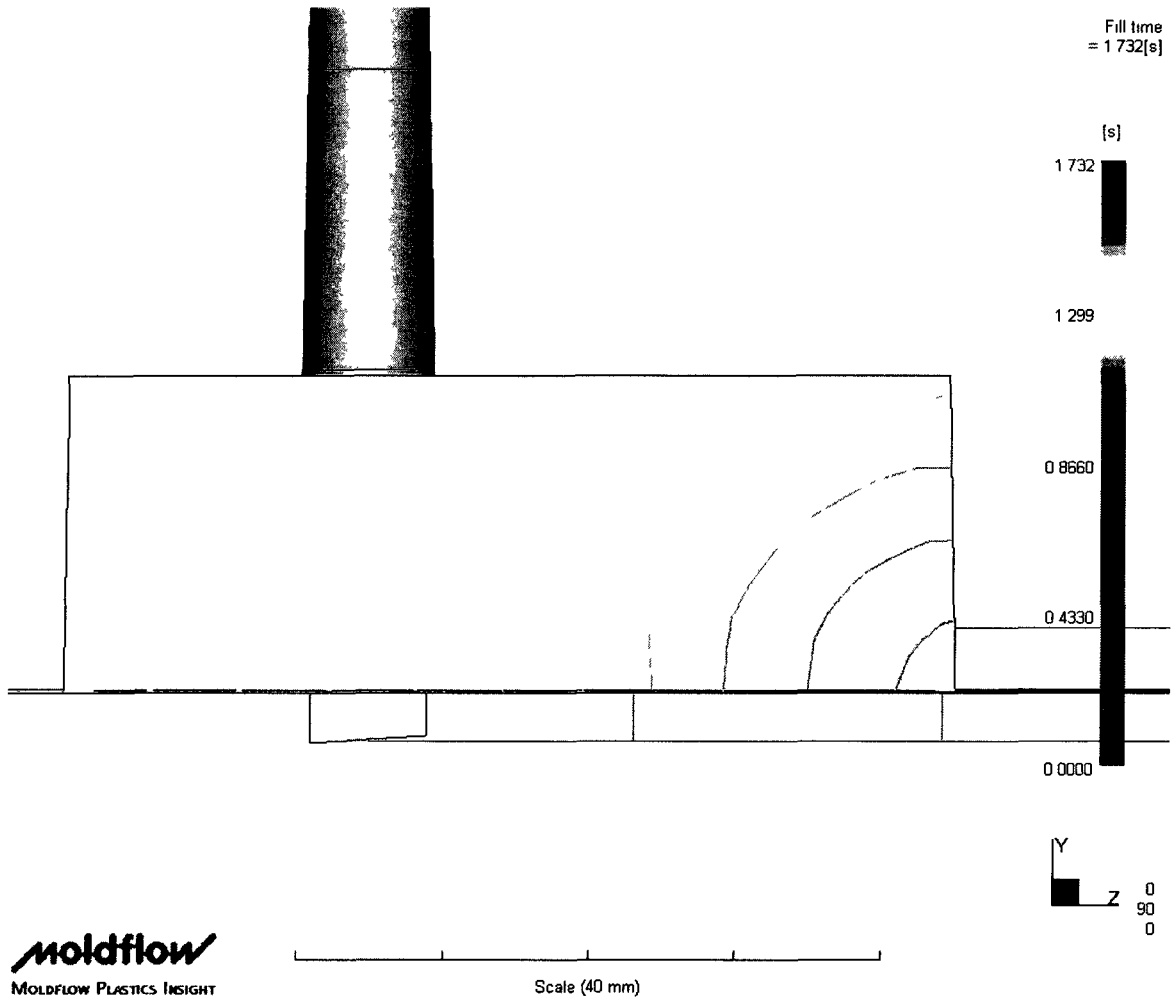


Figure 29-1a - Flow Front Profile (side) in 4 mm parallel rib cavity, mtl: 700GP @ 37.7 cc/s injection rate

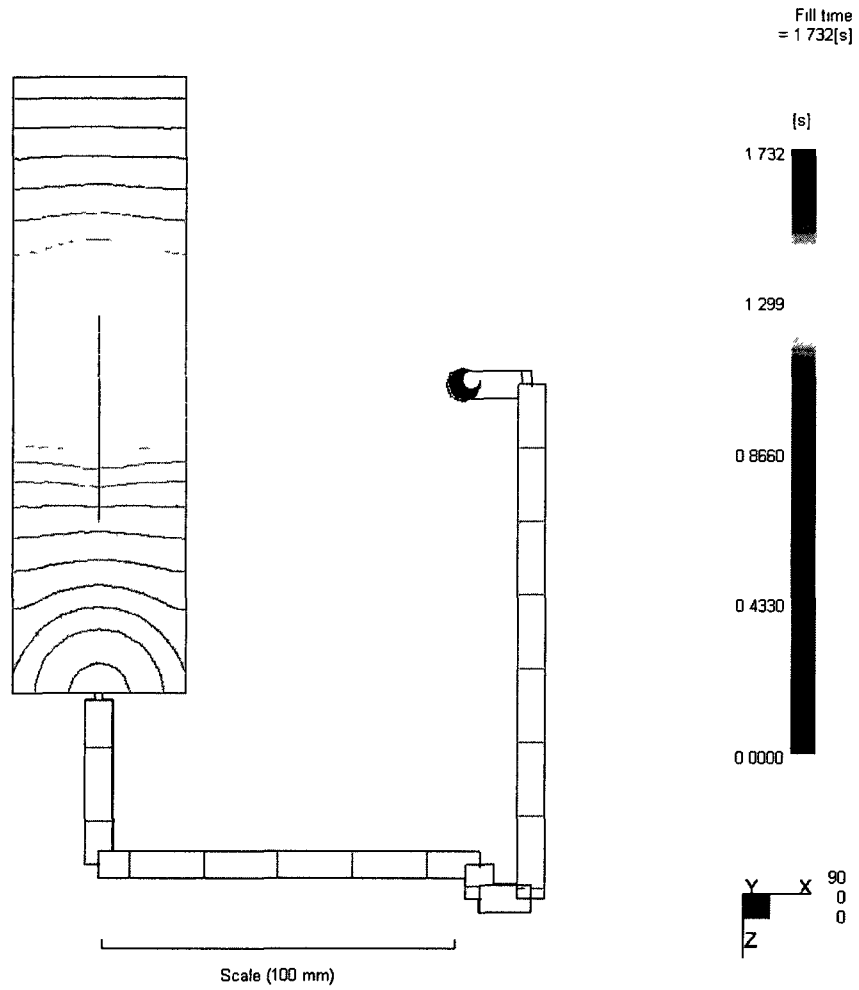


Figure 29-2a - Flow Front Profile (top) in 4 mm parallel rib cavity, mtl: 700GP @ 37.7 cc/s injection rate

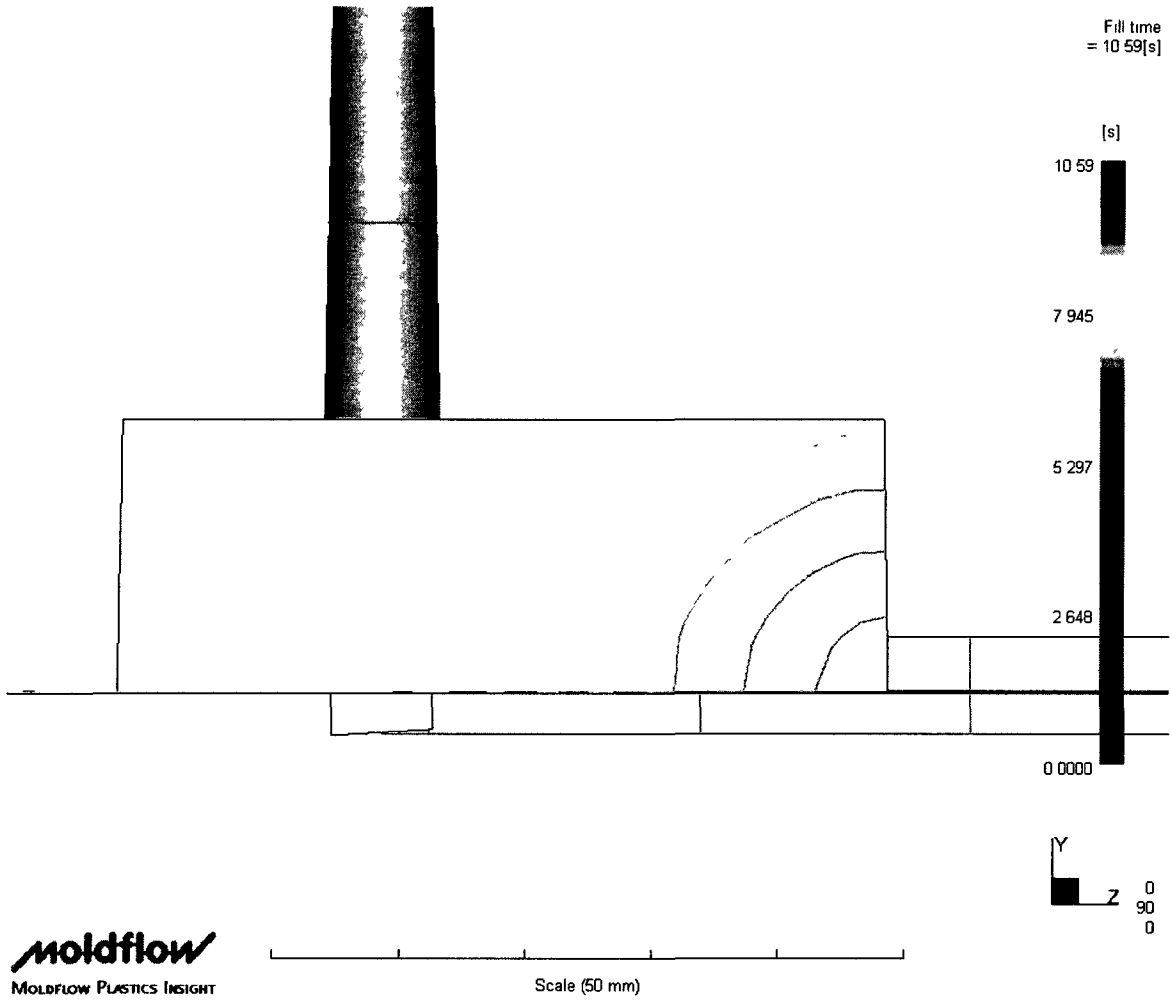


Figure 30-1a - Flow Front Profile (side) in 4 mm parallel rib cavity, mtl: 700GP @ 6.3 cc/s injection rate

moldflow
MOLDFLOW PLASTICS INSIGHT

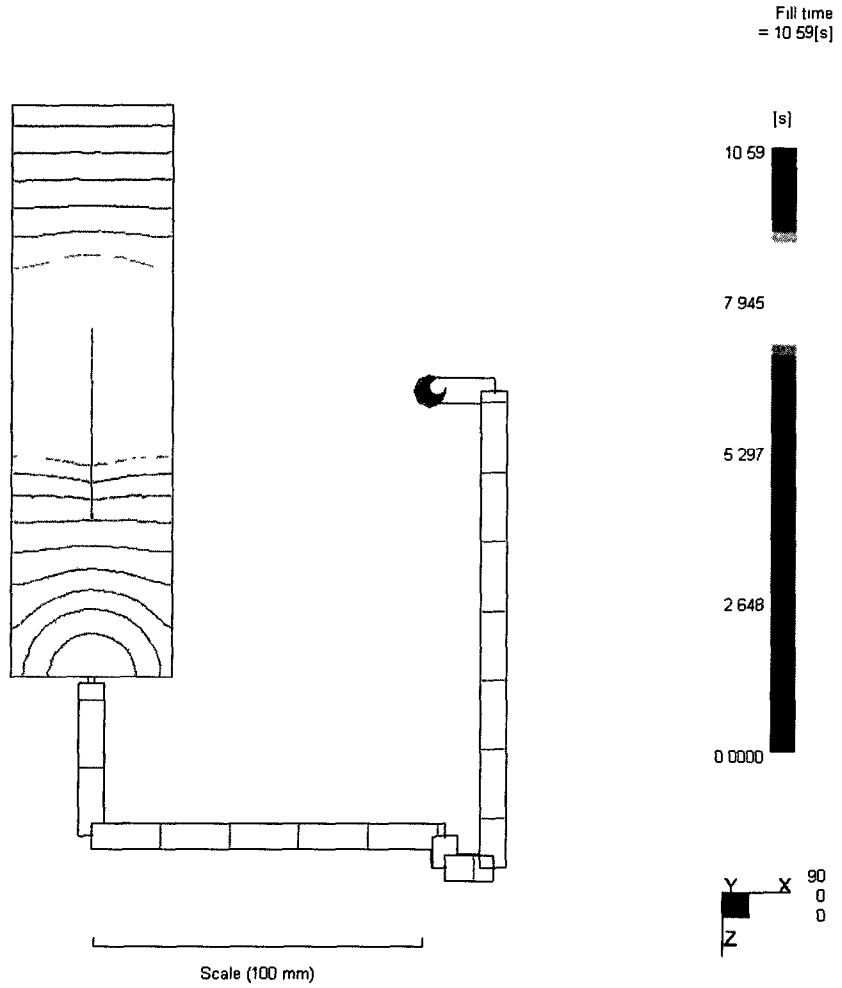


Figure 30-2a - Flow Front Profile (top) in 4 mm parallel rib cavity, mtl: 700GP @ 6.3 cc/s injection rate

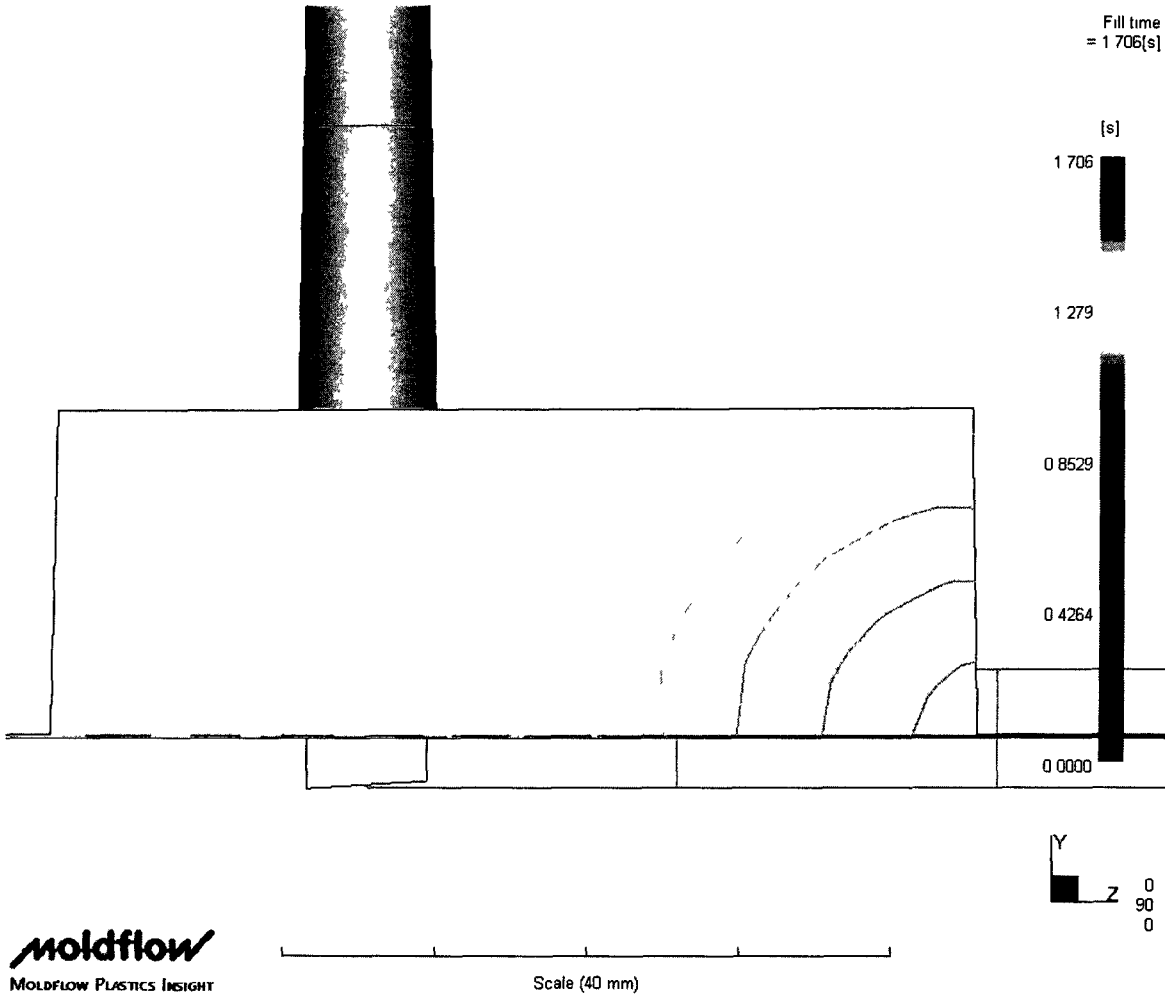
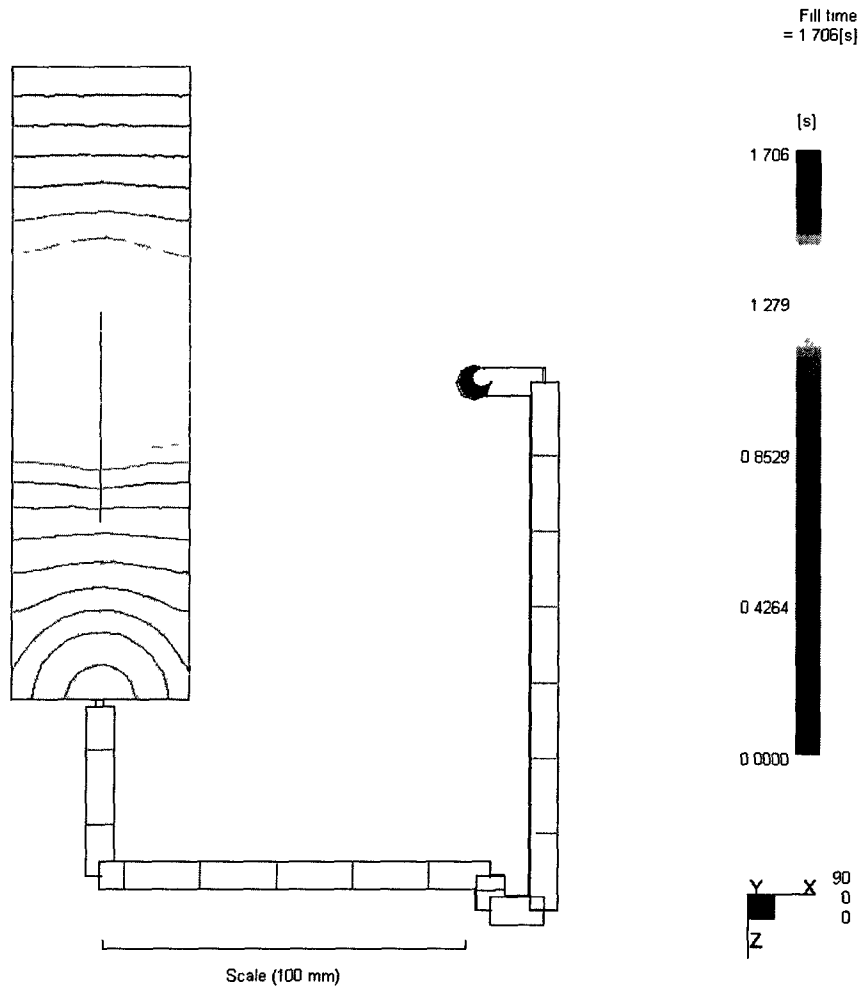


Figure 31-1a - Flow Front Profile (side) in 4 mm parallel rib cavity, mtl: 2000GP @ 37.7cc/s injection rate



**Figure 31-2a - Flow Front Profile (top) in 4 mm parallel rib cavity, mtl: 2000GP @
37.7cc/s injection rate**

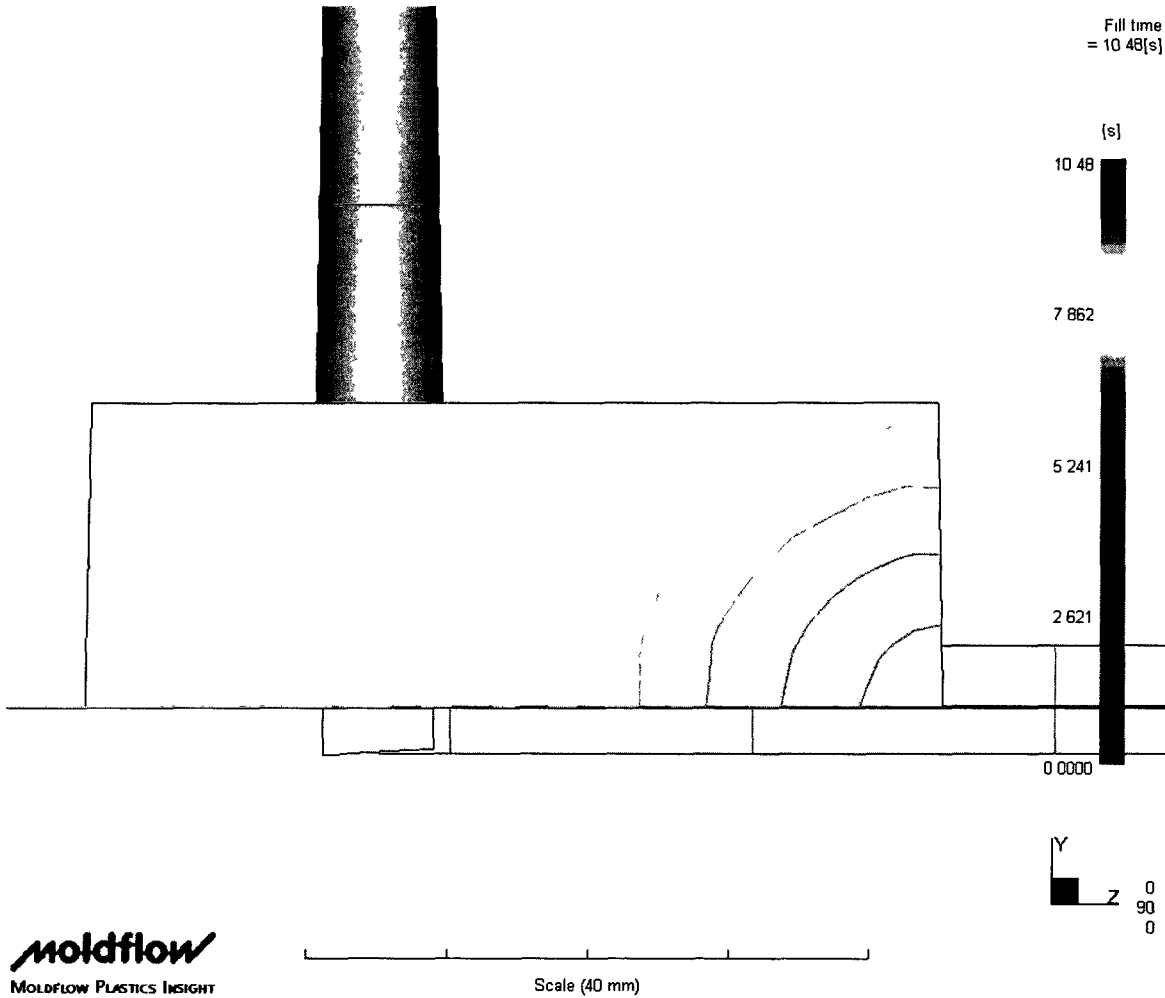


Figure 32-1a - Flow Front Profile (side) in 4 mm parallel rib cavity, mtl: 2000GP @ 6.3 cc/s injection rate

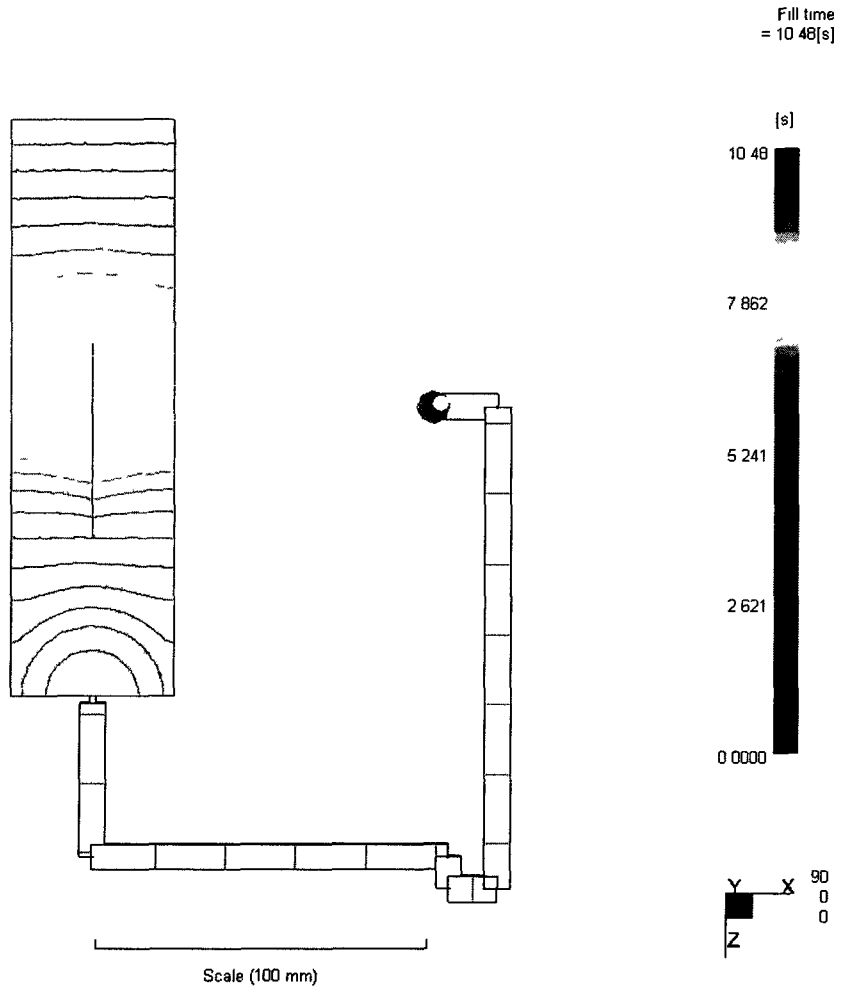
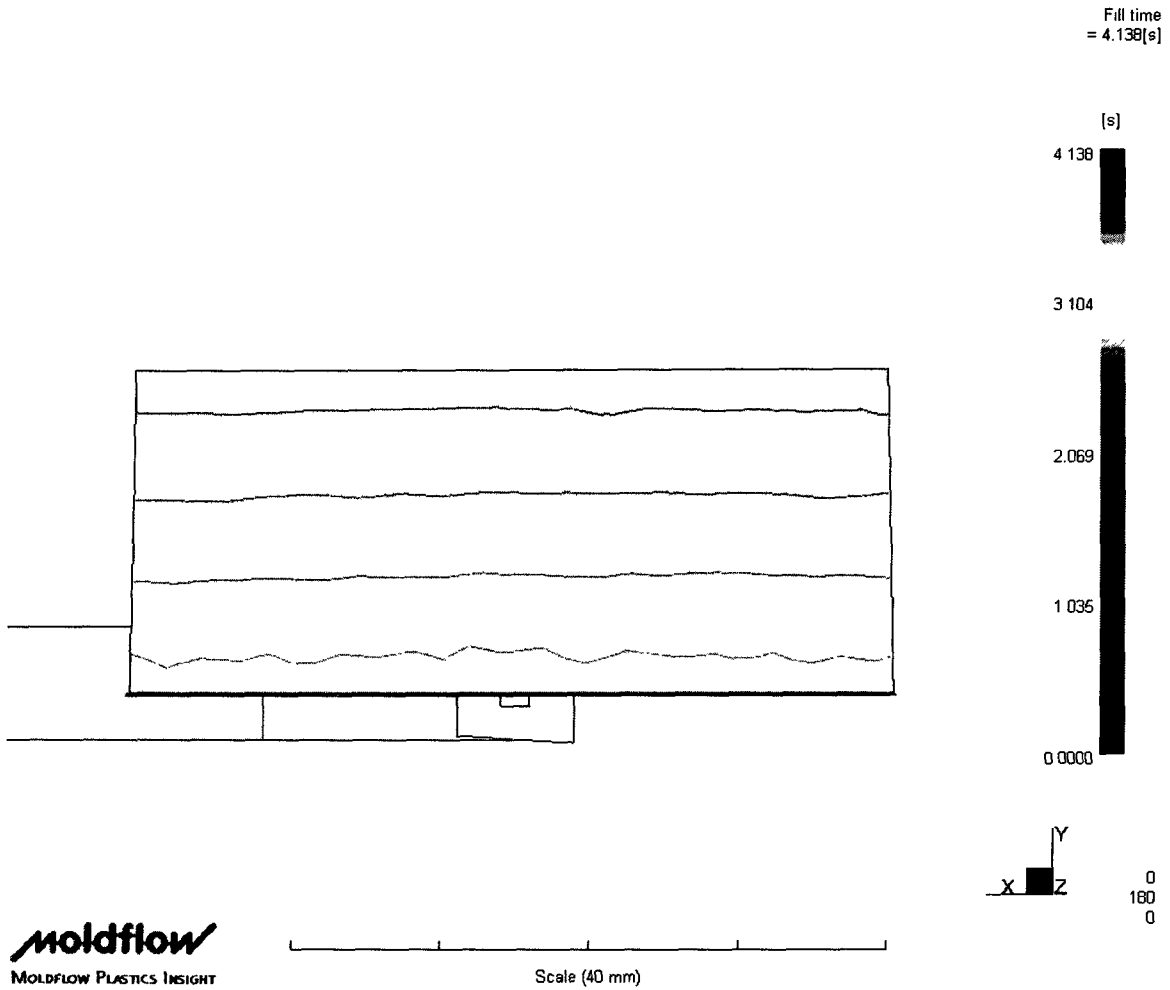
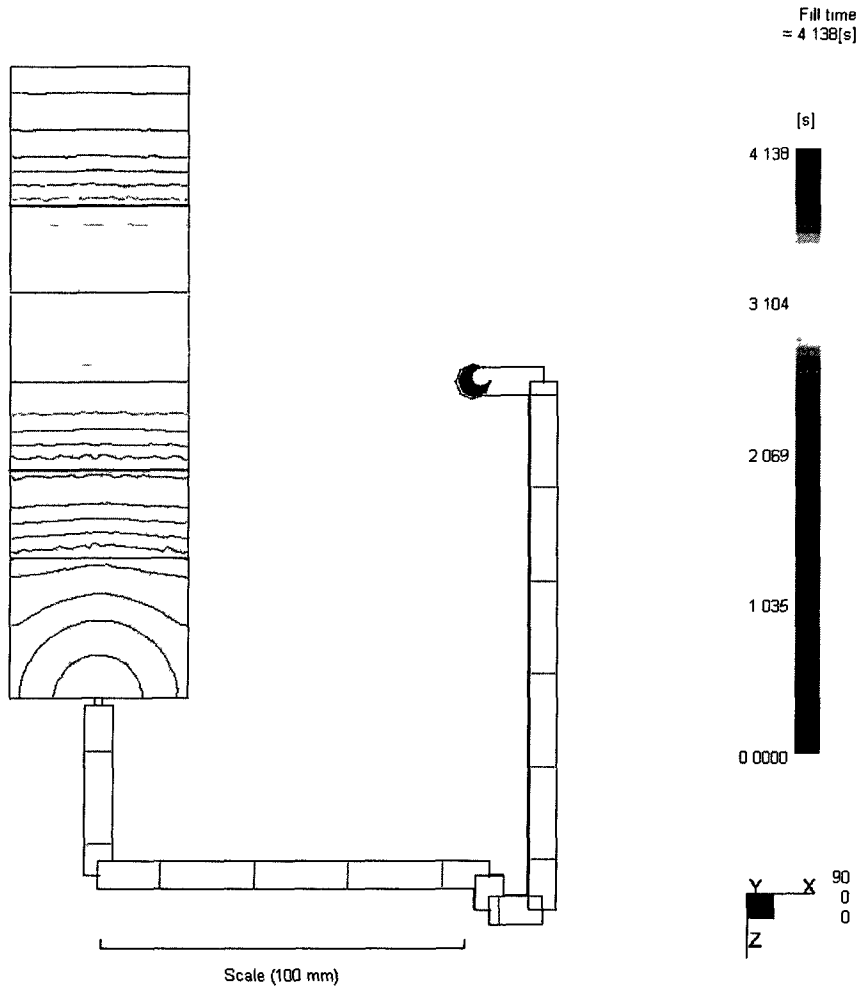


Figure 32-2a - Flow Front Profile (top) in 4 mm parallel rib cavity, mtl: 2000GP @ 6.3 cc/s injection rate



**Figure 33-1a - Flow Front Profile (last rib) in 4 mm perpendicular rib cavity, mtl:
CR3500 @ 18.8 cc/s injection rate**



**Figure 33-2a - Flow Front Profile (top) in 4 mm perpendicular rib cavity, mtl:
CR3500 @ 18.8 cc/s injection rate**

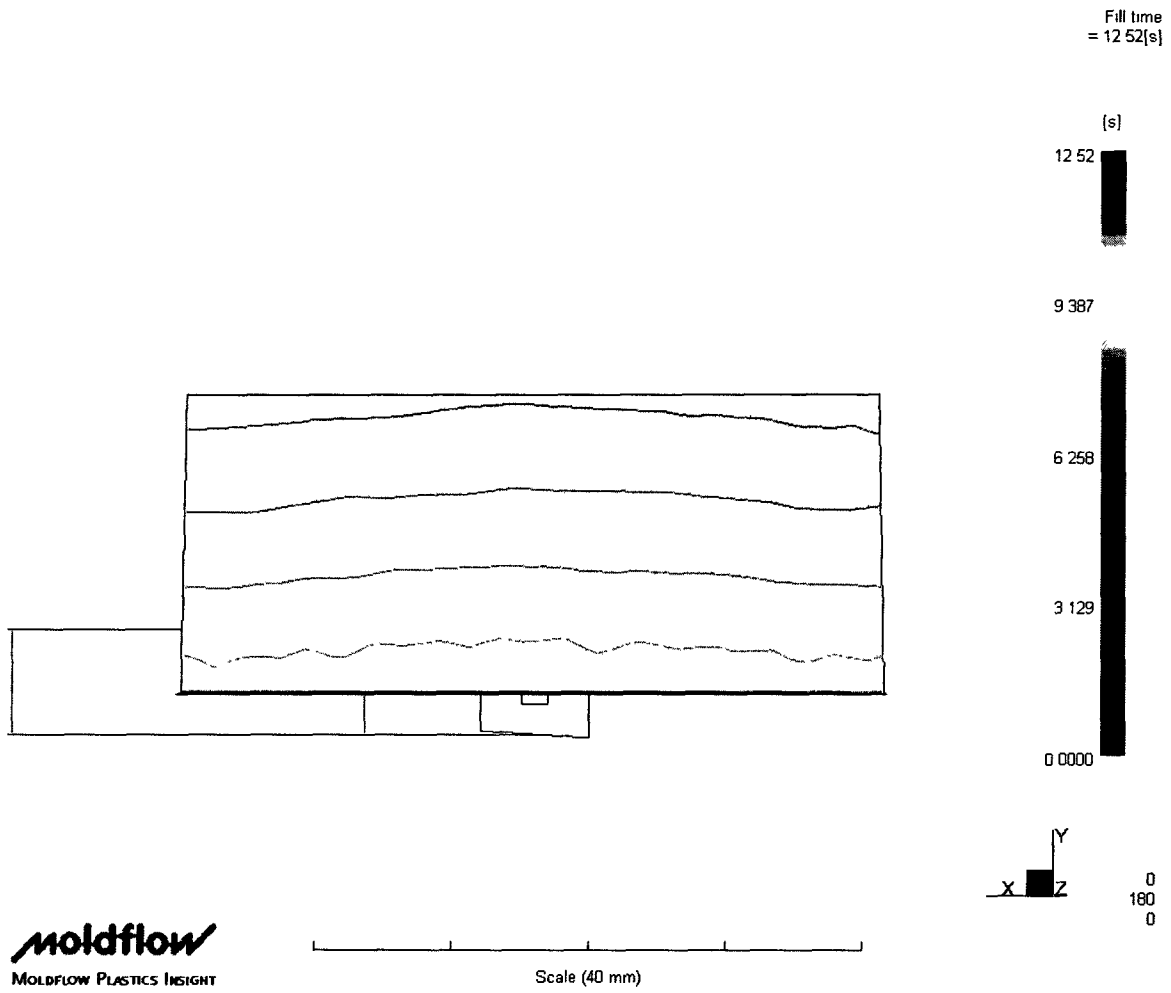


**Figure 34-1a - Flow Front Profile (last rib) in 4 mm perpendicular rib cavity, mtl:
CR3500 @ 6.3 cc/s injection rate**

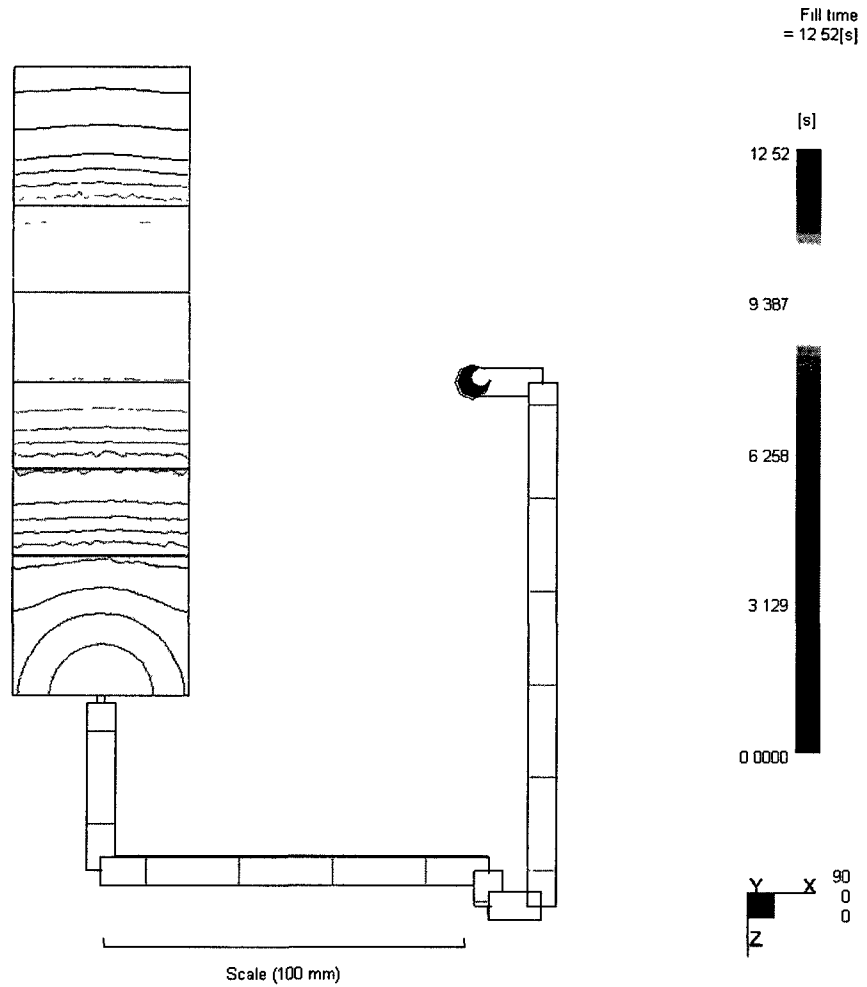
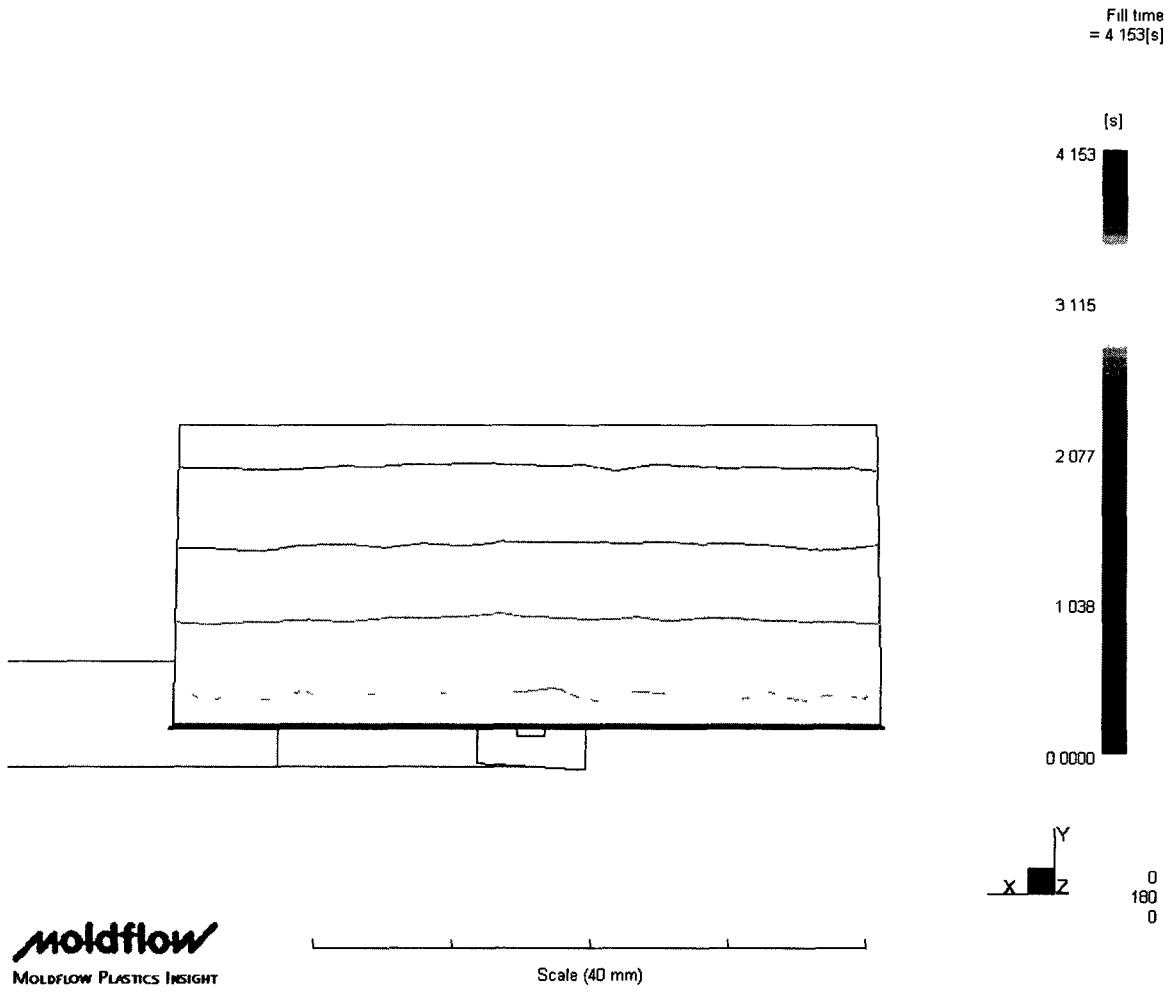
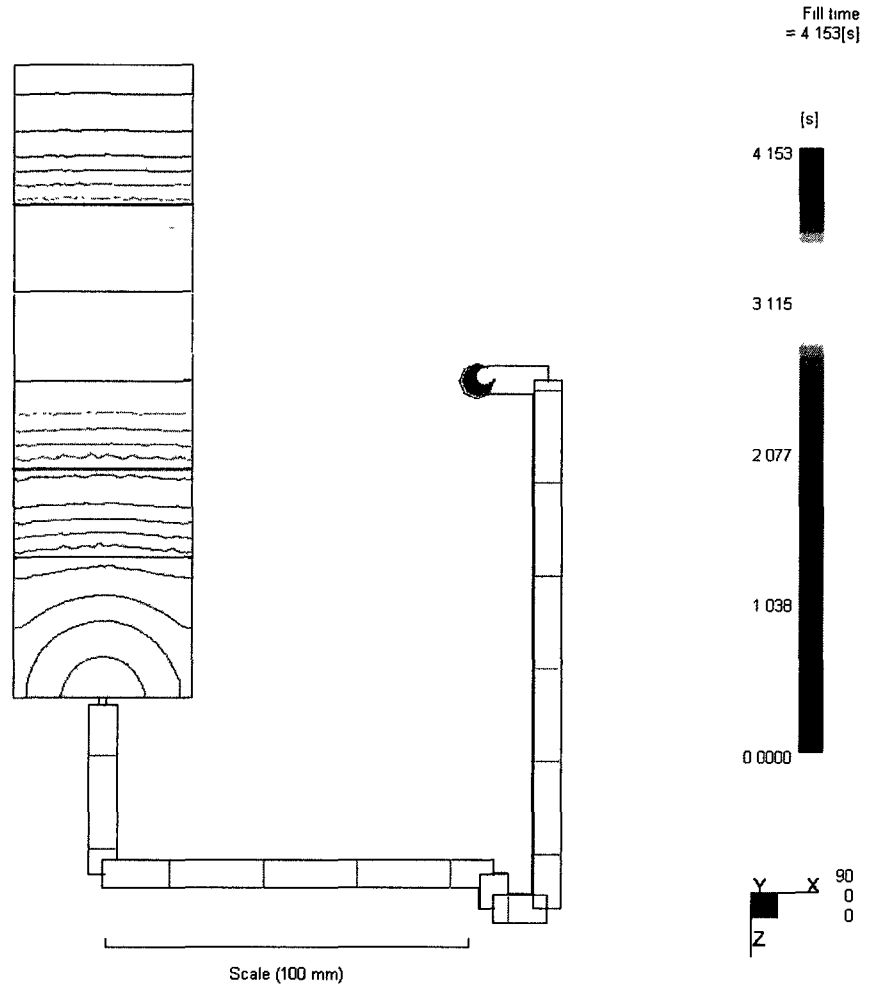


Figure 34-2a - Flow Front Profile (top) in 4 mm perpendicular rib cavity, mtl: CR3500 @ 6.3 cc/s injection rate



**Figure 35-1a - Flow Front Profile (last rib) in 4 mm perpendicular rib cavity, mtl:
CR4500 @ 18.8 cc/s injection rate**



**Figure 35-2a - Flow Front Profile (top) in 4 mm perpendicular rib cavity, mtl:
CR4500 @ 18.8 cc/s injection rate**

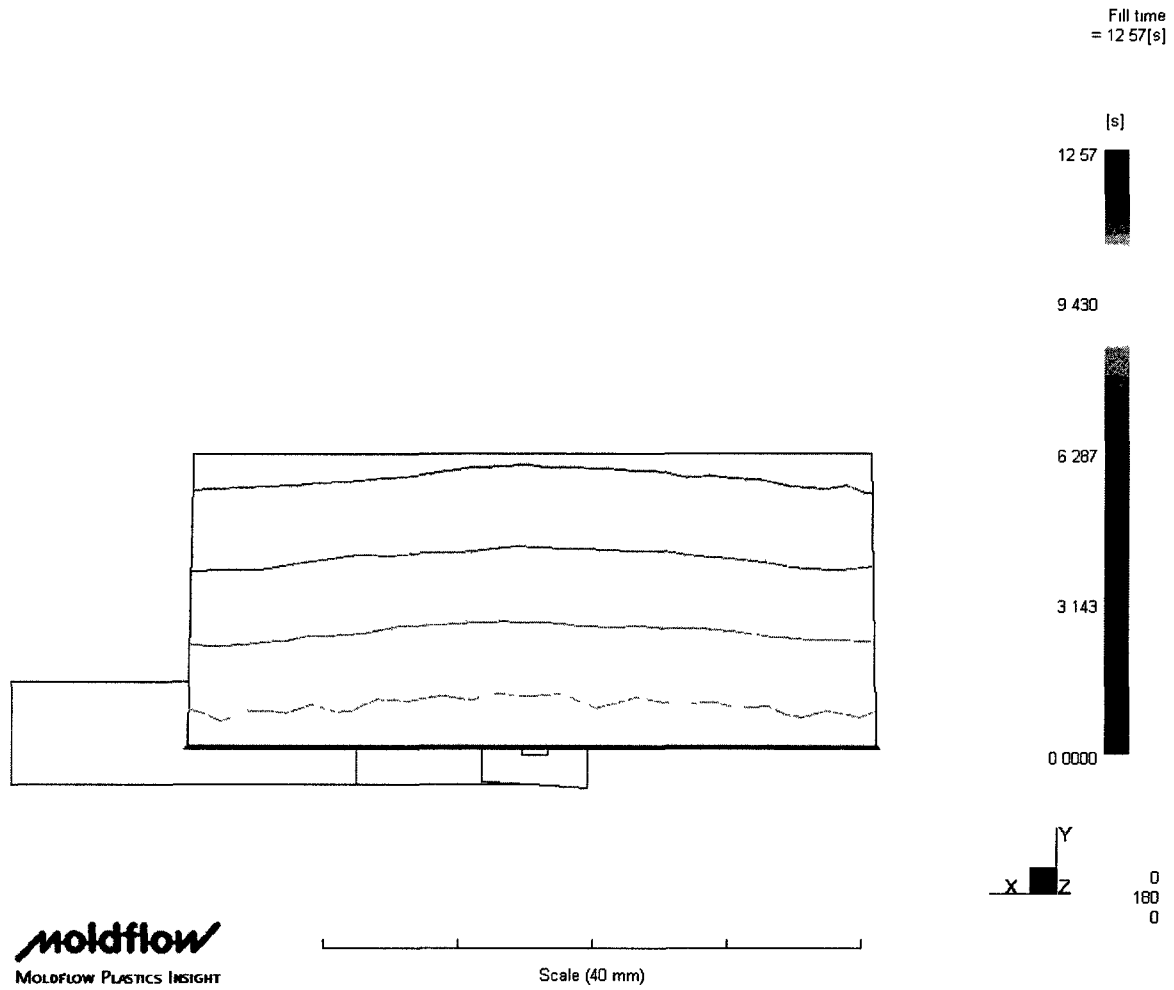


**Figure 36-1a - Flow Front Profile (last rib) in 4 mm perpendicular rib cavity, mtl:
CR4500 @ 6.3 cc/s injection rate**

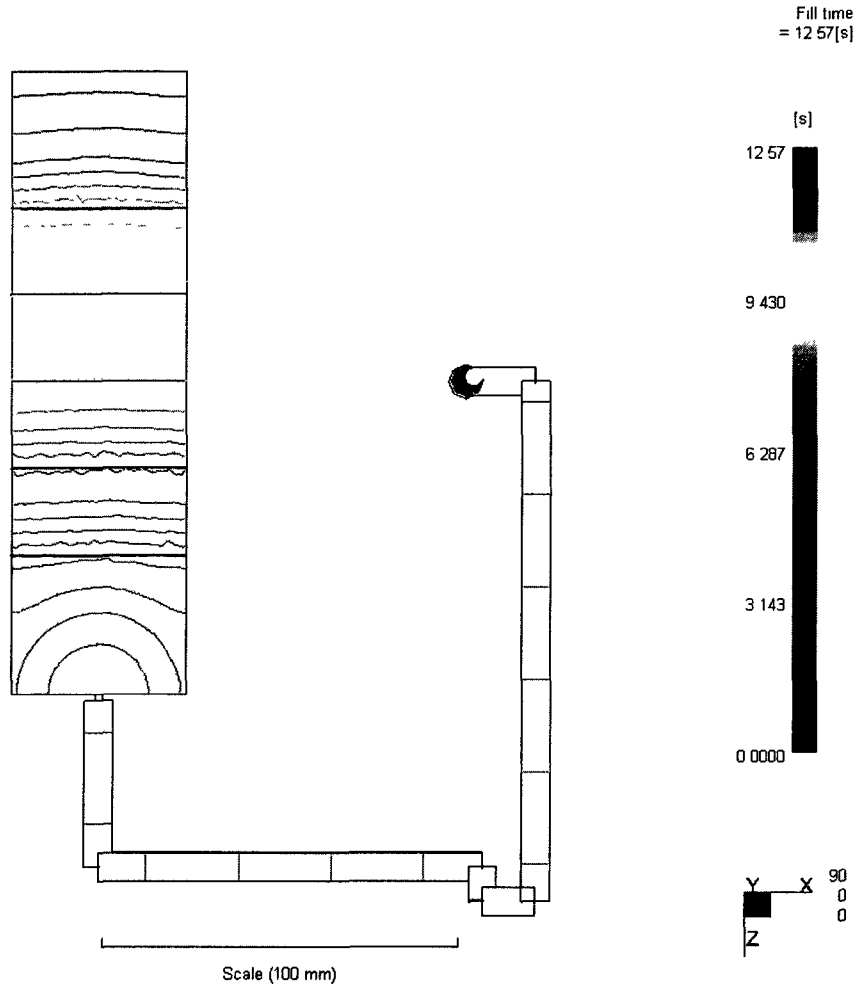


**Figure 36-2a - Flow Front Profile (top) in 4 mm perpendicular rib cavity, mtl:
CR4500 @ 6.3 cc/s injection rate**

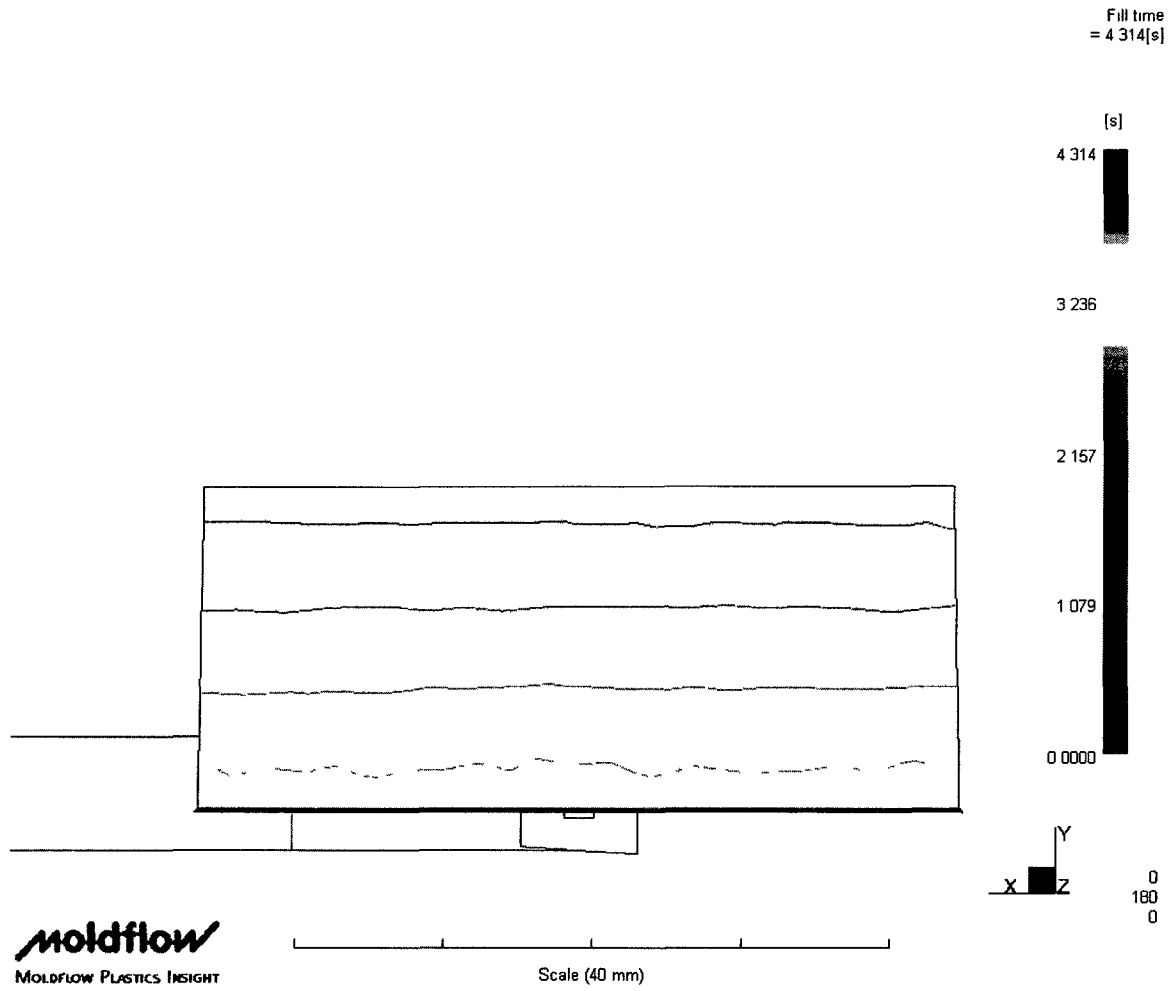
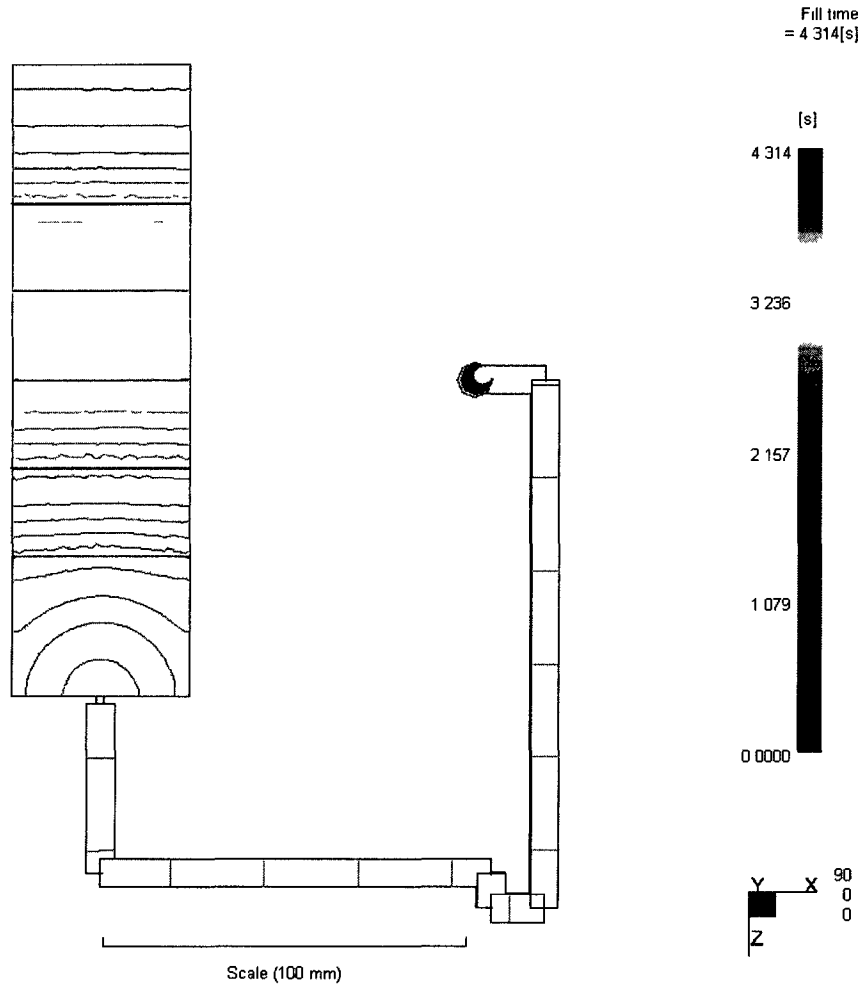
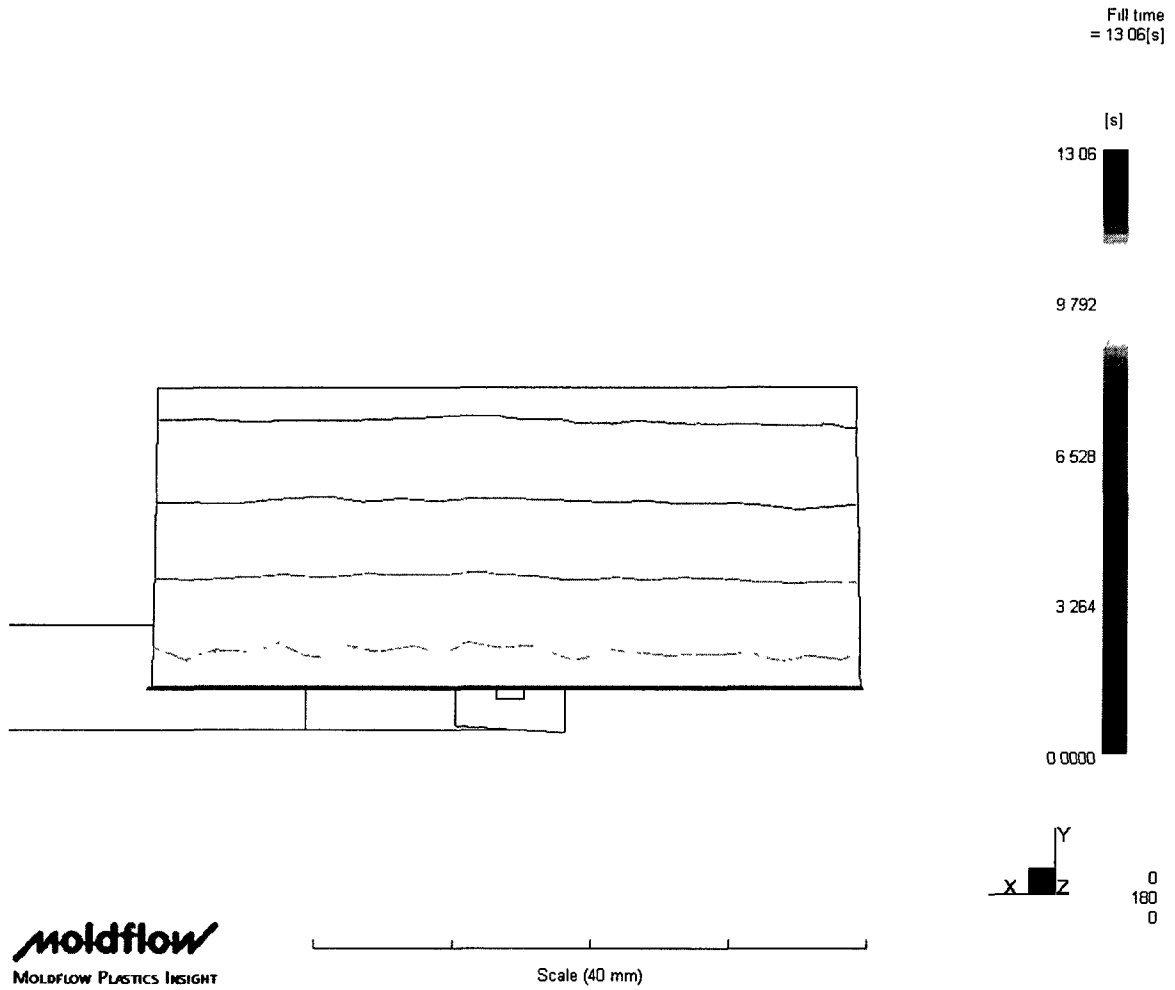


Figure 37-1a - Flow Front Profile (last rib) in 4 mm perpendicular rib cavity, mtl:
700GP @ 18.8 cc/s injection rate



**Figure 37-2a - Flow Front Profile (top) in 4 mm perpendicular rib cavity, mtl:
700GP @ 18.8 cc/s injection rate**



**Figure 38-1a - Flow Front Profile (last rib) in 4 mm perpendicular rib cavity, mtl:
700GP @ 6.3 cc/s injection rate**

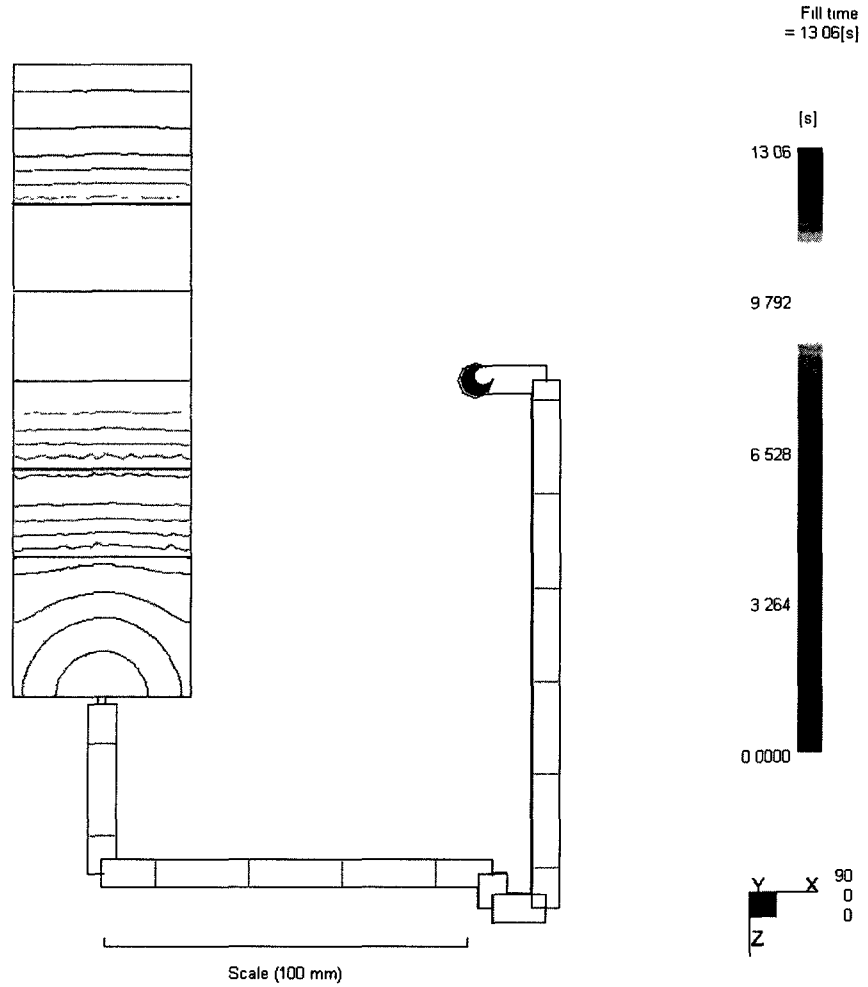


**Figure 38-2a - Flow Front Profile (top) in 4 mm perpendicular rib cavity, mtl:
700GP @ 6.3 cc/s injection rate**

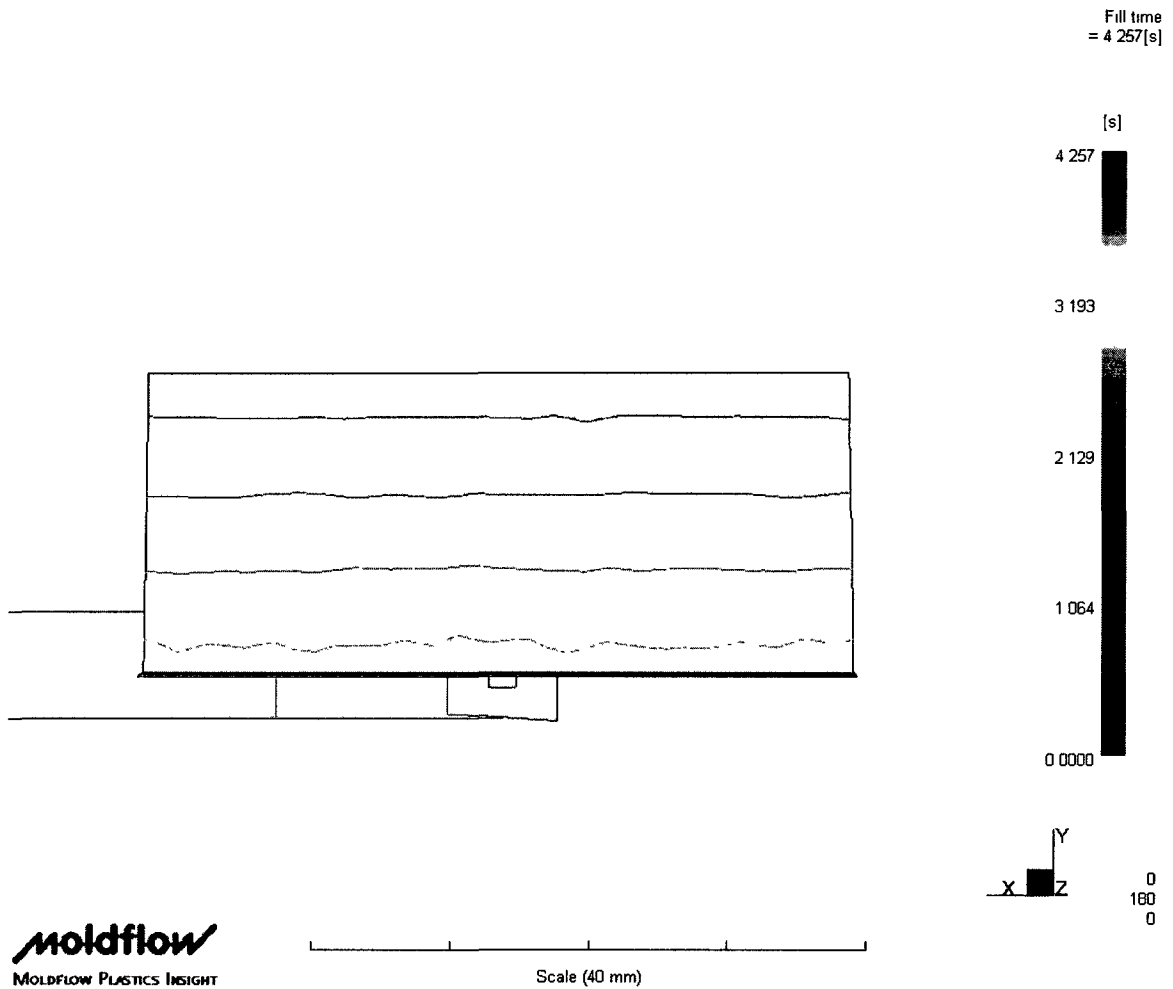


**Figure 39-1a - Flow Front Profile (last rib) in 4 mm perpendicular rib cavity, mtl:
2000GP @ 18.8 cc/s injection rate**

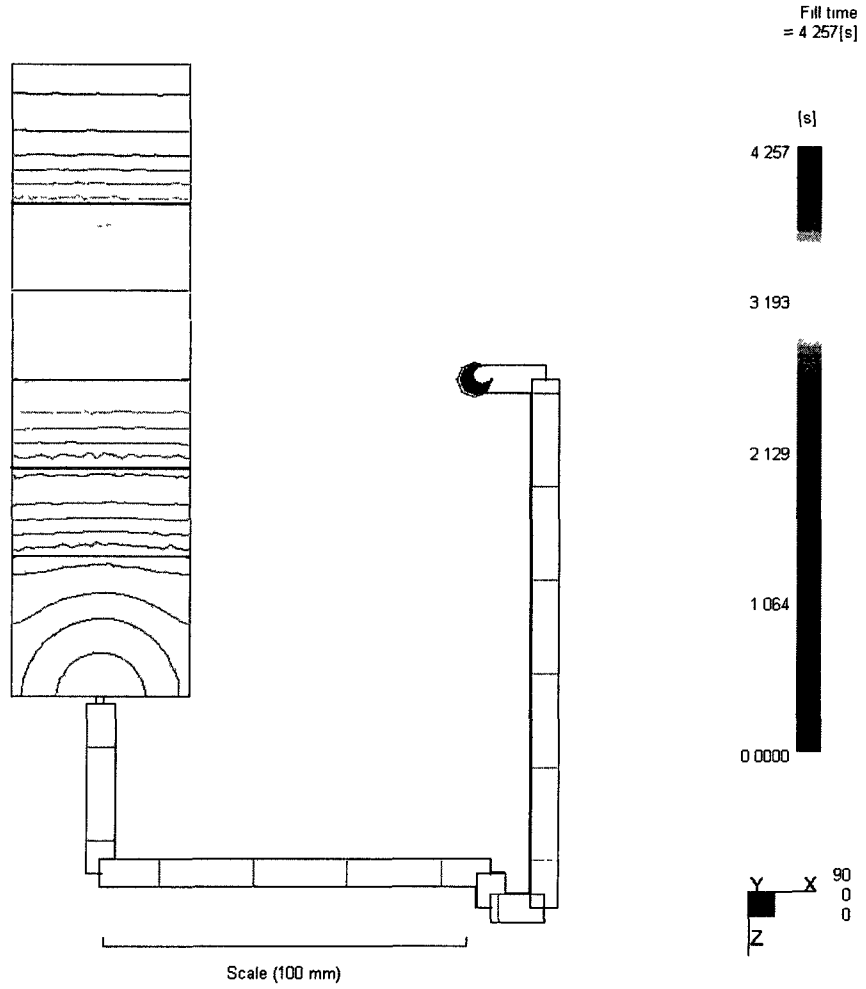


**Figure 39-2a - Flow Front Profile (top) in 4 mm perpendicular rib cavity, mtl:
2000GP @ 18.8 cc/s injection rate**

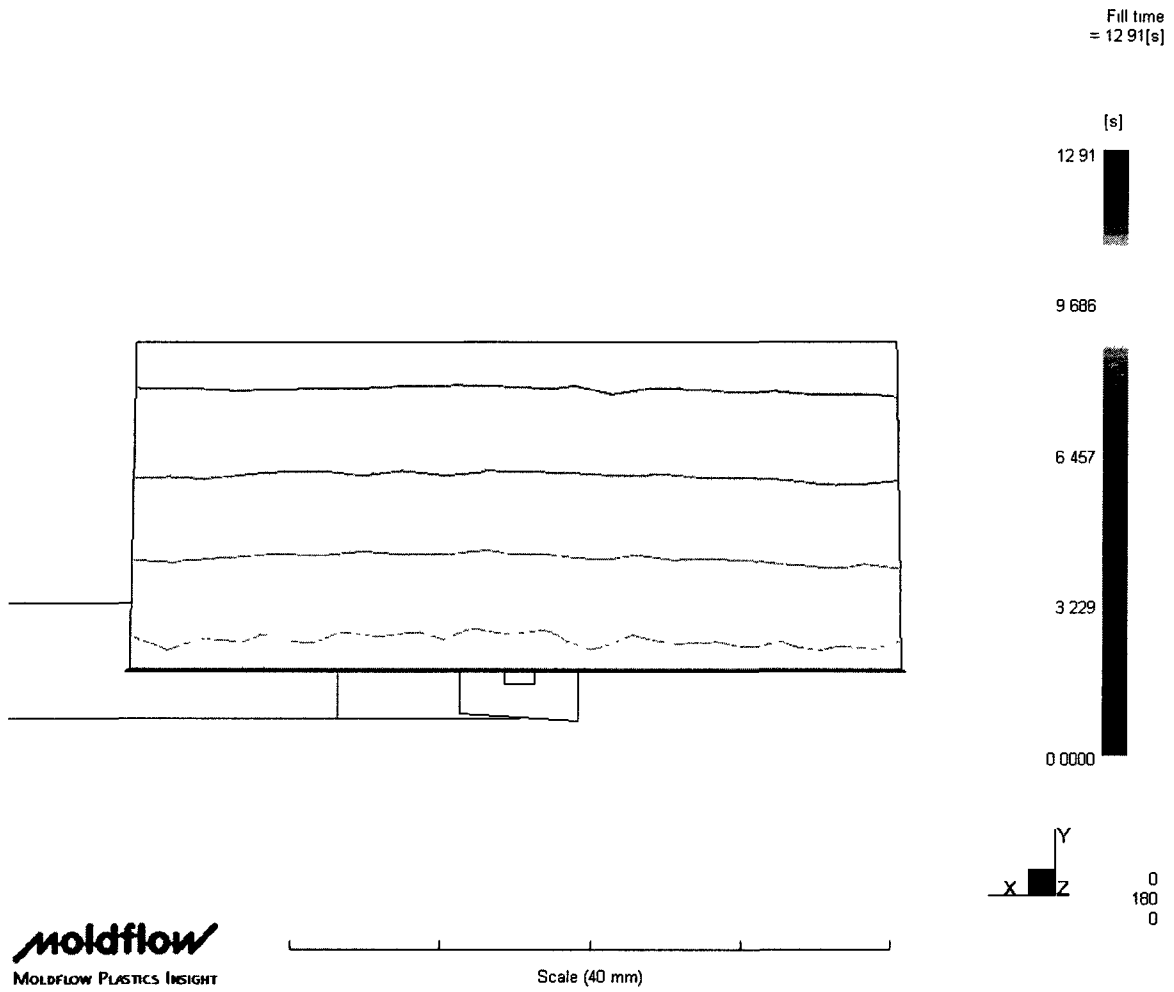


**Figure 40-1a - Flow Front Profile (last rib) in 4 mm perpendicular rib cavity, mtl:
2000GP @ 6.3 cc/s injection rate**

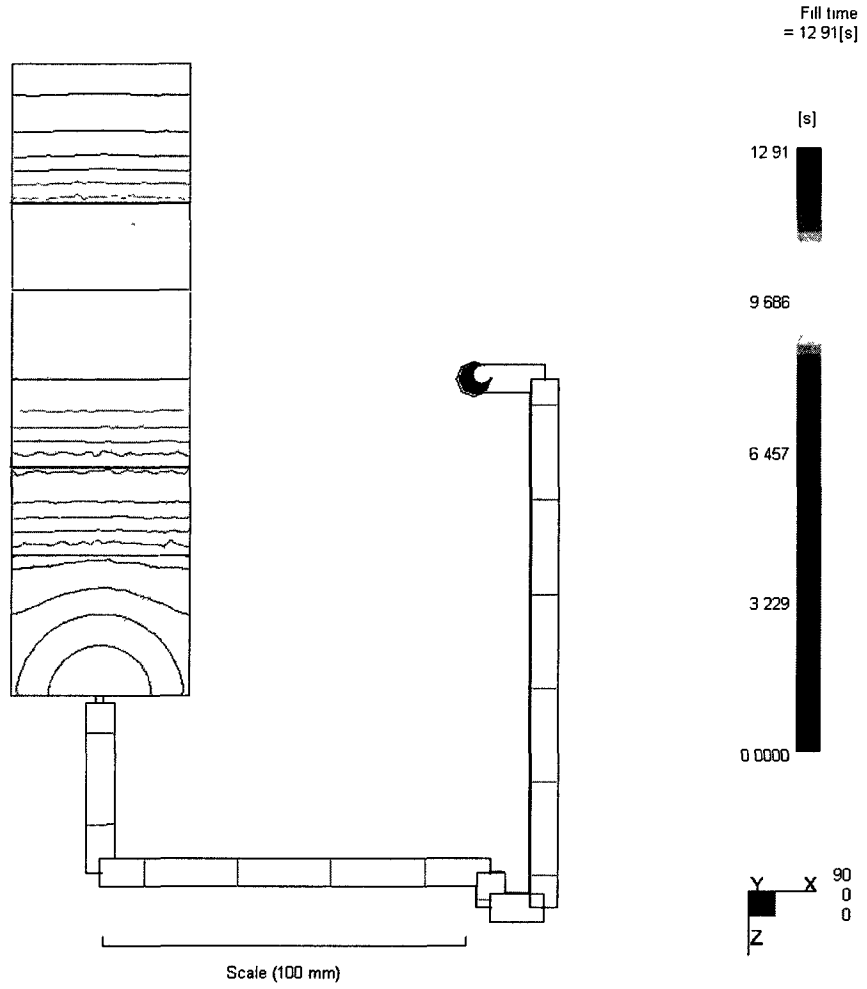


**Figure 40-2a - Flow Front Profile (top) in 4 mm perpendicular rib cavity, mtl:
2000GP @ 6.3 cc/s injection rate**

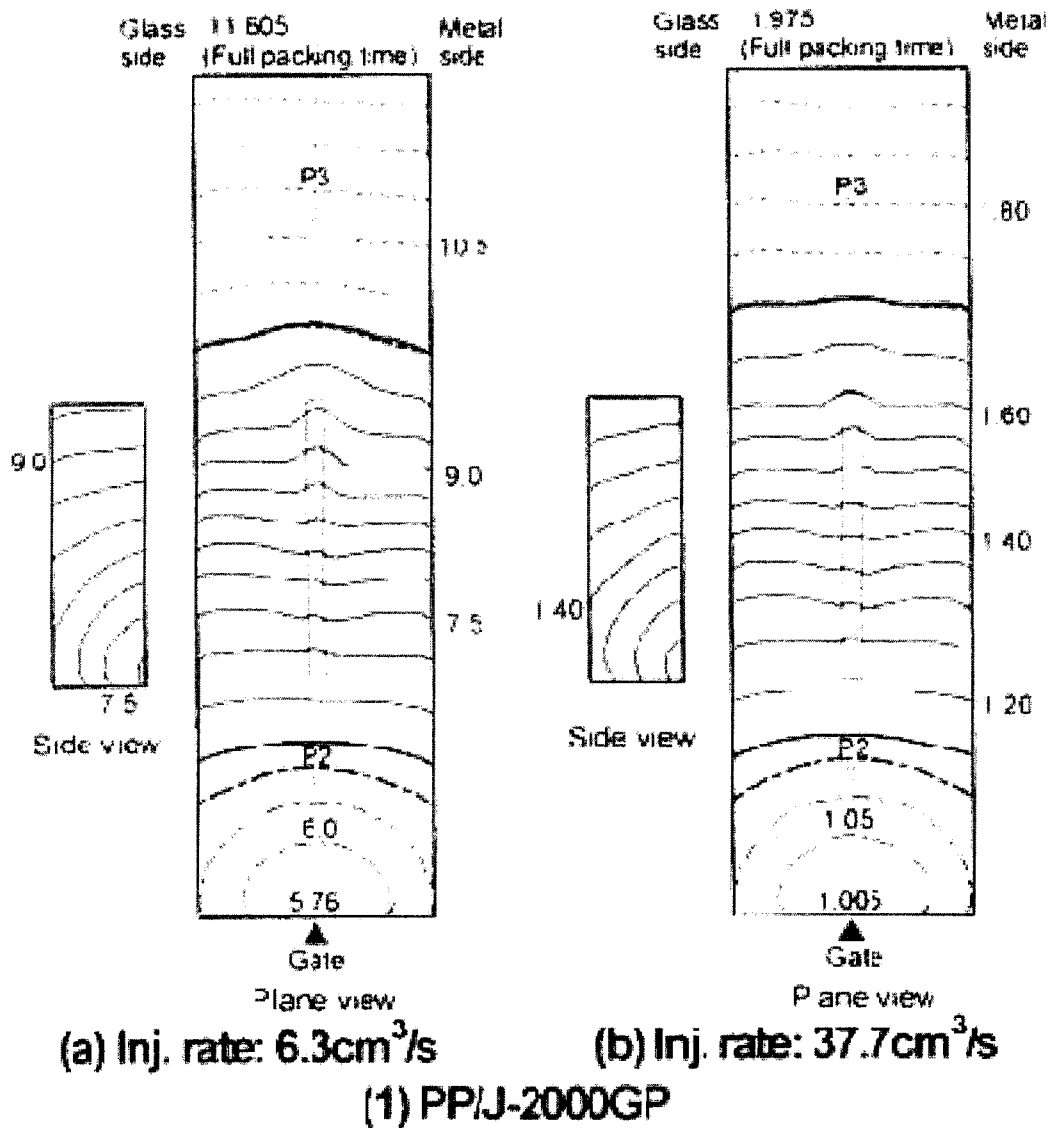


Figure 41a – Experimental Flow Pattern – 4 mm parallel rib cavity

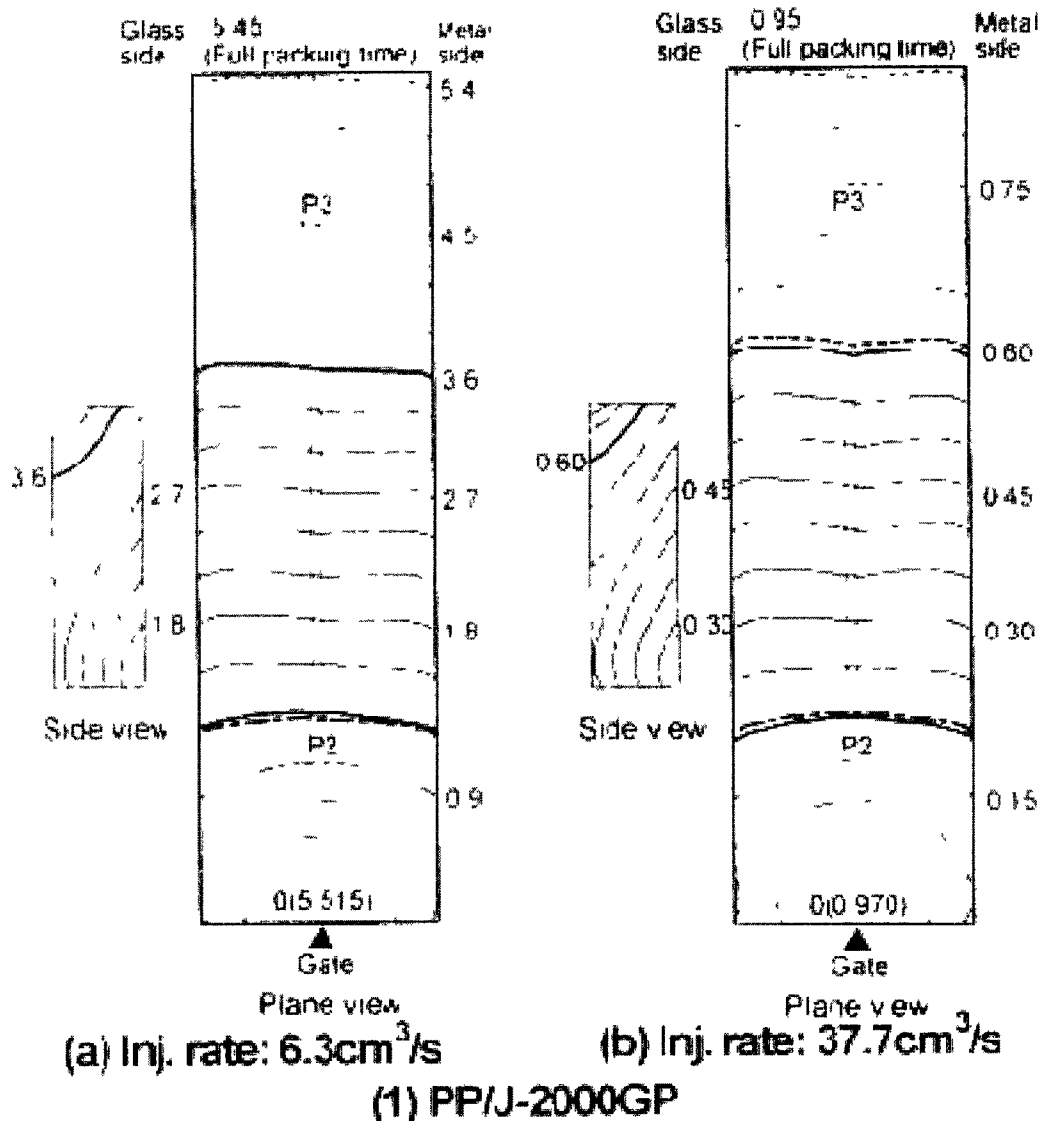


Figure 42a – Experimental Flow Pattern – 2 mm parallel rib cavity

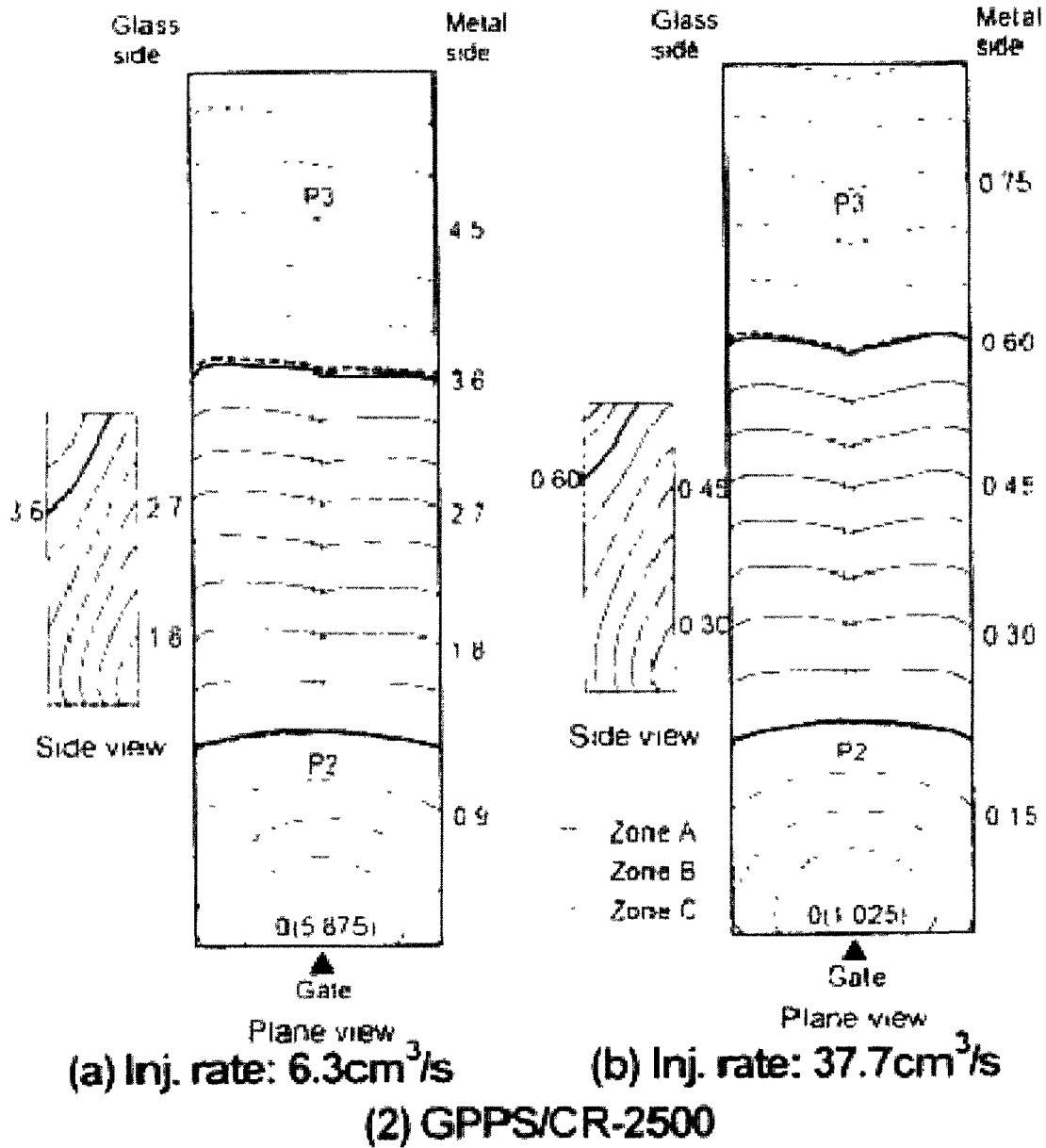


Figure 43a – Experimental Flow Pattern – 2 mm parallel rib cavity

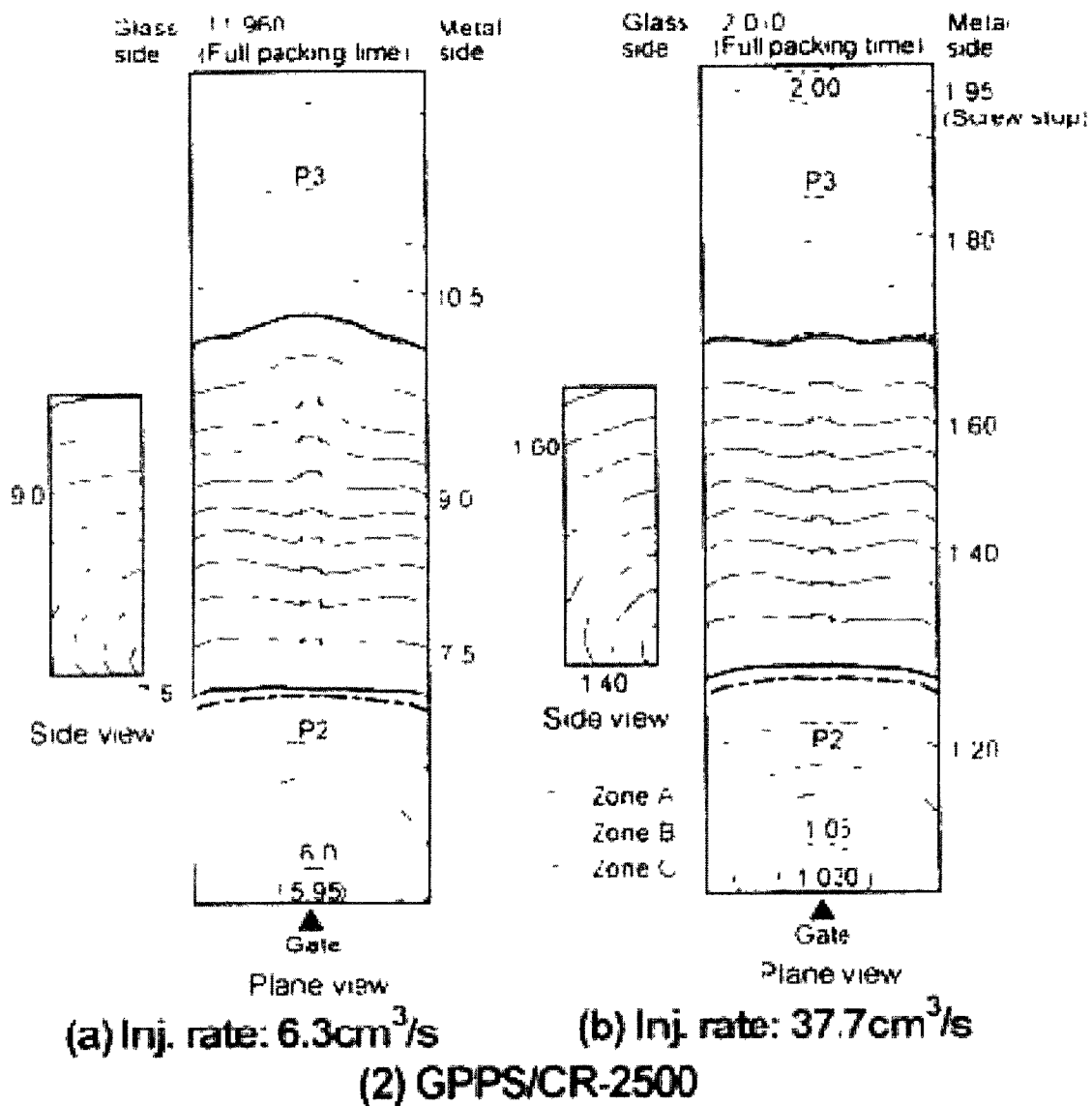
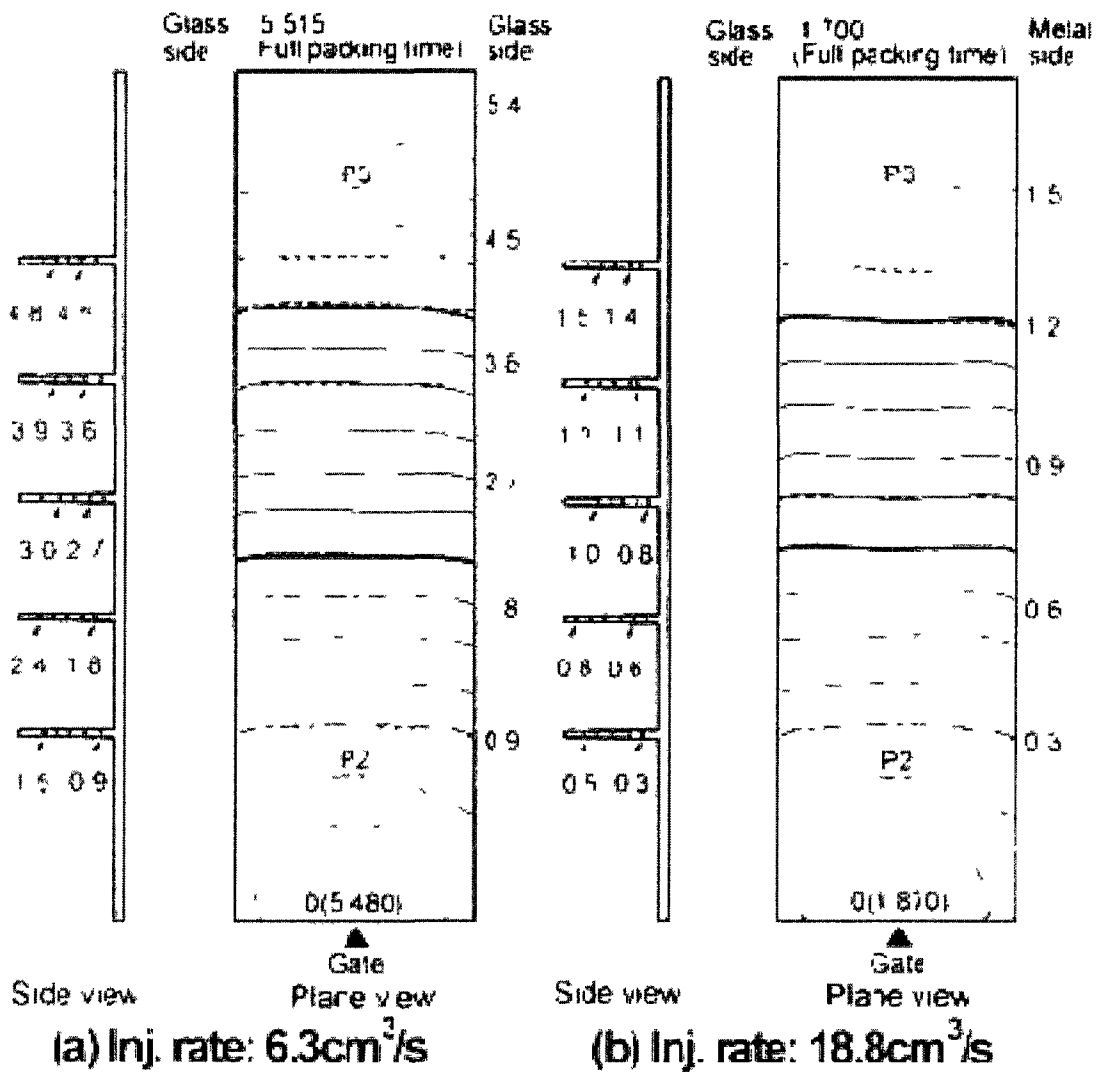


Figure 44a – Experimental Flow Pattern – 4 mm parallel rib cavity



(1) PP/J-2000GP

Figure 45a – Experimental Flow Pattern – 2 mm perpendicular rib cavity

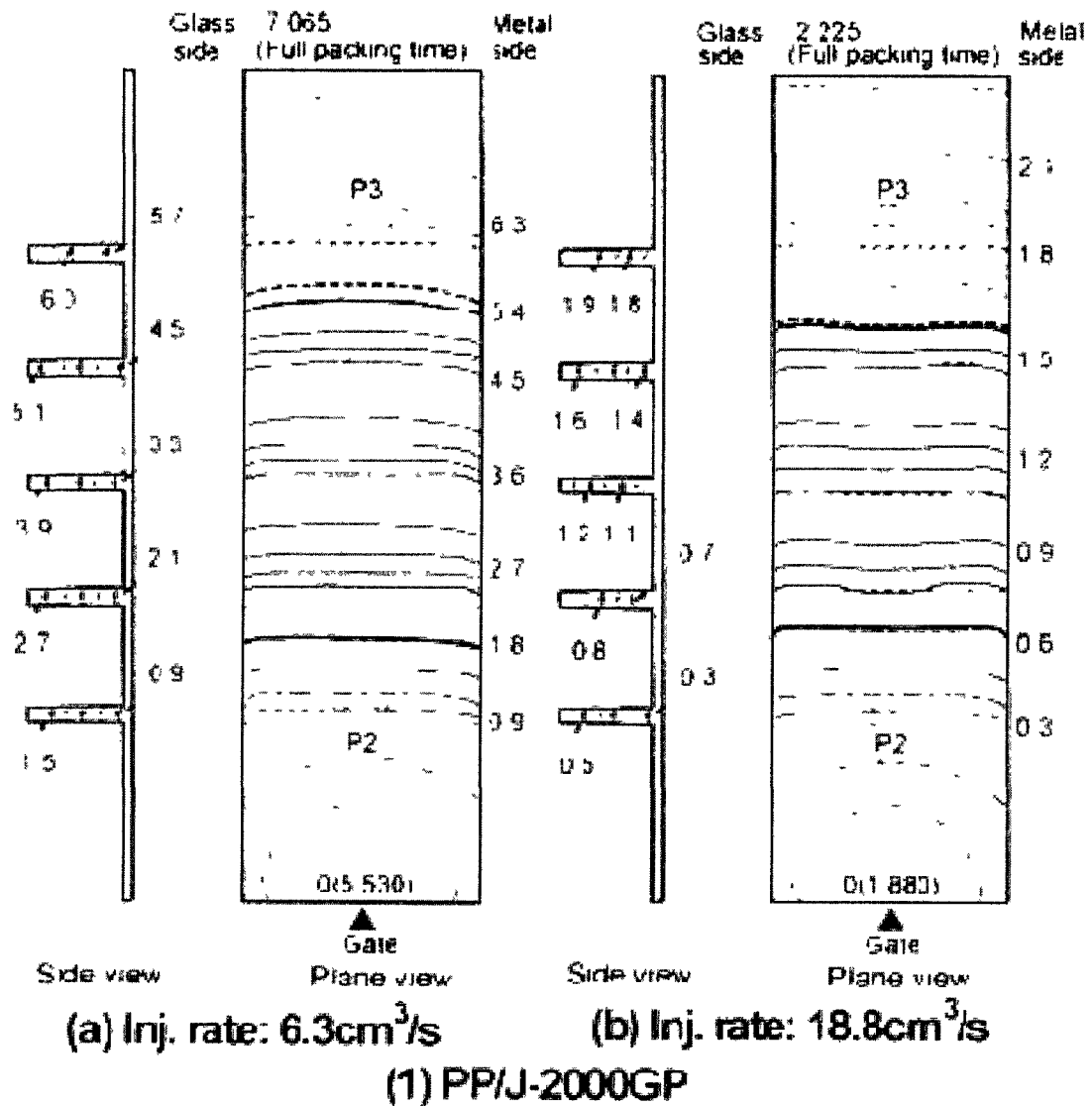
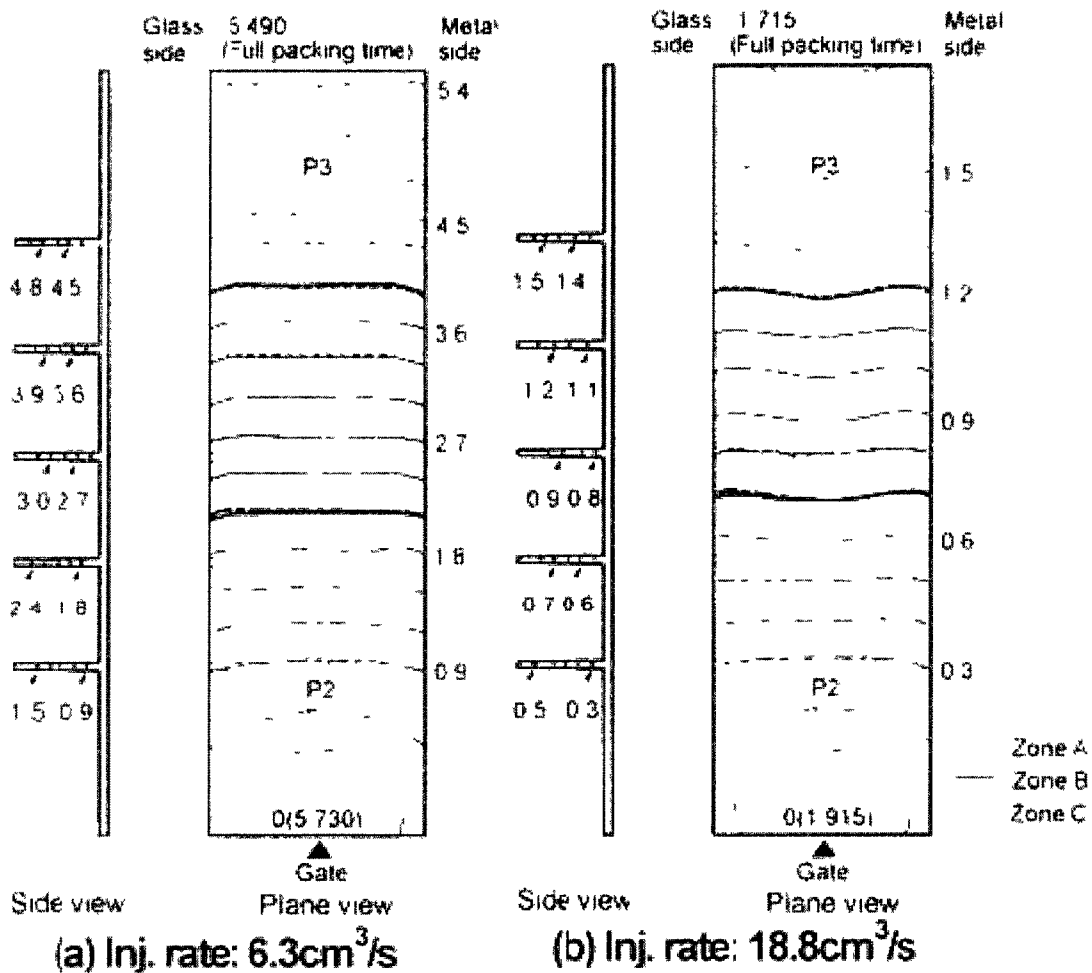


Figure 46a – Experimental Flow Pattern – 4 mm perpendicular rib cavity



(2) GPPS/CR-2500

Figure 47a – Experimental Flow Pattern – 2 mm perpendicular rib cavity

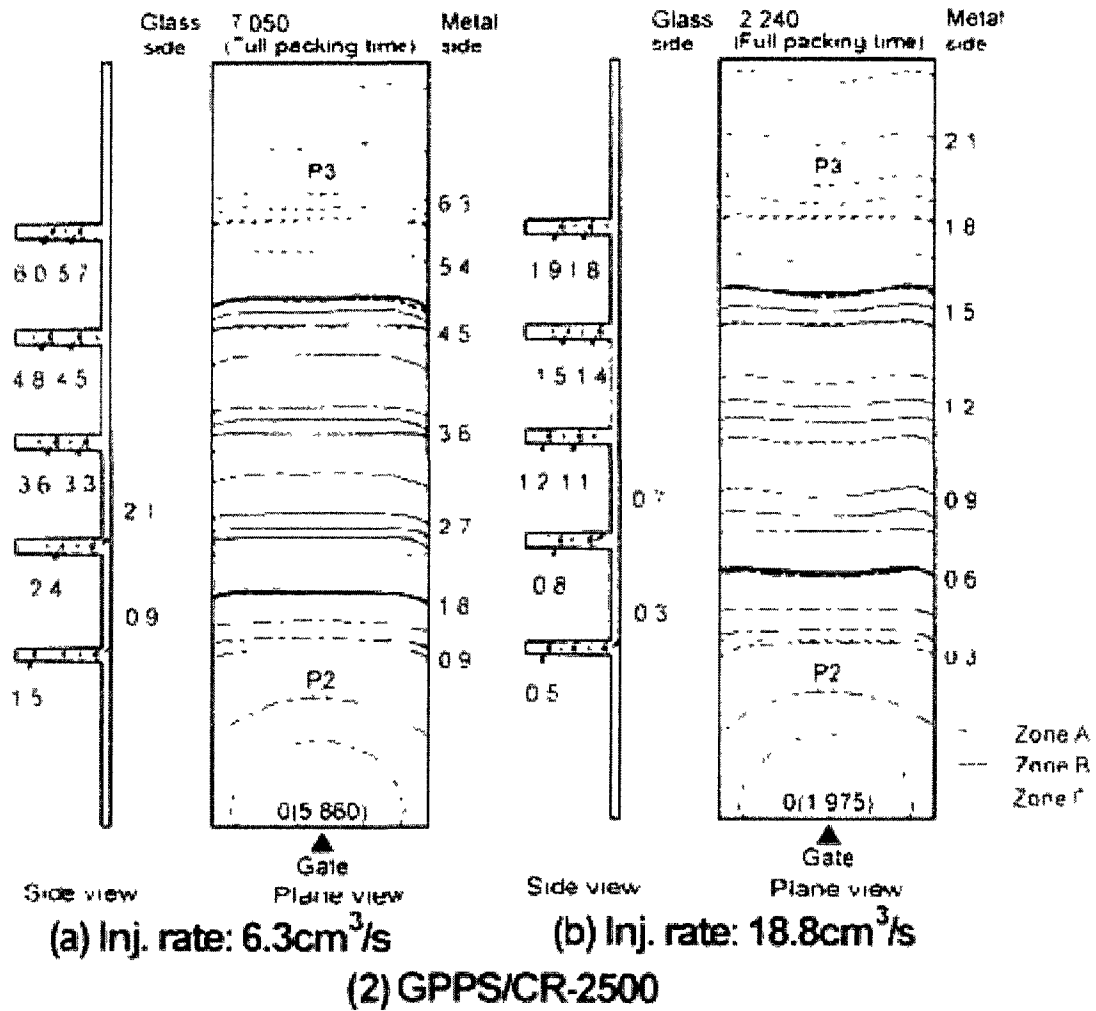
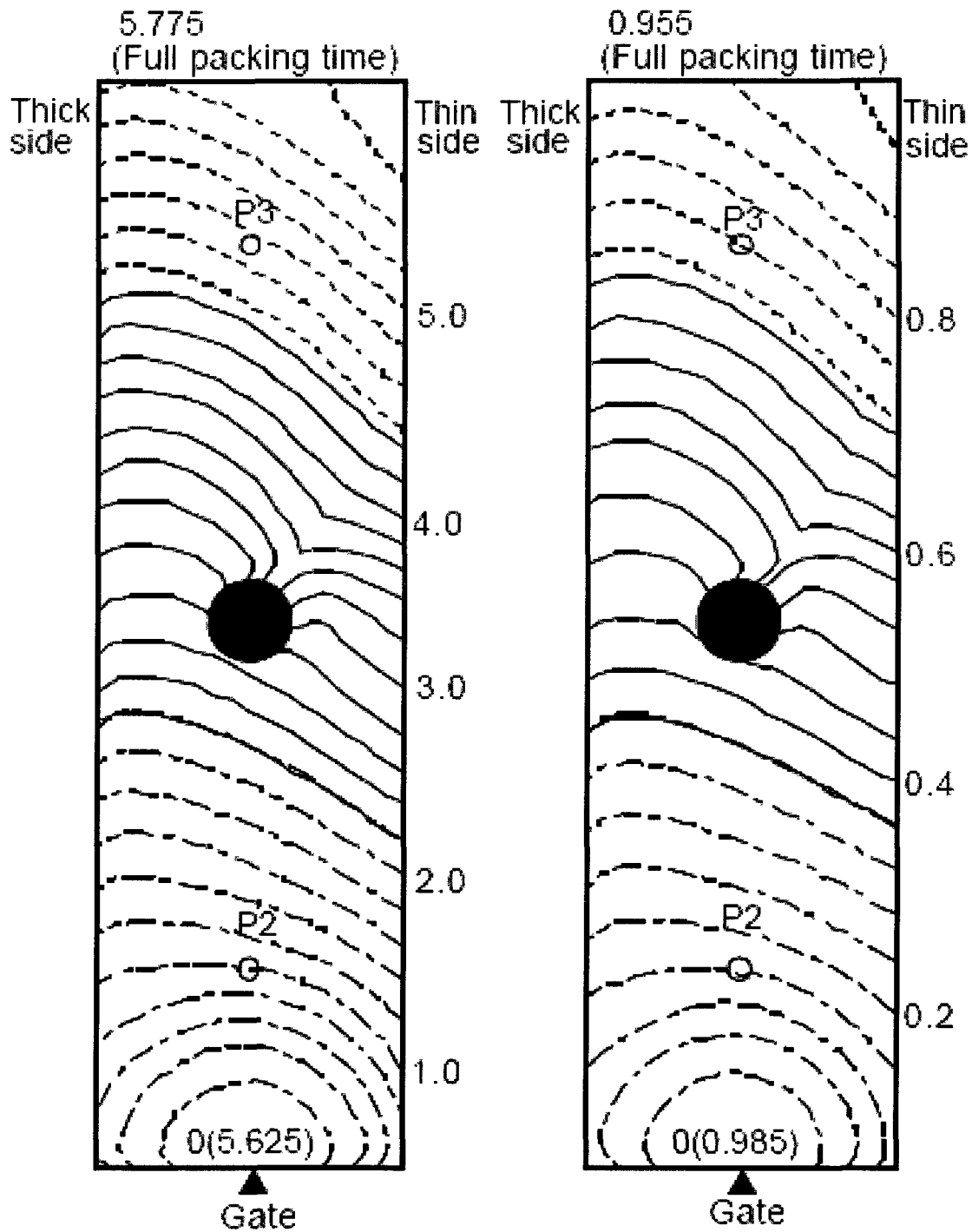


Figure 48a – Experimental Flow Pattern – 4 mm perpendicular rib cavity

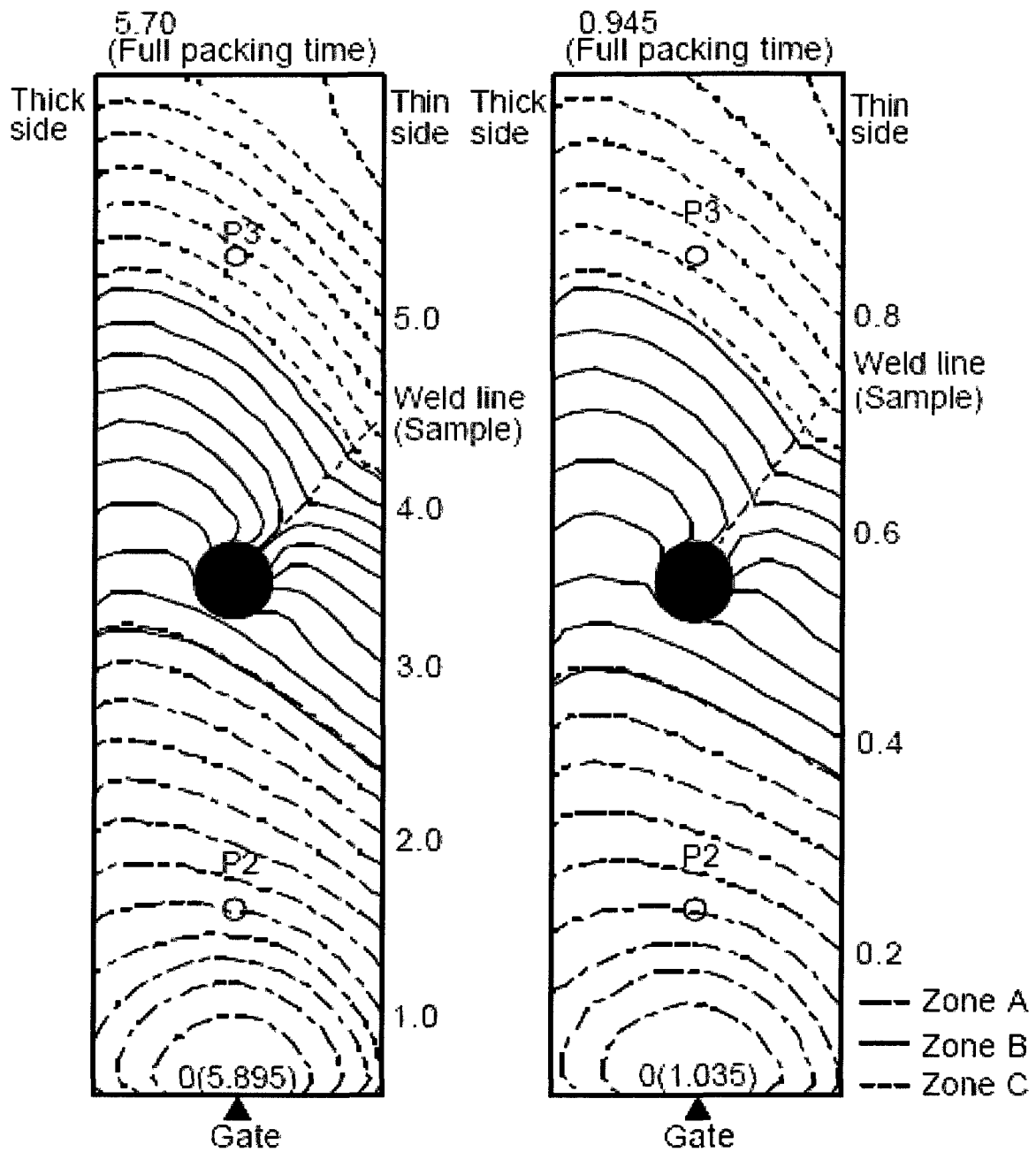


(a) Inj. rate: $6.3\text{cm}^3/\text{s}$

(b) Inj. rate: $37.7\text{cm}^3/\text{s}$

(1) PP

Figure 49a – Experimental Flow Pattern – Obstacle pin cavity J-2000GP



(a) Inj. rate: $6.3\text{cm}^3/\text{s}$ (b) Inj. rate: $37.7\text{cm}^3/\text{s}$

(2) GPPS

Figure 50a – Experimental Flow Pattern – Obstacle pin cavity CR-3500

Appendix B – Pressure Profile at Three Locations

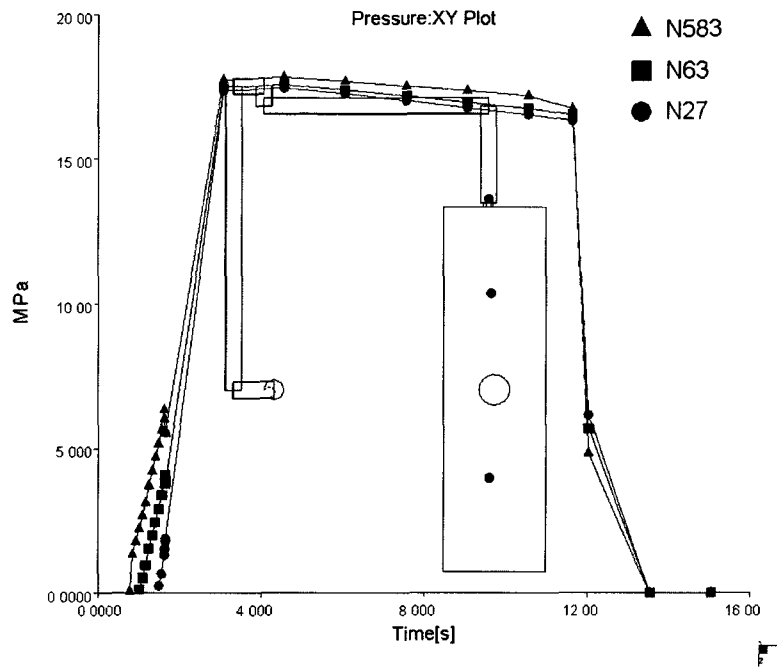


Figure 1b - Pressure profile at three locations in Obstacle Pin cavity, mtl: 700GP @ 37.7 cc/s injection rate

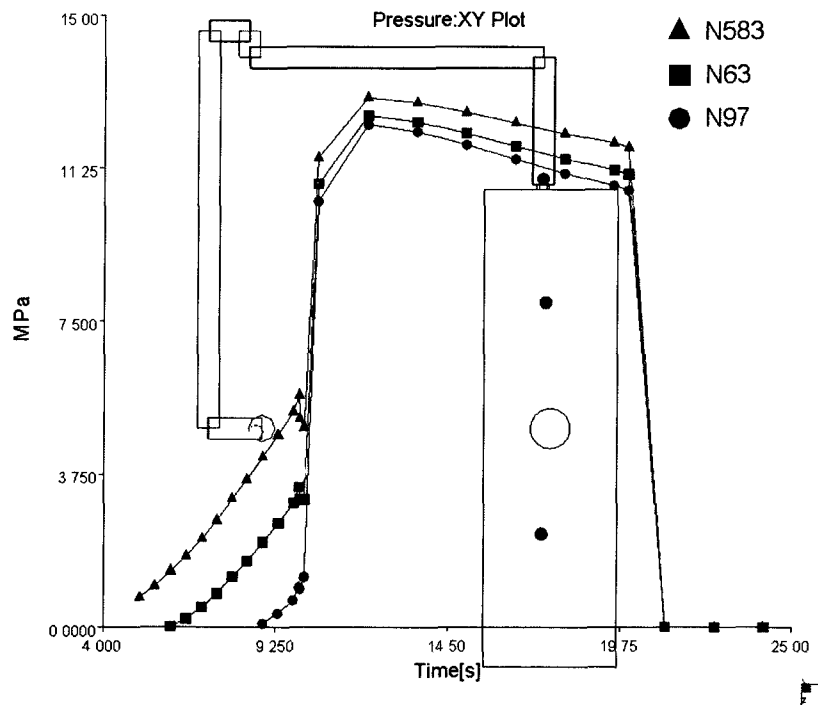


Figure 2b - Pressure profile at three locations in Obstacle Pin cavity, mtl: 700GP @ 6.3 cc/s injection rate

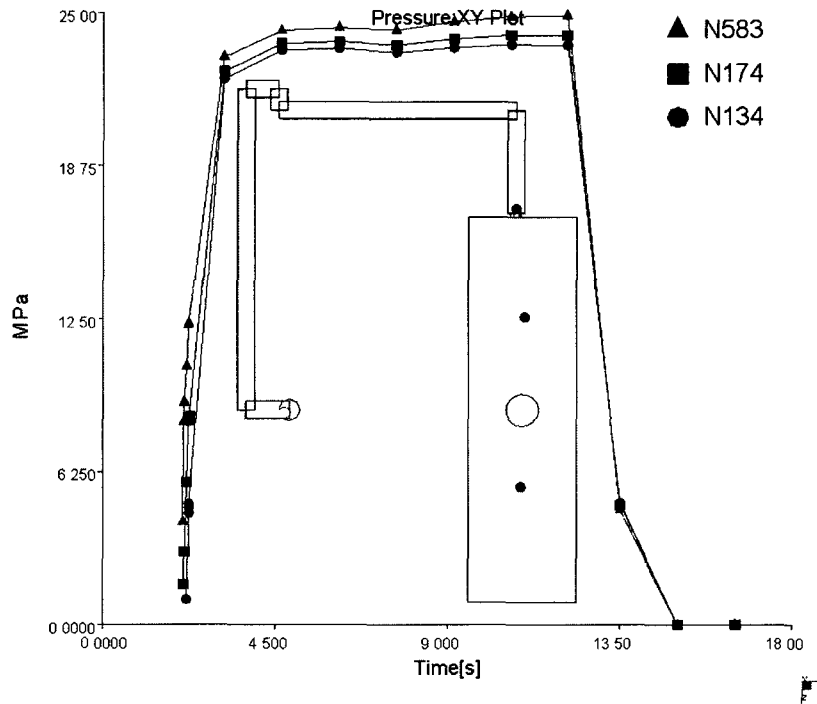


Figure 3b - Pressure profile at three locations in Obstacle Pin cavity, mtl: 2000GP @ 37.7 cc/s injection rate

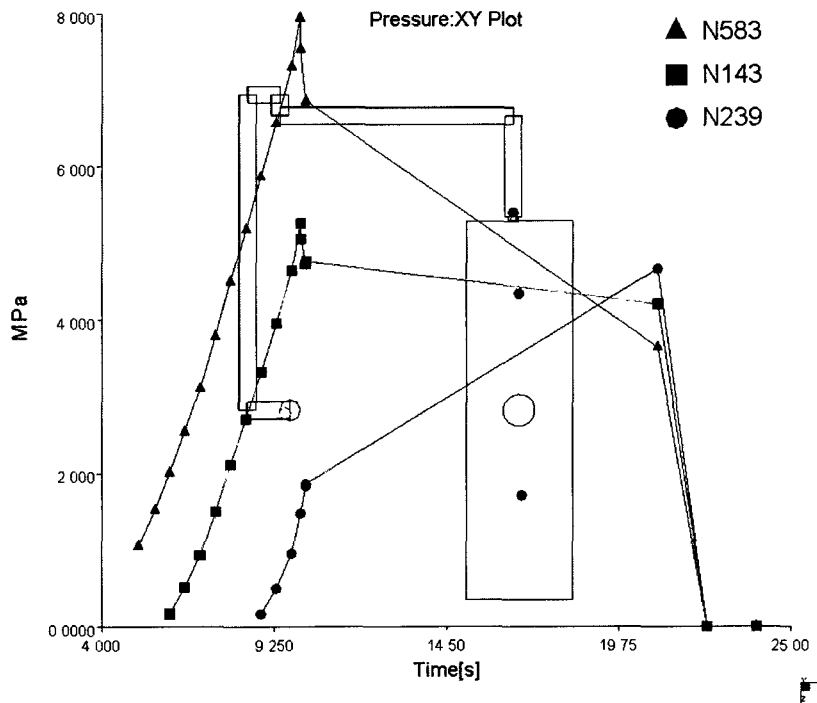


Figure 4b - Pressure profile at three locations in Obstacle Pin cavity, mtl: 2000GP @ 6.3 cc/s injection rate

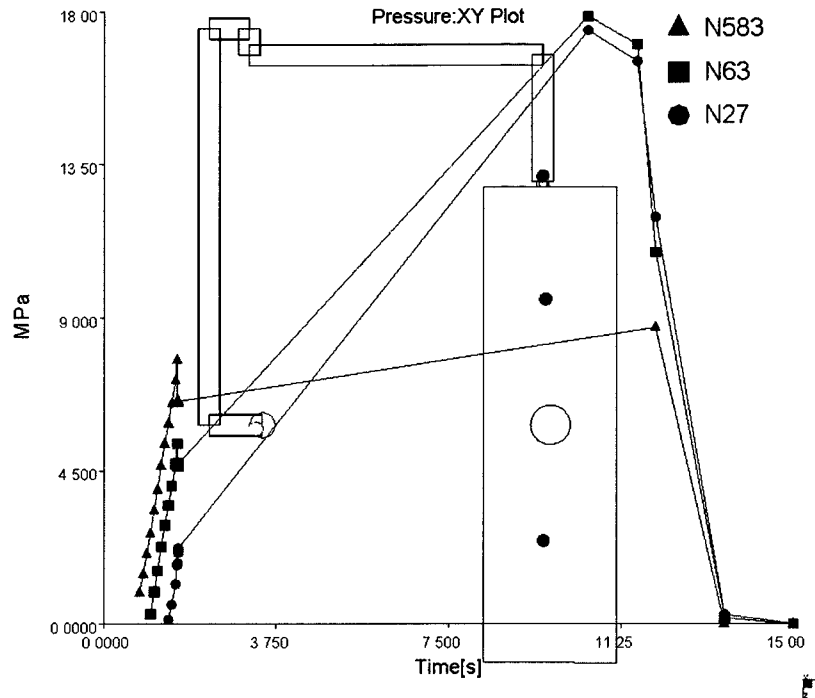


Figure 5b - Pressure profile at three locations in Obstacle Pin cavity, mtl: CR3500 @ 37.7 cc/s injection rate

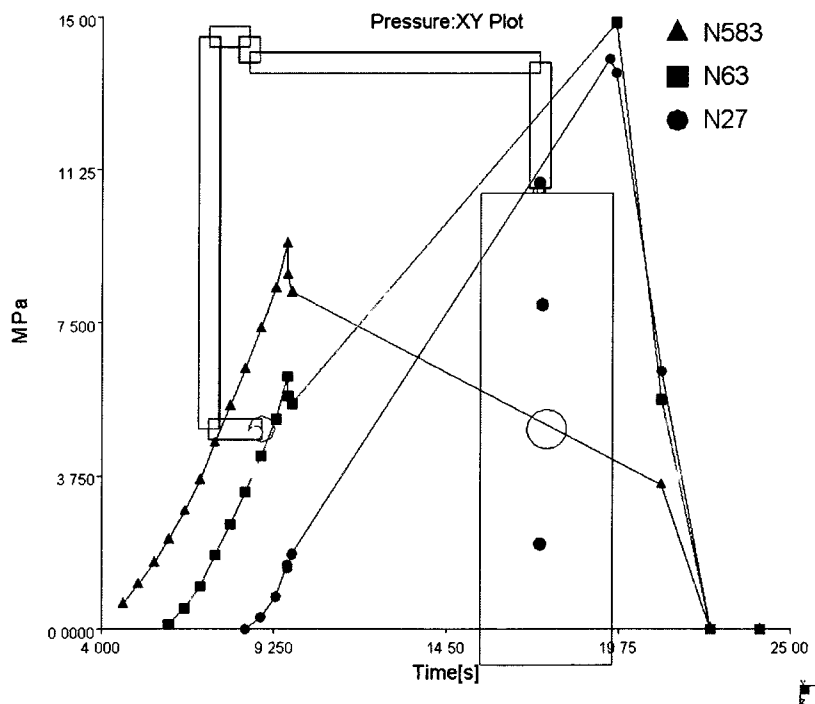


Figure 6b - Pressure profile at three locations in Obstacle Pin cavity, mtl: CR3500 @ 6.3 cc/s injection rate

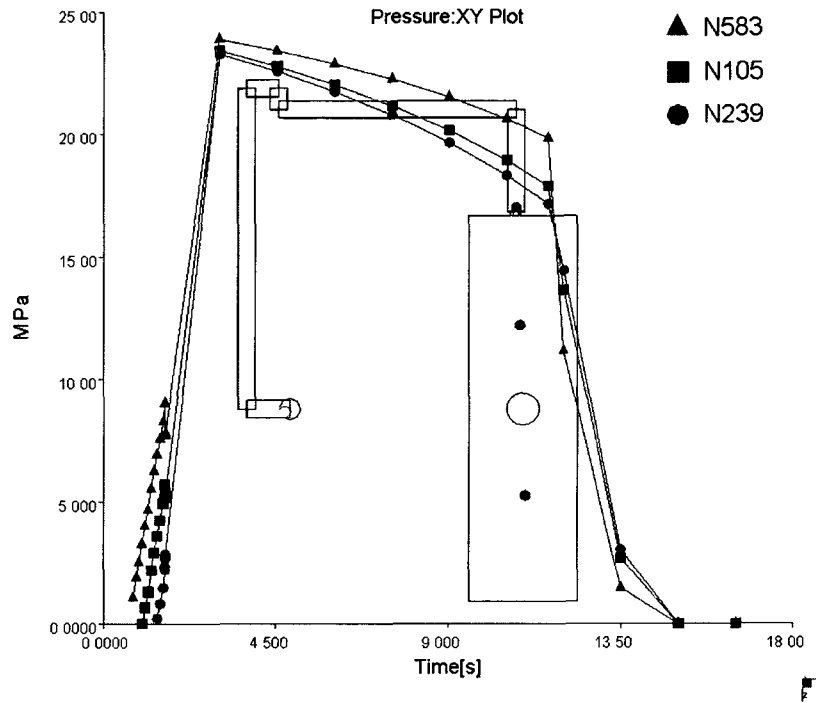


Figure 7b- Pressure profile at three locations in Obstacle Pin cavity, mtl: CR4500 @ 37.7 cc/s injection rate

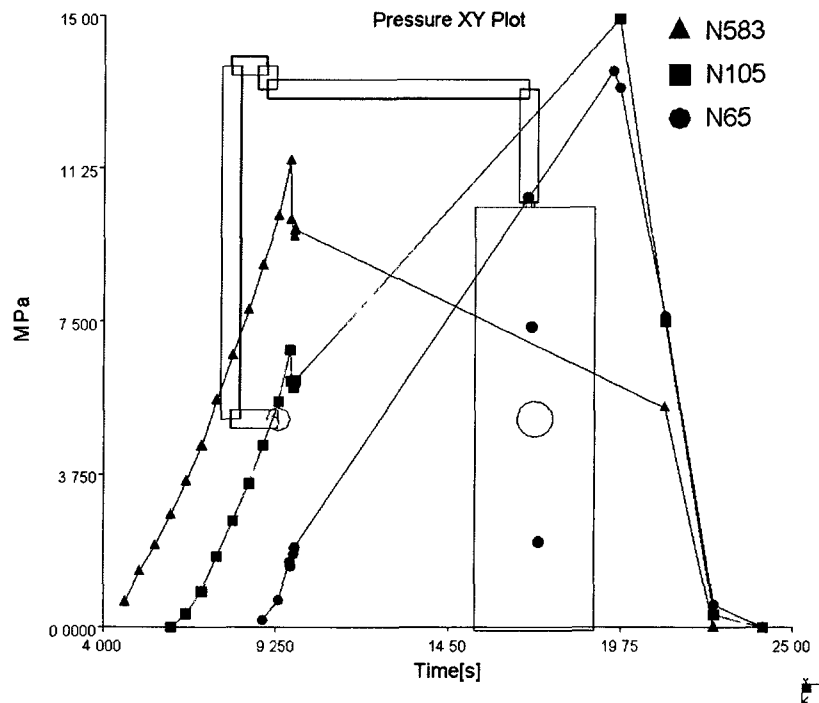
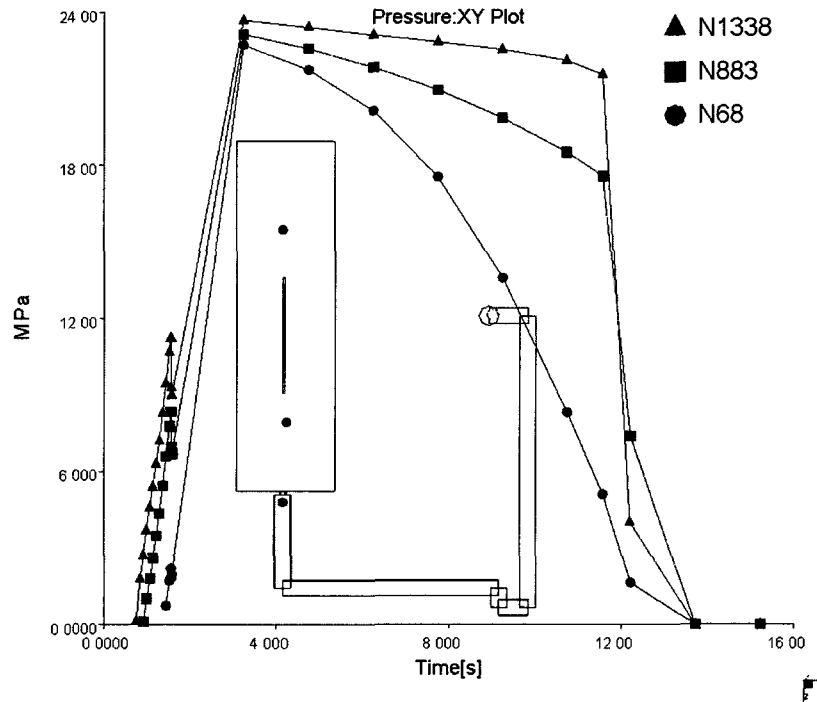
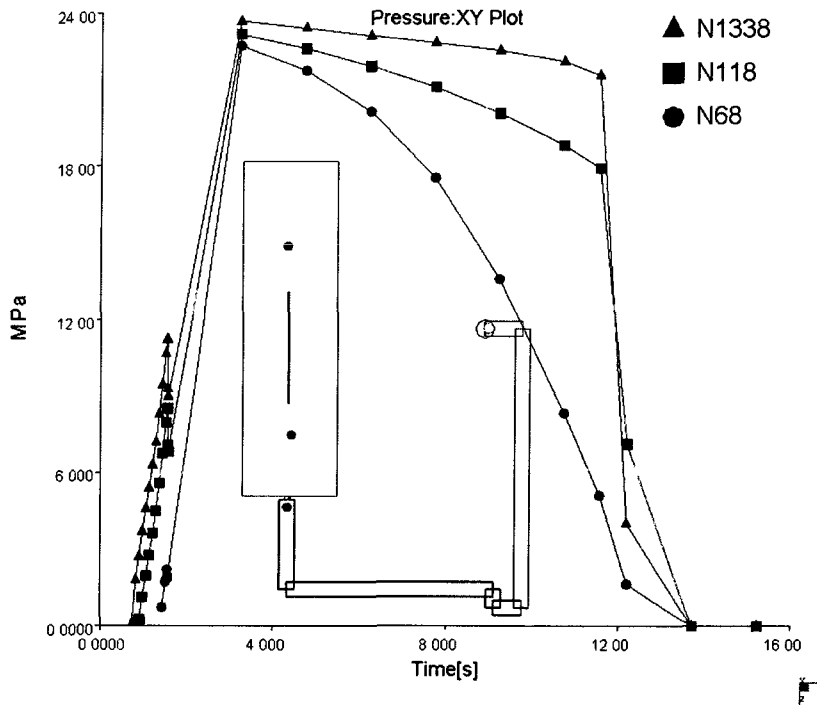


Figure 8b - Pressure profile at three locations in Obstacle Pin cavity, mtl: CR4500 @ 6.3 cc/s injection rate



**Figure 9b - Pressure profile at three locations in 2 mm parallel rib cavity, mtl:
CR3500 @ 37.7 cc/s injection rate**



**Figure 10b - Pressure profile at three locations in 2 mm parallel rib cavity, mtl:
CR4500 @ 37.7 cc/s injection rate**

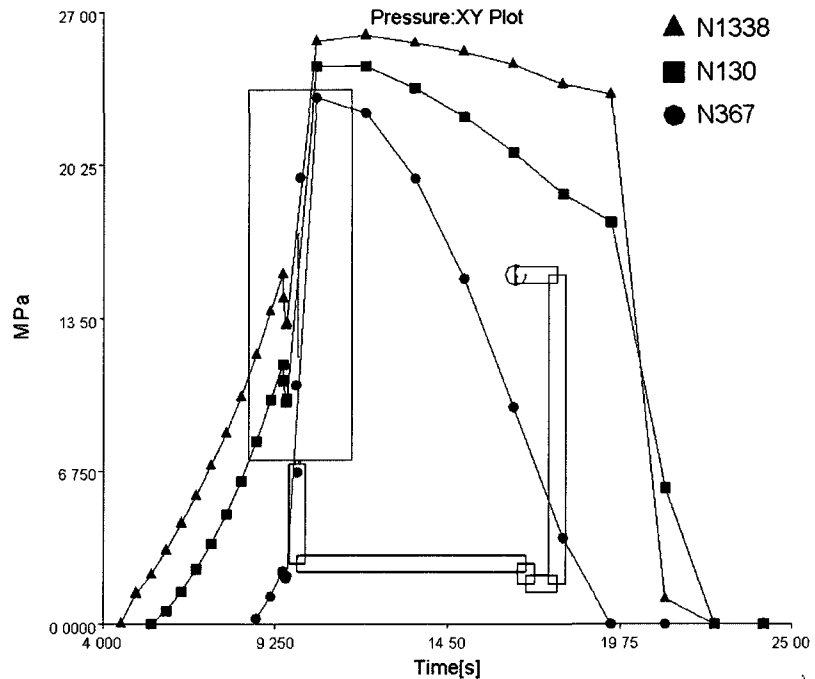


**Figure 11b - Pressure profile at three locations in 2 mm parallel rib cavity, mtl:
CR4500 @ 6.3 cc/s injection rate**

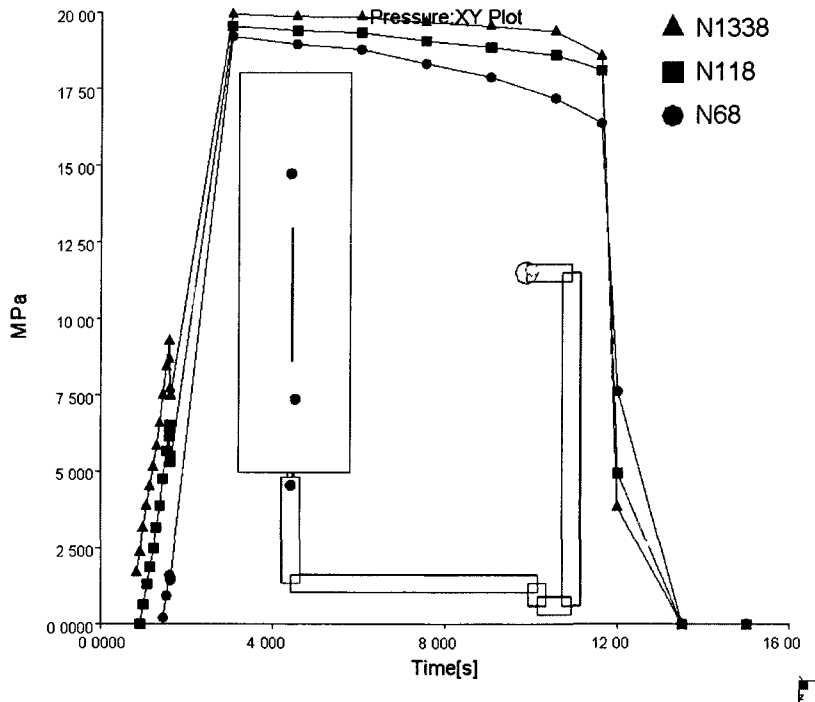


**Figure 12b - Pressure profile at three locations in 2 mm parallel rib cavity, mtl:
2000GP @ 37.7 cc/s injection rate**

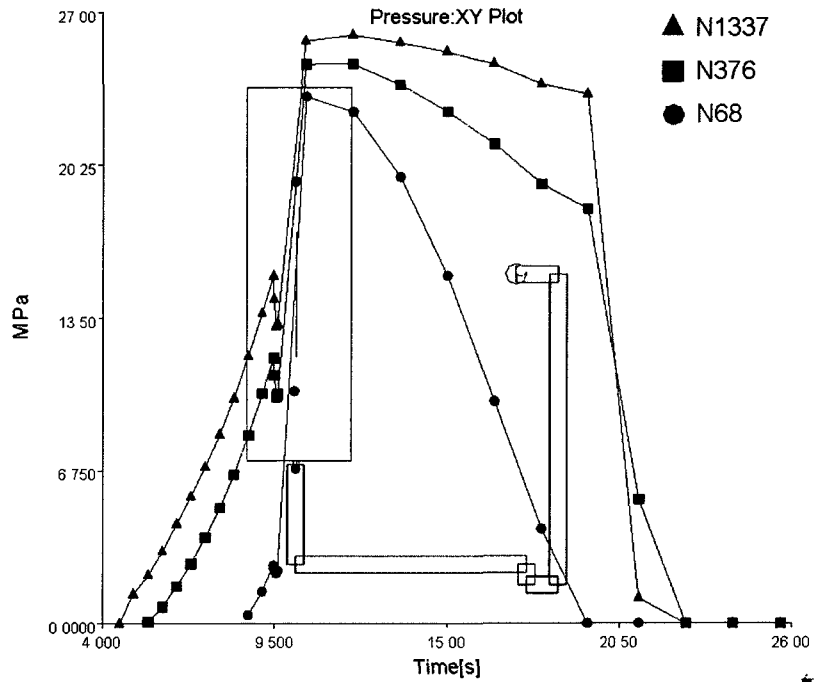


**Figure 13b - Pressure profile at three locations in 2 mm parallel rib cavity, mtl:
CR3500 @ 6.3 cc/s injection rate**

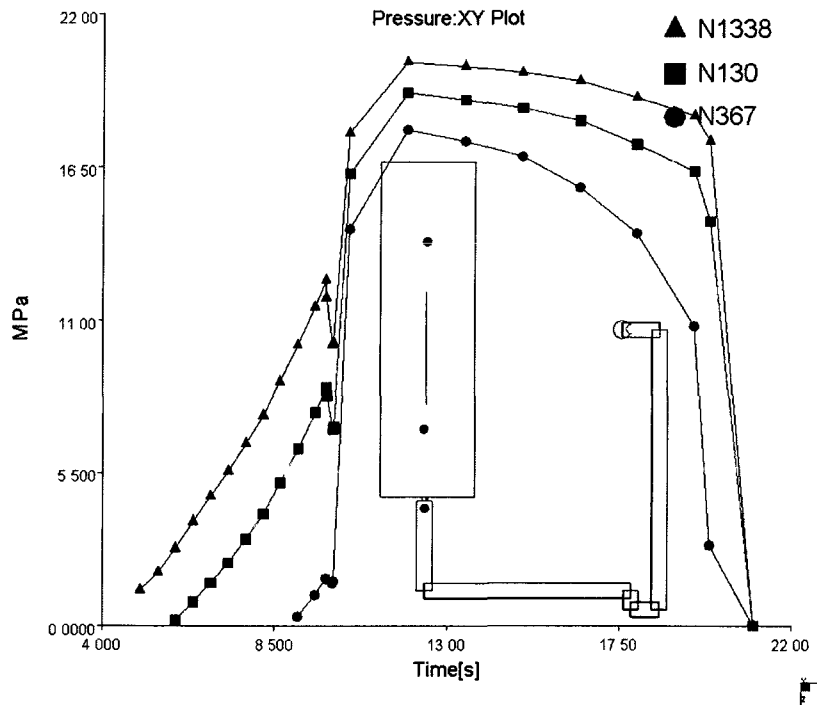


**Figure 14b - Pressure profile at three locations in 2 mm parallel rib cavity, mtl:
700GP @ 6.3 cc/s injection rate**

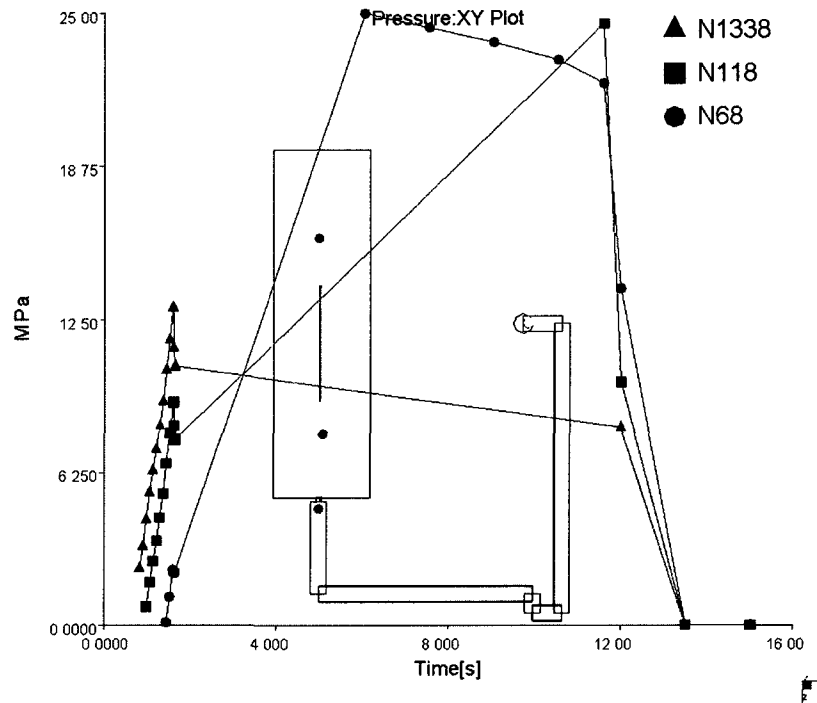


**Figure 15b - Pressure profile at three locations in 2 mm parallel rib cavity, mtl:
700GP @ 37.7 cc/s injection rate**

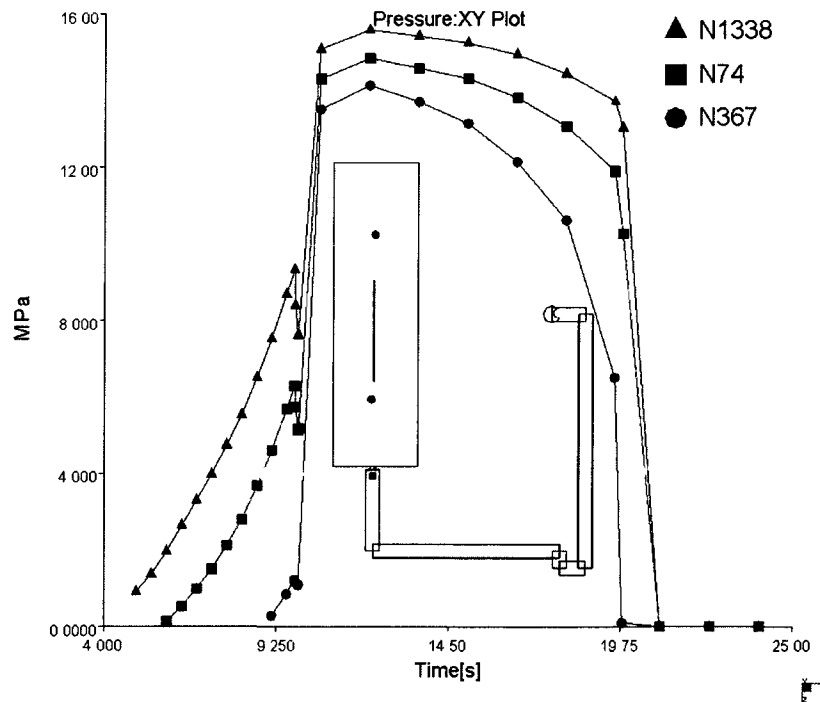


**Figure 16b - Pressure profile at three locations in 2 mm parallel rib cavity, mtl:
2000GP @ 6.3 cc/s injection rate**

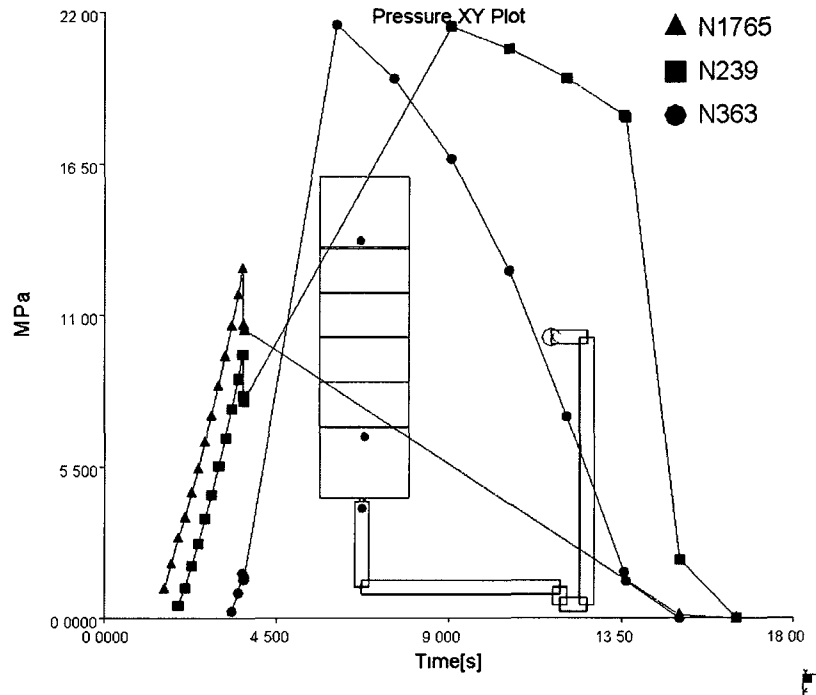


Figure 17b - Pressure profile at three locations in 2 mm perpendicular rib cavity, mtl: CR3500 @ 18.8 cc/s injection rate

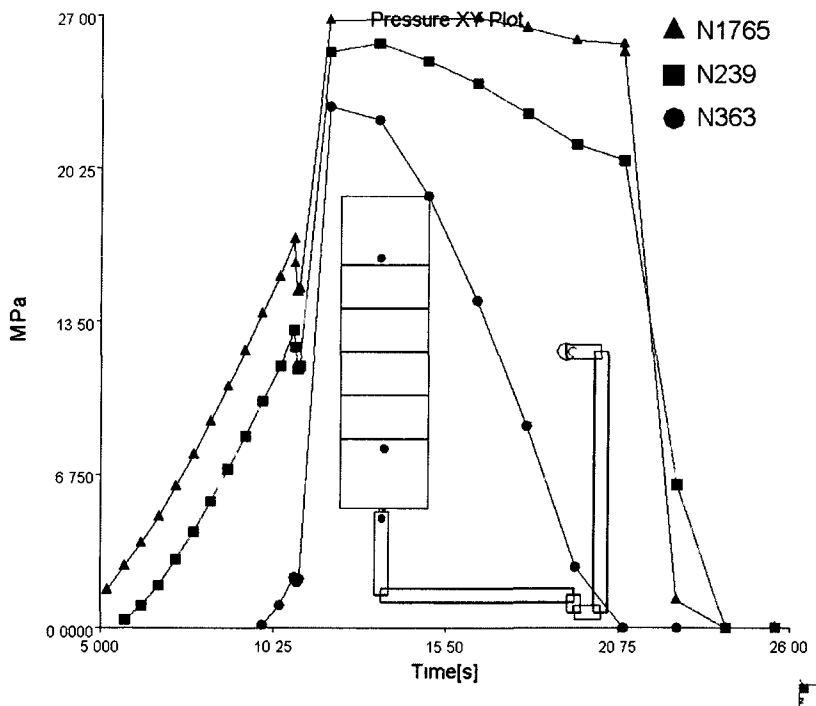


Figure 18b - Pressure profile at three locations in 2 mm perpendicular rib cavity, mtl: CR3500 @ 6.3 cc/s injection rate

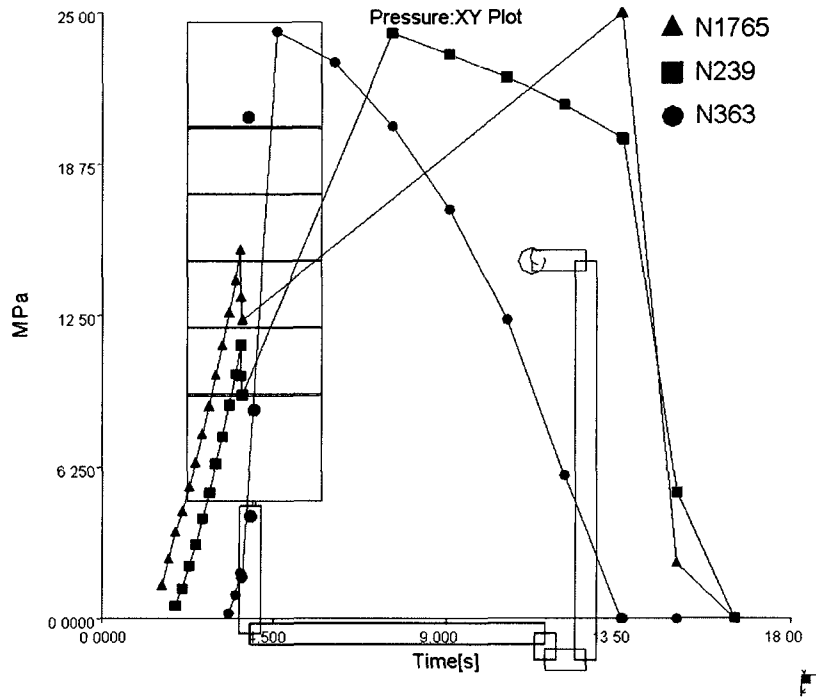


Figure 19b - Pressure profile at three locations in 2 mm perpendicular rib cavity, mtl: CR4500 @ 18.8 cc/s injection rate

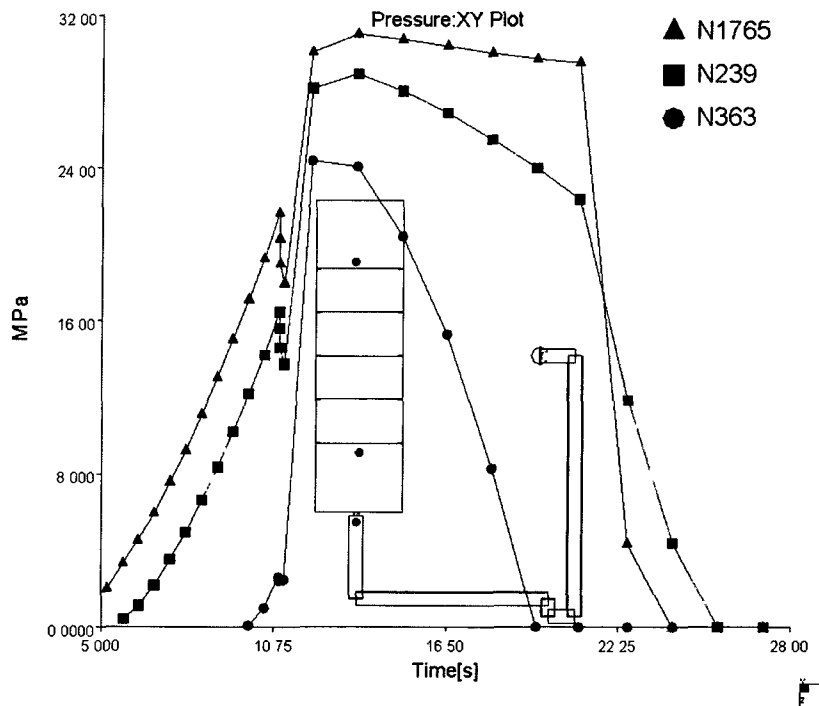


Figure 20b - Pressure profile at three locations in 2 mm perpendicular rib cavity, mtl: CR4500 @ 6.3 cc/s injection rate

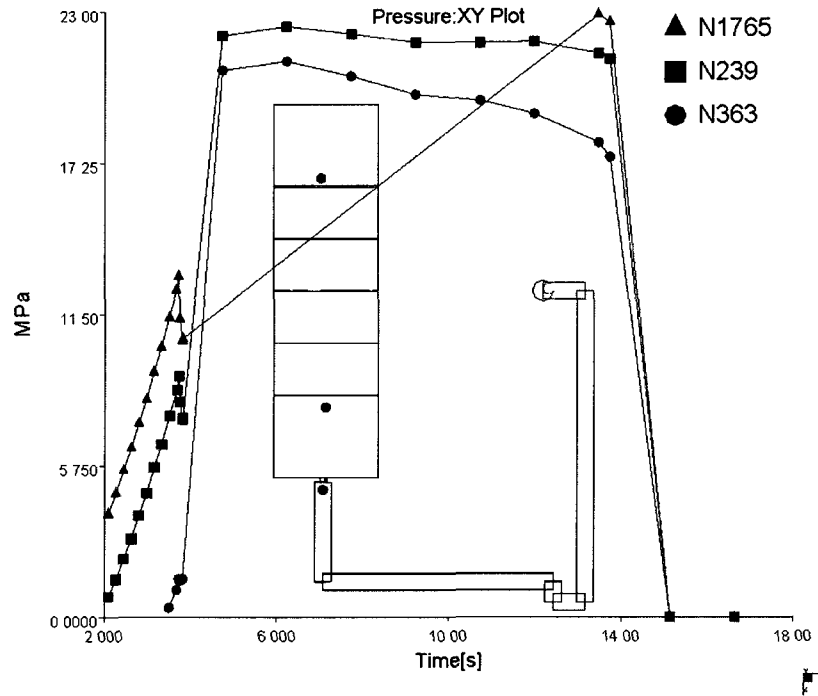


Figure 21b - Pressure profile at three locations in 2 mm perpendicular rib cavity, mtl: 700GP @ 18.8 cc/s injection rate

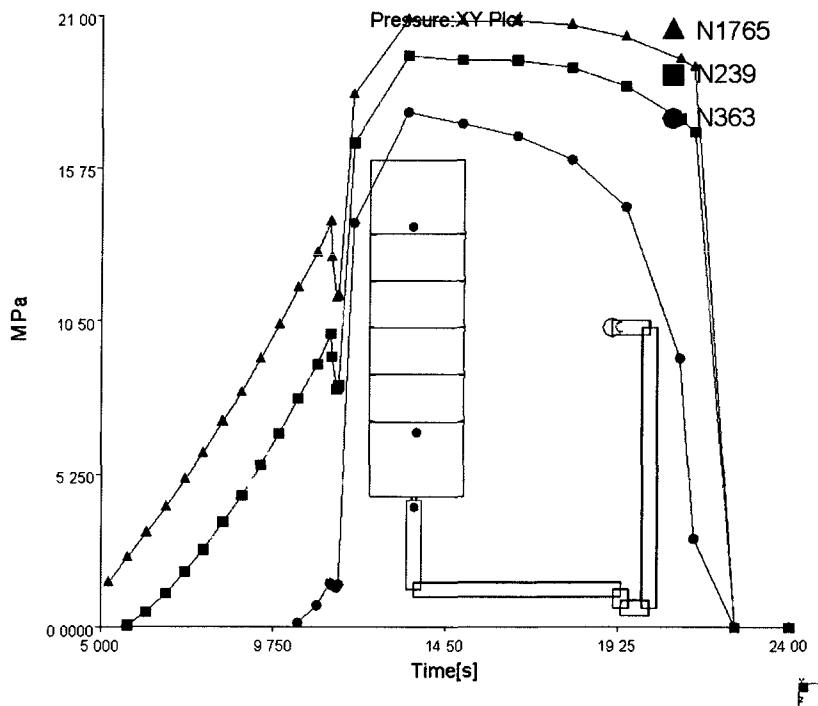


Figure 22b - Pressure profile at three locations in 2 mm perpendicular rib cavity, mtl: 700GP @ 6.3 cc/s injection rate

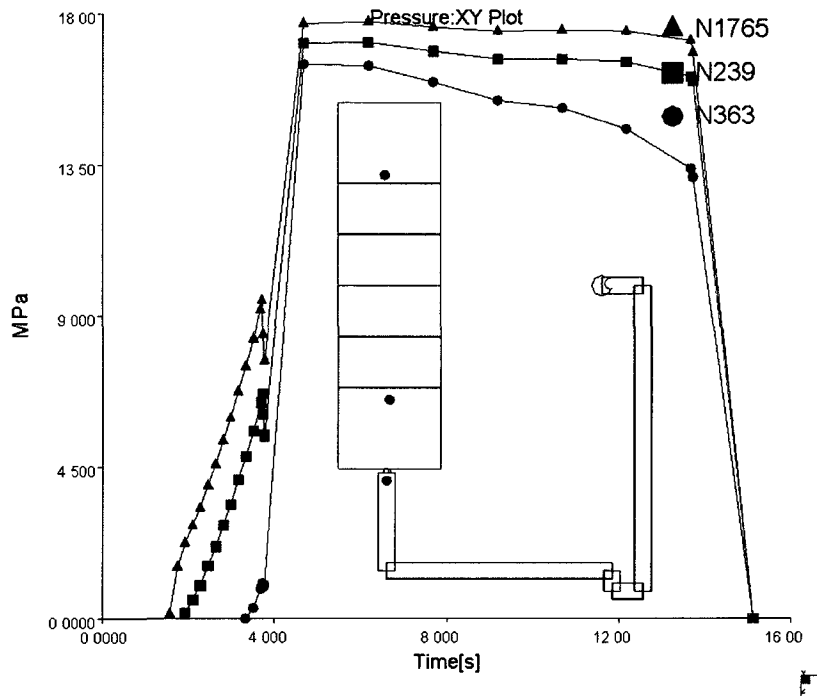


Figure 23b - Pressure profile at three locations in 2 mm perpendicular rib cavity, mtl: 2000GP @ 18.8 cc/s injection rate

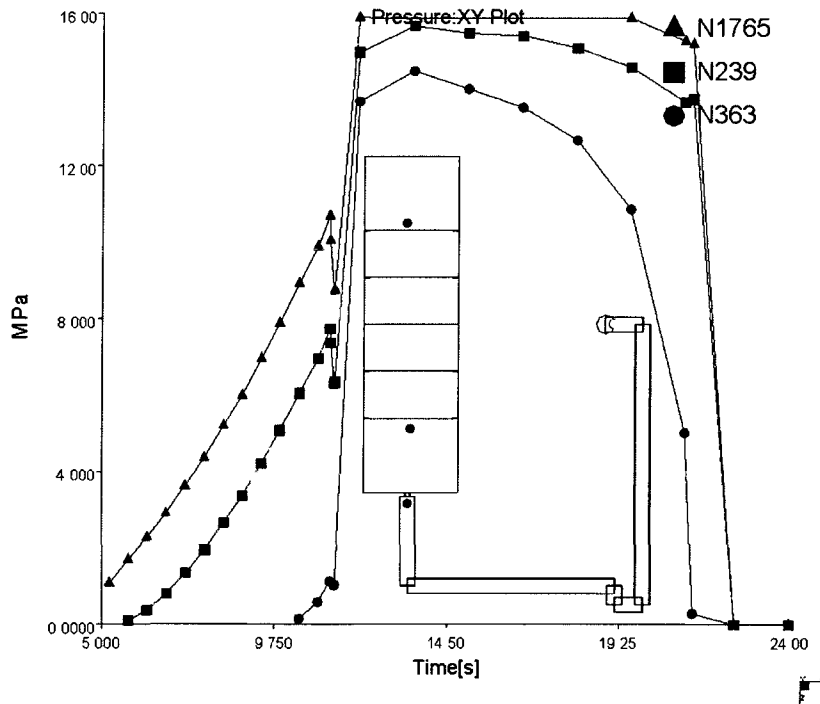


Figure 24b - Pressure profile at three locations in 2 mm perpendicular rib cavity, mtl: 2000GP @ 6.3 cc/s injection rate

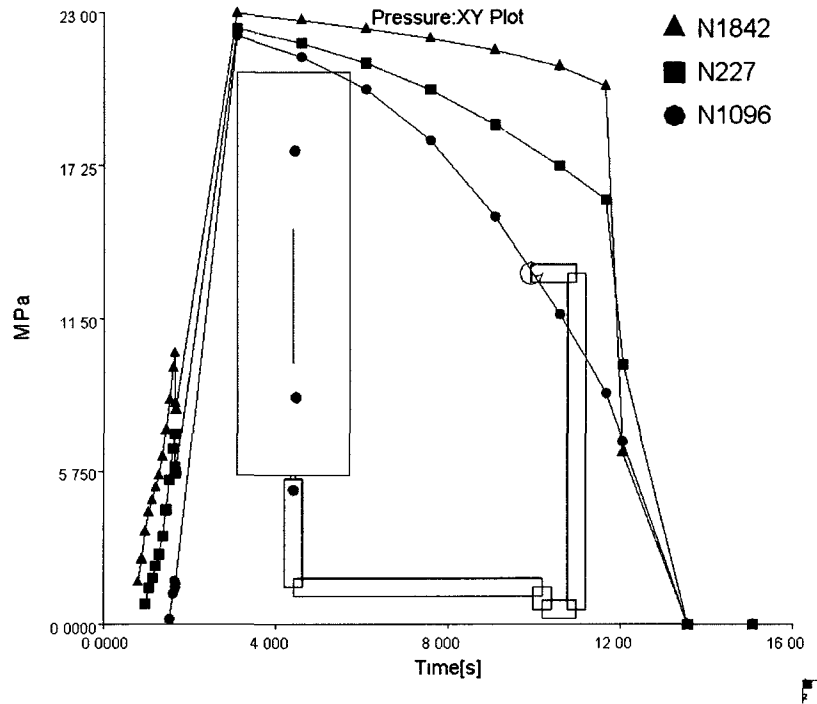


Figure 25b - Pressure profile at three locations in 4 mm parallel rib cavity, mtl: CR3500 @ 37.7 cc/s injection rate

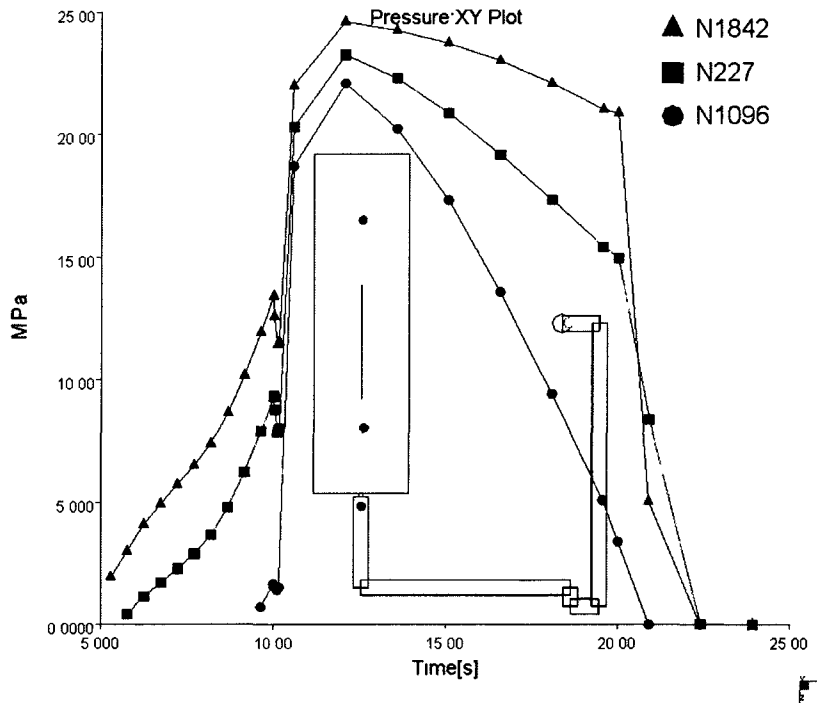
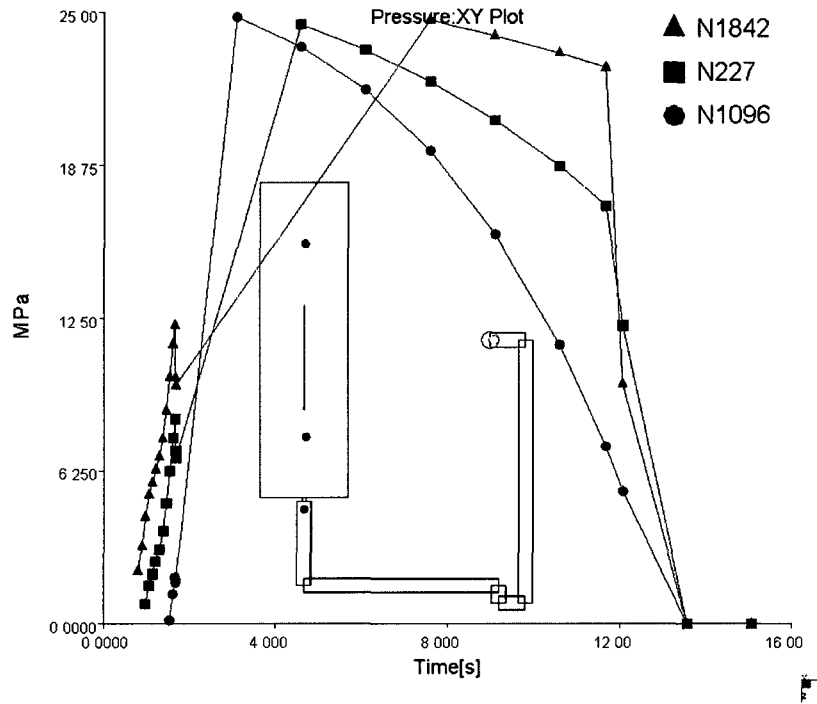
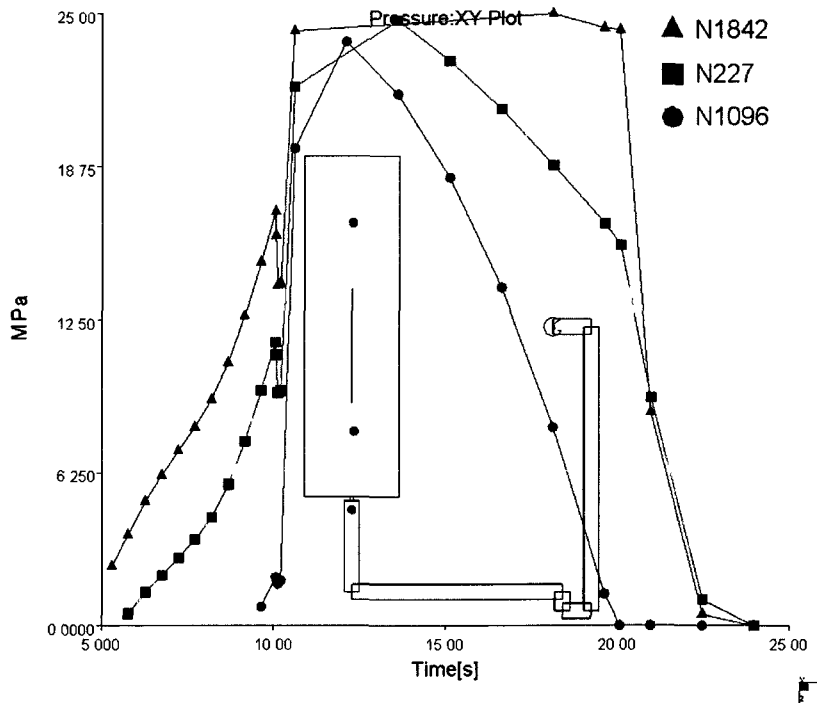


Figure 26b - Pressure profile at three locations in 4 mm parallel rib cavity, mtl: CR3500 @ 6.3 cc/s injection rate



**Figure 27b - Pressure profile at three locations in 4 mm parallel rib cavity, mtl:
CR4500 @ 37.7 cc/s injection rate**



**Figure 28b - Pressure profile at three locations in 4 mm parallel rib cavity, mtl:
CR4500 @ 6.3 cc/s injection rate**

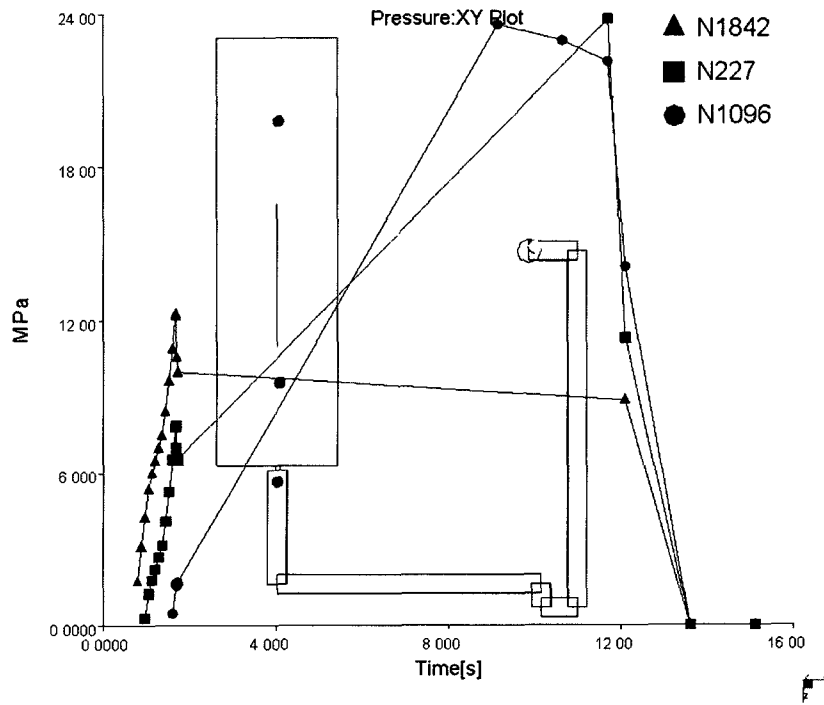


**Figure 29b - Pressure profile at three locations in 4 mm parallel rib cavity, mtl:
700GP @ 37.7 cc/s injection rate**

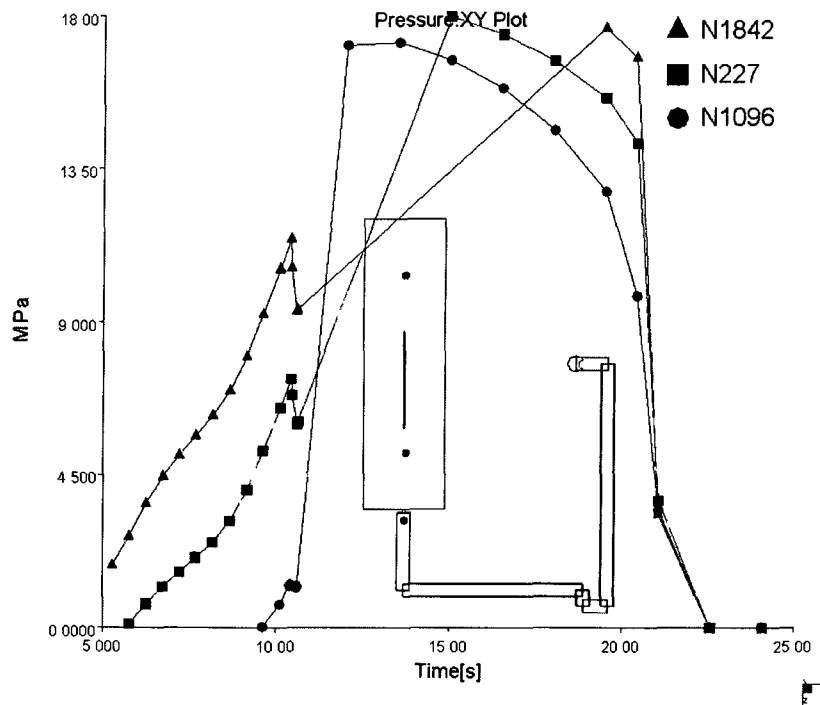


**Figure 30b - Pressure profile at three locations in 4 mm parallel rib cavity, mtl:
700GP @ 6.3 cc/s injection rate**

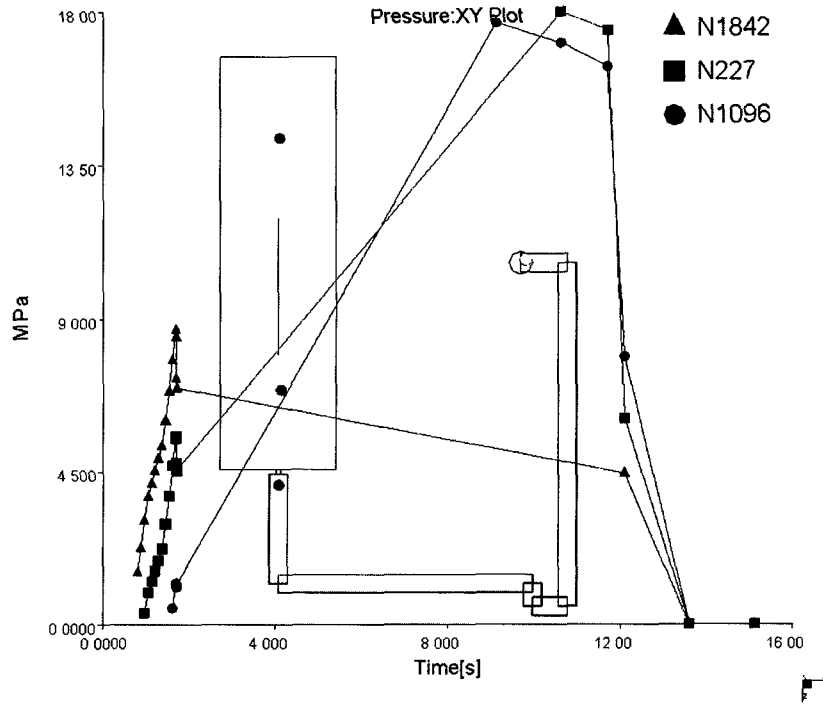


**Figure 31b - Pressure profile at three locations in 4 mm parallel rib cavity, mtl:
2000GP @ 37.7 cc/s injection rate**

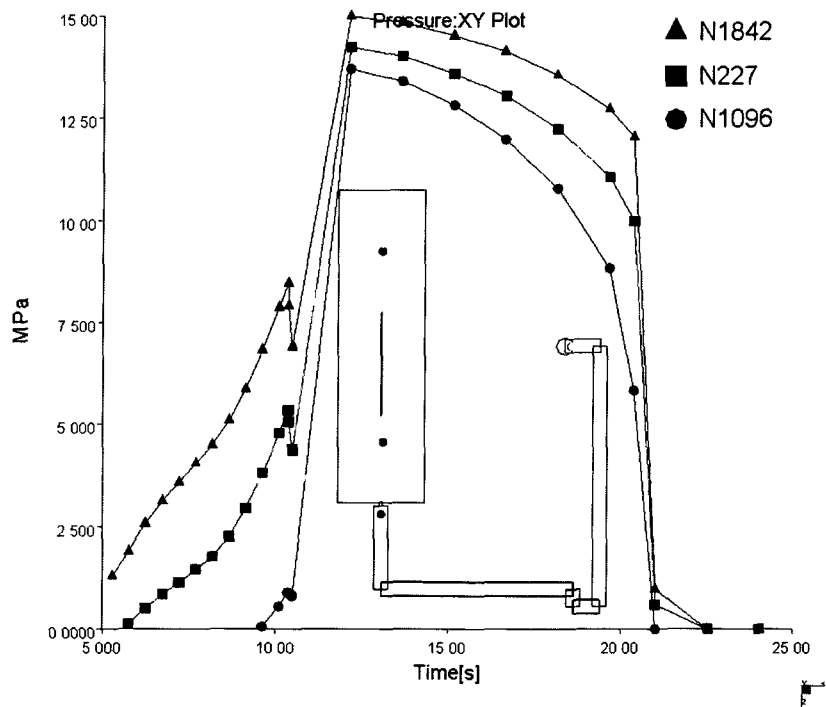


**Figure 32b - Pressure profile at three locations in 4 mm parallel rib cavity, mtl:
2000GP @ 6.3 cc/s injection rate**

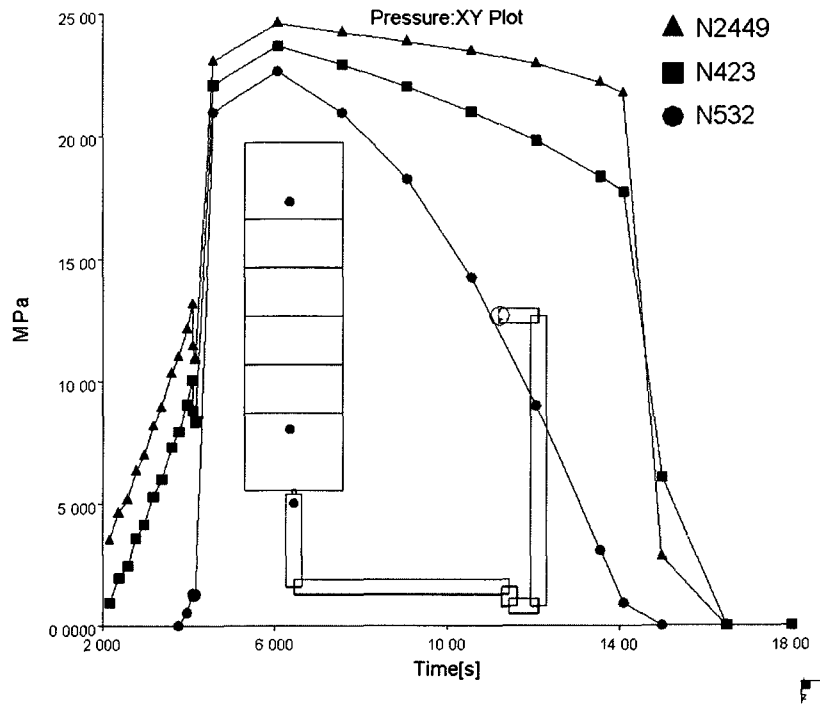


Figure 33b - Pressure profile at three locations in 4 mm perpendicular rib cavity, mtl: CR3500 @ 18.8 cc/s injection rate

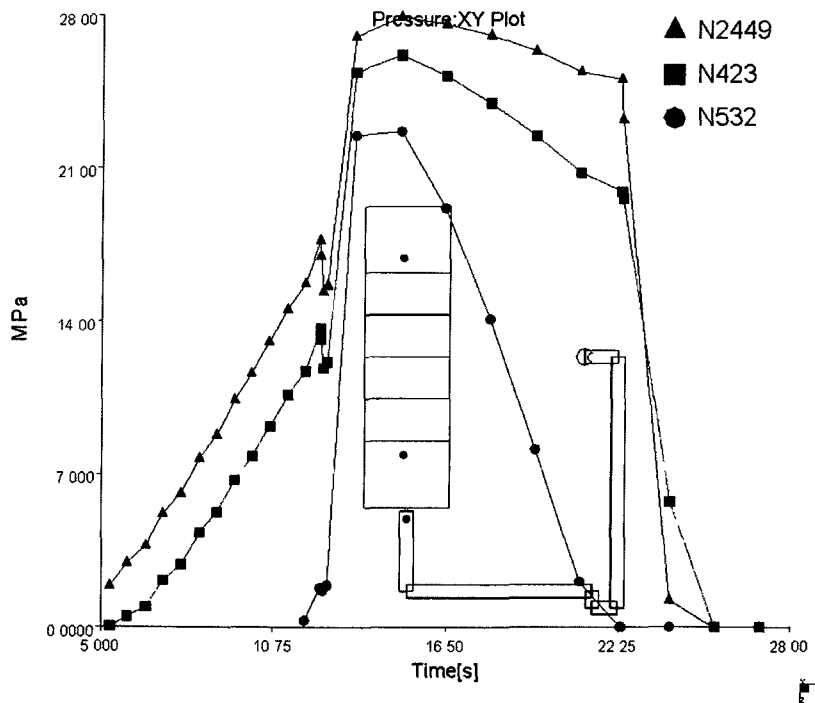


Figure 34b - Pressure profile at three locations in 4 mm perpendicular rib cavity, mtl: CR3500 @ 6.3 cc/s injection rate

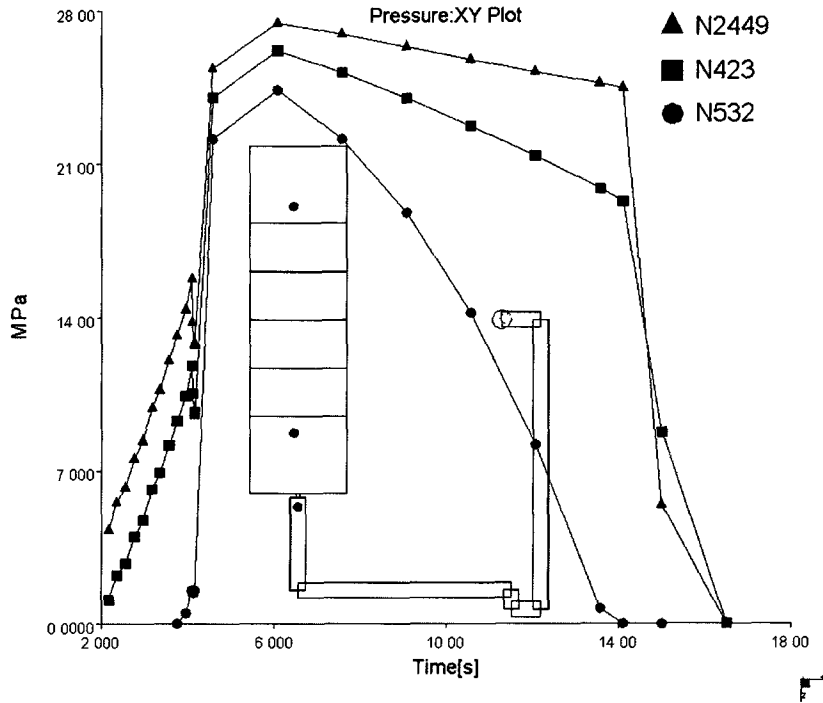


Figure 35b - Pressure profile at three locations in 4 mm perpendicular rib cavity, mtl: CR4500 @ 18.8 cc/s injection rate

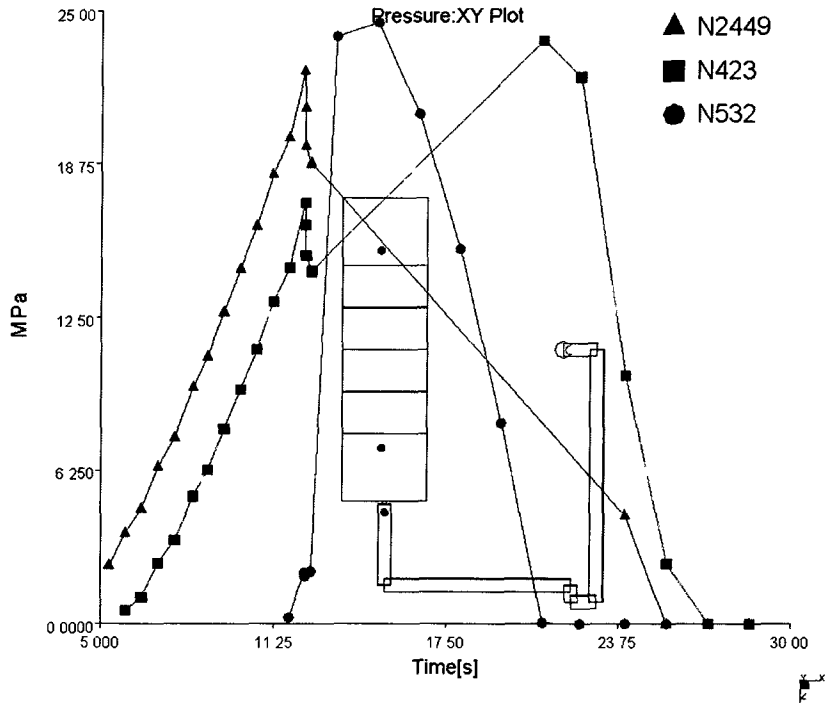


Figure 36b - Pressure profile at three locations in 4 mm perpendicular rib cavity, mtl: CR4500 @ 6.3 cc/s injection rate

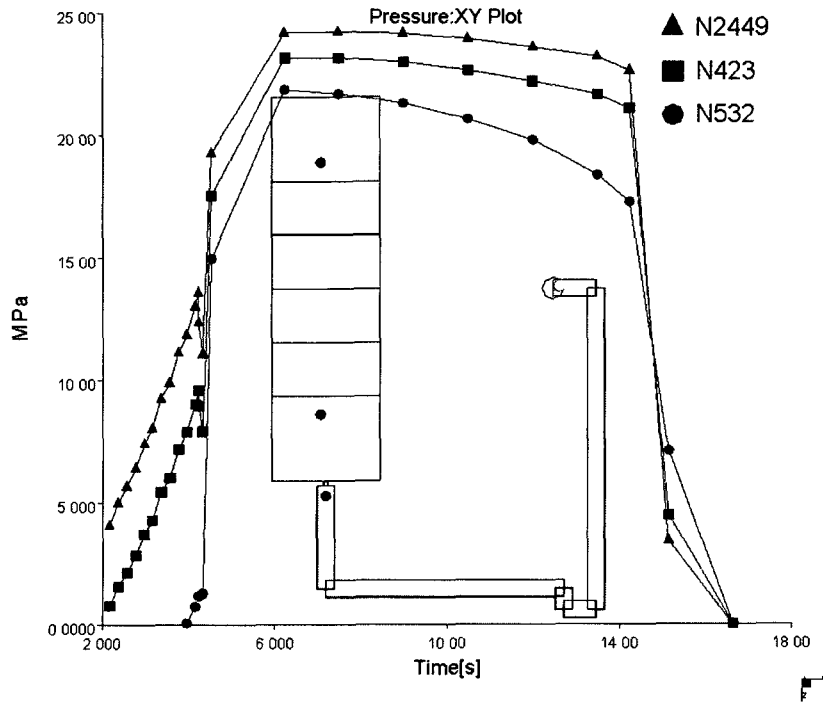


Figure 37b - Pressure profile at three locations in 4 mm perpendicular rib cavity, mtl: 700GP @ 18.8 cc/s injection rate

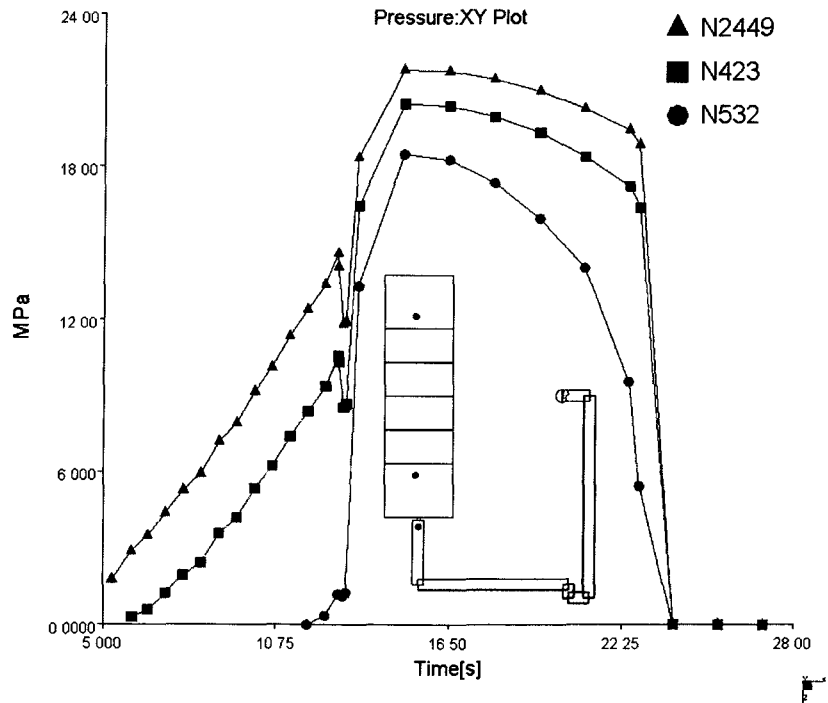


Figure 38b - Pressure profile at three locations in 4 mm perpendicular rib cavity, mtl: 700GP @ 6.3 cc/s injection rate

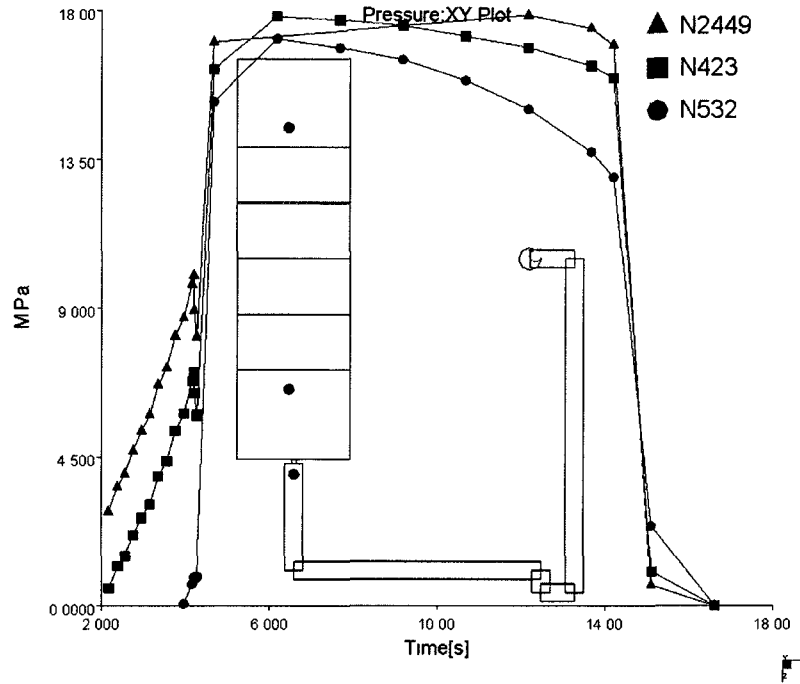


Figure 39b - Pressure profile at three locations in 4 mm perpendicular rib cavity, mtl: 2000GP @ 18.8 cc/s injection rate

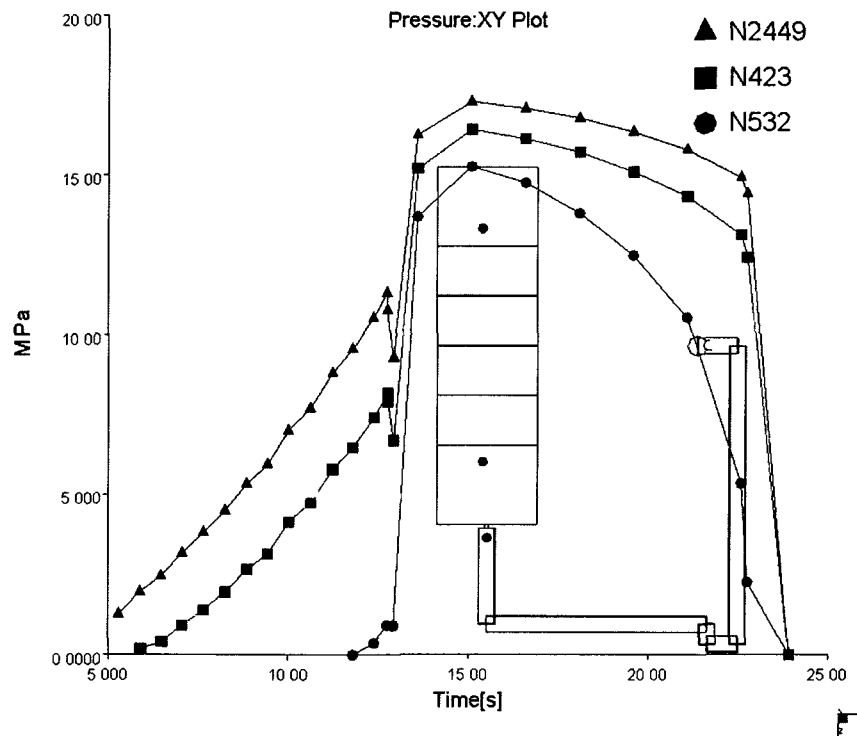


Figure 40b - Pressure profile at three locations in 4 mm perpendicular rib cavity, mtl: 2000GP @ 6.3 cc/s injection rate

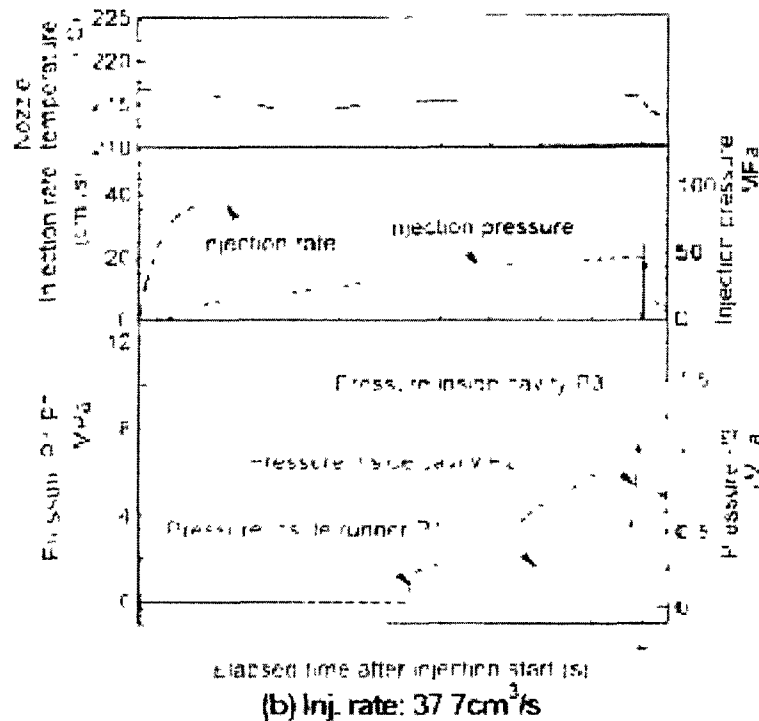
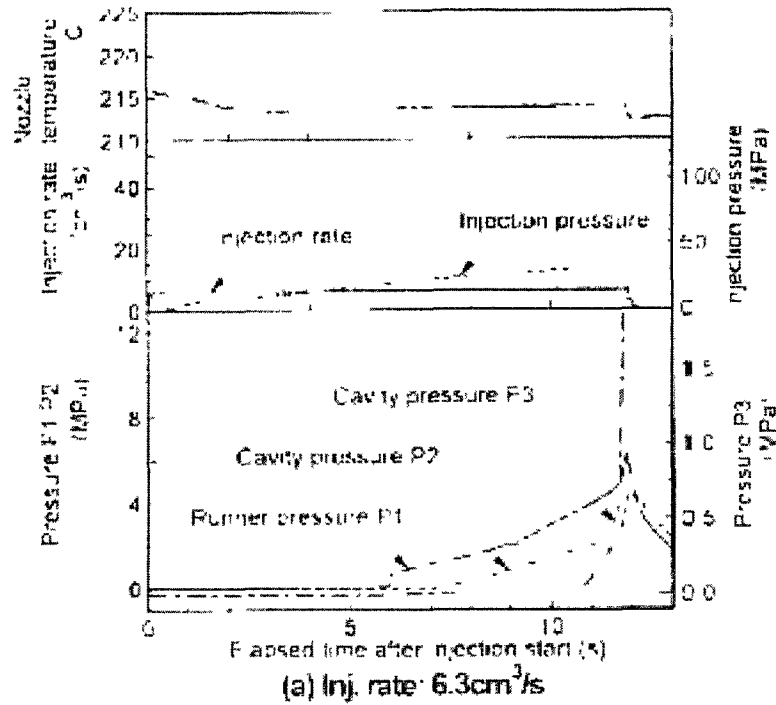


Fig.6 Pressure and temperature variation curves for PP/J-2000GP

Figure 41b – Experimental data of Pressure profile at three locations in obstacle pin cavity, mtl: J-2000GP

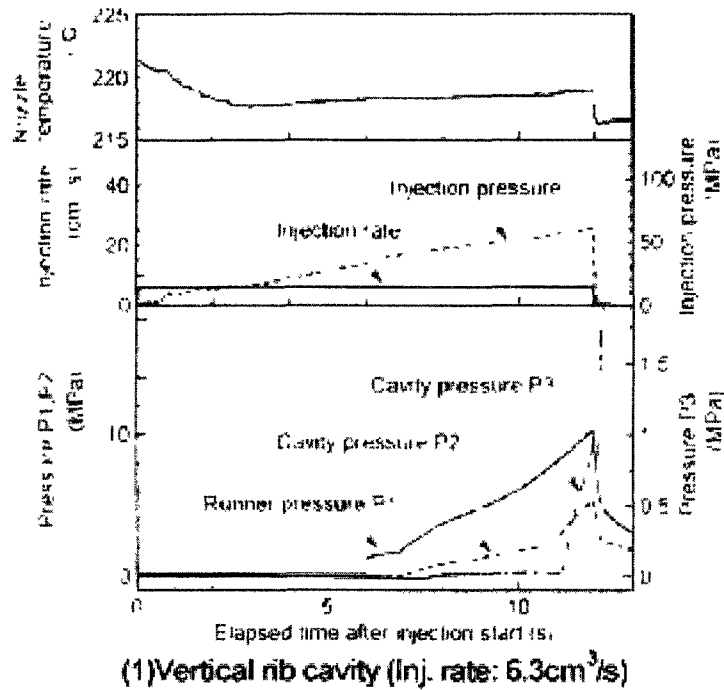


Figure 42b – Experimental data of Pressure profile at three locations in 4 mm parallel rib cavity, mtl: CR-2500

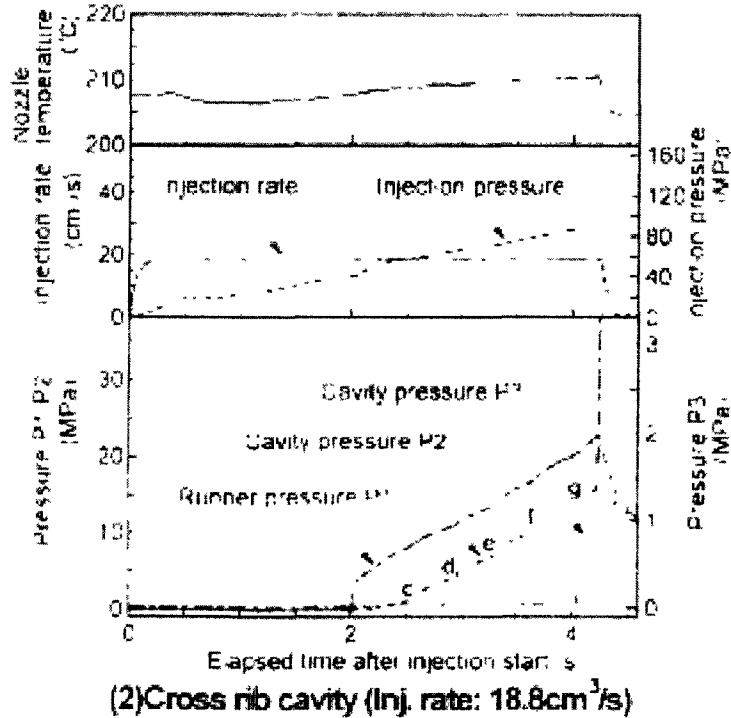


Figure 43b – Experimental data of Pressure profile at three locations in 4 mm perpendicular rib cavity, mtl: CR-2500

Appendix C -Tables

Table 1 – Pressure at different locations in obstacle pin cavity

	Pressure at location(Mpa)		Percent Difference
	Experiment	Moldflow	
	P1		
J-2000/6.3	5.1	6.0	-8.11%
J-2000/37.7	7.1	6.2	6.77%
J-700/6.3	9.9	11.9	-9.17%
J-700/37.7	9.8	8.5	7.10%
CR-3500/6.3	8.1	8.2	-0.61%
CR-3500/37.7	9.2	8.4	4.55%
CR-4500/6.3	10.0	14.0	-16.67%
CR-4500/37.7	10.1	13.0	-12.55%
	P2		
J-2000/6.3	4.2	4.1	1.20%
J-2000/37.7	6.0	4.0	20.00%
J-700/6.3	8.5	4.0	36.00%
J-700/37.7	7.9	5.0	22.48%
CR-3500/6.3	6.8	5.8	7.94%
CR-3500/37.7	7.8	5.8	14.71%
CR-4500/6.3	8.0	10.0	-11.11%
CR-4500/37.7	8.5	8.4	0.59%
		Avg.	3.94%
		Std. Dev.	14.28%

Table 2 – Peak injection pressure in obstacle pin cavity

	Peak Injection Pressure		
	Experiment	Moldflow	Percent Difference
J-2000/6.3	3500	1750	33.33%
J-2000/37.7	4900	2400	34.25%
J-700/6.3	5200	2500	35.06%
J-700/37.7	6800	3400	33.33%
CR-3500/6.3	5800	2800	34.88%
CR-3500/37.7	7500	2900	44.23%
CR-4500/6.3	9800	3300	49.62%
CR-4500/37.7	11500	3400	54.36%
		Avg.	39.88%
		Std. Dev.	8.36%

Table 3 – Fill time comparison in obstacle pin cavity

	Fill Time(s)		
	Experiment	Moldflow	Percent Difference
J-2000/6.3	11.25	10.05	5.63%
J-2000/37.7	1.92	1.712	5.73%
J-700/6.3	11.85	10.16	7.68%
J-700/37.7	1.98	1.724	6.91%
CR-3500/6.3	11.65	9.846	8.39%
CR-3500/37.7	1.95	1.624	9.12%
CR-4500/6.3	11.85	9.877	9.08%
CR-4500/37.7	1.98	1.68	8.20%
		Avg.	7.59%
		Std. Dev.	1.38%

Appendix D – Temperature at Flow Front

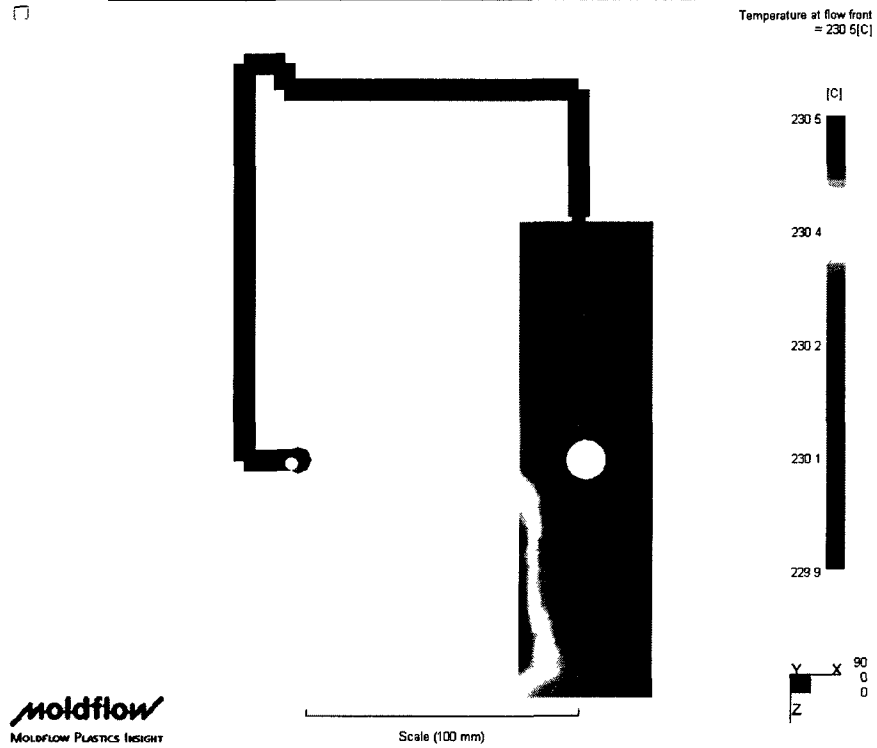


Figure 1d - Temperature at flow front in obstacle pin cavity, mtl: J700GP @ 37.7

cc/s

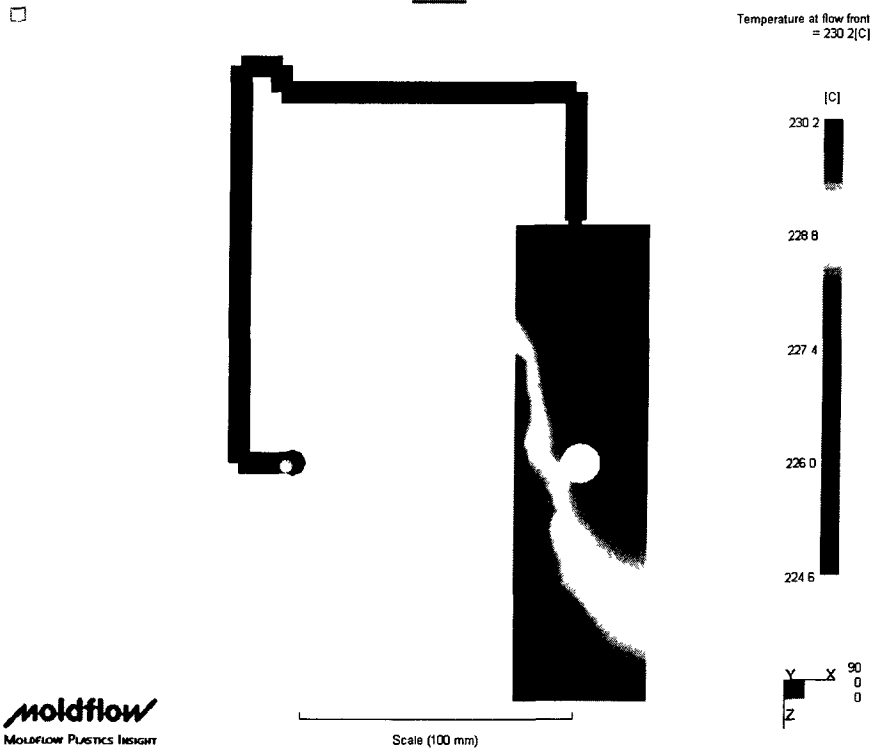


Figure 2d - Temperature at flow front in obstacle pin cavity, mtl: J700GP @ 6.3cc/s

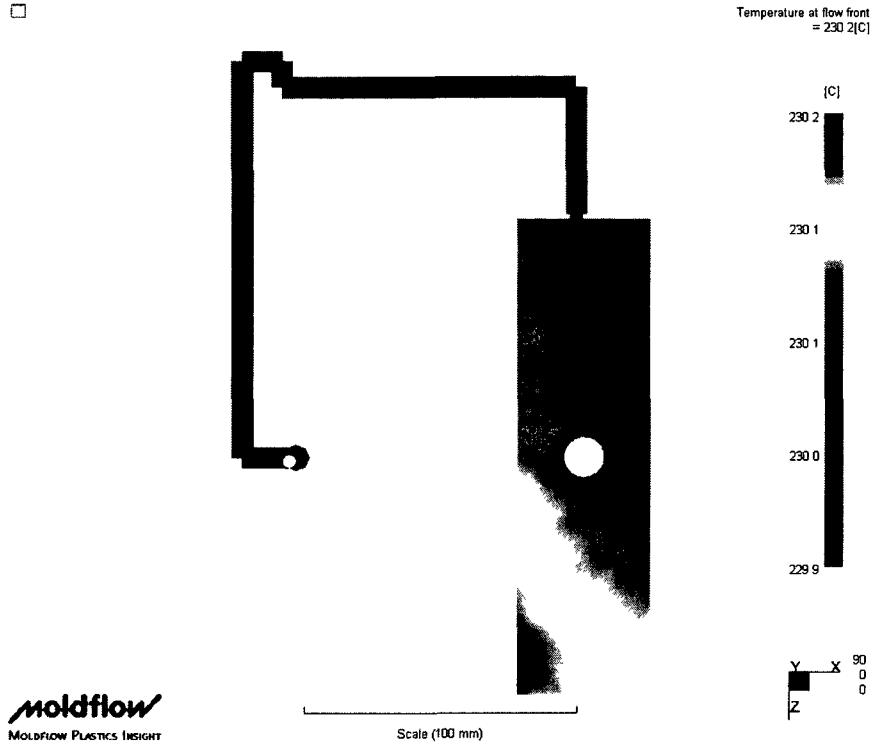


Figure 3d - Temperature at flow front in obstacle pin cavity, mtl: J2000GP @ 37.7

cc/s

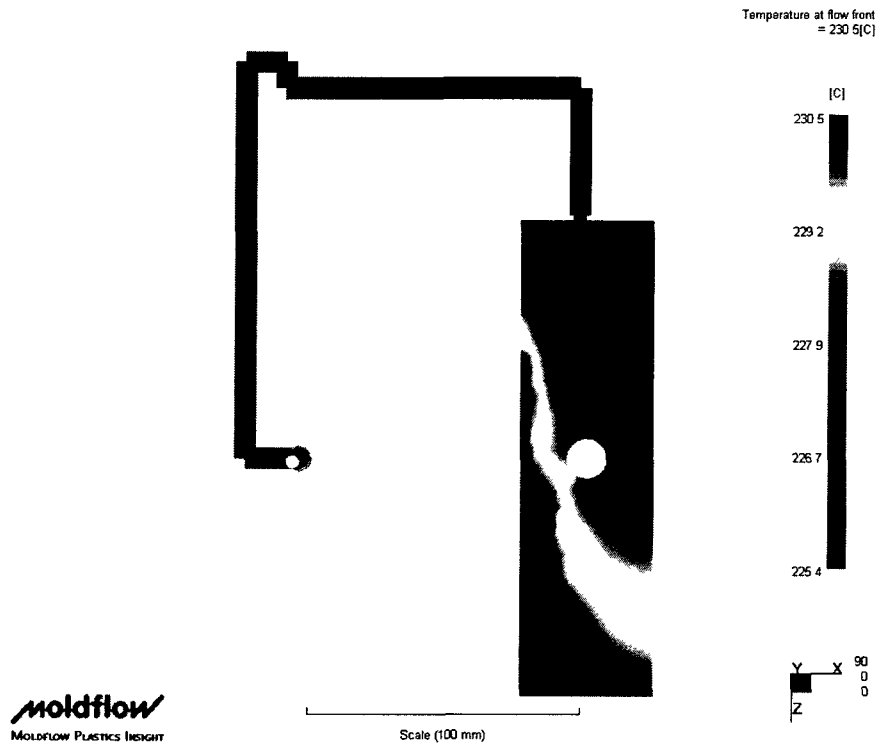


Figure 4d - Temperature at flow front in obstacle pin cavity, mtl: J2000GP @ 6.3

cc/s

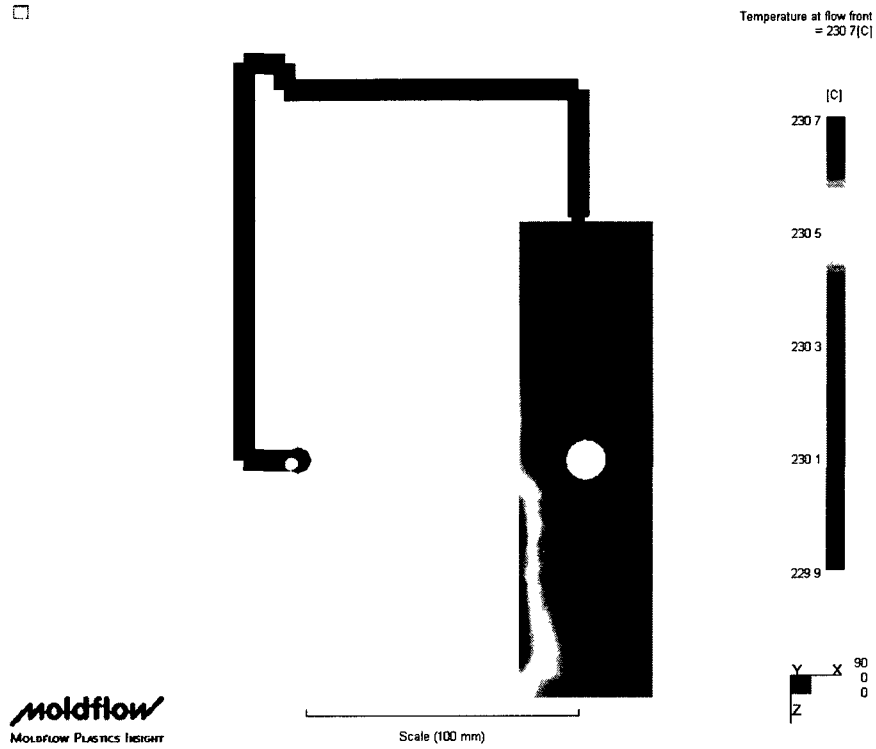


Figure 5d - Temperature at flow front in obstacle pin cavity, mtl: CR3500 @ 37.7

cc/s

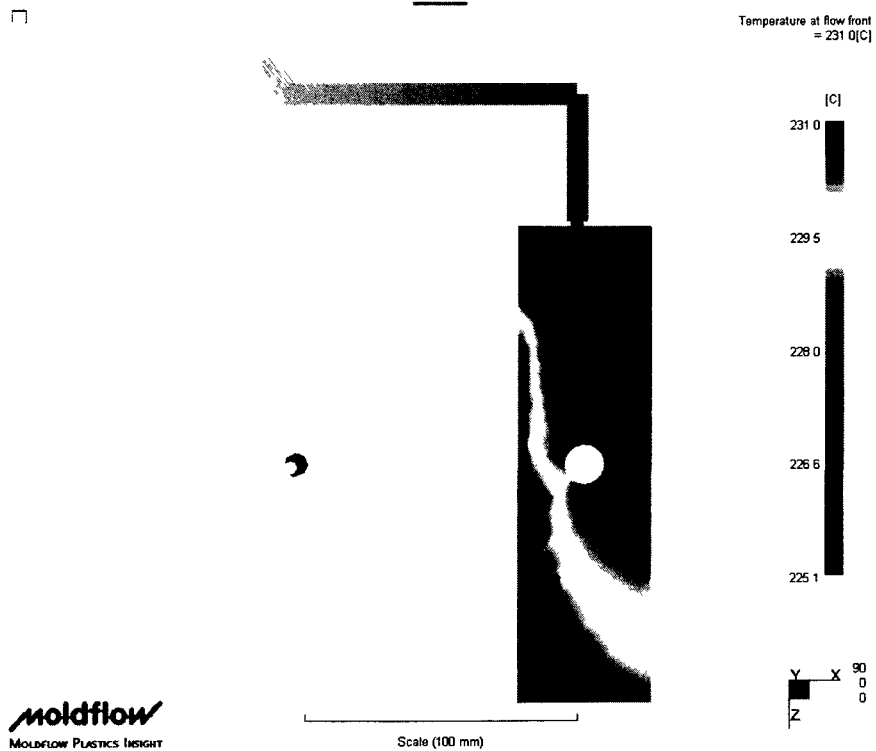


Figure 6d - Temperature at flow front in obstacle pin cavity, mtl: CR3500 @ 6.3 cc/s

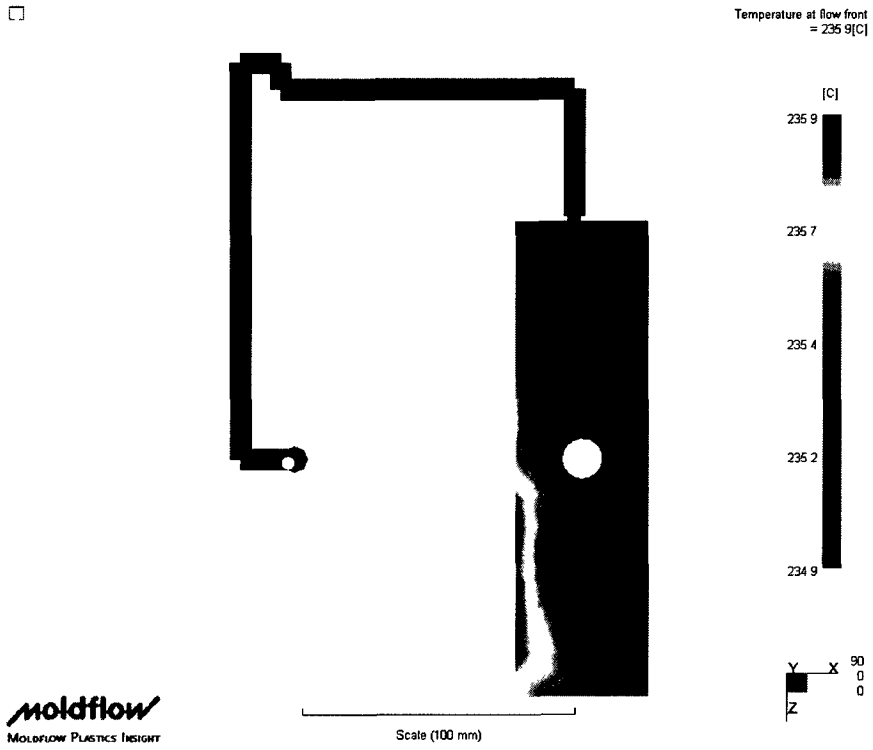


Figure 7d - Temperature at flow front in obstacle pin cavity, mtl: CR4500 @ 37.7

cc/s



Figure 8d - Temperature at flow front in obstacle pin cavity, mtl: CR4500 @ 6.3 cc/s

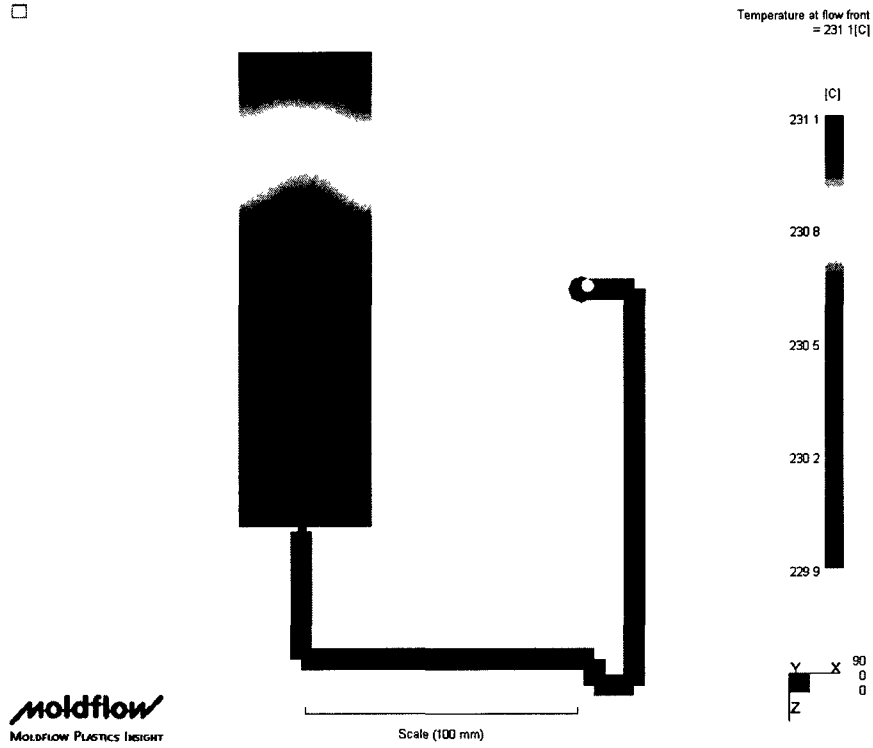


Figure 9d - Temperature at flow front in 2 mm parallel rib cavity, mtl: CR3500 @ 37.7 cc/s

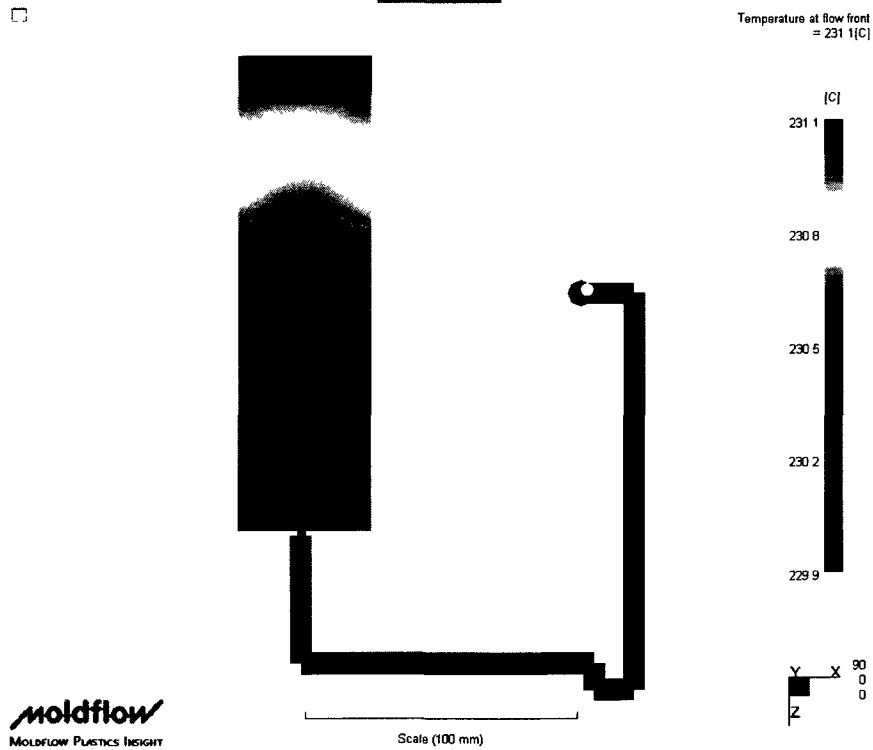


Figure 10d - Temperature at flow front in 2 mm parallel rib cavity, mtl: CR4500 @ 37.7 cc/s

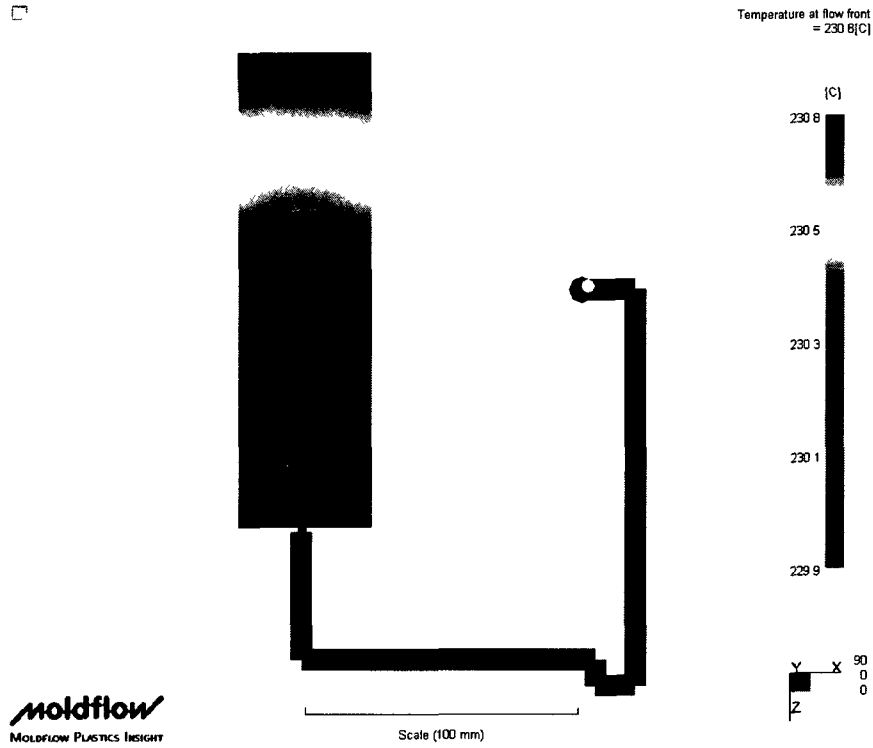


Figure 11d - Temperature at flow front in 2 mm parallel rib cavity, mtl: J2000GP @ 37.7 cc/s

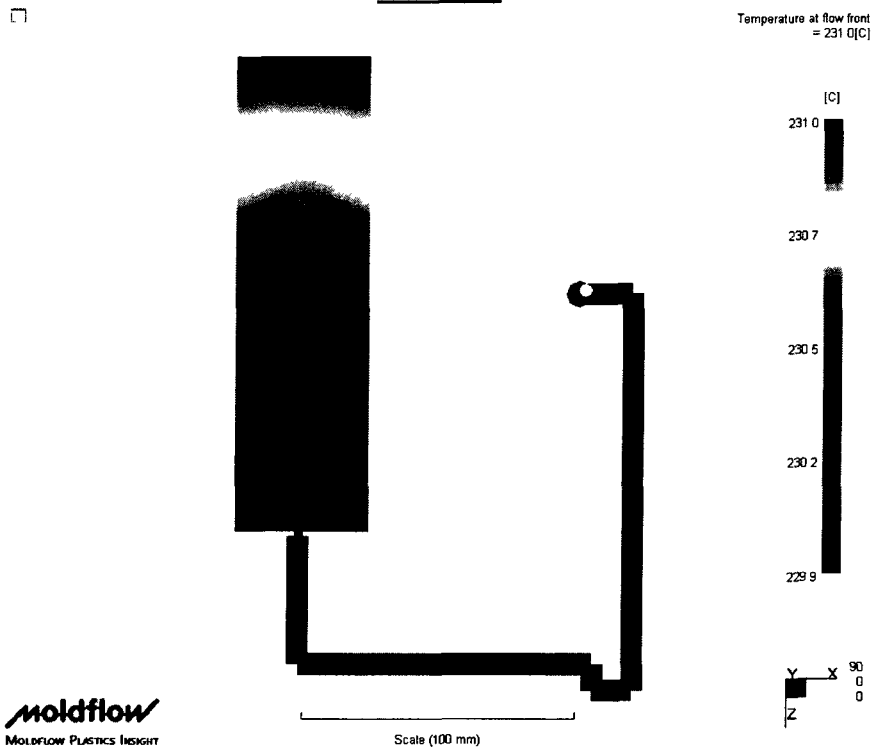


Figure 12d - Temperature at flow front in 2 mm parallel rib cavity, mtl: J700GP @ 37.7 cc/s

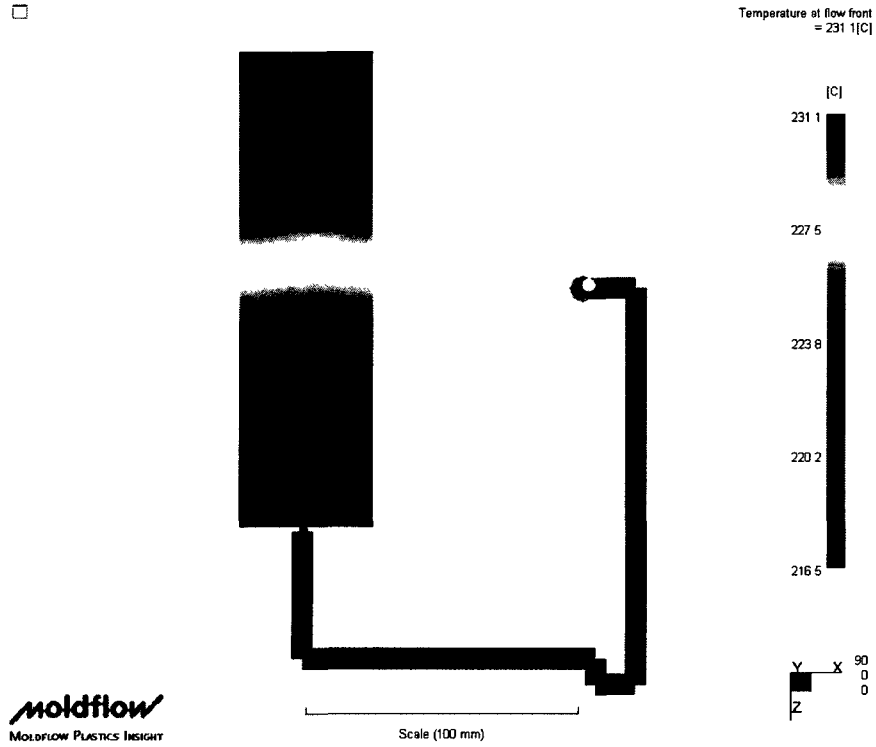


Figure 13d - Temperature at flow front in 2 mm parallel rib cavity, mtl: CR3500 @ 6.3 cc/s

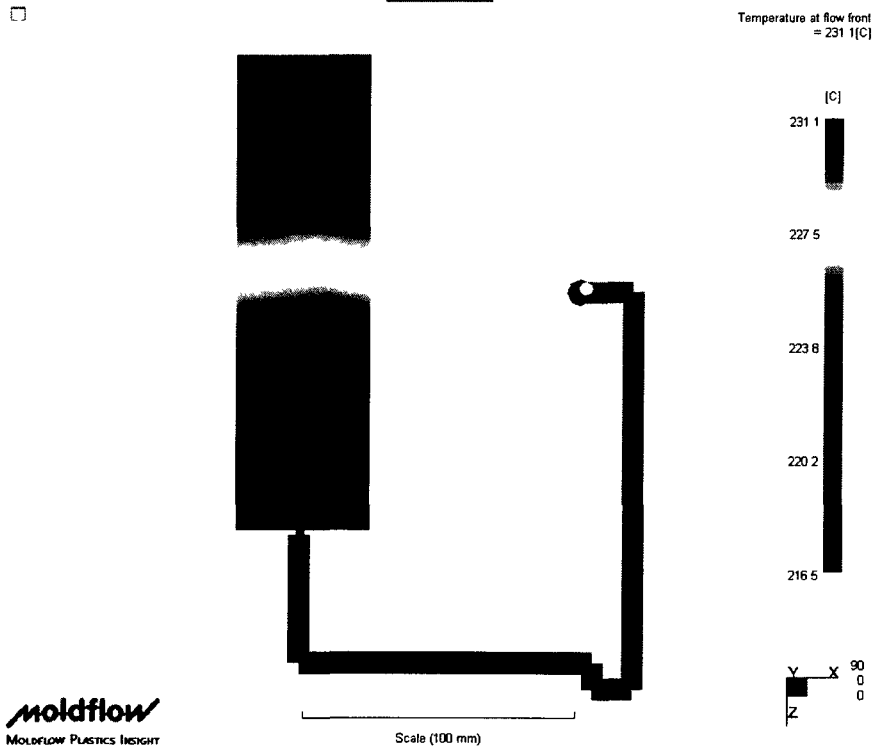


Figure 14d - Temperature at flow front in 2 mm parallel rib cavity, mtl: CR4500 @ 6.3 cc/s

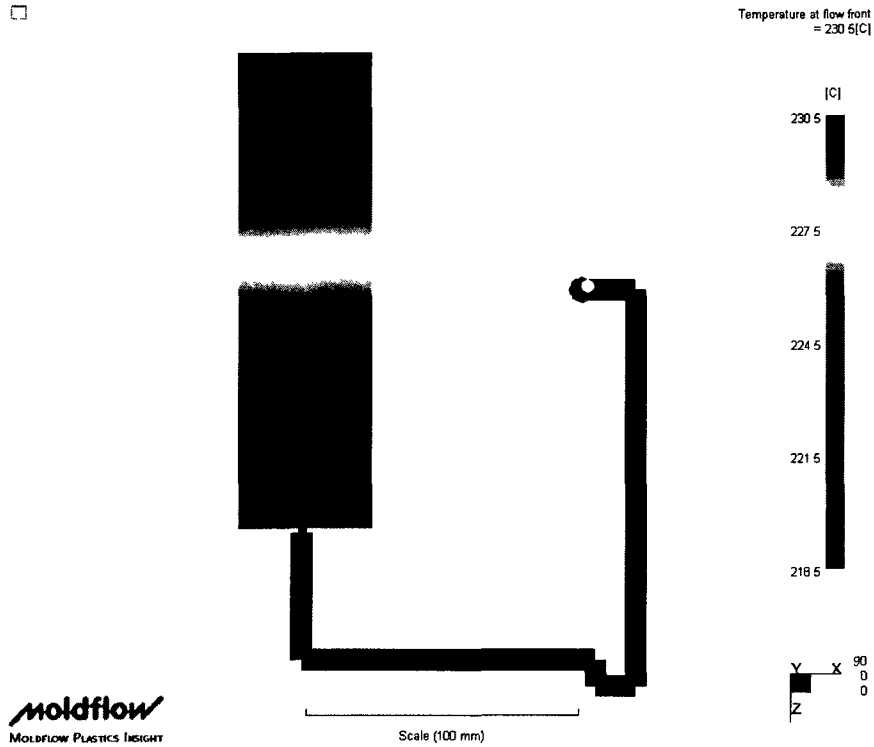


Figure 15d - Temperature at flow front in 2 mm parallel rib cavity, mtl: J700GP @ 6.3 cc/s

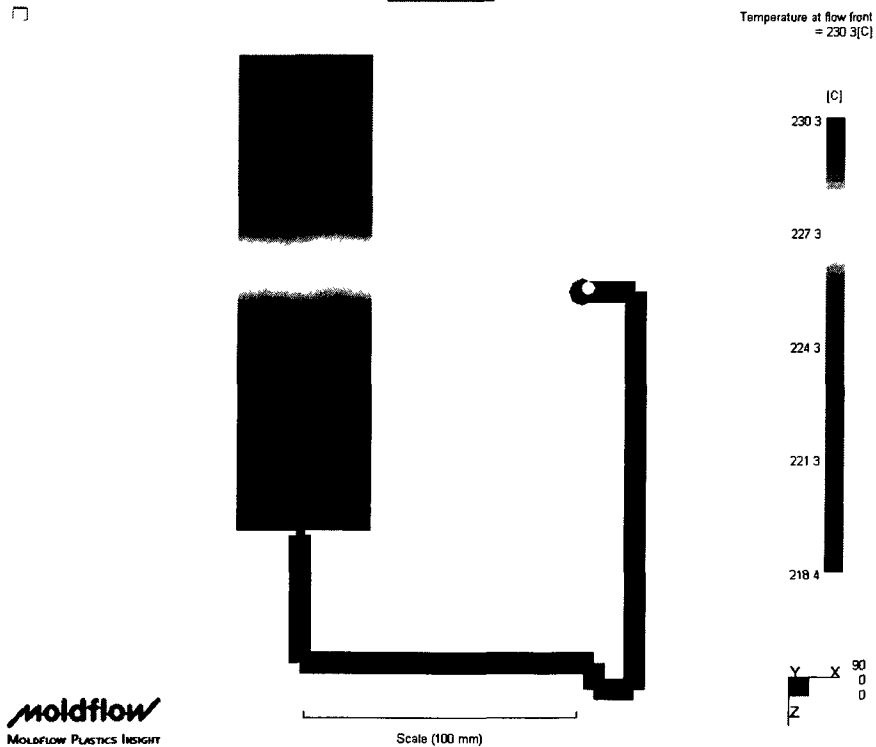
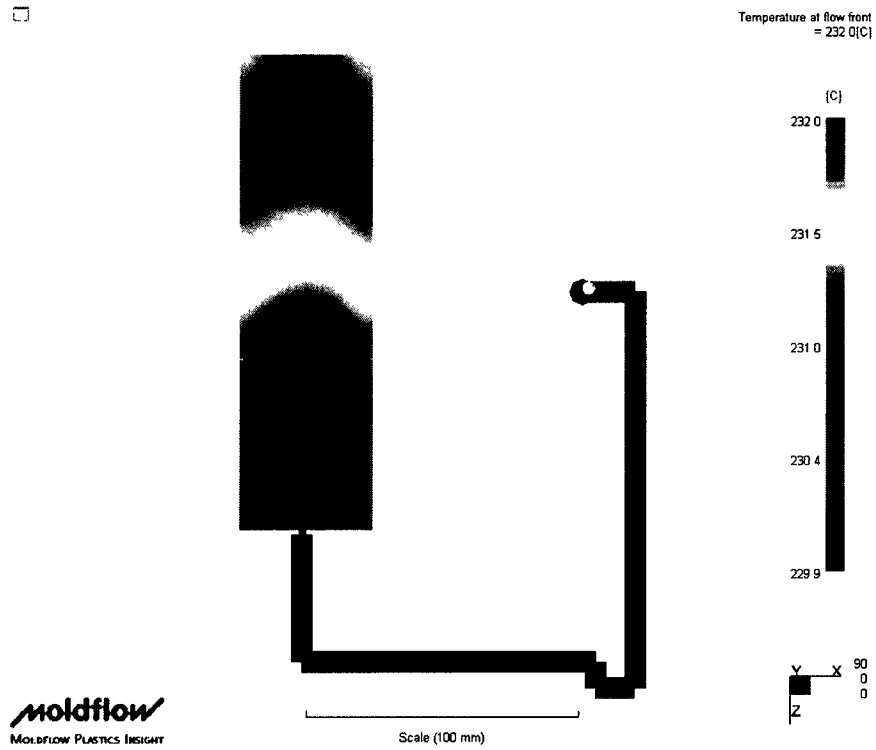
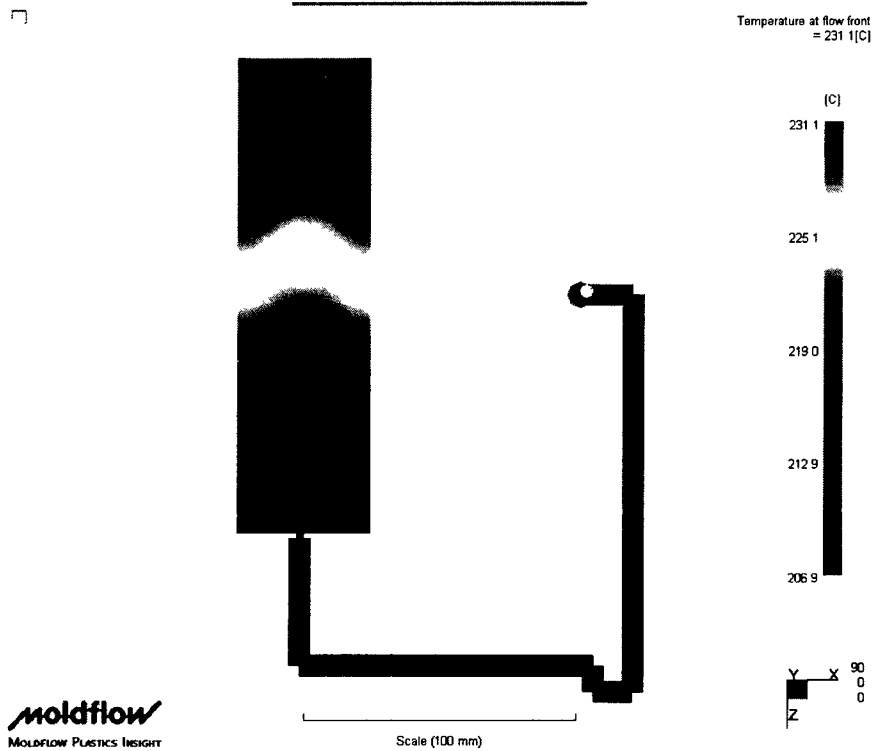


Figure 16d - Temperature at flow front in 2 mm parallel rib cavity, mtl: J2000GP @ 6.3 cc/s



**Figure 17d - Temperature at flow front in 2 mm perpendicular rib cavity, mtl:
CR3500 @ 18.8 cc/s**



**Figure 18d - Temperature at flow front in 2 mm perpendicular rib cavity, mtl:
CR3500 @ 6.3 cc/s**

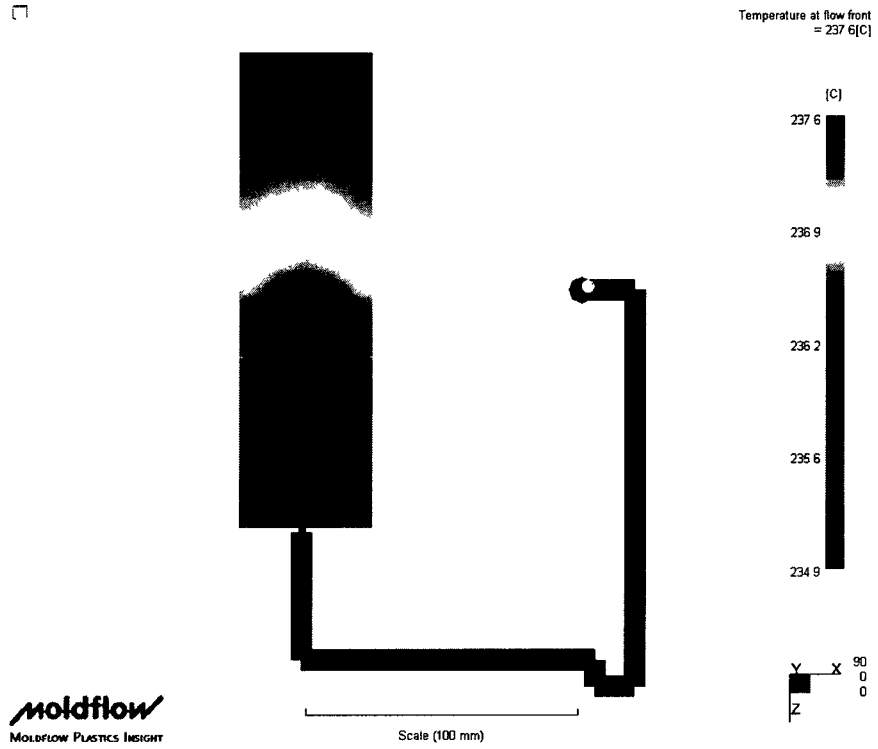


**Figure 19d - Temperature at flow front in 2 mm perpendicular rib cavity, mtl:
CR4500 @ 18.8 cc/s**

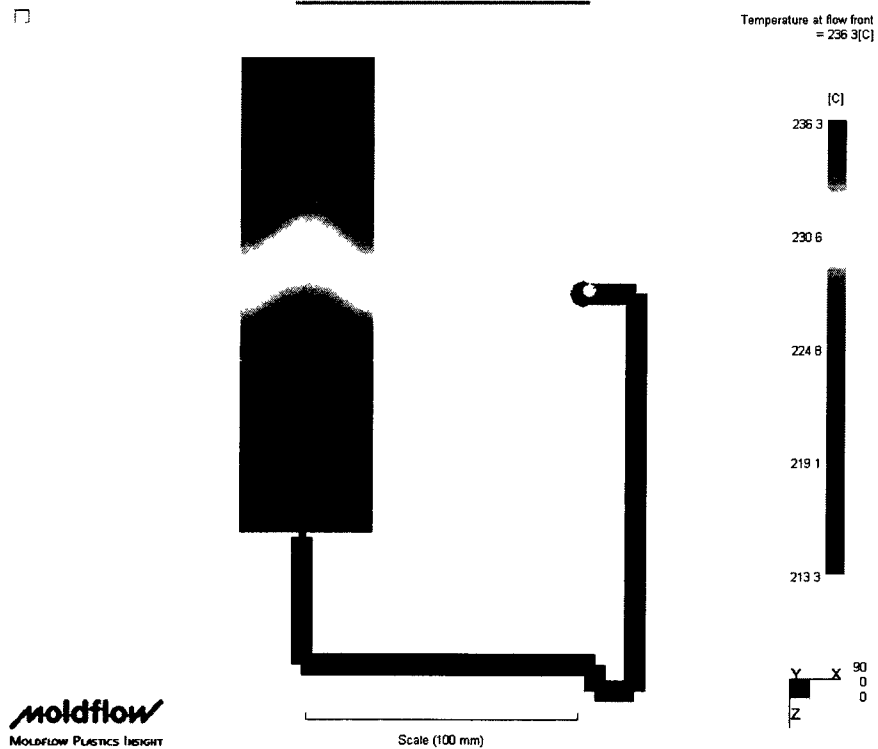


**Figure 20d - Temperature at flow front in 2 mm perpendicular rib cavity, mtl:
CR4500 @ 6.3 cc/s**

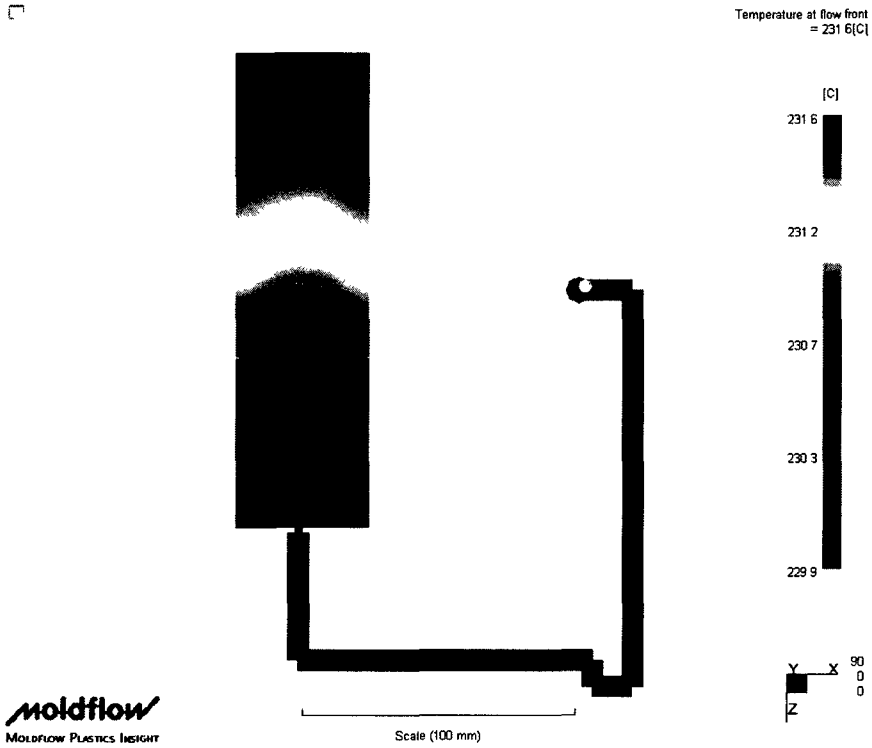


**Figure 21d - Temperature at flow front in 2 mm perpendicular rib cavity, mtl:
J700GP @ 18.8 cc/s**

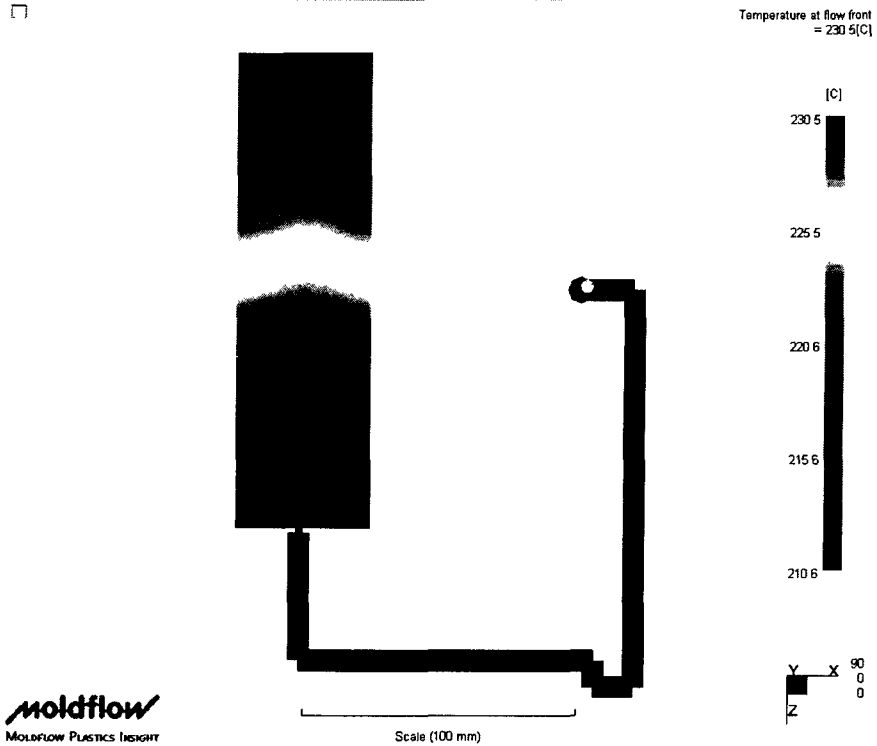


**Figure 22d - Temperature at flow front in 2 mm perpendicular rib cavity, mtl:
J700GP @ 6.3 cc/s**

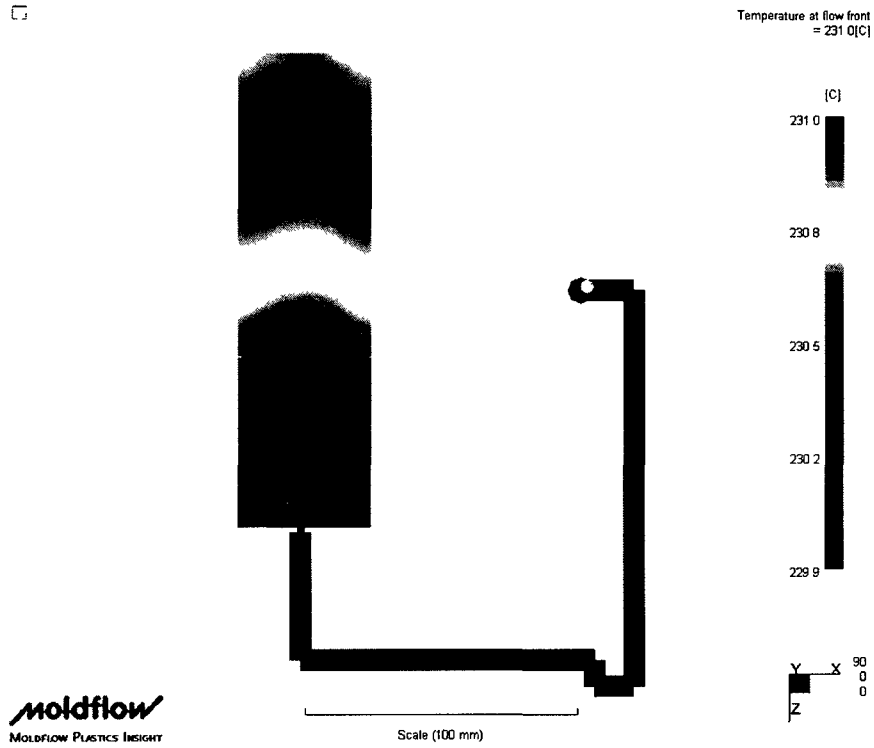


**Figure 23d - Temperature at flow front in 2 mm perpendicular rib cavity, mtl:
J2000GP @ 18.8 cc/s**

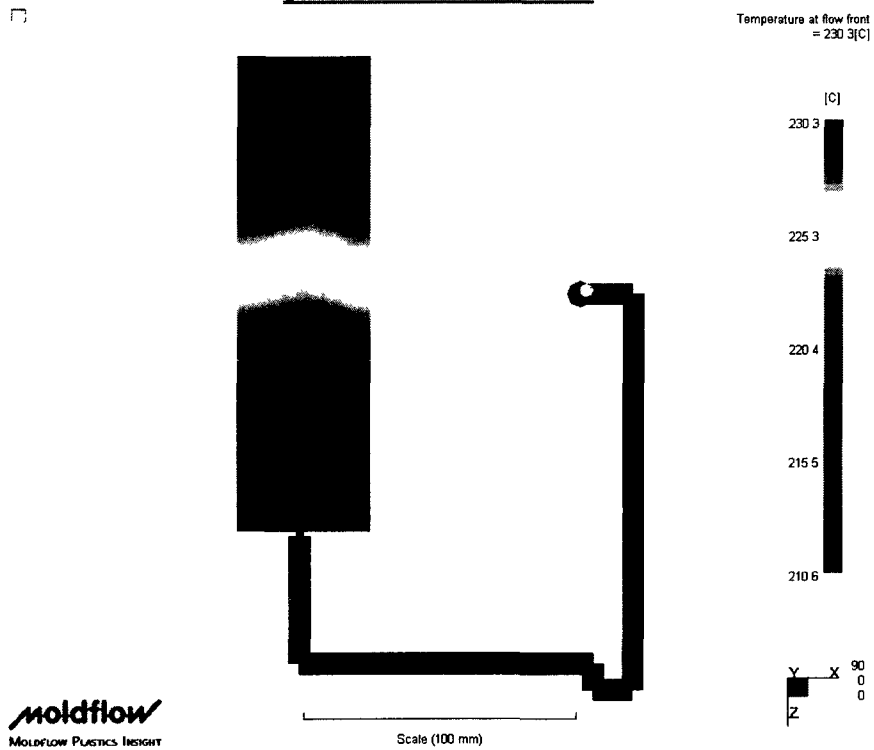


**Figure 24d - Temperature at flow front in 2 mm perpendicular rib cavity, mtl:
J2000GP @ 6.3 cc/s**

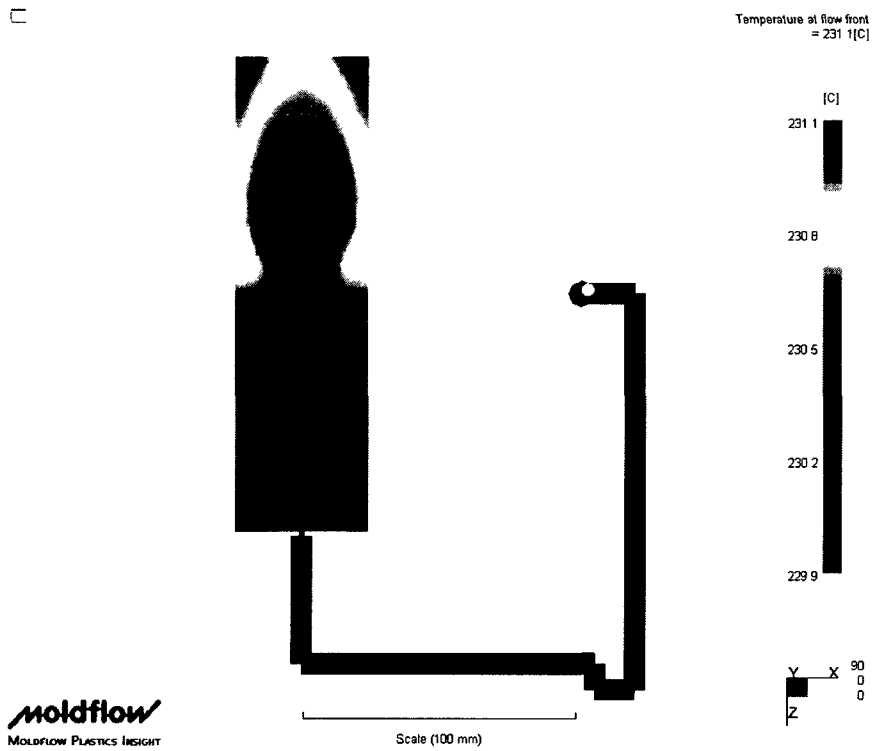


Figure 25d - Temperature at flow front in 4 mm parallel rib cavity, mtl: CR3500 @ 37.7 cc/s

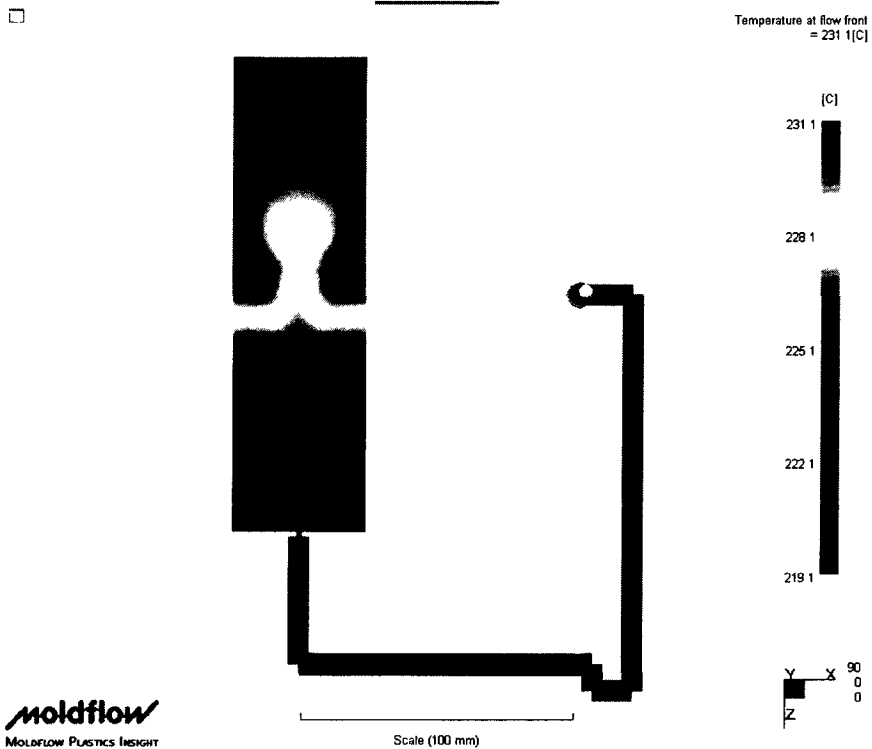


Figure 26d - Temperature at flow front in 4 mm parallel rib cavity, mtl: CR3500 @ 6.3 cc/s

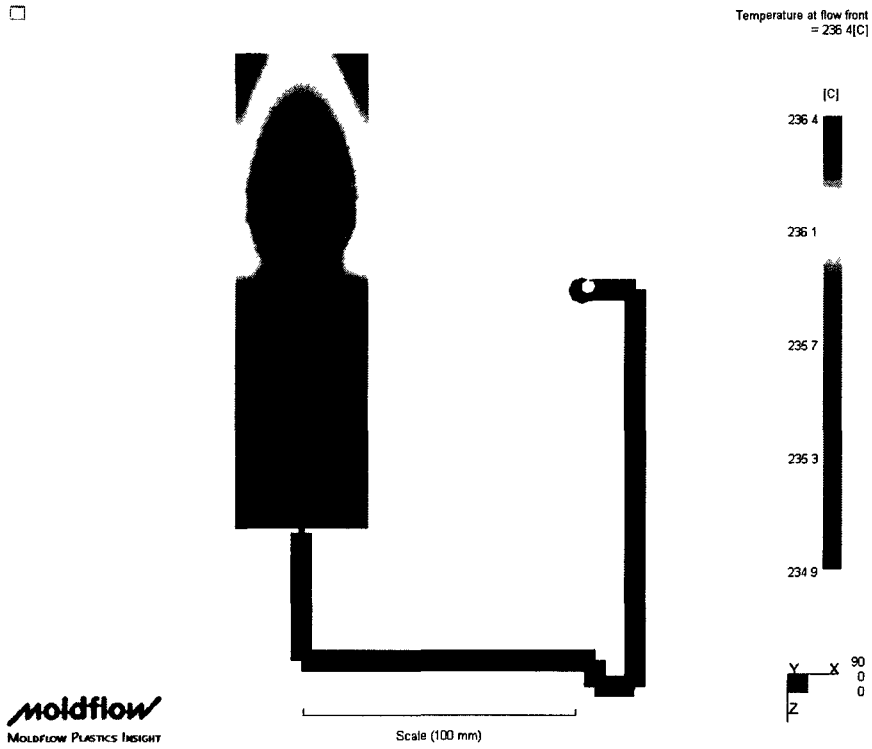


Figure 27d - Temperature at flow front in 4 mm parallel rib cavity, mtl: CR4500 @ 37.7 cc/s

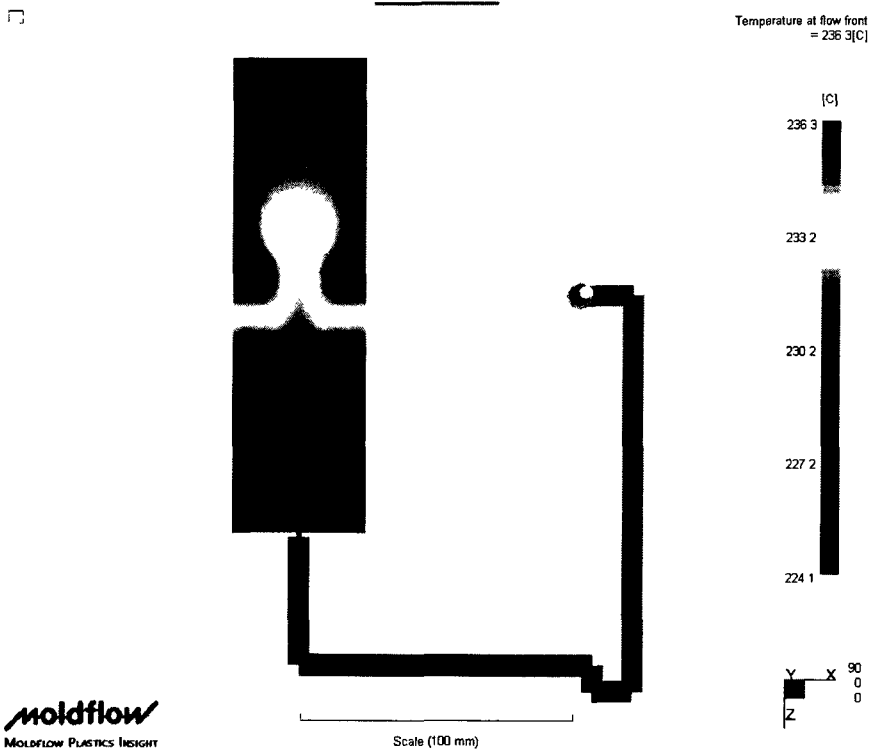


Figure 28d - Temperature at flow front in 4 mm parallel rib cavity, mtl: CR4500 @ 6.3 cc/s

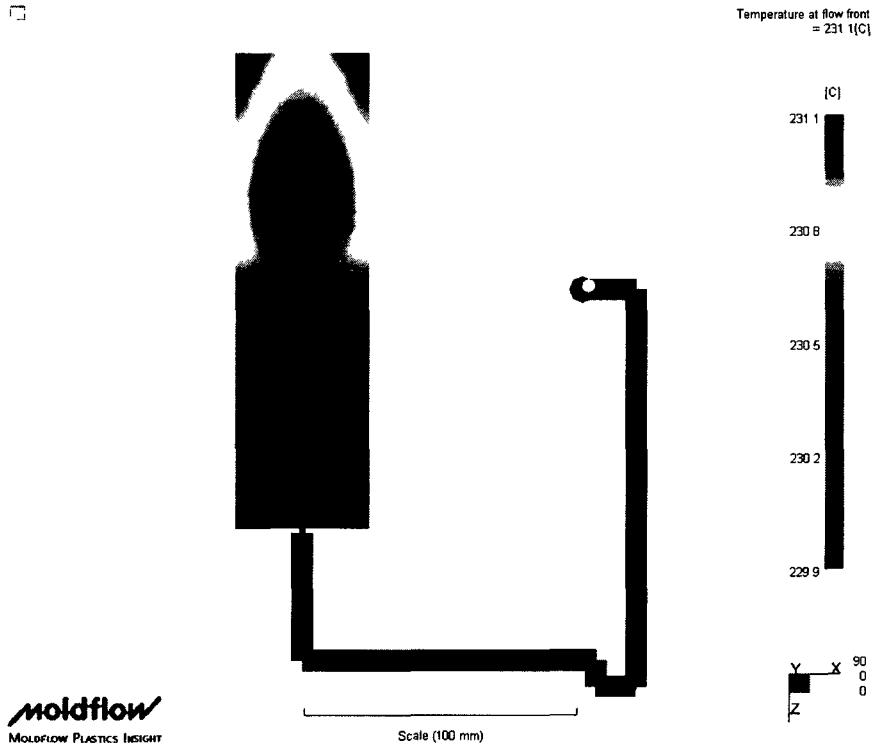


Figure 29d - Temperature at flow front in 4 mm parallel rib cavity, mtl: J700GP @ 37.7 cc/s

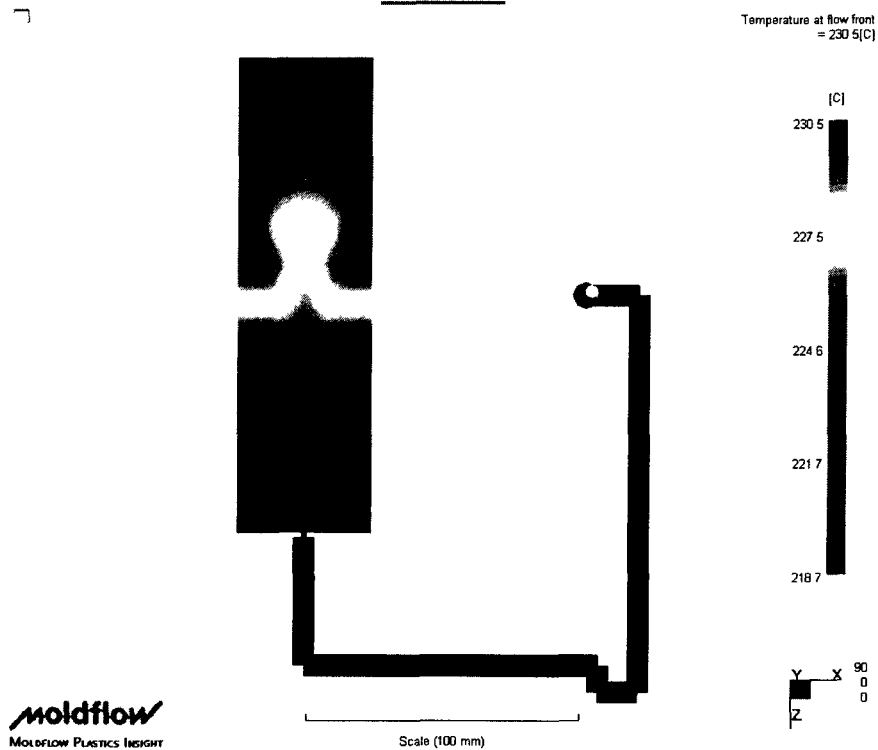


Figure 30d - Temperature at flow front in 4 mm parallel rib cavity, mtl: J700GP @ 6.3 cc/s

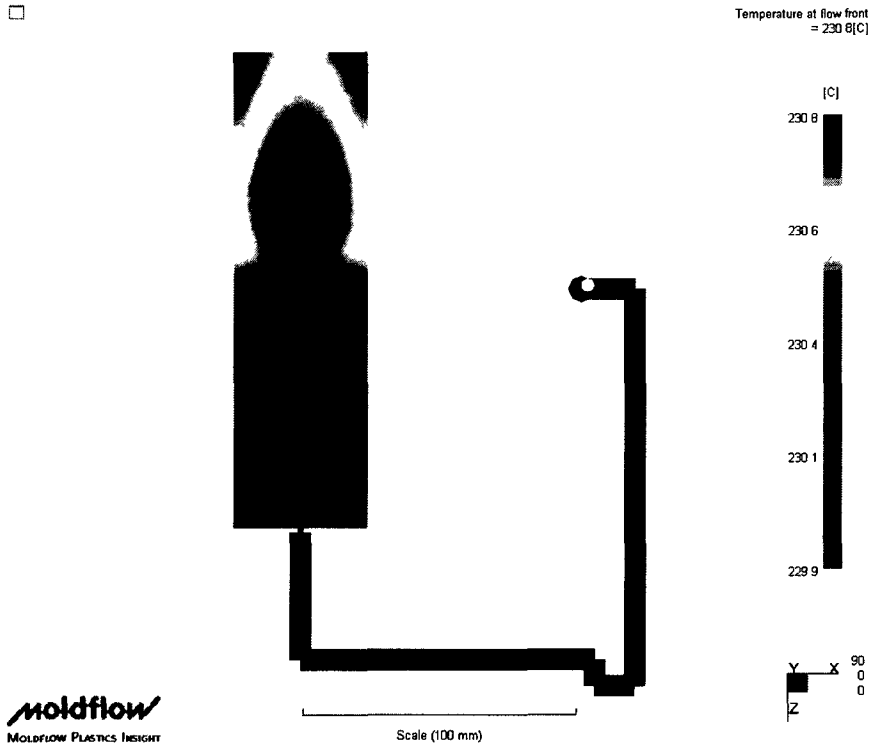


Figure 31d - Temperature at flow front in 4 mm parallel rib cavity, mtl: J2000GP @ 37.7 cc/s

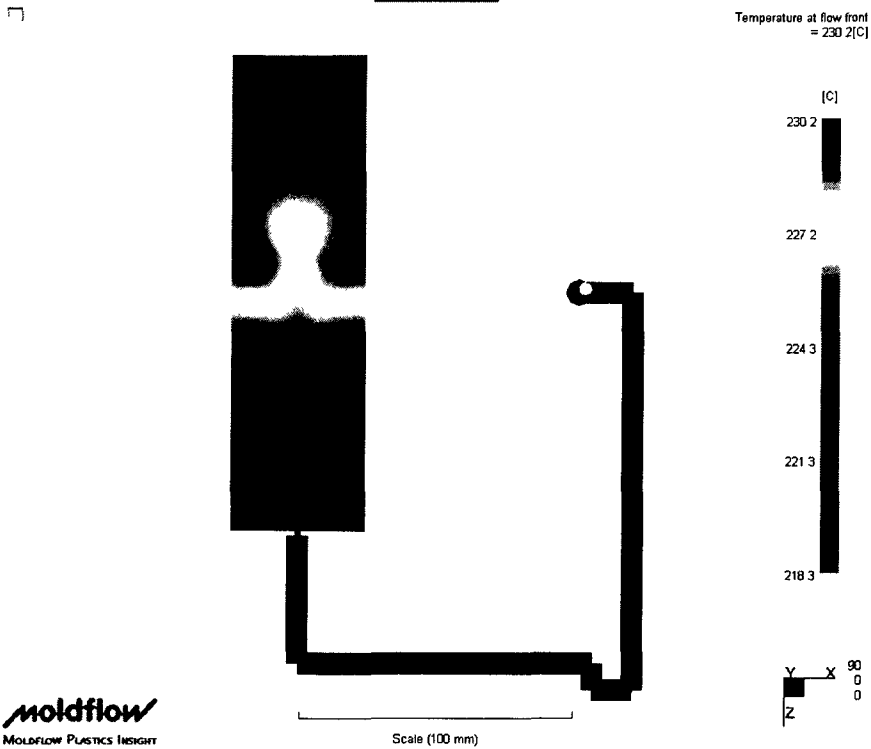
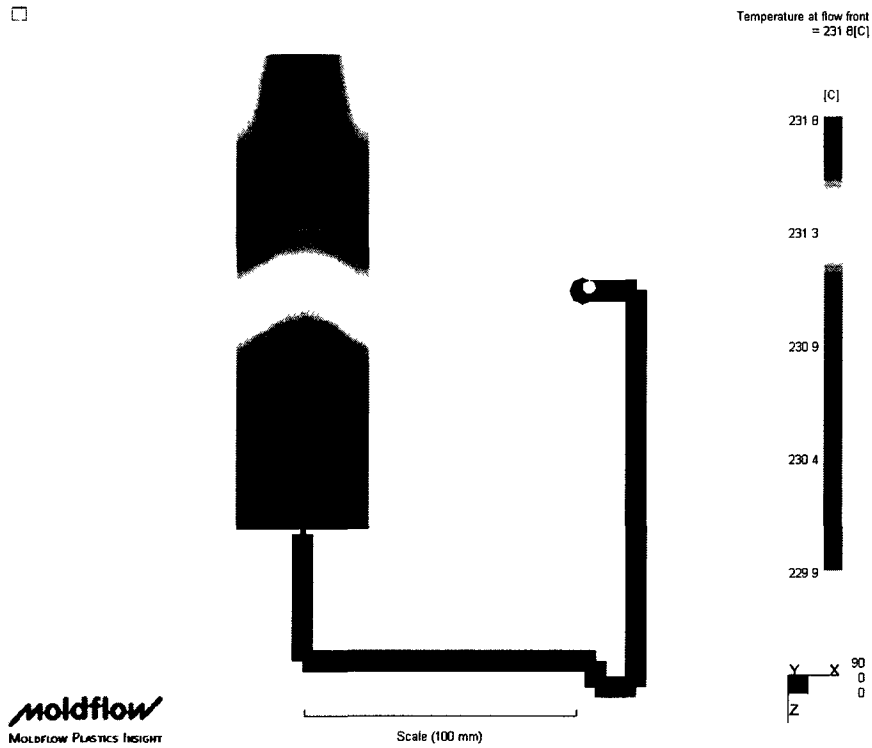
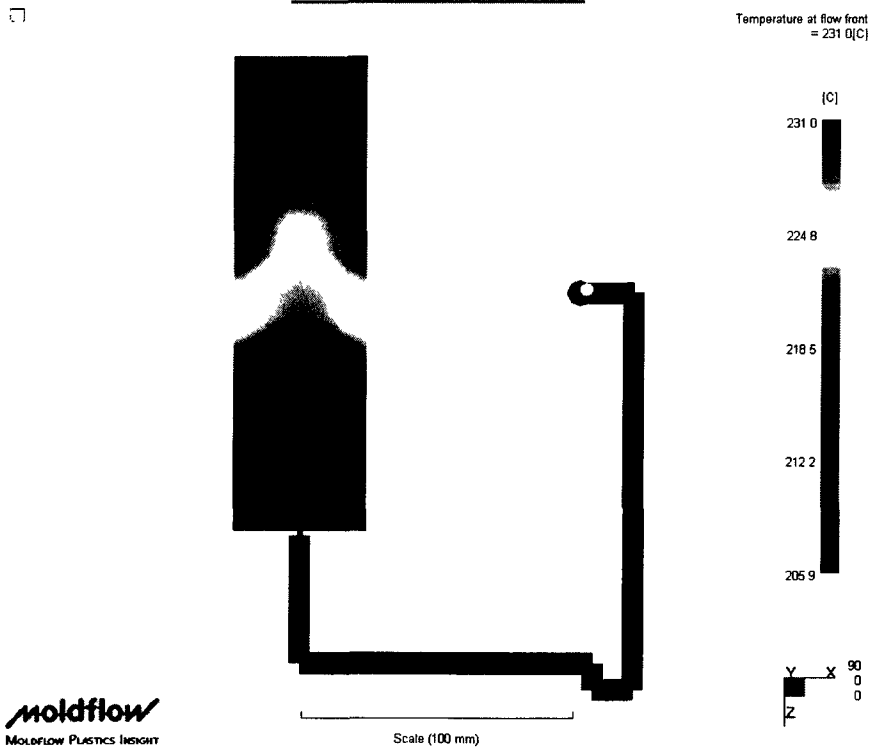


Figure 32d - Temperature at flow front in 4 mm parallel rib cavity, mtl: J2000GP @ 6.3 cc/s



**Figure 33d - Temperature at flow front in 4 mm perpendicular rib cavity, mtl:
CR3500 @ 18.8 cc/s**



**Figure 34d - Temperature at flow front in 4 mm perpendicular rib cavity, mtl:
CR3500 @ 6.3 cc/s**

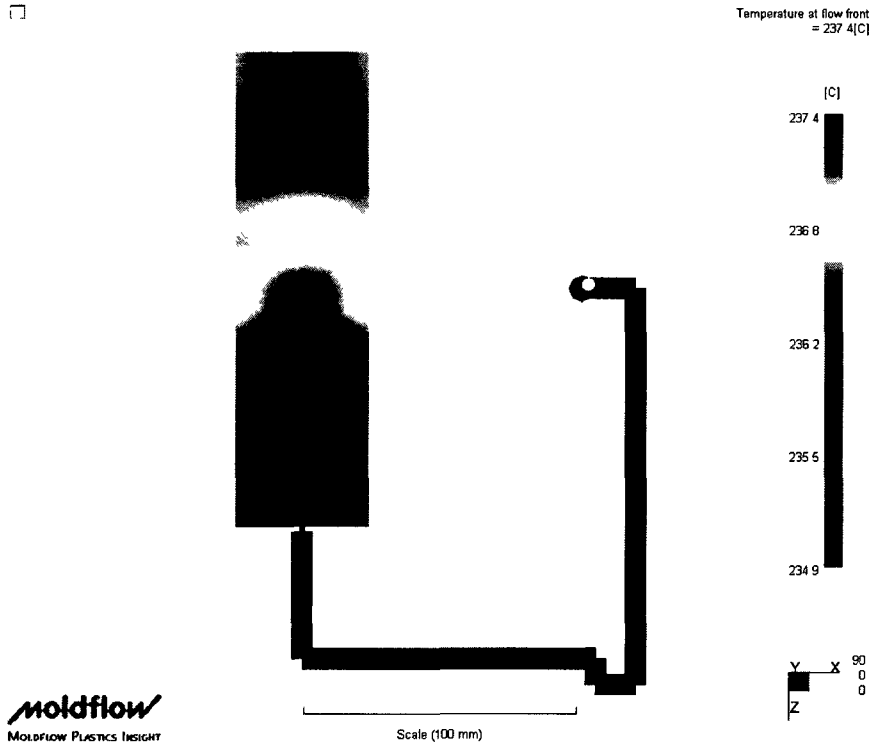


**Figure 35d - Temperature at flow front in 4 mm perpendicular rib cavity, mtl:
CR4500 @ 18.8 cc/s**

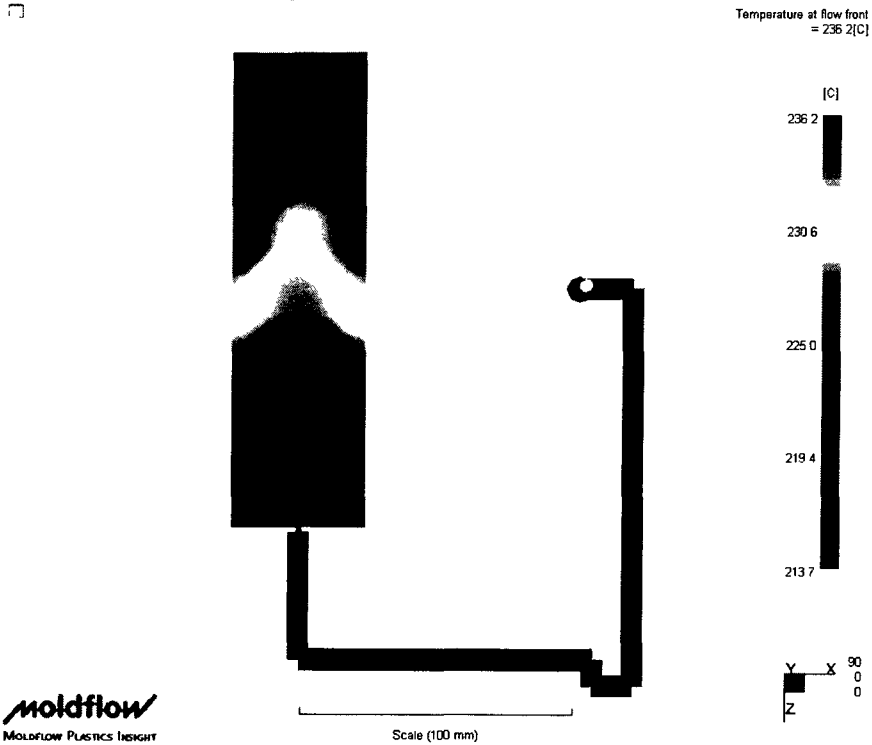


**Figure 36d - Temperature at flow front in 4 mm perpendicular rib cavity, mtl:
CR4500 @ 6.3 cc/s**

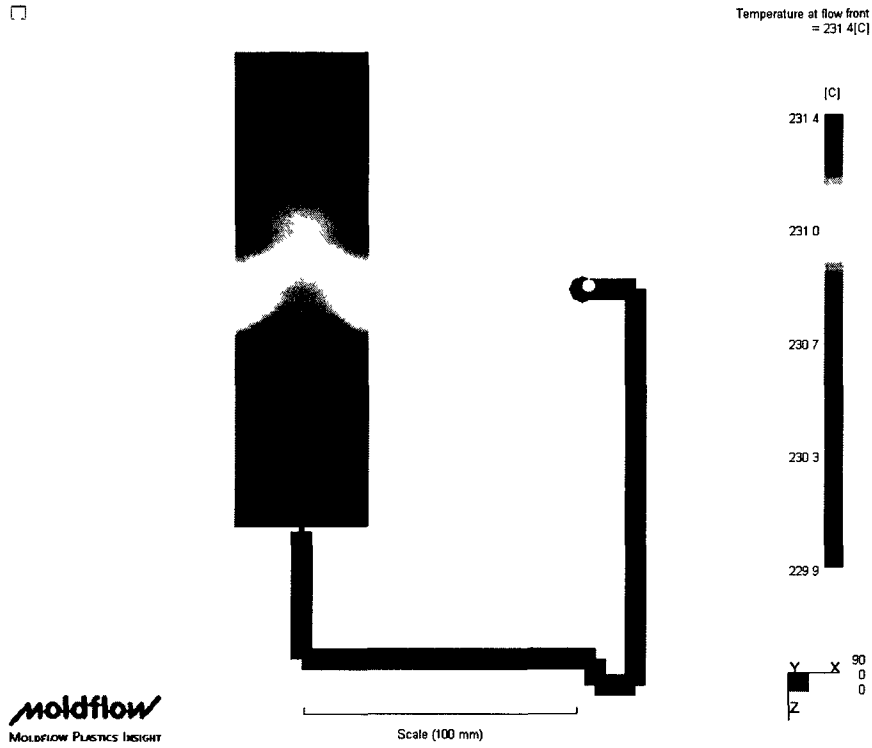


**Figure 37d - Temperature at flow front in 4 mm perpendicular rib cavity, mtl:
J700GP @ 18.8 cc/s**

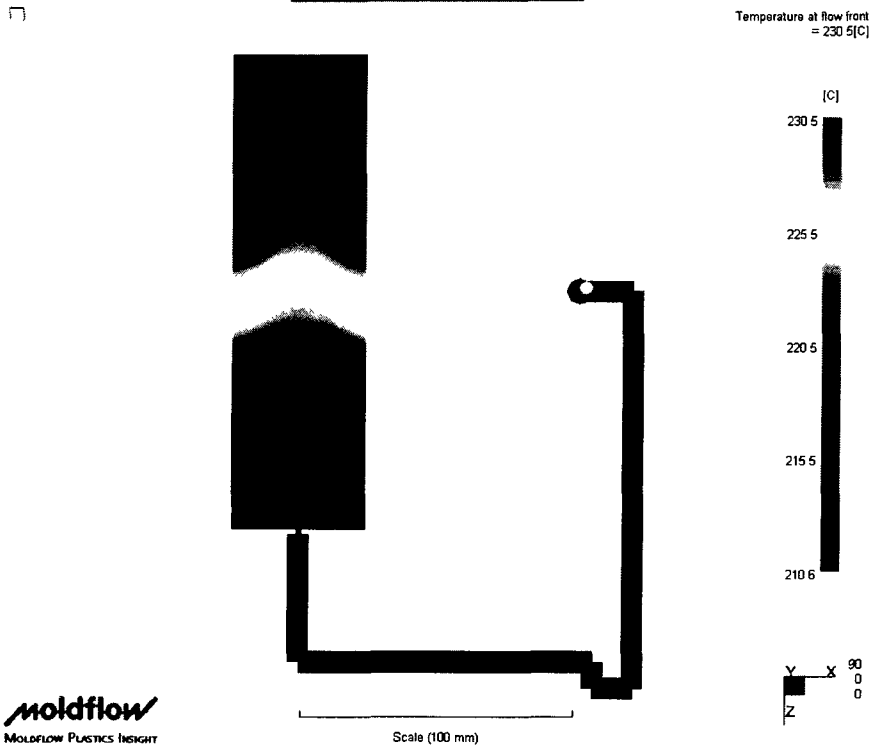


**Figure 38d - Temperature at flow front in 4 mm perpendicular rib cavity, mtl:
J700GP @ 6.3 cc/s**

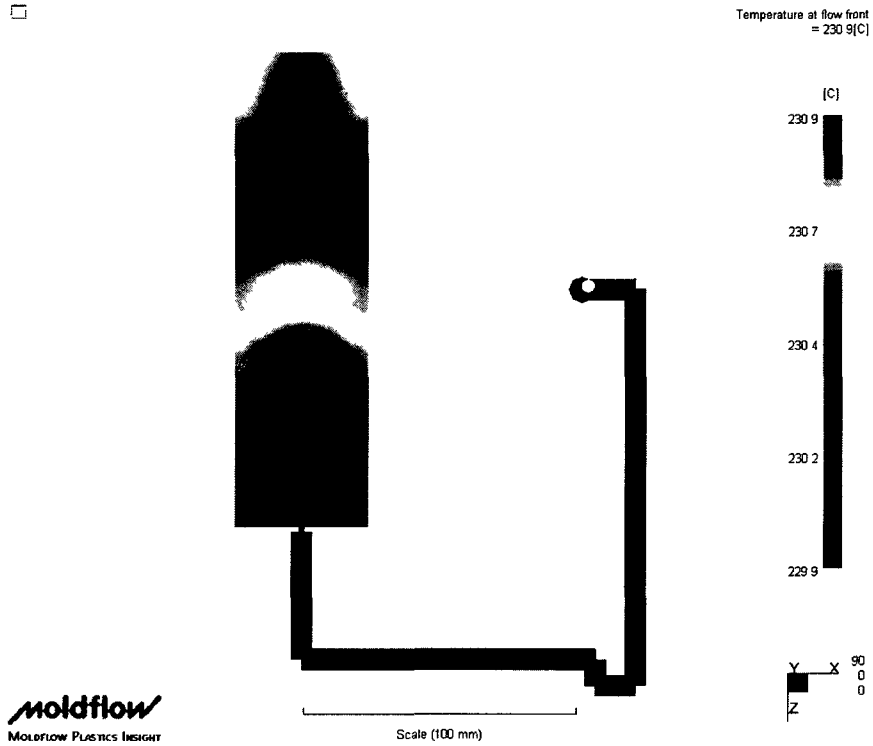


**Figure 39d - Temperature at flow front in 4 mm perpendicular rib cavity, mtl:
J2000GP @ 18.8 cc/s**

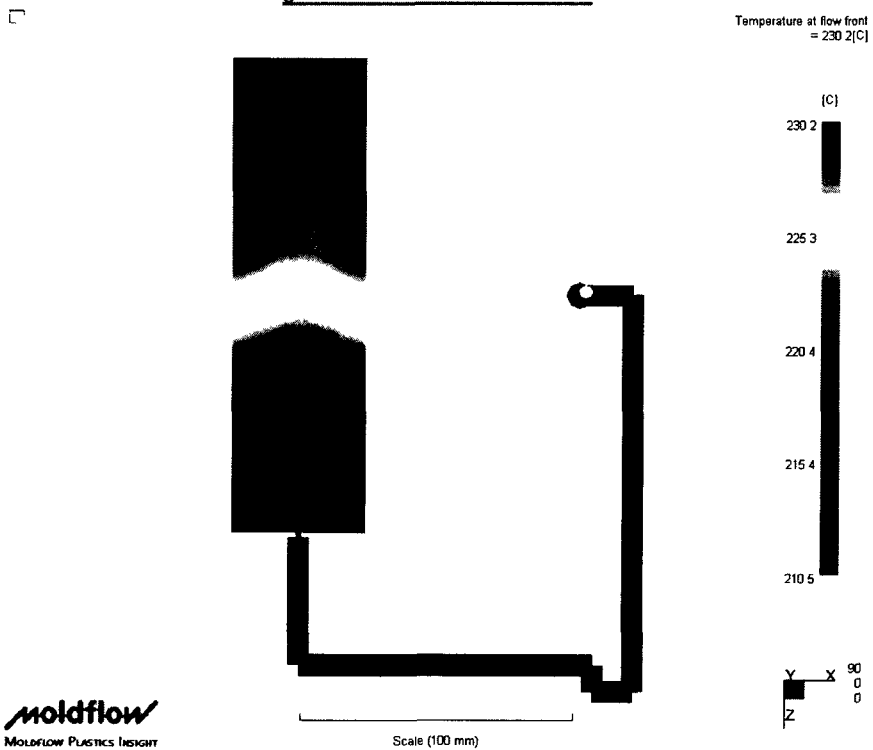


**Figure 40d - Temperature at flow front in 4 mm perpendicular rib cavity, mtl:
J2000GP @ 6.3 cc/s**

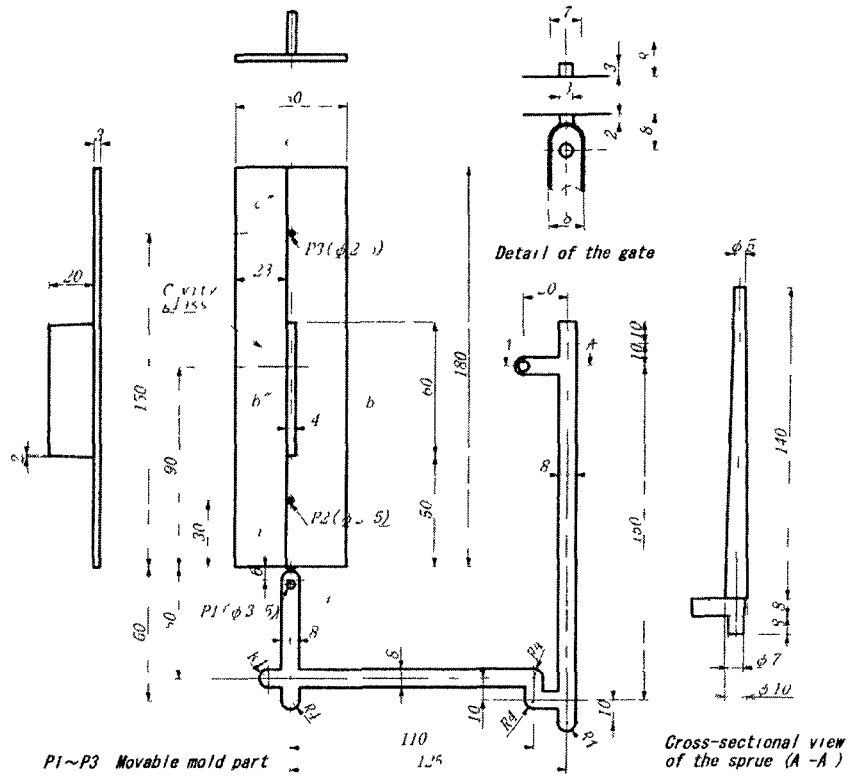


Figure 3c – Engineering Drawing of 4 mm Parallel Rib Cavity

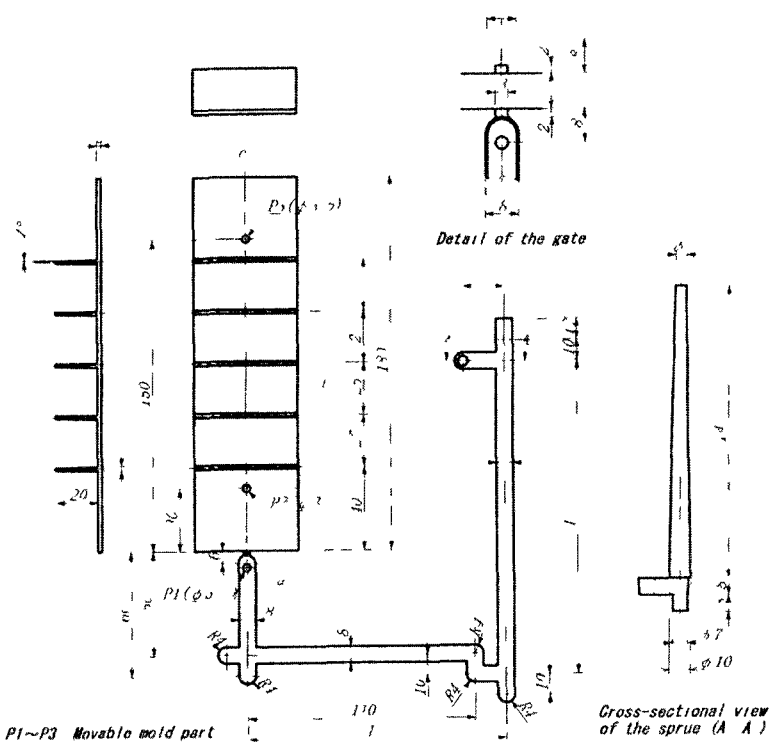


Figure 4e – Engineering Drawing of 2 mm Perpendicular Rib Cavity

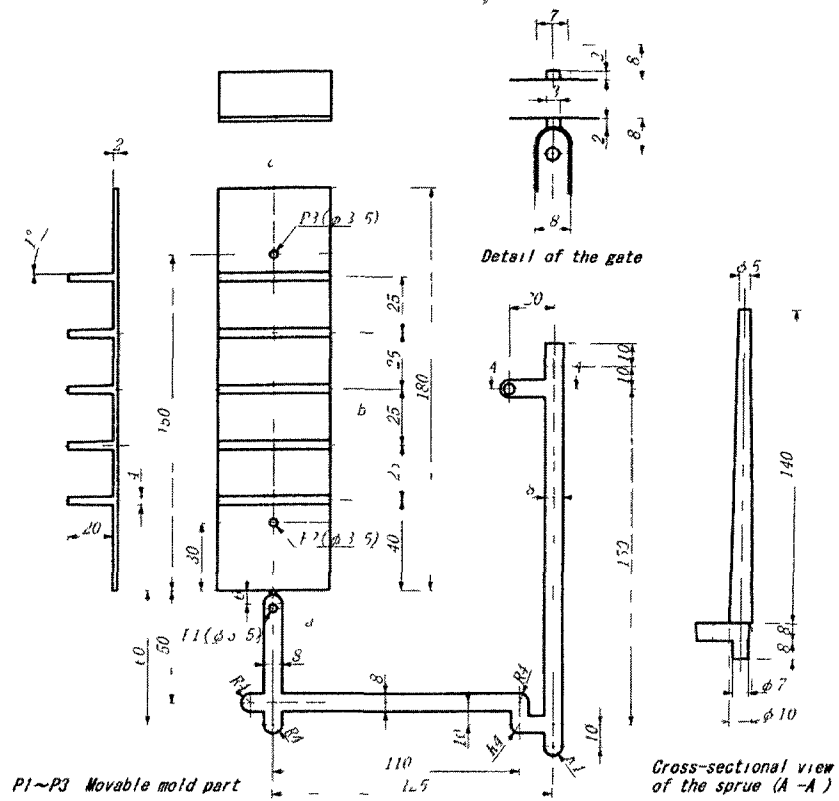


Figure 5e – Engineering Drawing of 4 mm Perpendicular Rib Cavity

Biographical Sketch of Author

Brian graduated from the University of Massachusetts Lowell, with a Bachelor of Science degree in Plastics Engineering, in 2008. He immediately began taking classes toward a Master of Science degree in Plastics Engineering. While taking classes in the evening Brian also worked in Chelmsford, MA for Rockwell Automation's engineering department. In early November 2009 Brian defended his thesis in front of Professors Lai, Driscoll, and Johnston; also present for the thesis defense were Brian's parents, Nancy and Alan, and girlfriend Alyson. The committee members approved the thesis and requested a few corrections and some additional information be added. The project was put on hold in mid November 2009 when Brian began working for The Haartz Corporation in Acton, MA as a Program Development Engineer. In the spring of 2010, Brian also began the process of opening a business; a paintball field in Connecticut with a lifelong friend as his business partner.

Working seven days a week between The Haartz Corporation and Modern Paintball, LLC Brian has struggled to find time to finish the corrections and additions. With the support of his family and girlfriend Alyson, Brian set out to finish the requests for a summer 2011 graduation.